Branched Glycopolymers

DISSERTATION

zur Erlangung des akademischen Grades eines
Doktors der Naturwissenschaften (Dr. rer. nat.)
im Fach Chemie der Fakultät für Biologie, Chemie und Geowissenschaften
der Universität Bayreuth

vorgelegt von

Sharmila Muthukrishnan

Geboren in Trichy/India

Bayreuth, 2005

Die vorliegende Arbeit wurde in der Zeit von März 2003 bis November 2005 in Bayreuth am Lehrstuhl Makromolekulare Chemie II unter Betreuung von Herrn Prof. Dr. Axel H. E. Müller angefertigt.

Promotionsgesuch eingereicht am:	29.11.2005
Zulassung durch die Promotionskommisssion:	07.12.2005
Wissenschaftliches Kolloquium:	08.02.2006

Amtierender Dekan: Prof. Dr. Carl Beierkuhnlein

Prüfungsausschuß:
Prof. Dr. A. H. E. Müller (Erstgutachter)
Prof. Dr. P. Strohriegl (Zweitgutachter)
Prof. Dr. K. Seifert (Vorsitzender)
Prof. Dr. H.G. Alt

Table of Contents

1. Introduction

The traditional view of carbohydrate polymers as nature´s energy source (starch and glycogen) and structural materials has expanded. Glycopolymers, synthetic sugar-containing polymers, are increasingly attracting the chemists due to their role as biomimetic analogues and their potential for commercial applications. There are different polymerization techniques which have enabled the synthesis of glycopolymers featuring a wide range of controlled architectures and functionalities. Methodologies for the synthesis of glycopolymers can be roughly classified into two main categories: (1) polymerization of sugar-bearing monomers and (2) chemical modifications of preformed polymers with sugar-containing reagents. In general, the latter method frequently results in glycopolymers having less regular structures because of incomplete reactions due to steric hindrance. Therefore, it is often better to use polymerizations of sugar-carrying monomers for synthesizing linear glycopolymers of well-defined architectures. In this thesis, well-defined glycopolymers of different topologies (Figure 1) have been synthesized by the polymerizations of sugar-carrying (meth)acrylate monomers using atom transfer radical polymerization (ATRP) and extensively characterized. Such glycopolymers of different architectures can be in future employed for several applications.

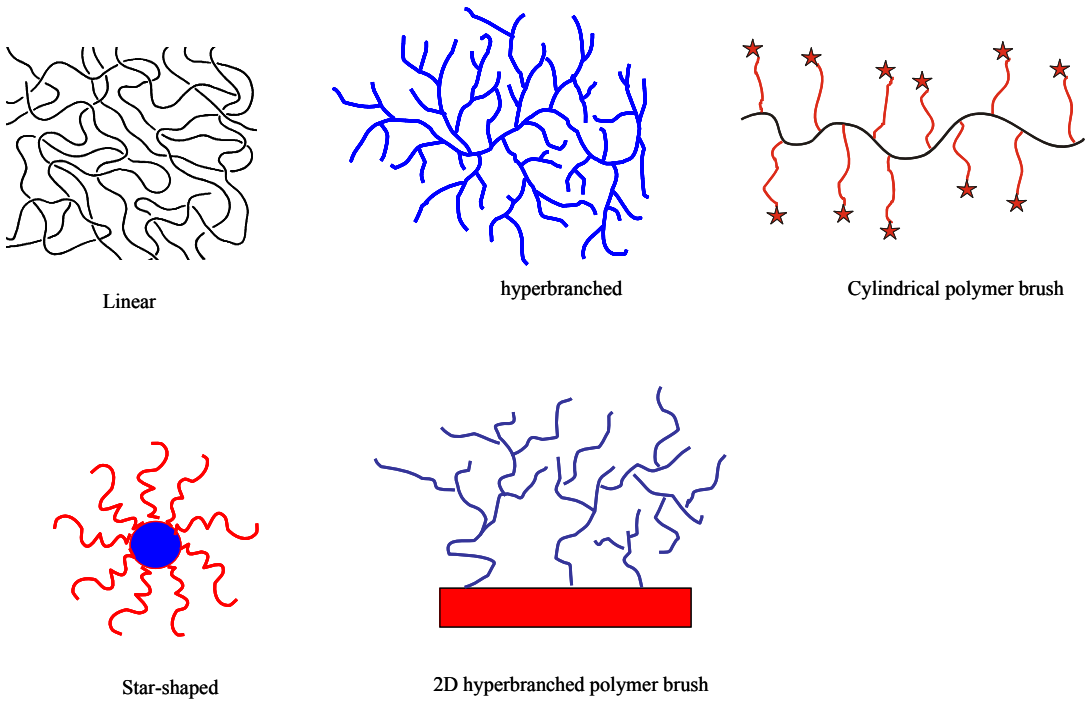

Figure 1. *Different topologies of sugar-carrying polymers.*

1.1. Atom transfer radical polymerization (ATRP)

Living ionic polymerization methods, like anionic polymerization has allowed the successful synthesis of well-defined polymers with controlled chain lengths and end functionalities, and the synthesis of well-defined block and graft copolymers. However, only a limited number of monomers can be used, and the presence of functionalities in the monomers causes undesirable side reactions. Moreover, these polymerizations have to be carried out with nearly complete exclusion of moisture and often at very low temperature.

The advent of controlled/"living" radical polymerization (CRP) has solved these problems and has provided numerous advantages over ionic polymerizations, like being suitable to a large number of monomers, tolerant to functional groups or impurities, allowing for mild reaction conditions, etc. In comparison to conventional radical polymerization, CRP has control with respect to molecular weight and polydispersity. The major difference between conventional radical polymerization and CRP is the lifetime of the propagating radical during the course of the reaction. In the conventional radical processes, radicals generated by decomposition of initiator undergo propagation and bimolecular termination reactions within a second. In contrast, in case of CRP, the lifetime of a growing radical can be extended to several hours enabling the preparation of polymers with predefined molecular weight, low polydispersity, controlled composition and functionality. In CRP, the mechanism to extend the lifetime of growing radical involves a dynamic equilibration between dormant and active sites with rapid exchange between the two states. It requires the use of either persistent radical species or transfer agents to react with propagating radicals to form the dormant species. Conversely, propagating radicals can be regenerated from the dormant species by an activation reaction.

There are mainly three different CRP techniques namely, nitroxide-mediated polymerization (NMP),[1] atom transfer radical polymerization (ATRP),[2] and reversible addition/fragmentation chain transfer (RAFT) polymerization.[3] All of these methods are based on establishing a rapid dynamic equilibration between a minute amount of growing free radicals and a large majority of the dormant species. But among them, the most successful and commonly used method is ATRP, in which the atom transfer step is the key elementary reaction responsible for the uniform growth of the polymeric chains.

1.1.1. Mechanism of ATRP

In order to obtain good control on a radical polymerization, two conditions should be met: (i) the equilibrium between the radicals and dormant species must lie strongly to the side of

the dormant species to assure that overall radical concentration remains very low and the rate of irreversible termination is negligible compared to the propagation rate; (ii) the exchange rate between radicals and dormant species must be faster than the rate of propagation so that all polymer chains have equal probability of growing. In ATRP, the propagating radicals are generated via reversible metal-catalyzed atom transfer, as shown in Scheme 1.

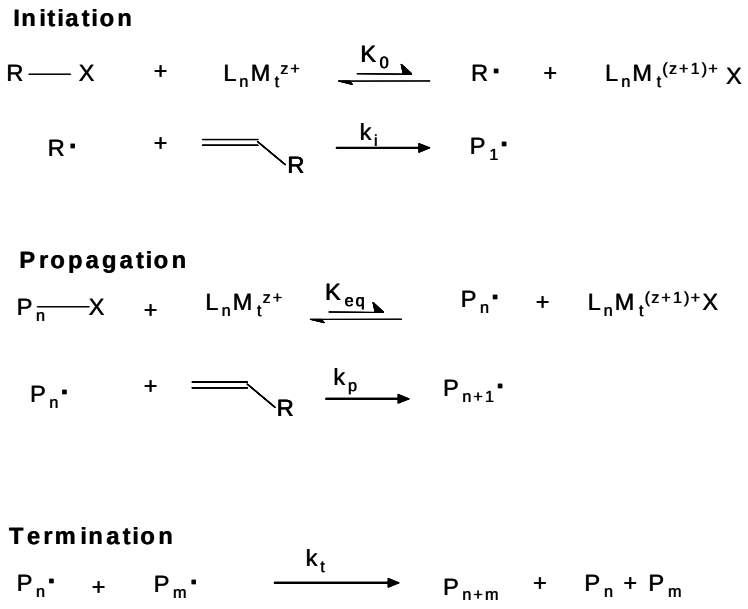

Scheme 1. *General mechanism for ATRP (RX: alkyl halide, initiator; L_n: Ligand; M_t: transition metal)*

With respect to kinetics, for a homogeneous system , the rate of ATRP has shown to be the first order with respect to the monomer and initiator as shown in eq. 1. For instance, in case of copper-mediated ATRP, the rate of propagation, R_p, is given by

$$R_p = k_{app}[P\cdot][M] = k_p K_{eq}[I]_0 \frac{[Cu(I)]}{[Cu(II)]}[M] \quad (1)$$

$$\text{where } K_{eq} = \frac{k_{act}}{k_{deact}} = \frac{[P.][Cu(II)]}{[PX][Cu(I)]} \quad (2)$$

As per the rate law, kinetic studies of ATRP using the soluble catalyst systems have proven that the rate of polymerization is first order with respect to alkyl halide (initiator), and copper(I) complex concentrations.[4] As can be seen from Scheme 1, a reactive radical and a

stable Cu(II) species are generated in the atom transfer step. If the initial concentration of Cu(II) is not high enough to ensure a fast deactivation, then the irreversible coupling and/or disproportionation of radicals can occur, and the concentration of Cu(II) builds up. Eventually, the concentration of Cu(II) is sufficiently high that the deactivation step is much faster than the rate at which the radicals react with each other in an irreversible termination step. This is called as persistent radical effect and a controlled polymerization is then obtained. A proper combination of initiator, metal, ligand, solvent, reaction time and temperature must be employed to obtained well-defined polymers by ATRP.

1.1.2. Monomers

A variety of monomers have been successfully polymerized using ATRP. Typical monomers include styrenes, (meth)acrylates, (meth)acrylamides, and acrylonitrile, which contain substituents that can stabilize the propagating radicals.[5,6] Each monomer has its own unique atom transfer equilibrium constant for its active and dormant species under the same conditions. In the absence of any side reactions other than radical termination by coupling or disproportionation, the magnitude of the equilibrium constant ($K_{eq} = k_{act}/k_{deact}$) determines the polymerization rate. Thus, for a specific monomer, the concentration of propagating radicals and the rate of radical deactivation need to be adjusted to maintain polymerization control. However, since ATRP is a catalytic process, the overall position of the equilibrium not only depends on the radical (monomer) and the dormant species but also can be adjusted by the amount and reactivity of the transition-metal catalyst added. Very recently, living radical polymerization of vinyl acetate[7] and vinyl chloride,[8] which lack a conjugating substituent, were reported using specially designed catalyst systems. In this thesis, sugar-carrying (meth)acrylate monomers, have been used for the well-defined synthesis of glycopolymers.

1.1.3. Initiators

The important role of the initiator is to determine the number of growing polymer chains. If the initiation is fast and transfer and termination negligible, then the number of growing chains is constant and equal to the initial initiator concentration. The theoretical molecular weight or degree of polymerization (DP) increases reciprocally with the initial concentration of initiator in a living polymerization. In ATRP alkyl halides are typically used as the initiator and the rate of the polymerization is first order with respect to the concentration of RX. To obtain well-defined polymers with narrow molecular weight distributions, the halide group, X, must rapidly and selectively migrate between the growing chain and the transition-

metal complex. So far, when X is either bromine or chlorine, the molecular weight control is the best. In general, any alkyl halide with activating substituents on the α-carbon, such as aryl, carbonyl, or allyl groups, can potentially be used as ATRP initiators. Polyhalogenated compounds (CCl_4, $CHCl_3$) and compounds with a weak RX bonds, such as N-X, S-X, and O-X can also be used as ATRP initiators. When the initiating moiety is attached to macromolecular species, macroinitiators are formed and can be used to synthesize block or graft copolymers.

It is important to note that the structure of the alkyl group (R) in the initiator should be similar to that of the dormant polymer species. This guideline holds good for secondary radicals but not for tertiary radicals. 1-phenylethyl halides resemble dormant polystyrene chains ends are good initiators for the polymerization of styrene and poor initiators for methyl methacrylate. For the selection of initiators that are not structurally related to the dormant polymer chain end, it is better to use organic halides that form less reactive radicals with higher efficiency than the dormant polymer chain ends. One should also consider the ratio of the apparent initiation rate constant (k_iK_0) to the apparent propagation rate constant (k_pK_{eq}). If the product k_iK_0 much lower than k_pK_{eq}, then initiation will be incomplete during the polymerization, consequently the molecular weights and polydispersities will be high.

1.1.4. Catalysts

The most important component of ATRP is the catalyst. It determines the position of the atom transfer equilibrium and the dynamics of exchange between the dormant and active species. There are several prerequisites for an efficient transition metal catalyst: (i) the metal center must have at least two readily accessible oxidation states separated by one electron, (ii) the metal center should have reasonable affinity toward a halogen, (iii) the coordination sphere around the metal should be expandable upon oxidation to selectively accommodate a (pseudo)halogen and the ligand should complex the metal relatively strongly. It is important to design the catalyst system where the position and dynamics of the ATRP equilibrium is appropriate. When bipyridine is used in copper-mediated ATRP, the copper halide is sparingly soluble in the polymerization medium. But, bipyridyl ligands with long alkyl chains at the 4,4`-position (such as dNbipy, 4,4´-di(5-nonyl)-2,2´-bipyridine) can completely solubilize the copper halide and lead to better control.[9] The position of equilibrium depends upon the nature of the metal and ligands. Generally, more electron-donating ligands better stabilize the higher oxidation state of the metal and accelerate the polymerization. A number of transition-metal complexes have been used in ATRP, including system based on Cu,[2] Ru,[10]

Fe,[11] and Ni,[12]. But copper(I)-catalyzed ATRP is the most successful and common one.

1.2. Hyperbranched polymers

Dendrimers are monodisperse molecules with well-defined, perfectly branched architectures, synthesized in a multi-step organic synthesis. In contrast, hyperbranched polymers are synthesized in a one-pot polymerization and are less regular in structure and their degree of branching (DB) typically does not exceed 50% of that of dendrimers. Hyperbranched polymers are very interesting to due an increasing number of end groups, compact structure in solution and ease in the synthesis, though they are less regular than those of dendrimers. In the past, hyperbranched polymers were mainly synthesized via polycondensation of AB_2 monomers and many reviews have been published.[13-16] After Kim and Webster[17,18] published the synthesis of pure "hyperbranched" polyarylenes from an AB_2 monomer, this class of polymers became a topic of intensive research by many groups.

Several methods can be employed for the synthesis of hyperbranched polymers. They can be classified into three categories[14,19]: (1) step-growth polycondensation of AB_x monomers; (2) chain-growth self-condensing vinyl polymerization (SCVP) of AB* initiator-monomers ("inimers"); (3) chain-growth self-condensing ring-opening polymerization of cyclic inimers. The most commonly used technique is the polycondensation of AB_x monomers, but vinyl monomers cannot be polymerized by that approach. Hence, the recent discovery of SCVP made it possible to utilize vinyl monomers for one-pot synthesis of hyperbranched polymers.[20-27]

The extension of SCVP is known as self-condensing vinyl copolymerization (SCVCP), which involves the copolymerization of AB* inimers with conventional monomers. This results in highly branched copolymers where the degree of branching is controlled by the comonomer ratio. By using SCVCP, a variety of hyperbranched polymers can be synthesized. Some AB* inimers used for SCV(C)P are listed in Figure 2, where the double bond is designated A and B* is a group capable of being activated to initiate the ATRP of vinyl groups. Cu-based atom transfer radical polymerization (ATRP) was employed for SCVP of these acrylate-type inimers having an acrylate (A) and a bromoester group (B*), capable to initiate ATRP.[28,29] For the synthesis of hyperbranched methacrylates, Cu-based ATRP with the addition of zero-valent copper for **5** and **6,**[30] Ni-based controlled radical polymerization for **6,**[31] and Cu-based ATRP for **7**[32] have been empolyed. However, methacrylate-type inimers, **5** and **6** as well as acrylate-type inimer, **2** could not be successfully polymerized by Cu-based ATRP despite variatons in ligand and temperature.[30] It was

speculated that the tertiary radical sites generated from methacrylate moieties (A) and/or the 2-bromoisobutyryloxy moieties (B*) coupled rapidly, forming an excess amount of deactivating Cu(II) species and prevented polymerization.

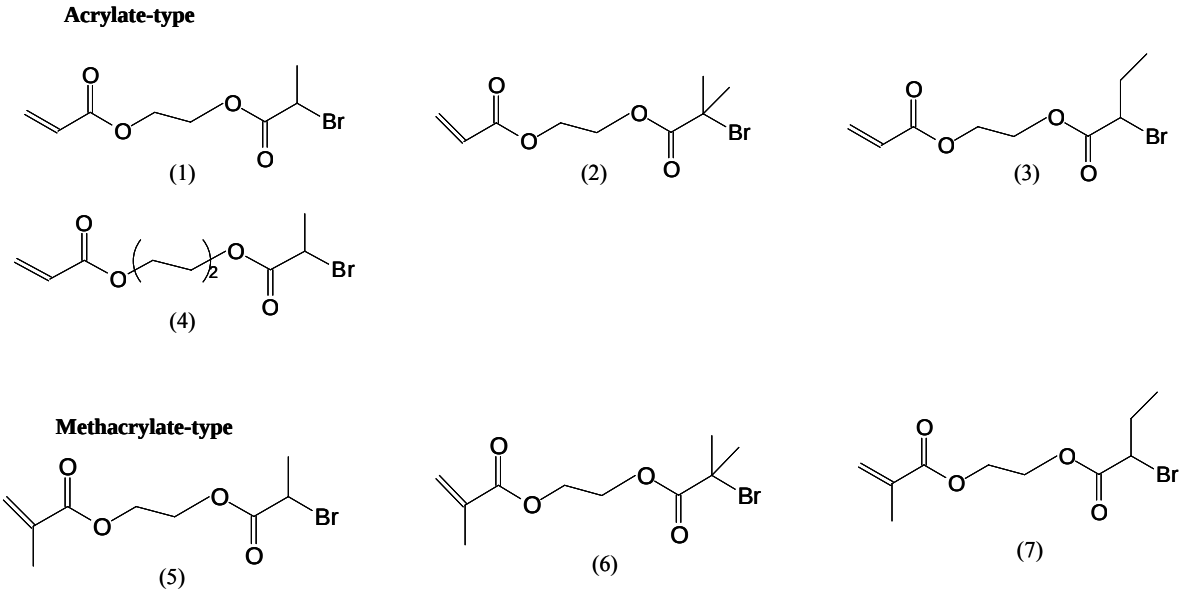

Figure 2. *Some structures of acrylate-type and methacrylate-type inimers.*

The basic mechanism for SCVCP via ATRP is shown in Scheme 2. It can be initiated in two ways: (i) by addition of the active B* group in an AB* inimer to the vinyl group A of another AB* inimer forming a dimer with two active sites, A* and B*, and (ii) by addition of a B* group to the vinyl group of monomer M forming a dimer with one active site, M*. Both the initiating B* group and the newly created propagating centres A* add M* can react with any vinyl group in the system. Thus we have three different types of active centers, A*, B*, and M* in the dimers, which can react with double bonds A (inimer and macromolecules; each macromolecule contains strictly one double bond) and M (monomer). Thus, copolymerization method is a facile approach to synthesize functionalized branched polymers, since different types of functional groups can be incorporated into a polymer, depending on the chemical nature of the comonomer. The architecture can be easily modified by a suitable choice of the comonomer ratio in the feed in an economic approach. A series of hyperbranched acrylates having different degree of branching (DB)s and MWs have been obtained using SCVCP of the acrylate-type inimer **1** tBuA via ATRP.[26]

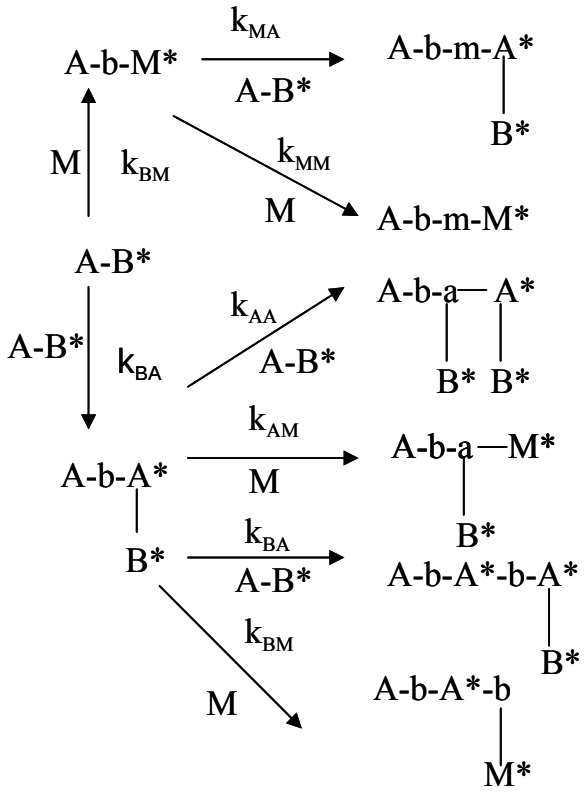

Scheme 2. *Mechanism of SCVCP for the synthesis of hyperbranched polymers.*

1.2.1. Degree of branching (DB)

DB can be defined as the ratio of the branched units in the polymer to those in a perfect dendrimer. Thus, the limiting values are DB = 0 for linear polymers and DB = 1 for a perfect dendrimer. If the vinyl group or the initiator unit ("core unit") is not taken into account then DB is defined as

$$DB = \frac{\text{(number of branched units) + (number of terminal units)-1}}{\text{(total number of units)-1}} \quad (3)$$

Here, one unit has been subtracted from the numberator and the denominator to take into account that even a linear polymer has got one initiating and one terminal unit. From the topology of the branched systems with trifunctional branchpoints, for any given molecule the number of branched units is equal to the number of terminal unit minus one. Hence, eq.3 can be further modified as

$$DB = \frac{\text{2x (number of branched units)}}{\text{(total number of units)-1}} \quad (4)$$

The DB obtainable in SCVP is DB = 0.465 for $r = k_A/k_B = 1$ (reactivity ratio of propagating and initiating groups), and reaches maximum, DB = 0.5, for $r = 2.6$.[33,34] This is similar to that obtained by AB_2 polycondensation when both B fuctions have the same reactivity.

For SCVCP, DB strongly depends on the comonomer ratio, $\gamma = [M]_0/[AB^*]_0$. In cases where all rate constant are equal, for $\gamma >> 1$, the final value of DB decreases with γ as $DB = 2/(\gamma + 1)$. For low values of γ ($\gamma \leq 1$), DB even exceeds the values for a homo-SCVP; a maximum of DB = 0.5 is reached at $\gamma \approx 0.6$. Depending on the reactivity ratios, the structure of the polymer obtained can change from "macroinimers" when the monomer M is much more reactive than the vinyl groups of inimer or polymer molecules to "hyperstars" in the opposite limiting case. DB can be evaluated for hyperbranched polymers using ^{1}H NMR. For hyperbranched acrylates obtained by SCV(C)P of the acrylate-type inimer **1**, DB has been evaluated using ^{1}H NMR.[26] The direct evaluation of DB for hyperbranched methacrylates obtained by SCVP is impossible due to overlapping of the signals required for evaluation.[30] However, DB of some hyperbranched methacrylates can be determined by ^{1}H NMR. NMR experiments afford a conclusive measurement of the degree of branching for lower γ values. In case of higher γ values, the low concentration of branchpoints in the copolymer does not permit the determination of the DB directly owing to the low intensities of the peaks required for the evaluation. However, for the case of high comonomer ratios, $\gamma >> 1$, the relation between DB_{theo} and γ becomes very simple and does not depend on the reactivity ratios of the various active centers and is represented as $DB_{theo} \approx 2/(\gamma + 1)$.

1.2.2. Solution properties

Hyperbranched polymers have characteristic properties, such as relatively compact shape, and absence of entanglements, in pronounced contrast to linear chains. They have low viscosity in bulk and solution and this strongly depends on MW and DB. Due to the difference in the hydrodynamic volume, the determination of MW is more complicated than that of linear polymers. The use of a linear calibration curve in SEC leads to erroneous results. Hence, mass-sensitive on-line detectors such as a multi-angle light scattering photometer (MALS)[35,36] or a viscosity detector using the universal calibration (UNICAL) principle.[37]

The relationship between the solution viscosity and MW has been investigated for many hyperbranched polymers and the Mark-Houwink exponent typically varies between 0.5 and 0.2, depending upon the DB. The exponent for linear homopolymers in a good solvent with a random coil conformation is in the region of 0.6-0.8. For branched PtBuAs obtained by

SCVCP of tBuA with acrylate-type inimer **1** via ATRP is found to have Mark-Houwink exponents, α in the region between 0.38-047 which is lower than that for linear PtBuA (α = 0.80).[29] The contraction factors,[38] $g = \langle R_g^2 \rangle_{branched} / \langle R_g^2 \rangle_{linear}$, $g` = [\eta]_{branched}/[\eta]_{linear}$, are another way of expressing the compact nature of branched polymers. It is computed experimentally at constant MW. The contraction factor can be expressed as the averaged value over the MWD or as a continuous function of MW. The ratios of hydrodynamic radius (R_h) and radius of gyration (R_g) for the hyperbranched methacrylates are investigated to be in the range of 0.75-0.84,[39] which are comparable to the value of hard spheres (0.775) and significantly lower than that of the linear unperturbed polymer coils (1.25-1.37).

1.3. Surface-grafted polymer brushes

Polymer brushes are defined as dense layers of chains tethered to a surface or interface where the distance between grafts is much less than the unperturbed dimensions of the tethered polymer. Due to the high steric crowding, grafted chains extend from the surface, thus residing in an entropically unfavorable conformation. They have been prepared by end-grafting of chains to flat surfaces that are either organic, or inorganic in nature. Since initial reports of this work in 1998 from flat silicon wafers,[40] surface-initiated ATRP has also been performed from flat gold surfaces,[41,42] inorganic particles/colloids, organic latexes,[43-46] nanopatterned networks,[47] dendrimers,[48-50] and highly functional linear polymers.[51,52] In terms of polymer chemical compositions, polymers grafted onto surfaces can be either linear or branched as shown in Figure 3. Depending upon the substrates, they can be divided into 3D, 2D, and one dimensional (1D) hybrids, which correspond to products grafted onto spherical particles, planar surfaces, and linear polymers, respectively.

There are basically two ways to fabricate polymer brushes: physisorption and covalent attachment as shown in Figure 4. For physisorption, block copolymers adsorb onto a suitable substrate with one block interacting strongly with the surface and the other block interacting weakly with the substrate.[53,54] Covalent attachment can be accomplished by either “grafting to” or “grafting from” approaches. In a “grafting to” technique, preformed end-functionalized polymer molecules react with an appropriate substrate to form polymer brushes.[55,56] The “grafting from” approach is more promising due to the fact that the resulting polymer brushes have a high grafting density. Unlike the situation in the “grafting to” technique, the substrate must be modified to generate the initiator functionality suitable for the polymer brush synthesis from surface. This surface modification can be performed using Langmuir-Blodgett techniques[57,58] or self-assembled monolyer (SAM) deposition.[59-61] Furthermore, depending

on the polymerization method, the initiator can be a free radical,[62,63] ionic,[64,65] ring-opening metathesis[66] or controlled radical polymerization type.[67,68] By varying the substrate (gold, silicon, nanoparticles, etc.), initiator deposition technique, and polymer synthesis route, virtually limitless possiblities present themselves for brush formation.

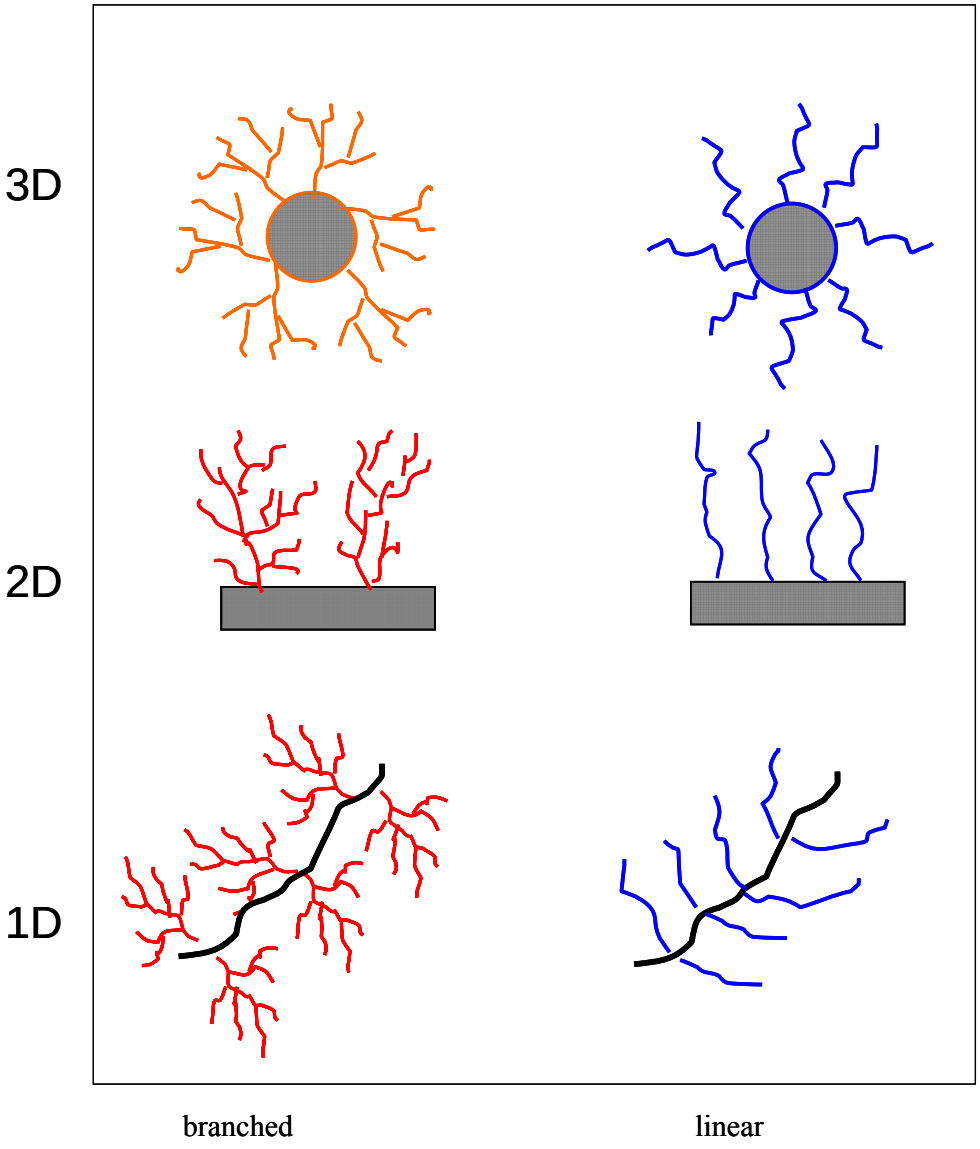

Figure 3. *Surface-grafted branched and linear polymers: from one-dimensional (1D) to three dimensional (3D) .*

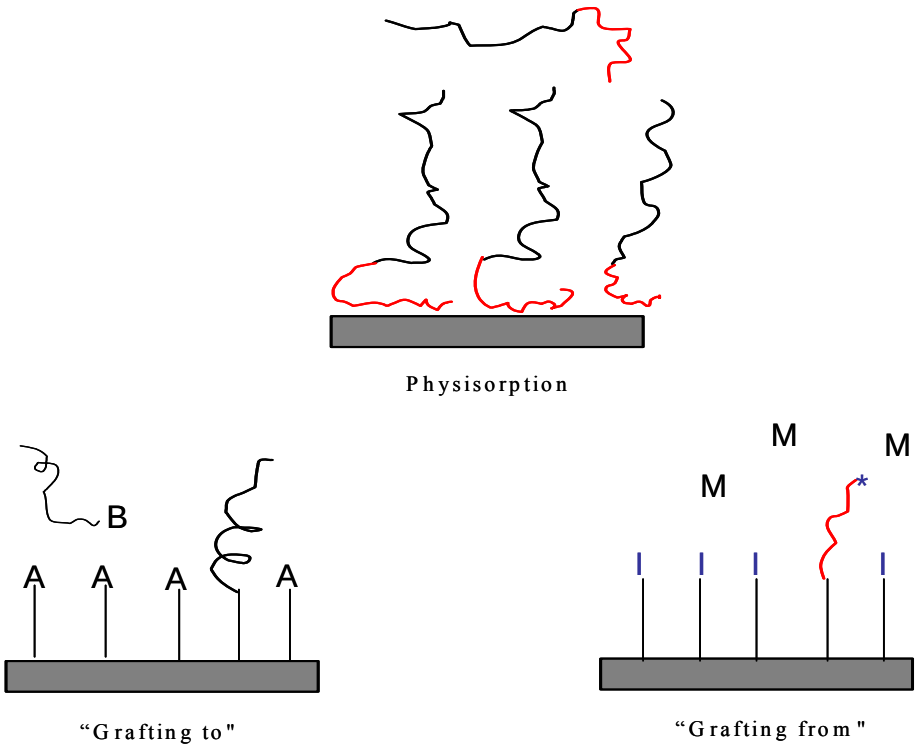

Figure 4. *Preparation of polymer brushes by physisorption, "grafting to" and "grafting from" approaches .*

The surface chemistry and interfacial properties of hyperbranched polymers have also become a field of growing interest.[69,70] In recent years, much interest has been paid to highly branched polymers grafted chemically onto surfaces, as their distinctive chemical and physical properties can be used advantageously as functional surfaces and as interfacial materials. Similar to that for the synthesis of linear polymer brushes, "grafting to" and "grafting from" methods can also be used to prepare surface-grafted branched polymer brushes. The one-step "grafting to" approach involves a reaction (or interaction) of one or several reactive groups of hyperbranched polymers with functional groups on the substrate.[71,72] In contrast, the "grafting from" technique is performed by an in-situ surface-initiated polymerization from immobilized initators.[73] Apart from these two methods, a multi-step grafting method can be employed which involves a series of repeated "grafting to" or "grafting from" steps. In this case, the branched architecture is formed during the repeated reactions. Zhou et al.[74] reported the preparation of a highly branched poly(acrylic acid) film attached to a self-assembled monolayer of mercaptonundecanoic acid on gold using the "grafting to" technique. The same strategy has been employed for the synthesis of

hyperbrancehd poly(acrlyic acid)s grafted on polyethylene, polypropylene etc. The most facile and straightforward strategy towards the synthesis of branched polymers from surfaces is by surface-initiated SCV(C)P.[31,75] Here, the functionalized surface as well as the AB* inimer have groups capable of initiating the polymerization and the chain growth can be started from both B* in the intiators immobilized on the silicon substrate, and a B* group in the inimer. Further addition of AB* inimer or dimer to A* , B* and M* centers results in highly branched polymers. Here, the polymers formed in solution may also add to active centers of attached polymers, so the method can be considered as a combination of "grafting from" and "grafting to" approaches. For the characterization of these systems, techniques such as ellipsometry, contact angle, X-ray photoelectron spectroscopy (XPS) and AFM are important in assessing whether the tethered polymers obtained from surface-initated polymerization possess precise molar mass and composition.

The surface-confined hyperbranched polymers are suitable for a number of technical applications, including corrosion inhibition, chemical sensing, cellular engineering, and micrometrscale patterning.[76-78] The surface-grafted polymers brushes are also useful in other applications such as new adhesive materials, protein-resistant biosurfaces, polymer surfactants and lubricants.[79-81]

1.4. Cylindrical brushes

As mentioned in the previous section, polymer brushes refer to an assembly of polymer chains which are tethered by one end to a polymer chain or a surface of a solid (Figure 3). ATRP has opened a wide range of possibilities to control and design the macromolecular architecture under mild reaction conditions. Cylindrical polymer brushes can be synthesized via ATRP in a controlled fashion. There are three main approaches to achieve these cylindrical polymer brushes: "grafting though",[82-84] "grafting onto",[85] and "grafting from",[86,87] respectively as shown in Figure 5.

The "grafting through" method involves the polymerization of macromonomers, which was the first method applied towards the synthesis of these cylindrical brushes. The first report using the radical polymerization of macromonomers was reported by Tsukahara e tal.[82,83] where oligomers prepared by anionic polymerization were end-functionalized to obtain macromonomers possessing a terminal vinyl group, which were subsequently polymerized using radical polymerization. The major limitation is the difficulty in obtaining complete conversion and precise size control of the polymer brushes formed. Due to the free radical polymerization, the brushes have broad distributions of the backbone length. Incomplete

conversion of the macromonomers causes difficulties in purification and fractionation is essentially required. Although other techniques aiming to achieve well-defined brushes were perfomed to polymerize the macromonomers using living anionic polymerization[88] and living ring-opening metathesis polymerization,[89] until now long and well-defined brushes have not been synthesized using this approach.

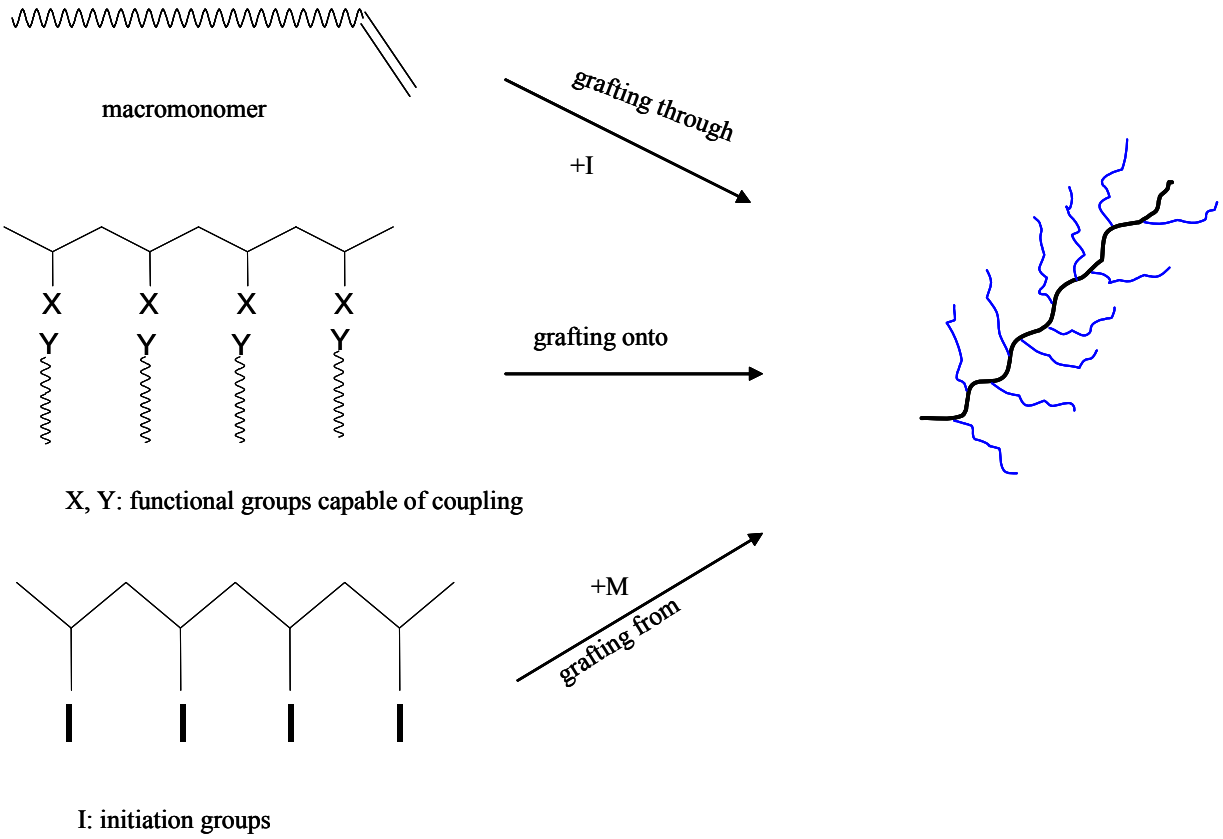

Figure 5. *Three different approaches to the synthesis of cylindrical polymer brushes .*

The "grafting onto" method involves the synthesis of the backbone and side chains separately. This involves coupling raction between the pendant functional groups (X) of backbone and the end-functional groups (Y) of the grafts. This technique often resulted in low grafting efficiency due to the steric hindrance in the case of long grafts. It is often difficult to control the degree of branching and incomplete coupling reaction could lead to problem of purification.

The "grafting from" approach is a very promising method to achieve well-defined cylindrical brushes. In this technique, a well-defined backbone is first prepared by living polymerization techniques, followed by functionalization to attach ATRP initiating groups to

the backbone (one initiating group per backbone monomer unit). The polymer brushes are then formed by ATRP from the pendant initiating groups on the backbone. This technique is useful in obtaining polymer brushes of high grafting density and narrow distribution of both the backbone and side chains. The purification is also not very tideous as in other two approaches.

1.4.1. Solution properties

The multibranched structure of these cylindrical brushes leads to very compact molecular dimension in solution compared to the corresponding linear polymer with the same molecular weight. These brushes have higher main-chain stiffness than linear flexible polymers in solution, due to the intramolecular repulsion between adjacent side chains. The persistence length (l_p) or Kuhn statistical segment length (l_k) of polymer brushes increases monotonously with increasing side chain length, and the contour length per main chain monomer unit was found to approach the limiting value, 0.25 nm, for large side chain lengths. Based on their chain stiffness, the cylindrical polymer brushes have been named as "rodlike" combs[90] or molecular "bottlebrushes".[84] Schmidt et al. reported a structural characterization of cylindrical polymer brushes with fixed side chain length in terms of absolute molar mass, M, the radius of gyration, R_g, and intrinsic viscosity, $[\eta]$.[90] For polymer brushes with fixed PS side-chain length but variable (PMA) main chain polymethacrylate, length, the relation of R_g vs. M is excellently described by the Kratky-Porod worm-like chain model.[91] They found out that these brushes exhibit a bottlebrush structure in which the PMA main chain adopts an extremely stiff conformation surrounded by the expanded but still flexible PS side chains. Nakamura et al.[92,93] investigated the solution properties by static light scattering and the viscosity measurements of series of brushes containing PS backbone and PS side chains of fixed side chain lengths. They concluded that the Kuhn segment length to be one order of magnitude larger than that of the linear chains at the Θ point, indicating that the high segment density around the main chain remarkably stiffens the backbone of the polymer brush. Additionally, the repulsions between the main chain and side chain and also between the neighbouring side chains play an important role in the high stiffness of polymer brushes. The intrinsic shape and size of the polymer brushes in solutions were also investigated by small angle X-ray scattering, aiming at determining the cross-sectional characteristics of polymer brushes.[94] The synthesis and characterization of cylindrical brushes are of growing interest due to their possible applications as templates for inorganic nanoparticle formation and novel nanosized organic/inorganic hybrids.[95,96]

1.5. Star polymers

The synthesis and characterization of star polymers has been a consistent area of exploration in the ongoing pursuit of structure-property relationships in macromolecular science.[97] Star polymers have different dynamic properties and higher degrees of chain end functionality compared to linear polymers of similar composition. Star polymers can be basically synthesized via two different methods: "arm first" and "core first" approaches. In the "arm first" approach, monofunctional, living linear macromolecules are initially synthesized. Star formation then occurs in one of two ways: a difunctional comonomer is used to provide cross-linking through propagation[98] or a multifunctional terminating agent is added connecting a precise number of arms to a central core molecule.[97] The former technique produces macromolecules with a large, often heterogeneous, number of arms while in the latter case separation techniques are used to isolate stars from uncoupled linear polymers. In the "core first" approach, multifunctional initiators are used to grow chains from a central core resulting in macromolecules with well-defined architectures in terms of arm number and arm length.[99] In many cases, the multifunctional initiators must be presynthesized. For well-defined synthesis of stars, its important to use a controlled polymerization technique. Several techniques like living ionic,[100] metathesis,[101] and group transfer polymerizations[102] were used but they all require strenuous methods of reagent purification. Hence controlled/"living" free radical polymerization has opened a wide range of possibilities. In the case of "arm-first" approach, divinylbenzene was used to produce microgels in the radical polymerization of styrene.[103] The first report on using the "core first" approach described the hexakis-(bromomethyl)benzene-initiated ATRP of styrene, methyl acrylate, and methyl methacrylate.[99] 2-bromoisobutyrate functions attached to sugars, like α-D-glucose, saccharose and β-cyclodextrin have also resulted in well-defined star-shaped polymers via the "core-first" approach.[104-106] Nowadays, efforts to develop organic/inorganic nanocomposites are in progress wherein cubic silsesquioxanes are used as a core and organic star polymers or oligomers are synthesized using "core first" approach via ATRP.[107,108] This trend is due to the increasing interest in combining the potential applications of hybrid materials with the facility with which branched polymers can be processed.

1.5.1. Solution properties

Branched polymers, as mentioned in earlier sections, are found to have reduced viscosity compared to their linear analogues with the same molecular weight. This effect becomes more and more pronounced with increasing number of branches. The exponent for the

relation between intrinsic viscosity and molecular weight, $[\eta] = KM^{\alpha}$, is the same for a linear polymer and a star with a constant number of arms.[109] This implies that in a Mark-Houwink plot of a star polymer which grows by adding monomer to the arms, results in a parallel line to the linear one, but shifted to lower viscosity. Star polymers prepared by the the arm-first approach with a bifunctional monomer have an interesting feature that they do not have a constant number of arms. Here the molecular weight increases with the number of arms and hence the structure changes within the sample. This results in a smaller Mark-Houwink exponent.[38,110] For the relation between the radius of gyration and the molecular weight of star polymers in a good solvent Daoud and Cotton[111] calculated a dependence of $R_g \propto N^{0.6} \cdot f^{0.2}$ (N = number of segments per arm). For N = constant, this results in $R_g \propto M^{0.2}$. For a constant number of arms, the dependence will be $R_g \propto M^{0.6}$.

The dependence of the dimensions of a star upon its functionality can be expressed by means of the dimensionless parameters.[112]

$$g = \frac{< R_g^2 >}{< R_g^2 >_L} \tag{5}$$

$$\text{and} \quad g` = \frac{[\eta]}{[\eta]_L} \tag{6}$$

where $< R_g^2 >_L$ and $[\eta]_L$ indicate the root-mean-square radius of gyration and the intrinsic viscosity of the linear polymer molecule with identical molar mass, respectively. According to Zimm and Stockmayer,[112] $g_{0,ZS}$ for star polymers with a freely jointed chain (random-walk) is given by

$$g_{0,ZS} = \frac{(3f - 2)}{f^2} \tag{7}$$

In order to estimate non-uniformity in *f*, the following *g* factor proposed by Burchard[38] can be applied

$$g_{0,B} = \frac{6f}{(f+1)^2} \tag{8}$$

Zimm and Kilb[113] made a first attempt to calculate *g`* for star branched macromolecules on the basis of the Kirkwood-Riseman approximation for the hydrodynamic interaction. They came to the conclusion that

$$g` = g^{0.5} \tag{7}$$

The ratio of R_g/R_h is a sensitive fingerprint of the inner density profile of star molecules. It is well known that R_g/R_h for linear unperturbed polymers is in the range 1.25-1.37 and 0.775 for hard spheres of uniform density.[38] However, for regular star polymers, the value approaches unity and around 1.225 for stars with polydisperse arms for $f >> 1$ under θ conditions.[38]

In this thesis, well-defined glycostars using a silsesquioxane-based macroinitiator via ATRP are synthesized and their solution properties are extensively investigated.

1.6. Motivation of this thesis

The basic motivation for this work is to develop a simplest methodology to synthesize well-defined and novel hybrid glycopolymers. Glycopolymers of different topologies are synthesized using via atom transfer radical polymerization (ATRP) of sugar-carrying (meth)acrylate monomers. Hyperbranched glycopolymers of sugar-carrying (meth)acrylate monomers, 3-*O*-(meth)acryloyl-1,2:5,6-di-*O*-isopropylidene-D-glucofuranose ((M)AIGlc) are synthesized by self-condensing vinyl copolymerization (SCVCP) via ATRP. Their solution properties are then compared to those of linear glycopolymers. The same strategy is then extended to the surface of the silicon wafers to prepare novel and smart branched copolymer surfaces and linear polymer brushes. Molecular sugar sticks or glycocylidrical brushes are also synthesized using a well-defined polyinitiator backbone and a sugar-carrying methacrylate monomer, MAIGlc. The morphology is then examined using scanning force micoroscopy. Glycostars or glycopolymer/nanoparticle hybrid stars are obtained via "core first" approach using a silsesquioxane-based macoinitiator and the monomer, MAIGlc via ATRP and their solution properties are extensively investigated.

Such well-defined glycopolymers of different architectures are then deprotected and converted to water-soluble glycopolymers. Such sugar-carrying polymers have high density of sugar moieties resulting in enhanced biocompatibility and hydrophilicity. Hence, one of the objectives of this work is to explore the easiest and more efficient pathway to prepare biocompatible materials. In future, they can serve as useful tools in understanding carbohydrate-protein interactions and also for drug delivery.

1.7. References

(1) Hawker, C. J.; Bosman, A. W.; Harth, E. *Chemical Reviews* **2001**, *101*, 3661-3688.

(2) Wang, J.-S.; Matyjaszewski, K. *J. Am. Chem. Soc.* **1995**, *117*, 5614-5615.

(3) Chiefari, J.; Chong, Y. K. B.; Ercole, F.; Kristina, J.; Jeffery, J.; Le, T. P. T.; Mayadunne, R. T. A.; Meijs, G. F.; Moad, C. L.; Moad, G.; Rizzardo, E.; Thang, S. H. *Macromolecues* **1998**, *31*, 5559-5562.

(4) Matyjaszewski, K.; Patten, T. E.; Xia, J. *J. Am. Chem. Soc.* **1997**, *119*, 674-680.

(5) Patten, T. E.; Matyjaszewski, K. *Advanced Materials* **1998**, *10*, 901.

(6) Matyjaszewski, K. *Chem.--Eur. J.* **1999**, *5*, 3095-3102.

(7) Wakioka, M.; Baek, K.-Y.; Ando, T.; Kamigaito, M.; Sawamoto, M. *Macromolecules* **2002**, *35*, 330-333.

(8) Percec, V.; Popov, A. V.; Ramirez-Castillo, E.; Monteiro, M.; Barboiu, B.; Weichold, O.; Asandei, A. D.; Mitchell, C. M. *Journal of the American Chemical Society* **2002**, *124*, 4940-4941.

(9) Patten, T. E.; Xia, J.; Abernathy, T.; Matyjaszewski, K. *Science* **1996**, *272*, 866-868.

(10) Kato, M.; Kamigaito, M.; Sawamoto, M.; Higashimura, T. *Macromolecules* **1995**, *28*, 1721.

(11) Zhu, L.; Tong, X.; Li, M.; Wang, E. *Journal of Polymer Science, Part A: Polymer Chemistry* **2000**, *38*, 4282-4288.

(12) Granel, C.; Dubois, P.; Jerome, R.; Teyssie, P. *Macromolecules* **1996**, *29*, 8576-8582.

(13) Ishida, Y.; Sun, A. C. F.; Jikei, M.; Kakimoto, M.-a. *Macromolecules* **2000**, *33*, 2832-2838.

(14) Jikei, M.; Kakimoto, M. *Progress in Polymer Science* **2001**, *26*, 1233-1285.

(15) Voit, B. *J. Polym. Sci., Part A: Polym. Chem.* **2000**, *38*, 2505-2525.

(16) Hult, A.; Johansson, M.; Malmstrom, E. *Advances in Polymer Science* **1999**, *143*, 1-34.

(17) Kim, Y. H.; Webster, O. W. *J. Am. Chem. Soc.* **1990**, *112*, 4592.

(18) Kim, Y. H.; Webster, O. W. *Macromolecules* **1992**, *25*, 5561-5572.

(19) Sunder, A.; Heinemann, J.; Frey, H. *Chemistry--A European Journal* **2000**, *6*, 2499-2506.

(20) Fréchet, J. M. J.; Henmi, M.; Gitsov, I.; Aoshima, S.; Leduc, M. R.; Grubbs, R. B. *Science* **1995**, *269*, 1080.

(21) Baskaran, D. *Macromolecular Chemistry and Physics* **2001**, *202*, 1569-1575.

(22) Simon, P. F. W.; Radke, W.; Müller, A. H. E. *Macromol. Rapid Commun.* **1997**, *18*, 865-873.

(23) Hawker, C. J.; Fréchet, J. M. J.; Grubbs, R. B.; Dao, J. *J. Am. Chem. Soc.* **1995**, *117*, 10763-10764.

(24) Matyjaszewski, K.; Gaynor, S. G.; Kulfan, A.; Podwika, M. *Macromolecules* **1997**, *30*, 5192.

(25) Matyjaszewski, K.; Gaynor, S. G. *Macromolecules* **1997**, *30*, in press.

(26) Mori, H.; Seng, D. C.; Lechner, H.; Zhang, M. F.; Müller, A. H. E. *Macromolecules* **2002**, *35*, 9270-9281.

(27) Mori, H.; Walther, A.; André, X.; Lanzendörfer, M. G.; Müller, A. H. E. *Macromolecules* **2004**, *37*, 2054-2066.

(28) Matyjaszewski, K.; Gaynor, S. G.; Müller, A. H. E. *Macromolecules* **1997**, *30*, 7034-7041.

(29) Mori, H.; Chan Seng, D.; Lechner, H.; Zhang, M.; Müller, A. H. E. *Macromolecules* **2002**, *35*, 9270-9281.

(30) Matyjaszewski, K.; Pyun, J.; Gaynor, S. G. *Macromol. Rapid Commun.* **1998**, *19*, 665-670.

(31) Mori, H.; Böker, A.; Krausch, G.; Müller, A. H. E. *Macromolecules* **2001**, *34*, 6871-6882.

(32) Hong, C. Y.; Pan, C. Y.; Huang, Y.; Xu, Z. D. *Polymer* **2001**, *42*, 6733-6740.

(33) Yan, D.; Müller, A. H. E.; Matyjaszewski, K. *Macromolecules* **1997**, *30*, 7024.

(34) Holter, D.; Frey, H. *Acta Polym.* **1997**, *48*, 298-309.

(35) Wyatt, P. J. *Journal of Chromatography* **1993**, *648*, 27-32.

(36) Wyatt, P. J. *Anal. Chim. Acta* **1993**, *272*, 1.

(37) Benoît, H.; Grubisic, Z.; Rempp, P.; Decker, D.; Zilliox, J. G. *J. Chem. Phys.* **1966**, *63*, 1507.

(38) Burchard, W. *Adv. Polym. Sci.* **1999**, *143*, 113-194.

(39) Ishizu, K.; Shibuya, T.; Mori, A. *Polymer International* **2002**, *51*, 424-428.

(40) Ejaz, M.; Yamamoto, S.; Ohno, K.; Tsujii, Y.; Fukuda, T. *Macromolecules* **1998**, *31*, 5934-5936.

(41) Kim, J. B.; Bruening, M. L.; Baker, G. L. *J Am Chem Soc* **2000**, *122*, 7616-7617.

(42) Huang, W. X.; Kim, J. B.; Bruening, M. L.; Baker, G. L. *Macromolecules* **2002**, *35*, 1175-1179.

(43) Guerrini, M. M.; Charleux, B.; Vairon, J. P. *Macromol Rapid Comm* **2000**, *21*, 669-674.

(44) Jayachandran, K. N.; Takacs-Cox, A.; Brooks, D. E. *Macromolecules* **2002**, *35*, 4247-4257.

(45) Bontempo, D.; Tirelli, N.; Masci, G.; Crescenzi, V.; Hubbell, J. A. *Macromol Rapid Comm* **2002**, *23*, 418-422.

(46) Bontempo, D.; Tirelli, N.; Feldman, K.; Masci, G.; Crescenzi, V.; Hubbell, J. A. *Adv Mater* **2002**, *14*, 1239-+.

(47) von Werne, T. A.; Germack, D. S.; Hagberg, E. C.; Sheares, V. V.; Hawker, C. J.; Carter, K. R. *J Am Chem Soc* **2003**, *125*, 3831-3838.

(48) Leduc, M. R.; Hawker, C. J.; Dao, J.; Frechet, J. M. J. *J Am Chem Soc* **1996**, *118*, 11111-11118.

(49) Heise, A.; Hedrick, J. L.; Frank, C. W.; Miller, R. D. *J Am Chem Soc* **1999**, *121*, 8647-8648.

(50) Inoue, K. *Prog Polym Sci* **2000**, *25*, 453-571.

(51) Beers, K. L.; Gaynor, S. G.; Matyjaszewski, K.; Sheiko, S. S.; Moeller, M. *Macromolecules* **1998**, *31*, 9413-9415.

(52) Chang, J. Y.; Ji, H. J.; Han, M. J.; Rhee, S. B.; Cheong, S.; Yoon, M. *Macromolecules* **1994**, *27*, 1376-1380.

(53) Bug, A. L. R.; Cates, M. E.; Safran, S. A.; Witten, T. A. *J Chem Phys* **1987**, *87*, 1824-1833.

(54) Marra, J.; Hair, M. L. *Colloid Surface* **1989**, *34*, 215-226.

(55) Koutsos, V.; van der Vegte, E. W.; Hadziioannou, G. *Macromolecules* **1999**, *32*, 1233-1236.

(56) Koutsos, V.; vanderVegte, E. W.; Pelletier, E.; Stamouli, A.; Hadziioannou, G. *Macromolecules* **1997**, *30*, 4719-4726.

(57) Devaux, C.; Chapel, J. P.; Beyou, E.; Chaumont, P. *Eur Phys J E* **2002**, *7*, 345-352.

(58) Ejaz, M.; Ohno, K.; Tsujii, Y.; Fukuda, T. *Macromolecules* **2000**, *33*, 2870-2874.

(59) Prucker, O.; Rühe, J. *Macromolecules* **1998**, *31*, 592-601.

(60) Prucker, O.; Rühe, J. *Macromolecules* **1998**, *31*, 602-613.

(61) Prucker, O.; Ruhe, J. *Langmuir* **1998**, *14*, 6893-6898.

(62) Minko, S.; Gafijchuk, G.; Sidorenko, A.; Voronov, S. *Macromolecules* **1999**, *32*, 4525-4531.

(63) Minko, S.; Sidorenko, A.; Stamm, M.; Gafijchuk, G.; Senkovsky, V.; Voronov, S. *Macromolecules* **1999**, *32*, 4532-4538.

(64) Jordan, R.; Ulman, A.; Kang, J. F.; Rafailovich, M. H.; Sokolov, J. *J Am Chem Soc* **1999**, *121*, 1016-1022.

(65) Jordan, R.; Ulman, A. *J Am Chem Soc* **1998**, *120*, 243-247.

(66) Buchmeiser, M. R.; Sinner, F.; Mupa, M.; Wurst, K. *Macromolecules* **2000**, *33*, 32-39.

(67) Ejaz, M.; Tsujii, Y.; Fukuda, T. *Polymer* **2001**, *42*, 6811-6815.

(68) Marutani, E.; Yamamoto, S.; Ninjbadgar, T.; Tsujii, Y.; Fukuda, T.; Takano, M. *Polymer* **2004**, *45*, 2231-2235.

(69) Voit, B. *J Polym Sci Pol Chem* **2000**, *38*, 2505-2525.

(70) Tully, D. C.; Frechet, J. M. J. *Chem Commun* **2001**, 1229-1239.

(71) Hierlemann, A.; Campbell, J. K.; Baker, L. A.; Crooks, R. M.; Ricco, A. J. *J Am Chem Soc* **1998**, *120*, 5323-5324.

(72) Li, J.; Piehler, L. T.; Qin, D.; Baker, J. R.; Tomalia, D. A.; Meier, D. J. *Langmuir* **2000**, *16*, 5613-5616.

(73) Nakayama, Y.; Sudo, M.; Uchida, K.; Matsuda, T. *Langmuir* **2002**, *18*, 2601-2606.

(74) Zhou, Y. F.; Bruening, M. L.; Bergbreiter, D. E.; Crooks, R. M.; Wells, M. *J Am Chem Soc* **1996**, *118*, 3773-3774.

(75) Mori, H.; Müller, A. H. E. *Top Curr Chem* **2003**, *228*, 1-37.

(76) Franchina, J. G.; Lackowski, W. M.; Dermody, D. L.; Crooks, R. M.; Bergbreiter, D. E.; Sirkar, K.; Russell, R. J.; Pishko, M. V. *Anal Chem* **1999**, *71*, 3133-3139.

(77) Lackowski, W. M.; Ghosh, P.; Crooks, R. M. *J Am Chem Soc* **1999**, *121*, 1419-1420.

(78) Aoki, A.; Ghosh, P.; Crooks, R. M. *Langmuir* **1999**, *15*, 7418-7421.

(79) Joanny, J. F. *Langmuir* **1992**, *8*, 989-995.

(80) Milner, S. T. *Science* **1991**, *251*, 905-914.

(81) Amiji, M.; Park, K. *J Biomat Sci-Polym E* **1993**, *4*, 217-234.

(82) Tsukahara, Y.; Mizuno, K.; Segawa, A.; Yamashita, Y. *Macromolecules* **1989**, *22*, 1546-1552.

(83) Tsukahara, Y.; Tsutsumi, K.; Yamashita, Y.; Shimada, S. *Macromolecules* **1990**, *23*, 5201-5208.

(84) Wintermantel, M.; Gerle, M.; Fischer, K.; Schmidt, M.; Wataoka, I.; Urakawa, H.; Kajiwara, K.; Tsukahara, Y. *Macromolecules* **1996**, *29*, 978-983.

(85) Ryu, S. W.; Hirao, A. *Macromolecules* **2000**, *33*, 4765-4771.

(86) Beers, K. L.; Gaynor, S. G.; Matyjaszewski, K.; Sheiko, S. S.; Möller, M. *Macromolecules* **1998**, *31*, 9413-9415.

(87) Börner, H. G.; Beers, K.; Matyjaszewski, K.; Sheiko, S. S.; Möller, M. *Macromolecules* **2001**, *34*, 4375-4383.

(88) Tsukahara, Y.; Inoue, J.; Ohta, Y.; Kohjiya, S.; Okamoto, Y. *Polym. J* **1994**, *26*, 1013-1018.

(89) Feast, W. J.; Gibson, V. C.; Johnson, A. F.; Khosravi, E.; Mohsin, M. A. *Polymer* **1994**, *35*, 3542-3548.

(90) Wintermantel, M.; Schmidt, M. *Makromol. Chem., Rapid Commun.* **1994**, *15*, 279.

(91) Kratky, O.; Porod, G. *Rec. trav. chim.* **1949**, *68*, 1106-1122.

(92) Terao, K.; Takeo, Y.; Tazaki, M.; Nakamura, Y.; Norisuye, T. *Polymer Journal* **1999**, *31*, 193-198.

(93) Terao, K.; Nakamura, Y.; Norisuye, T. *Macromolecules* **1999**, *32*, 711-716.

(94) Wataoka, I.; Urakawa, H.; Kajiwara, K.; Schmidt, M.; Wintermantel, M. *Polymer International* **1997**, *44*, 365-370.

(95) Zhang, M.; Drechsler, M.; Müller, A. H. E. *Chemistry of Materials* **2004**, *16*, 537-543.

(96) Zhang, M.; Mueller, A. H. E. *Journal of Polymer Science, Part A: Polymer Chemistry* **2005**, *43*, 3461-3481.

(97) Simms, J. A.; Spinelli, H. J. *In Macromolecular Design of Polymeric Materials*; Hatada, K., Kitayama, T., Vogl, O., Eds.; Marcel Dekker: New York, 1997.

(98) Morton, M.; Helminiak, T. E.; Gadkary, S. D.; Bueche, F. J. *J Polym. Sci.* **1962**, *57*, 471.

(99) Wang, J.-S.; Greszta, D.; Matyjaszewski, K. *Polym. Mater. Sci. Eng.* **1995**, *73*, 416-417.

(100) Kennedy, J. P.; Jacob, S. *Accounts Chem Res* **1998**, *31*, 835-841.

(101) Risse, W.; Wheeler, D. R.; Cannizzo, L. F.; Grubbs, R. H. *Macromolecules* **1989**, *22*, 3205-3210.

(102) Simms, J. A. *Rubber Chemistry and Technology* **1991**, *64*, 139-151.

(103) Xia, J.; Zhang, X.; Matyjaszewski, K. *Macromolecules* **1999**, *32*, 4482-4484.

(104) Haddleton, D. M.; Edmonds, R.; Heming, A. M.; Kelly, E. J.; Kukulj, D. *New J Chem* **1999**, *23*, 477-479.

(105) Plamper, F.; Becker, H.; Lanzendörfer, M.; Patel, M.; Wittemann, A.; Ballauff, M.; Müller, A. H. E. *Macromol. Chem. Phys.,* **2005**, *206*, 1813-1825.

(106) Stenzel-Rosenbaum, M. H.; Davis, T. P.; Chen, V. K.; Fane, A. G. *Macromolecules* **2001**, *34*, 5433-5438.

(107) Pyun, J.; Matyjaszewski, K. *Macromolecules* **2000**, *33*, 217-220.

(108) Costa, R. O. R.; Vasconcelos, W. L.; Tamaki, R.; Laine, R. M. *Macromolecules* **2001**, *34*, 5398-5407.

(109) Roovers, J.; Zhou, L. L.; Toporowski, P. M.; Vanderzwan, M.; Iatrou, H.; Hadjichristidis, N. *Macromolecules* **1993**, *26*, 4324-4331.

(110) Held, D.; Müller, A. H. E. *Macromol. Symp.* **2000**, *157*, 225-237.

(111) Daoud, M.; Cotton, J. P. *Journal de Physique* **1982**, *43*, 531.

(112) Zimm, B. H.; Stockmayer, W. H. *J. Chem. Phys.* **1949**, *17*, 1301.

(113) Zimm, B. H.; Kilb, R. W. *J. Polym. Sci.* **1959**, *37*, 19.

2. Overview of thesis – Results

This thesis includes five publications which are presented in Chapters 3 to 7.

First, the sugar-carrying acrylate monomer, 3-*O*-acryloyl-1,2:5,6-di-*O*-isopropylidene-α-D-glucofuranose (AIGlc), was synthesized. It was then used to obtain linear and branched poly(AIGlc)s via atom transfer radical polymerization (ATRP), which were then extensively characterized to understand their solution properties. (Chapter 3)

The sugar-carrying methacrylate monomer, 3-*O*-methacryloyl-1,2:5,6-di-*O*-isopropylidene-α-D-glucofuranose (MAIGlc), was synthesized and thereafter utilized for the preparation of linear and branched poly(MAIGlc)s using ATRP. The Degrees of branching (DB) of the branched polymers were also evaluated indicating the formation of branched architectures. These linear and branched polymers were then converted to water-soluble glycopolymers. (Chapter 4)

Then the chemistry of self-condensing vinyl copolymerization (SCVCP) was extended to the surfaces of the silicon wafers. Branched polymer brushes grafted from the surface of silicon wafers were synthesized using SCVCP via ATRP of glycomethacrylate monomer MAIGlc. A Linear polymer brush was also obtained and its characteristic morphology as well as chemical composition was compared to those of the branched copolymer brushes. (Chapter 5)

Then, the synthesis of glycopolymers of different topologies was investigated. The synthesis and characterization of glycocylindrical brushes or "sugar sticks" using MAIGlc as monomer and poly(2-(2-bromoisobutyryloxy)ethyl methacrylate) as polyinitiator using "grafting from" approach via ATRP appeared to be very promising, as it involved the grafting of a bulky sugar-carrying monomer and its impact on the morphology of the resulting cylindrical brushes. (Chapter 6)

Finally, glycomethacrylate stars of ca. 25 arms were synthesized using a silsesquioxane nanoparticle-based macroinitiator and MAIGlc as monomer. The solution properties of the resulting stars and morphology were investigated extensively. The efficiency of the initiation sites were determined by basic solvolysis and thoroughly characterized. (Chapter 7)

In the following, a summary of the main results is presented.

2.1. Linear and branched glycoacrylates

The synthesis of the sugar-carrying acrylate monomer, 3-*O*-acryloyl-1,2:5,6-di-*O*-isopropylidene-α-D-glucofuranose (AIGlc), was conducted according to the method reported by Fukuda et al[1] and Ouchi et al[2] with slight modifications. In this study, we used CuBr/pentamethyldiethylenetriamine (PMDETA) catalyst system via ATRP to prepare well-defined and mondisperse linear poly(AIGlc)s. For an ideal self-condensing vinyl copolymerization (SCVCP) process for the synthesis of highly branched glycopolymers, living polymerization systems are required to avoid crosslinking reactions and gelation due to chain transfer or recombination reactions.[3-6] Hence the important step was to find suitable conditions where both homoplymerization of AIGlc and homo-SCVP of the inimer can proceed in controlled/"living" fashion.

The homopolymerization of AIGlc was conducted under various conditions, aiming at increasing the polymerization rate as well as understanding the effects of solvent and temperature using ethyl 2-bromo-2-isobutyrate as initiator and CuBr/PMDETA catalyst system. The polymerization in ethyl acetate at 80 ºC led to increase of the reaction rate, but gave a bimodal distribution curve, as shown in Figure 1a. The polymerization in anisole at 80 ºC and 100 ºC also gave polymers having bimodal distribution (Figure 1b). This could be due to recombination occuring at higher temperatures. Hence, CuBr/PMDETA system at 60 ºC in ethyl acetate (50 wt% to AIGlc) was found to be a suitable system for controlled polymerization of AIGlc.

Randomly branched poly(AIGlc)s having different molecular weights and degree of branching were synthesized by self-condensing vinyl copolymerization (SCVCP) of an acrylic AB* inimer, 2-(2-bromopropionyloxy)ethyl acrylate (BPEA)[7,8] with AIGlc via ATRP using CuBr/PMDETA system at 60 ºC in ethyl acetate (50 wt% to AIGlc). The effect of the comonomer ratio, $\gamma = [AIGlc]_0/[BPEA]_0$, on SCVCP of BPEA with AIGlc was investigated with the CuBr/PMDETA system in ethyl acetate. The copolymerization was carried out at 60 ºC at different comonomer ratios, $1 \leq \gamma \leq 10$, keeping the comonomer-to-catalyst ratio at a constant value of $\mu = ([AIGlc]_0 + [BPEA]_0)/[CuBr]_0 = 100$.

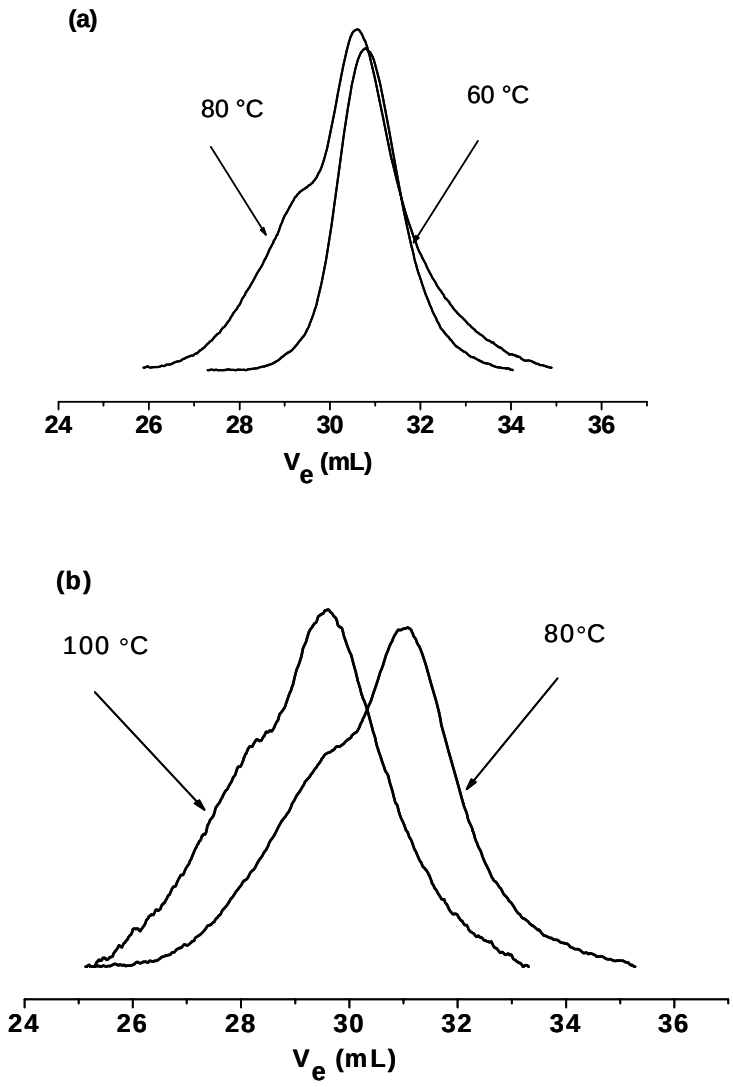

Figure 1. *GPC traces of linear poly(AIGlc)s (a) in ethyl acetate at 60 ºC and 80 ºC ($[M]_0/[I]_0$ = 50), (b) in anisole at 80 ºC ($[M]_0/[I]_0$ = 50) and 100 ºC ($[M]_0/[I]_0$ = 100).*

The linear and branched polymers obtained from AIGlc were evaluated by conventional GPC and GPC/viscosity systems, as the relation between molecular weight and hydrodynamic volume of branched polymers differs substantially from the linear ones. In addition, the bulky side group in poly(AIGlc) may lead to different hydrodynamic volume compared to that obtained by conventional GPC using PtBuA standards.

Mark-Houwink plots and contraction factors,[9] $g' = [\eta]_{branched}/[\eta]_{linear}$, as a function of the molecular weight for representative branched polymers obtained by SCVCP are shown in Figure 2. Relationships between dilute solution viscosity and molecular weight were determined, and the Mark-Houwink exponent typically varies between 0.28 and 0.2,

depending on the degree of branching. In contrast, the exponent is typically in the region of 0.6-0.8 for linear homopolymers[5,10] in a good solvent with a random coil conformation. The Mark-Houwink exponent of the mixture of linear poly(AIGlc)s ($\alpha = 0.52 \pm 0.03$) is lower than that of poly(*tert*-butyl acrylate) ($\alpha = 0.80$), indicating less favorable interaction with the solvent.

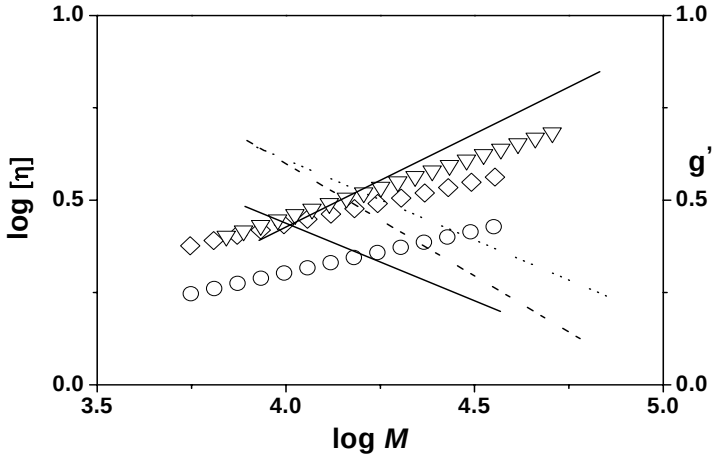

Figure 2. *Mark-Houwink plots for the polymers obtained by copolymerizations of BPEA and AIGlc: γ = 1 (○), 2.5 (◊), 5 (▽). The intrinsic viscosity of a linear poly(AIGlc) (—) is given for comparison. Contraction factors, g′=*$[\eta]_{branched}/[\eta]_{linear}$*, for the polymers obtained by SCVCP of BPEA and AIGlc: γ = 1 (—), 2.5 (- - -), 5.0 (·····).*

The hydrolysis of the isopropylidene groups in the linear and branched poly(AIGlc)s was performed by treating the samples with formic acid.[1] The final product was obtained by freeze-drying from dioxane after the deprotected polymer was dialyzed against water. The complete hydrolysis of linear and branched poly(AIGlc)s were confirmed by ^{1}H NMR, GPC and FT-IR measurements.

2.2. Linear and branched glycomethacrylates

The synthesis of linear and hyperbranched glycoacrylates were successful using the CuBr/PMDETA system under appropriate reaction conditions as discussed earlier. However, the system had several drawbacks, including limited molecular weights and extremely low polymerization rate; for example branched poly(AIGlc) with number-average molecular weight of 13,000 at a comonomer ratio, $\gamma = 10$ was obtained after 120 h. These difficulties

may lead to limitations of the hyperbranched glyocopolymers to be employed for various biological, pharmaceutical, and medical applications. In addition, the purification of the glycoacrylate monomer is quite difficult. These drawbacks motivated us to investigate the corresponding methacrylates.

The sugar-carrying methacrylate monomer, 3-*O*-methacryloyl-1,2:5,6-di-*O*-isopropylidene-α-D-glucofuranose (MAIGlc) was synthesized as reported by Klein et al.[11] In order to find a suitable catalyst system for the synthesis of highly branched glycopolymers by SCVCP via ATRP, we initially investigated the influence of the catalyst system (Cu- and Ni-based catalysts) on the homopolymerization of MAIGlc. The homopolymerization of MAIGlc was conducted using three different catalyst systems with ethyl 2-bromoisobutyrate (EBIB), which has a same initiating group as in a methacrylic inimer (BIEM). The homopolymerization proceeded smoothly with CuBr/hexamethyltriethylenetetramine (HTMTETA) and $(PPh_3)_2NiBr_2$ catalyst systems in solution resulting in linear poly(MAIGlc)s having controlled molecular weights and narrow molecular weight distributions as shown in Figure 3.

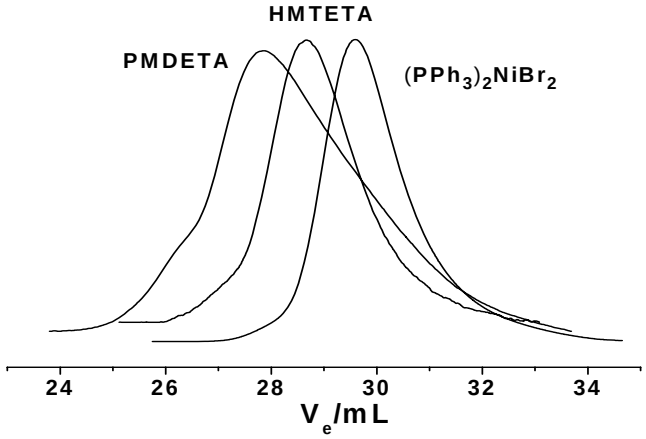

Figure 3. *GPC traces of linear poly(MAIGlc)s prepared with various catalyst systems.*

Water-soluble hyperbranched glycopolymethacrylates were synthesized by self-condensing vinyl copolymerization (SCVCP) of the methacrylic AB* inimer, 2-(2-bromoisobutyryloxy)ethyl methacrylate (BIEM) with MAIGlc using $(PPh_3)_2NiBr_2$ in ethyl acetate (50 wt% to MAIGlc) via atom transfer radical polymerization (ATRP), followed by deprotection of the isopropylidene protecting groups. The linear and hyperbranched poly(MAIGlc)s were then characterized by GPC, GPC/viscosity, ^1H, ^{13}C, and 2D NMR measurements. Figure 4 shows the ^1H NMR spectra of the linear and branched

glycomethacrylates. The characteristic peaks are at 1.2-1.4 ppm (isopropylidene protons), 3.8-5.0 and 5.7-6.0 ppm for the linear poly(MAIGlc). In the case of the copolymers, besides the signal of poly(MAIGlc) segment, the BIEM inimer signals appear at 4.1-4.5 and 1.9-2.0 ppm which correspond to the protons of the ethylene linkage of BIEM and methyl protons adjacent to a bromine atom (A* and M* in the polymer chain end and B* in the 2-bromoisobutyryloxy group), respectively.

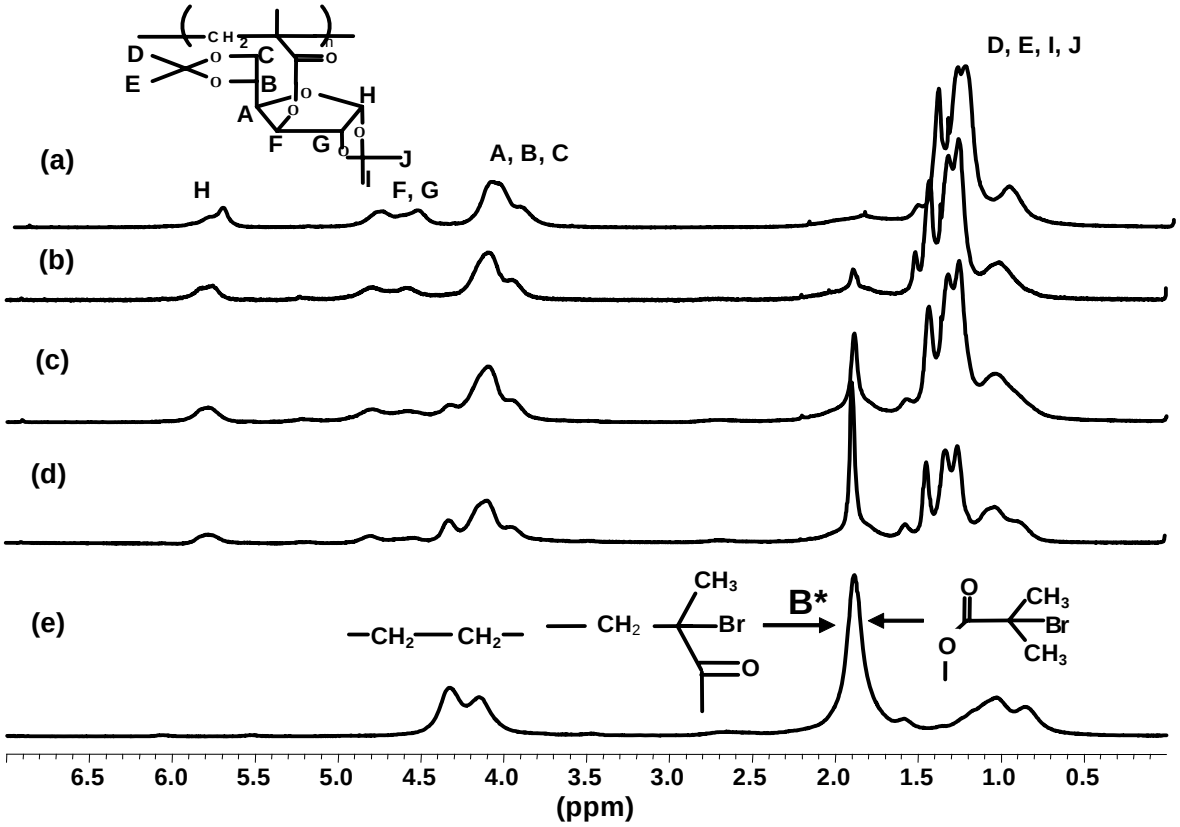

Figure 4. *^{1}H NMR spectra ($CDCl_3$) of the linear (a) and branched poly(MAIGc): γ = 10 (b), 2.5 (c), 1.0 (d), and poly(BIEM) (e).*

The bulky isopropylidene-protected sugar moiety in MAIGlc had no significant influence on the polymerization rate as in the case of AIGlc, and both the homopolymerization and SCVCP proceeded smoothly within reasonable polymerization time. The water-soluble linear and branched poly(MAGlc)s obtained after deprotection can be employed as effective tools for various biological and medicinal applications.

2.3. Surface-grafted branched glycomethacrylates

The concept of SCVCP in solution was then extended to modify the surfaces of the silicon wafers by using the "grafting from" approach to prepare surface-grafted hyperbranched

glycopolymers. Hyperbranched glycopolymers were grafted from a silicon wafer consisting of a covalently attached initiator layer of α-bromoester fragments by using SCVCP of the methacrylic AB* inimer, BIEM and a sugar-carrying methacrylate monomer, MAIGlc via atom transfer radical polymerization (ATRP). A linear poly(MAIGlc) brush was also synthesized in the presence of a sacrificial initiator in order to compare its morphology, thickness and composition with branched ones.

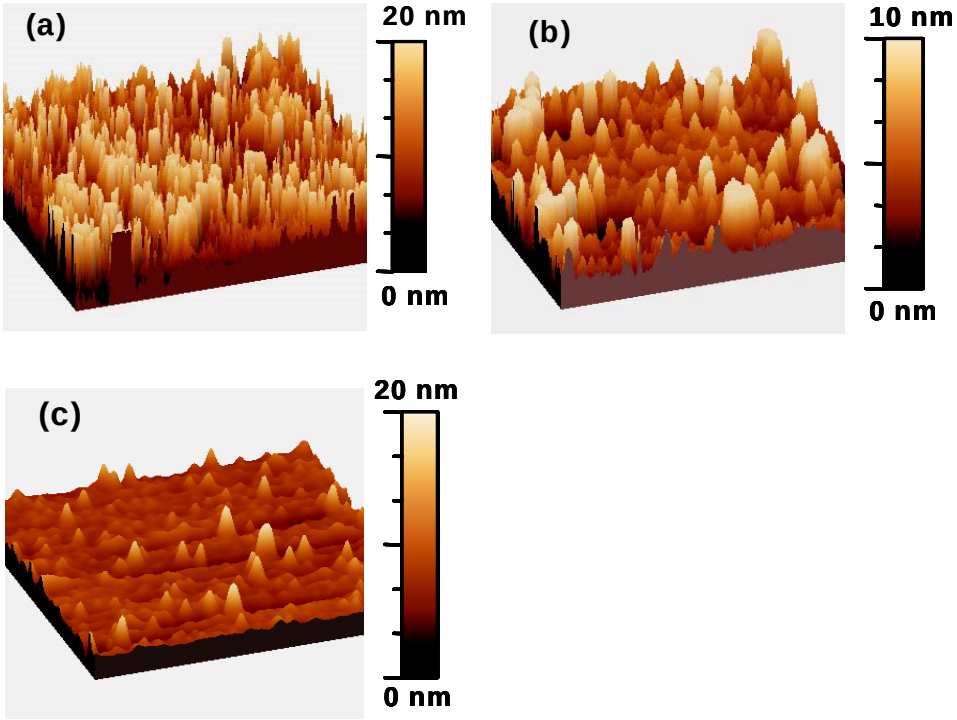

Figure 5. *Three-dimensional height images of the grafted polymers obtained from (a) SCVCP of BIEM and MAIGlc at* $\gamma = [MAIGlc]_0:[BIEM]_0 = 1$*, (b) 10, and (c) homopolymerization of MAIGlc. The X, Y scale is 5 μm.*

It was found that the thickness and roughness of the resulting surfaces depend on the catalyst amount and the comonomer ratio, $\gamma = [MAIGlc]_0/[BIEM]_0$. Figure 5 shows the scanning force microscopy (SFM) images of the brushes obtained at two different comonomer ratios, γ and of the linear polymer brush, respectively. The mean thickness and roughness of the resulting polymer films after Soxhlet extraction decrease with increasing comonomer ratio, γ. In the case of branched copolymer surfaces, the protrusions are irregularly distributed whereas, the linear polymer brush has a relatively smooth and homogeneous surface (Figure 5c). The significant difference in Br content between linear and branched polymers brushes was observed by X-ray photoelectron spectroscopy (XPS) which demonstrates the feasibility to control and modify the surface chemical functionality.

Deprotection of the isopropylidene groups of the branched and linear polymer brushes resulted in hydrophilic surfaces as investigated by contact angle measurements. The quantitative deprotection was also confirmed by diffuse-reflectance infrared spectroscopy (DRIFT-IR) and XPS. Such surfaces can be further modified and employed for understanding carbohydrate-protein interactions and as models for understanding nature ´s complicated multivalent processes.

2.4. Glycocylindrical brushes ("sugar sticks")

The synthesis of glycopolymers of different architectures was then focussed. The sugar-carrying methacrylate monomer, MAIGlc was used to synthesize glycocylindrical brushes or "molecular sugar sticks". The cylindrical brushes of different backbone lengths were obtained by a "grafting from" approach of the polyinitiator poly(2-(2-bromoisobutyryloxy)ethyl methacrylate), (PBIEM), where the precursor, poly(2-hydroxyethyl methacrylate), (PHEMA), was made via ATRP[12,13] as well as anionic polymerization.[13] In this work, we chose CuBr/HMTETA for the synthesis of glycocylindrical brushes. The formation of well-defined brushes with narrow length distribution was confirmed by GPC-MALS and ^{1}H NMR.

The initiating efficency of the initiating sites of the polyinitiator, PBIEM were determined to be in the range of $0.23 < f < 0.38$ by cleaving the side chains from the backbone via base-catalyzed transesterification in methanol.[14] In spite of the rather low initiating efficiency, the glycocylindrical brushes show the characteristic worm-like structure, as visualized by SFM shown in Figure 6. The number-average and weight-average lengths of 160 cylinders are L_n = 138 nm and L_w = 147 nm, respectively, with a polydispersity L_w/L_n = 1.06 which agrees well with the polydispersity of the backbone (M_w/M_n = 1.08). The number-average brush length of

138 nm corresponds to a length per main chain monomer unit of 0.09 nm, which is much smaller than the maximum value of 0.25 nm, indicating that the main chain is not completely stretched out but locally coiled. This could be due to the rather low grafting efficency (f = 23 %) of the brush.

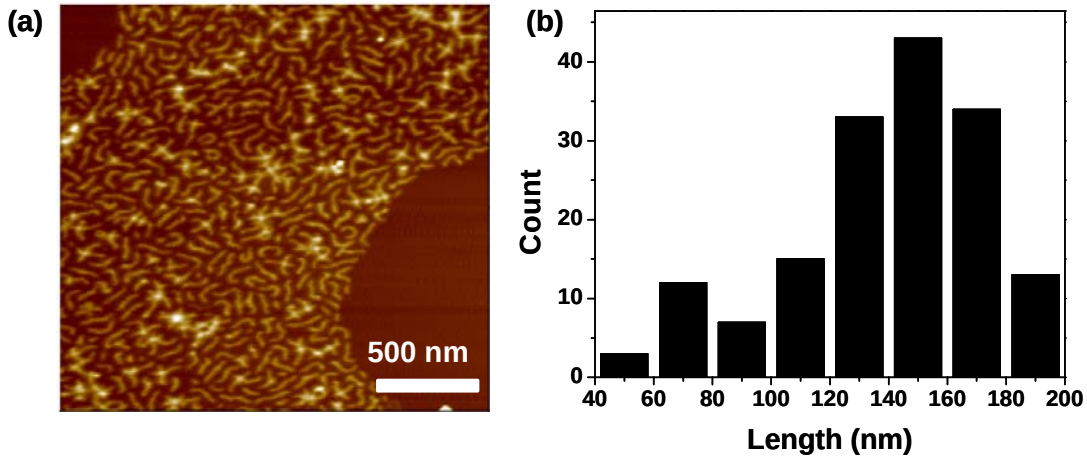

Figure 6. *(a) SFM Tapping Mode height image of the long glycocylindrical brush, dip-coated from dilute THF solution on mica, (z-range: 15 nm) and (b) histogram of the lengths from 160 molecules.*

The deprotection of the isopropylidene groups of the PMAIGlc side chains resulted in water-soluble glycocylindrical brushes. The structure of the deprotected glycocylindrical brush in aqueous solution was characterized using cryo-TEM. This tool allows to directly image the original shape and size of the polymers in solution, since the sample is vitrified before the measurement (Figure 7). The cryo-TEM image of the deprotected brush shows worm-like cylinders as before hydrolysis indicating the structure of the brushes are retained during the process of hydrolysis.

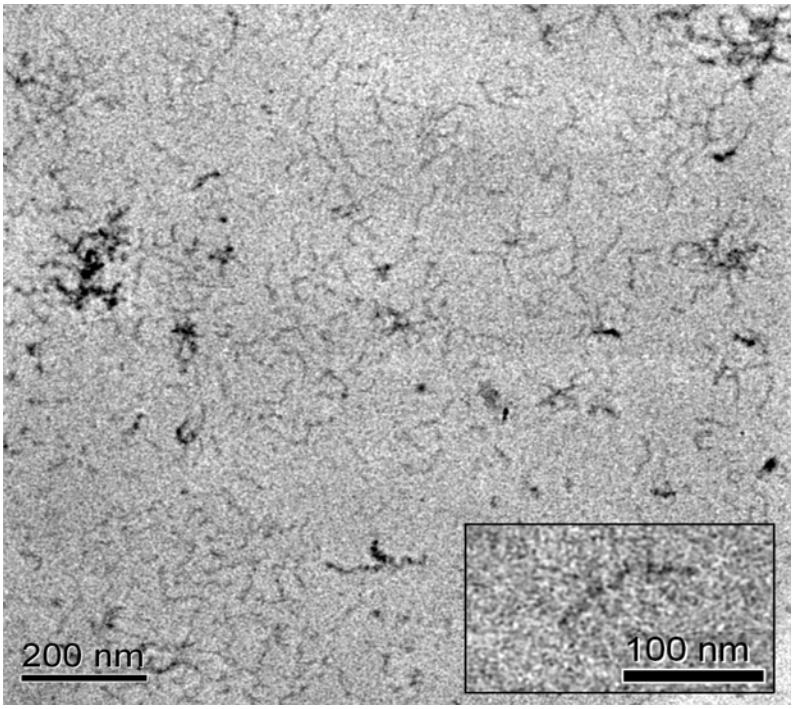

Figure 7. *Cryo-TEM image of the deprotected brush.*

2.5. Glycomethacrylate hybrid stars

A silsesquioxane nanoparticle-based macroinitiator of ca. 58 functions was used to synthesize glycomethacrylate stars with approximately 25 arms of different lengths using the sugar-carrying methacrylate monomer MAIGlc via atom transfer radical polymerization (ATRP). Well-defined glycostars could be synthesized by restricting the polymerization to low conversion. GPC coupled with an online viscometer (GPC/viscosity) and GPC with a multi-angle light scattering detector (GPC-MALS) were used to determine the absolute molecular weights and solution properties of the glycostars. The molecular weights obtained by GPC/viscosity and GPC-MALS are found to be higher than those obtained by conventional GPC using PtBMA calibration indicating their compact nature.

The morphology of these hybrid glycostars was characterized by scanning force microscopy (SFM). Figure 8 displays an SFM image of the glycostar. Spherical isolated particles are clearly seen indicating the uniform and well-defined formation of hybrid stars. The diameter of the particle marked by a rectangle in Figure 8a is 46 nm (non-corrected for the tip radius) and the height is ~ 5 nm which is somewhat higher than the diameter of the starting silsesquioxane nanoparticles (~ 3 nm).

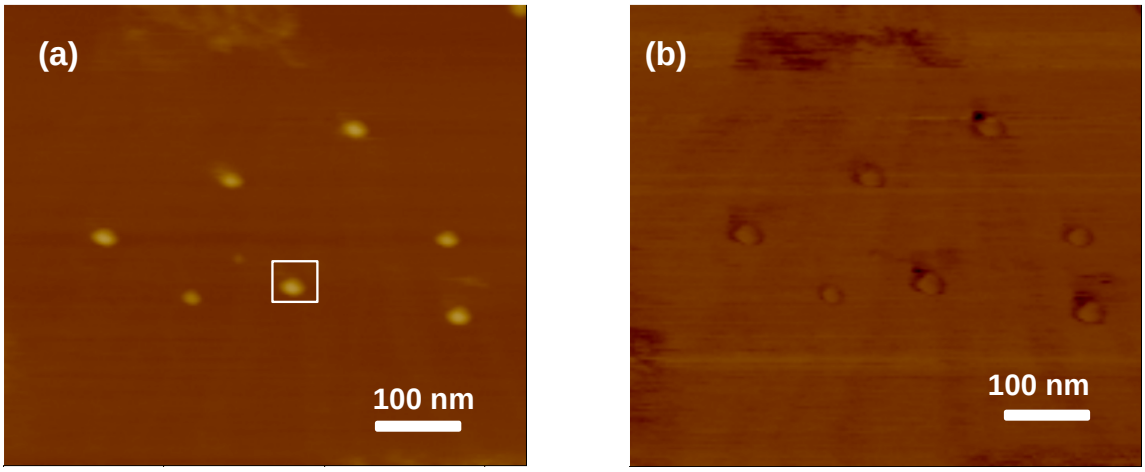

Figure 8. *SFM Tapping Mode images of glycomethacrylate stars, spin-coated from dilute THF solution on to mica, (a) height image (z-range: 20 nm), (b) phase image (range: 45°).*

Analysis of the arms cleaved by basic solvolysis indicated the initiation site efficiency of the silsesquioxane-based macroinitiator is about 44 % which could be due to bulkiness of the monomer, MAIGlc as well as the influence of the structure of the macroinitiator, some functions possibly being less accessible than others. The deprotection of the isopropylidene groups resulted in water-soluble glycomethacrylate hybrid stars. The deprotected glycostars also have a spherical structure in water solution as investigated by different methods, indicating the successful synthesis of water-soluble glycopolymer hybrid stars of well-defined structure and morphology.

2.6. Individual contributions to joint publications

The results presented in this thesis were obtained in collaboration with others, and published as indicated below. In the following, the contributions of all the coauthors to the different publications are specified. The asterisk denotes the corresponding author.

Chapter 3

This work is published in *Macromolecules* **2005**, 38, p. 9, under the title **"Synthesis of Hyperbranched Glycopolymers via Self-Condensing Atom Transfer Radical Copolymerization of Sugar-Carrying Acrylate"** S. Muthukrishnan, G. Jutz, X. André, H. Mori and Axel H. E. Müller*.

I have performed all the experiments presented in this work and the publication was written by me.

G. Jutz was involved in measuring MALDI-TOF spectrometry.

X. André was involved in GPC/viscosity measurements.

I was introduced to ATRP technique by H. Mori. I have profited from scientific discussions with H. Mori and Axel H. E. Müller.

Chapter 4

This work is published in *Macromolecules* **2005**, 38, p. 3108, under the title **"Synthesis and Characterization of Methacrylate-Type Hyperbranched Glycopolymers via Self-Condensing Atom Transfer Radical Copolymerization"** S. Muthukrishnan, H. Mori and Axel H. E. Müller*.

I have done all the experiments and characterizations presented in this work. The publication was written by me.

H. Mori and Axel H. E. Müller were involved in the scientific discussions related to this work.

Chapter 5

This work is submitted to *Macromolecules* under the title **"Synthesis and Characterization of Surface-Grafted Hyperbranched Glycomethacrylates"** S. Muthukrishnan, Dominik P. Erhard, H. Mori and Axel H.E. Müller*.

Dominik P. Erhard performed some of the experiments for this work within the scope of his Hauptpraktikum under my guidance. The publication was written by me.

H. Mori and Axel H.E. Müller were involved in scientific discussions, comments and suggestions.

Chapter 6

This work is published in *Macromolecules* **2005**, 38, p. 7926, under the title **"Molecular Sugar Sticks: Cylindrical Glycopolymer Brushes"** S. Muthukrishnan, M. Zhang, M. Burkhardt, M. Drechsler, H. Mori and Axel H. E. Müller*.

I have performed all the experiments for this work and the publication was written by me.

M. Zhang (presently at University of Massachusetts, Amherst (USA)) and M. Burkhardt contributed to the discussions regarding DLS data.

M. Drechsler performed the measurement of cryo-TEM.

H. Mori and Axel H. E. Müller contributed to the scientific discussions and comments.

Chapter 7

This work is published in *Macromolecules*, **2005,** 38, p. 10631, under the title **"Synthesis and Characterization of Glycomethacrylate Hybrid Stars from Silsesquioxane Nanoparticles"** S. Muthukrishnan, F. Plamper, H. Mori and Axel H. E. Müller*.

I have performed all the experiments for this work and the publication was written by me.

F. Plamper was involved in the synthesis and characterization of the silsesquioxane-based macroinitiator.

H. Mori and Axel H. E. were involved in corrections of this manuscript and scientific discussions.

2.7. References

(1) Ohno, K.; Izu, Y.; Yamamoto, S.; Miyamoto, T.; Fukuda, T. *Macromolecular Chemistry and Physics* **1999**, *200*, 1619-1625.

(2) Ouchi, T.; Jokei, S.; Chikashita, H. *Journal of Heterocyclic Chemistry* **1982**, *19*, 935-936.

(3) Litvinenko, G. I.; Simon, P. F. W.; Müller, A. H. E. *Macromolecules* **1999**, *32*, 2410-2419.

(4) Simon, P. F. W.; Müller, A. H. E. *Macromolecules* **2001**, *34*, 6206-6213.

(5) Mori, H.; Walther, A.; André, X.; Lanzendörfer, M. G.; Müller, A. H. E. *Macromolecules* **2004**, *37*, 2054-2066.

(6) Litvinenko, G. I.; Simon, P. F. W.; Muller, A. H. E. *Macromolecules* **2001**, *34*, 2418-2426.

(7) Matyjaszewski, K.; Gaynor, S. G.; Kulfan, A.; Podwika, M. *Macromolecules* **1997**, *30*, 5192-5194.

(8) Mori, H.; Böker, A.; Krausch, G.; Müller, A. H. E. *Macromolecules* **2001**, *34*, 6871-6882.

(9) Burchard, W. *Adv. Polym. Sci.* **1999**, *143*, 113-194.

(10) Mori, H.; Seng, D. C.; Lechner, H.; Zhang, M. F.; Müller, A. H. E. *Macromolecules* **2002**, *35*, 9270-9281.

(11) Klein, J.; Herzog, D.; Hajibegli, A. *Makromolekulare Chemie-Rapid Communications* **1985**, *6*, 675-678.

(12) Cheng, G.; Böker, A.; Zhang, M.; Krausch, G.; Müller, A. H. E. *Macromolecules* **2001**, *34*, 6883-6888.

(13) Zhang, M.; Breiner, T.; Mori, H.; Müller, A. H. E. *Polymer* **2003**, *44*, 1449-1458.

(14) Neugebauer, D.; Sumerlin, B. S.; Matyjaszewski, K.; Goodhart, B.; Sheiko, S. S. *Polymer* **2004**, *45*, 8173-8179.

3. Synthesis of Hyperbranched Glycopolymers via Self-Condensing Atom Transfer Radical Copolymerization of a Sugar-Carrying Acrylate

Sharmila Muthukrishnan, Günter Jutz, Xavier Andre, Hideharu Mori[§], Axel H. E. Müller[*]

Makromolekulare Chemie II and Bayreuther Zentrum für Kolloide und Grenzflächen, Universität Bayreuth, D-95440 Bayreuth, Germany

[*] To whom correspondence should be addressed. e-mail: *Axel.Mueller@uni-bayreuth.de*, Phone:+49 (921) 55-3399, Fax: +49 (921) 55-3393

[§] Present address; Department of Polymer Science and Engineering, Faculty of Engineering, Yamagata University, 4-3-16, Jonan, Yonezawa, 992-8510, Japan

Published in *Macromolecules* 2005, 38, p. 9.

Abstract: Hyperbranched glycopolymers were synthesized by self-condensing vinyl copolymerization (SCVCP) of an acrylic AB* inimer, 2-(2-bromopropionyloxy)ethyl acrylate (BPEA) with 3-*O*-acryloyl-1,2:5,6-di-*O*-isopropylidene-α-D-glucofuranoside (AIGlc) via atom transfer radical polymerization (ATRP), followed by deprotection of the isopropylidene protecting groups. Homopolymerization of AIGlc with CuBr/pentamethyldiethylenetriamine (PMDETA) catalyst system in solution resulted in linear poly(AIGlc) having controlled molecular weights and narrow molecular weight distribution, which were characterized using GPC, GPC/viscosity and MALDI-TOF mass spectrometry. The catalyst system could be applied for SCVCP to synthesize hyperbranched poly(AIGlc)s, in which the molecular weights, the composition of AIGlc segment, and the branched structures can be adjusted by an appropriate choice of the comonomer ratio, γ. Deprotection of the isopropylidene protecting groups of the branched poly(AIGlc)s resulted in water-soluble glycopolymers with randomly branched architectures.

3.1. Introduction

Synthetic carbohydrate-based polymers are now being used as very important tools to investigate carbohydrate-based interactions.[1,2] Carbohydrates are involved in various biological functions in living systems. For instance, heparin, which is a natural polyanion composed of repeating dissaccharide units, is a first polysaccharide applied in medicine and plays an important role in blood coagulation.[3] Synthetic carbohydrate polymers with biocompatible and biodegradable properties are used in tissue engineering and controlled drug release devices. Many of them are used also as surfactants,[4] and biologically active polymers.[5]

The new era of "glycomimics", which are synthetic complex carbohydrates and carbohydrate-based polymers, are increasingly used for investigating glycopolymer-protein interactions.[6] These glycopolymers are widely investigated for pharmaceutical and medical applications in the treatment of infectious diseases.[7] Glycopolymers generally include natural as well as synthetic carbohydrate-bearing polymers, whereas synthetic polymers containing sugar moieties as pendant groups can be referred in a narrower sense as glycopolymers.[8] There are various types of synthetic sugar-carrying polymers. Linear polymers, comb-shaped polymers, dendrimers and cross-linked hydrogels represent the four major classes.[9] Due to their biocompatibility and hydrophilicity sugar-based hydrogels are used in biomedical engineering as superabsorbents, contact lenses and matrices for drug delivery systems.[10,11]

Highly branched glycopolymers have adopted nature's multivalent approach to their work,[12] and therefore they have been used to understand the multivalent processes. It has been reported that polyvalent saccharide ligands inhibit the protein-carbohydrate interaction providing the best therapeutic strategy for the treatment of myriad human diseases.[13] Silylated glycodendrimers have been tested in bacterial adhesion hemagglutination assays.[14] Dendrimers with covalently attached glycoside residues in the outer layer are well defined glycopolymer models of cell surface multiantennary glycoproteins.[15] The polyvalency inherent in carbohydrate-based polymers, especially in branched polymers, is an important feature, which allows these materials to serve as cell surface mimics to understand and manipulate carbohydrate-protein interactions.

The recent developments in the field of glycoscience, glycotechnology, and the potential applications of glycopolymers have attracted researchers to develop new synthetic routes to design a variety of sugar-containing polymers with controlled architectures and functionalities. Various polymerization techniques have been developed to synthesize sugar-

containing polymers with well-defined structures, which involve cationic polymerization[16], ring-opening polymerization[17], ring-opening metathesis polymerization[18], and free radical polymerization.[19] Although a variety of glycopolymers has been synthesized by conventional free radical polymerization of vinyl monomers carrying sugar residues, it was difficult to control molecular weights and architecture. Controlled/"living" radical polymerization has allowed well-defined and controlled synthesis of glycopolymers by a very facile and simple approach. For example, Fukuda et al. has reported the synthesis of styryl and methacryloyl monomers having a saccharide residue by using nitroxide-mediated polymerization[20] and atom transfer radical polymerization (ATRP).[21] They also have reported the synthesis of glycopolymers by nitroxide-mediated polymerization of a sugar-carrying acrylate, but the system gave polymers with limited conversion.[22] Gotz et al. have reported the synthesis of new lipo-glycopolymer amphiphiles, which were prepared by nitroxide-mediated polymerization with a dioctadecyl-substituted nitroxide initiator and 1,2,5,6-di(isopropylidene)-D-Glucose-2-propenoate as monomer.[23] ATRP has been used for the synthesis of many sugar-carrying block[24,25] and graft polymers.[26] Very recently, Narain and Armes reported the first ATRP of unprotected sugar-based monomers.[27,28]

This paper reports the synthesis of randomly branched glycopolymers using self-condensing vinyl copolymerization (SCVCP) of an acrylic AB* inimer, 2-(2-bromopropionyloxy)ethyl acrylate (BPEA) with 3-*O*-acryloyl-1,2:5,6-di-*O*-isopropylidene-α-D-glucofuranoside (AIGlc) via ATRP. The synthetic route to highly branched glycopolymers is given in Scheme 1. The curved lines represent polymer chains. A*, B*, and M* are active units, whereas a, b, and m are reacted ones. A is an acryloyl group. M and m stand for AIGlc units at the chain end and in the linear segment, respectively. SCVCP of AB* inimers with conventional monomers is a facile approach to obtain functional branched polymers because different types of functional groups can be incorporated into a polymer, depending on the chemical nature of the comonomer.[29-32] In this study, an isopropylidene-protected sugar-carrying acrylate, AIGlc, was selected as a comonomer for the synthesis of water-soluble highly branched glycopolymers. For an ideal SCVCP process, living polymerization systems are required to avoid crosslinking reactions and gelation due to chain transfer or recombination reactions. Hence the important step is to find suitable conditions where both homoplymerization of AIGlc and homo-SCVP of the inimer can proceed in controlled/"living" fashion. In general, Cu-based ATRP was employed for SCV(C)P of acrylate-type inimers having an acrylate (A) and a bromoester group (B*), capable to initiate ATRP.[33] In this study, we used the CuBr/pentamethyldiethylenetriamine (PMDETA) catalyst system to prepare well-defined and

monodisperse linear poly(AIGlc). Effects of temperature and solvents were investigated in terms of the polydispersity and polymerization rate. Randomly branched poly(AIGlc)s having different molecular weights and degree of branching were synthesized by SCVCP with different comonomer ratios, γ, via ATRP.

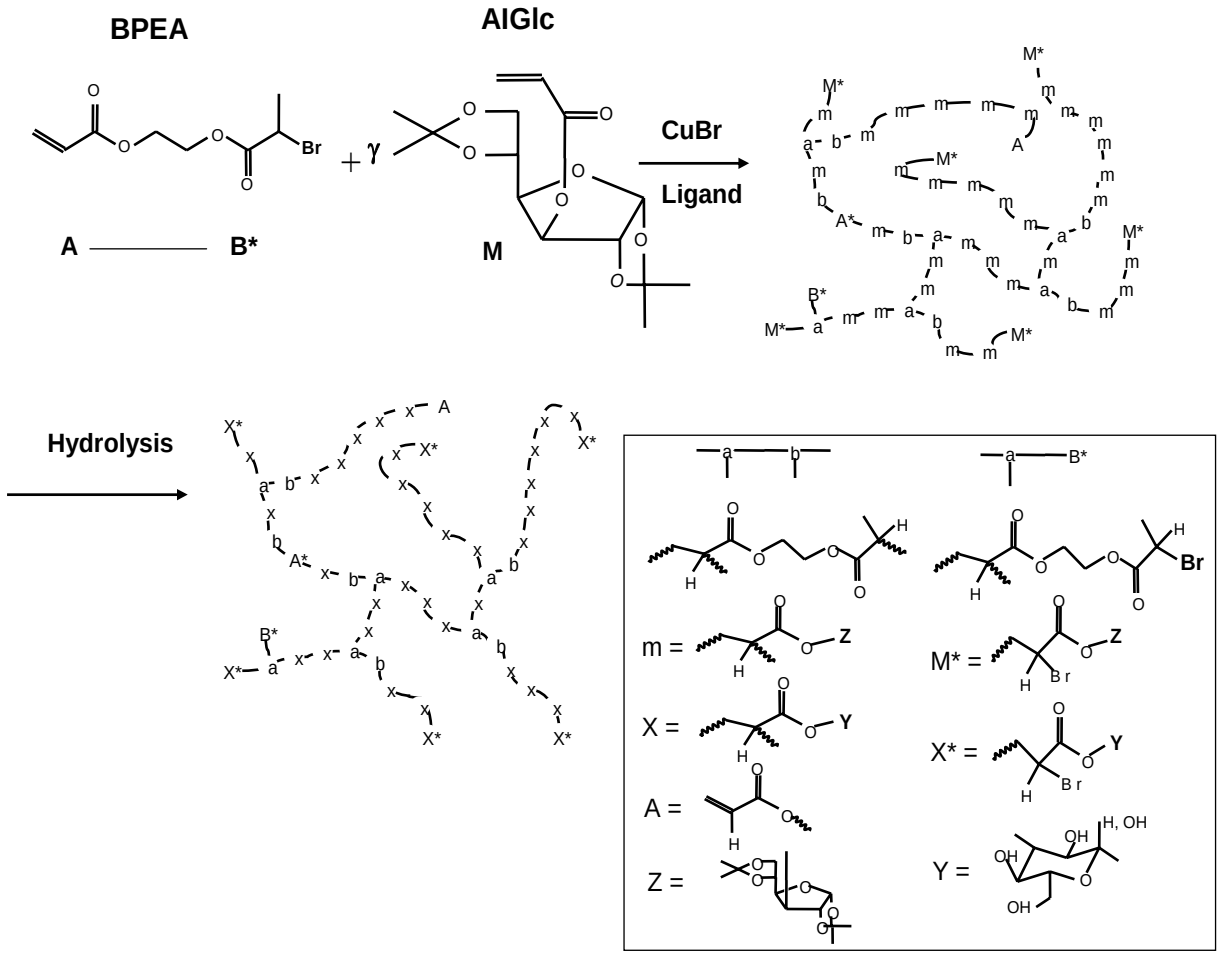

Scheme 1. *General route to branched glycopolymers via self-condensing vinyl copolymerization, followed by deprotection of isopropylidene protecting groups.*

3.2. Experimental Section

Materials. CuBr (95%, Aldrich) was purified by stirring overnight in acetic acid. After filtration, it was washed with ethanol, ether, and then dried. N,N,N',N",N"-pentamethyldiethylenetriamine (PMDETA, 99 %, Aldrich) and ethyl 2-bromo-2-isobutyrate (98%, Aldrich) were distilled and degassed. Synthesis of an acrylic AB* inimer, 2-(2-bromopropionyloxy)ethyl acrylate (BPEA), was conducted by the reaction of 2-bromo-propinoyl bromide with 2-hydroxyethyl acrylate in the presence of pyridine as reported previously.[34,35] The inimer was degassed by three freeze-thaw cycles. Other reagents were commercially obtained and used without further purification.

Synthesis of 3-*O*-Acryloyl-1,2:5,6-di-*O*-isopropylidene-α-D-glucofuranoside (AIGlc). The synthesis of AIGlc was carried out according to the method reported by Fukuda et al[22] and Ouchi et al.[36] with slight modifications. To a solution of 1,2:5,6-di-*O*-isopropylidene-D-glucofuranose (10g, 38.5 mmol) in acetone (50 ml) was added a 5N solution of NaOH (11.55 ml, 57.8 mmol) and then acryloyl chloride (3.4 ml, 38.5 mmol) was added dropwise to the mixture with stirring in an ice bath. After one hour it was allowed to stir at room temperature for 48 h. Then the reaction mixture was diluted with 100 ml of water and extracted with n-hexane. The aqueous layer was washed two times with hexane and the combined extract was washed three times with water to remove the salts. It was then dried over anhydrous sodium sulfate. The drying agent was filtered off and the filtrate was evaporated under reduced pressure to give a crude syrup. The crude syrup was distilled under a very high vacuum (90 ° C, 1x 10^{-2} mbar) to give white solid, 5.0 g (41%). ^{1}H NMR ($CDCl_3$): δ = 1.25-1.55 (m., 12H, isopropylidene units), 4.05, 4.25, 5.29, 5.87 (7H, sugar moiety), 5.85-6.50 (3H, three vinyl protons). ^{13}C NMR ($CDCl_3$): δ = 165.05 (C=O), 131.6 (CH_2=), 128.09 (CH=), 27.18, 27.07, 26.56, 25.59 (CH_3 in isopropylidene groups).

Atom Transfer Radical Polymerization of AIGlc. All polymerizations were carried out in a round bottom flask sealed with a plastic cap. A representative example is as follows: Ethyl 2-bromo isobutyrate (0.0254 g, 0.127 mmol) was added to a round bottom flask containing CuBr(I) (0.0178 g, 0.127 mmol), PMDETA (0.0219 g, 0.127 mmol) and AIGlc (0.80 g, 2.54 mmol) in ethyl acetate (0.80 g, 50 wt% to AIGlc). As soon as the initiator was added to the mixture, the colour changed into green, indicating the start of the polymerization. The flask was placed in an oil bath at 60º C for 48 h. Conversion of the double bonds, as detected by ^{1}H NMR, was 88 %. The content in the flask was viscous which was dissolved in

THF. The solution was passed through a silica column, and the polymer was precipitated from THF into hexane. Finally the product was freeze-dried from dioxane and dried under vacuum at room temperature. The polymer had M_n = 5,900 and M_w/M_n = 1.09 according to conventional GPC, and M_n = 6,600 and M_n/M_w = 1.13 according to GPC/visosity using universal calibration, and M_n = 5,400 and M_w/M_n = 1.09 according to MALDI-TOF MS measurement.

A mixture of linear poly(AIGlc)s with various molecular weights was used as comparison in the solution viscosity studies. Molecular weight for this sample: M_n = 13,800 and M_w/M_n = 1.64 (determined by GPC/viscosity using universal calibration) as shown in Figure S-1 (see supporting information).

Self-Condensing Vinyl Copolymerization. A representative example for the copolymerization ($\gamma = [AIGlc]_0/[BPEA]_0 = 1$), is as follows: BPEA (0.3995 g, 1.592 mmol) was added to a round bottom flask containg CuBr(I) (0.00478 g, 0.0318 mmol), PMDETA (0.00549 g, 0.0318 mmol), AIGlc (0.5 g, 1.592 mmol), and ethyl acetate (0.5 g , 50 wt% to AIGlc). As soon as BPEA was added to the mixture, the colour changed into green, indicating the start of the polymerization. The flask was placed in an oil bath at 60 º C for 4 h. The mixture was completely solidified after 4 h when the conversion reached a certain level. Conversion of the double bonds, as detected by ^{1}H NMR, was 90 %. After the mixture was dissolved in THF, and was passed through a silica column, the polymer was precipitated from THF into hexane. Then the product was freeze-dried from dioxane and finally dried under vacuum at room temperature to yield a white powder. The polymer had M_n = 7,800 and M_w/M_n = 1.43 according to conventional GPC and M_n = 9,200 and M_w/M_n = 2.84 according to GPC/viscosity using universal calibration. The resulting polymer was soluble in chloroform, THF, and acetone, but insoluble in methanol, hexane, and water.

Deprotection. Transformation of randomly branched poly(AIGlc) into branched poly(3-*O*-acryloyl-α,β-D-glucopyranoside) (AGlc) was achieved under mild acidic condition. The branched poly(AIGlc) (γ = 1, 85 mg) was dissolved in 80 % formic acid (10 ml) and stirred for 48 h at room temperature. Then, 4 ml of water was added and it was stirred for another 3 h. The solution was dialysed using Spectra/Por^R (MWCO: 1000) against millipore water for 2 days. The solution was evaporated under reduced pressure and the resulting polymer was freeze-dried from dioxane, and dried under vacuum. The deprotected hyperbranched polymer (γ = 1) was obtained as white powder in a quantitative yield (75 mg, yield = 88 %), which was insoluble in water, methanol, and acetone and completely soluble in DMSO. The

deprotection was done in a similar way in the case of linear poly(AIGlc), which gave water-soluble glycopolymers.

Characterization. The linear and branched polymers obtained from AIGlc were characterized by conventional GPC and GPC/viscosity using THF as eluent at a flow rate of 1.0 ml/min at room temperature. A conventional THF-phase GPC system was used to obtain apparent molecular weights. GPC system I; column set: 5µm PSS SDV gel, 10^2, 10^3, 10^4, 10^5 Å, 30 cm each; detectors: Waters 410 differential refractometer and Waters photodiode array detector operated at 254 nm. Narrow PtBuA standards (PSS, Mainz) were used for the calibration of the column set I. Molecular weights of the branched polymers were determined by the universal calibration principle[37] using the viscosity module of the PSS-WinGPC scientific V 6.1 software package. Linear PMMA standards (PSS, Mainz) were used to construct the universal calibration curve. GPC system II; column set: 5µ PSS SDV gel, 10^3 Å, 10^5 Å and 10^6 Å, 30cm each; detectors: Shodex RI-71 refractive index detector; Jasco Uvidec-100-III UV detector (λ = 254 nm); Viscotek viscosity detector H 502B. A 1-methyl-2-pyrrolidone (NMP)-phase GPC system was used to obtain apparent molecular weights of the hydrolysed polymers. GPC system III; column set: two PSS GRAM 7µm, 1000 and 100 Å columns thermostated at 70 °C; detectors: Waters 486 UV detector (λ = 270 nm), and Bischoff RI-Detector 8110. 50 µL of the sample diluted in NMP (containing 0.05 M LiBr) were injected at a flow rate of 1 mL/min. Linear PS standards were used for calibration.

MALDI-TOF mass spectrometry was performed on a Bruker Reflex III instrument equipped with a 337 nm N_2 laser in the reflector mode and 20 kV acceleration voltage. 2,5-Dihydroxy benzoic acid (Aldrich, 97%) was used as a matrix. Samples were prepared from THF solution by mixing matrix (20 mg/mL) and polymer (10 mg/mL) in a ratio of 4:1. The number-average molecular weights, of the polymers were determined in the linear mode.

^{1}H and ^{13}C NMR spectra were recorded with a Bruker AC-250. FT-IR spectra were recorded on a Bruker Equinox 55 spectrometer. The elemental analyses were performed by Ilse Beetz Mikroanalytisches Laboratorium (Kulmbach).

3.3. Results and Discussion

Effect of Polymerization Conditions on the Homopolymerization of AIGlc. To find the suitable polymerization conditions for the synthesis of highly branched glycopolymers by SCVCP, we first investigated the effect of polymerization conditions on ATRP of AIGlc. In a previous paper, we have demonstrated that the synthesis of randomly branched polymers by

SCVCP of *tert*-butyl acrylate with BPEA was achieved using CuBr/PMDETA catalyst system.[38] Hence the CuBr/PMDETA catalyst system was employed for ATRP of AIGlc. When AIGlc was polymerized using CuBr/PMDETA with ethyl 2-bromo isobutyrate ($[M]_0/[I]_0 = 20$) at 60 ºC in ethyl acetate, as shown in Table 1, the conversion reached 88 % (as determined by ^{1}H NMR) after 48 h. The number-average molecular weight of poly(AIGlc) as determined by conventional GPC using PtBuA standards was M_n = 5,900, which is almost the same as the theoretical value (M_n = 5,500), and the polydispersity index was M_w/M_n = 1.09. As can be seen later, the linear and branched polymers obtained from AIGlc were evaluated by conventional GPC and GPC/viscosity systems, as the relation between molecular weight and hydrodynamic volume of branched polymers differs substantially from the linear ones. In addition, the bulky side group in poly(AIGlc) may lead to different hydrodynamic volume compared to that of standard PtBuA. In order to clarify these points, further characterization was conducted using GPC/viscosity and MALDI-TOF mass spectrometry (MS). As can be seen in Figure 1, the molecular weights and molecular weight distributions obtained from MALDI-TOF MS (M_n = 5,400 and M_w/M_n = 1.09) and GPC/viscosity (M_n = 6,600 and M_w/M_n = 1.09) are in agreement with those obtained from the conventional GPC using PtBuA standards and with the theoretical values.

Table 1 shows the results of homopolymerization obtained at different monomer to initiator ratios, $[M]_0/[I]_0$. For the cases of the polymerization at $[M]_0/[I]_0$ = 100, a longer polymerization time was required to attain higher conversion (conversion = 84 % for 120 h and 33 % for 48 h). The polymerization mixture was still liquid after 48 h, but it became viscous and the polymerization was stopped after 120 h, whereas almost full conversion was obtained after 72 h in the case of $[M]_0/[I]_0$ = 50. As can be seen in Table 1, the polymerization in ethyl acetate using the CuBr/PMDETA system gave linear poly(AIGlc)s with low narrow polydispersity ($1.05 < M_w/M_n < 1.14$) with predicted molecular weights in the range of $[M]_0/[I]_0 = 20 \sim 100$. These results suggest that the CuBr/PMDETA catalyst at 60 ºC is a suitable system for the controlled polymerization of AIGlc. In all cases, the expected molecular weights and narrow molecular weight distributions could be achieved regardless of $[M]_0/[I]_0$, suggesting that the extremely slow polymerization compared to other type of acrylates is simply due to the steric hindrance by the bulky side group in the sugar-carrying acrylate. A similar tendency was also observed in the nitroxide-mediated polymerization of AIGlc, which resulted in limited conversion (~55 %) and molecular weights (M_n = ~13,000) with relatively low polydispersity ($1.2 < M_w/M_n < 1.6$).[22] On the

other hand, our ATRP system provided polymers with almost full conversion having higher molecular weights (M_n > 2 x 10^4) and narrower molecular weight distributions (M_w/M_n < 1.14).

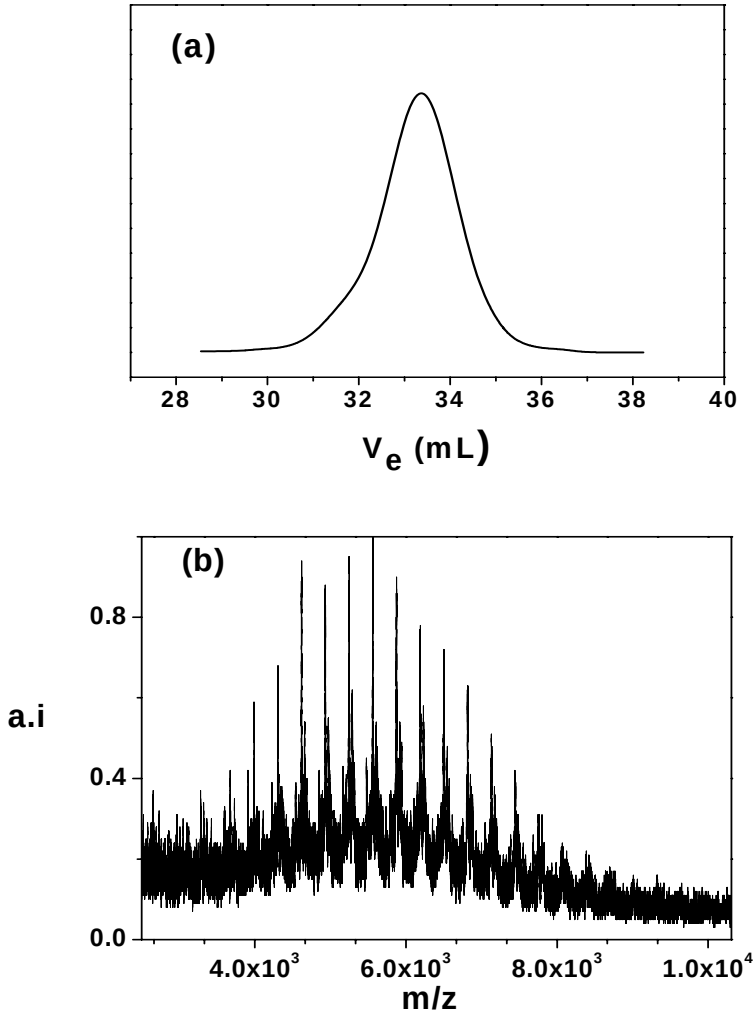

Figure 1. *(a) GPC trace (RI signal), and (b) MALDI-TOF mass spectrum (linear mode) of linear poly(AIGlc) obtained by CuBr/PMDETA at* $[M]_0/[I]_0 = 20$. *See Table 1 for detailed polymerization conditions.*

Table 1. Homopolymerization of 3-*O*-acryloyl-1,2:5,6-di-*O*-isopropylidene-α-glucofuranoside (AIGlc) with CuBr/PMDETA at 60 ºC in ethyl acetate (50 wt%)[a]

$[M]_0 / [I]_0$	Time (h)	Conv[b] (%)	$M_{n,\,calcd}$[c]	$M_{n,\,GPC}$[d] (M_w/M_n)	$M_{n,GPC\text{-}VISCO}$[e] (M_w/M_n)	$M_{n,\,MALDI}$[f] (M_w/M_n)
15	18	73	3,400	4,100 (1.05)		3,200 (1.14)
20	48	88	5,500	5,900 (1.09)	6,600 (1.13)	5,400 (1.09)
50	72	93	14,600	13,400 (1.09)	18,500 (1.25)	13,600 (1.11)
100	48	33	10,300	9,260 (1.06)	14,800 (1.17)	9,400 (1.13)
100	120	84	26,300	24,200 (1.14)	30,900 (1.37)	29,200 (1.12)

[a]Solution polymerization with ethyl 2-bromo isobutyrate; $[I]_0 : [CuBr]_0 : [PMDETA]_0 = 1 : 1 : 1$. [b]Monomer conversion as determined by ^{1}H NMR. [c]Theoretical number-average molecular weight as calculated from the monomer conversion. [d]Determined by GPC using THF as eluent with PtBuA standards. [e]Determined by GPC-Viscosity measurement. [f]Determined by MALDI-TOF MS measurement using universal calibration.

The homopolymerization of AIGlc was conducted under various conditions, aiming at increasing the polymerization rate as well as understanding the effects of solvent and temperature. The results are summarized in Table 2. The polymerization in ethyl acetate at 80 ºC led to increase of the reaction rate, but gave a bimodal distribution curve, as shown in Figure 2a. Note that the polymerization at higher concentration (with less solvent) is also not suitable, because the solubility of the monomer is not so high; the solubilization process is slow even in ethyl acetate (50 wt% to AIGlc) and takes prolonged time to dissolve completely. The polymerization in anisole at 80 ºC and 100 ºC also gave polymers having bimodal distribution (Figure 2b). This could be due to recombination occuring at higher temperatures. These results suggest that CuBr/PMDETA system at 60 ºC in ethyl acetate (50 wt% to AIGlc) is a suitable system for controlled polymerization of AIGlc, but the increase of the polymerization temperature may lead to unfavorable side reactions

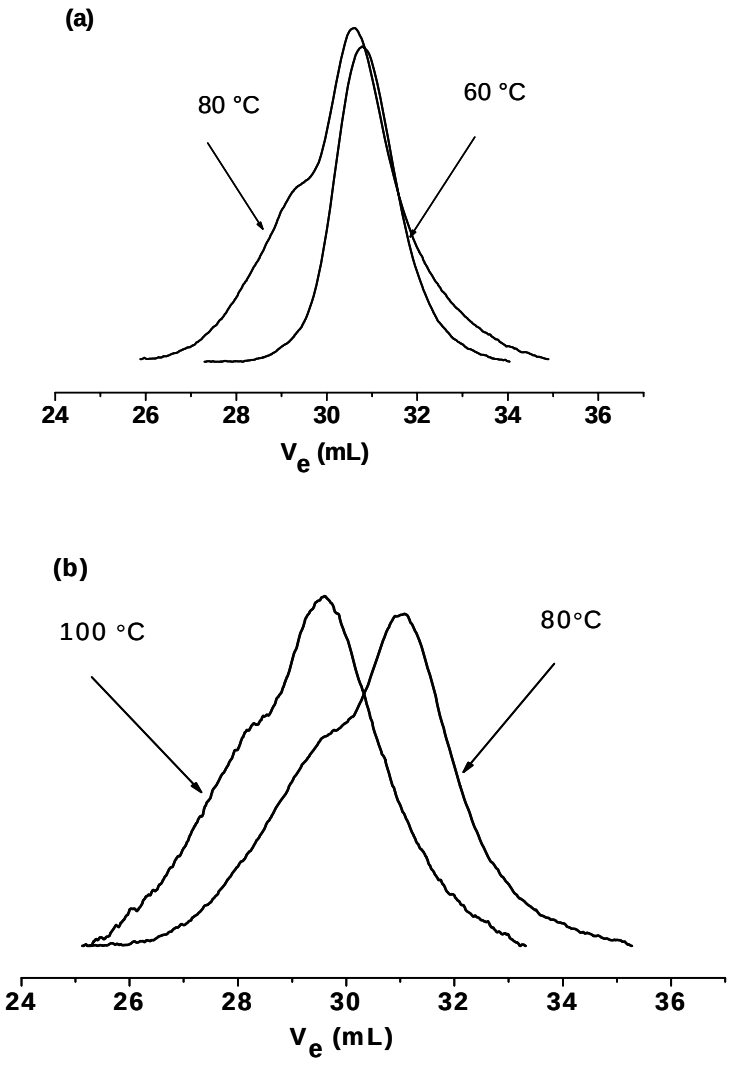

Figure 2. *GPC traces of linear poly(AIGlc) (a) in ethyl acetate at 60 ºC and 80 ºC ($[M]_0/[I]_0$ = 50), (b) in anisole at 80 ºC ($[M]_0/[I]_0$ = 50) and 100 ºC ($[M]_0/[I]_0$ = 100). See Table 2 for polymerization conditions.*

Table 2. Effects of solvent and temperature on homopolymerization of AIGlc with CuBr/PMDETA

Solvent [a]	Temp. (ºC)	$[M]_0 / [I]_0$	Time (h)	Conv.[b] (%)	$M_{n, calcd}$	$M_{n, GPC}$[c] (M_w/M_n)
Ethyl acetate	60	50	72	93	14,600	13,400 (1.09)
Ethyl acetate	60	100	48	33	10,300	9,260 (1.06)
Ethyl acetate	80	50	48	77	12,800	14,900 (1.27)
Ethyl acetate	80	100	24	47	14,700	13,500 (1.18)
Anisole	80	50	24	93	15,700	14,700 (1.25)
Anisole	100	100	24	79	23,100	24,800 (1.26)

[a]50 wt%; $[I]_0 : [CuBr]_0 : [PMDETA]_0 = 1 : 1 : 1$. [b]Monomer conversion as determined by ^{1}H NMR. [c]Determined by GPC using THF as eluent with PtBuA standards.

Effect of Polymerization Conditions on SCVCP of BPEA with AIGlc. Copolymerizations were conducted with CuBr/PMDETA in ethyl acetate at a constant comonomer-to-catalyst ratio, $\mu = ([AIGlc]_0+[BPEA]_0)/[CuBr]_0 = 100$, and a constant comonomer ratio, $\gamma = [AIGlc]_0/[BPEA]_0 = 1.5$. The results are summarized in Table 3. The comparisons of the Mark-Houwink plots are given in Figure 3.

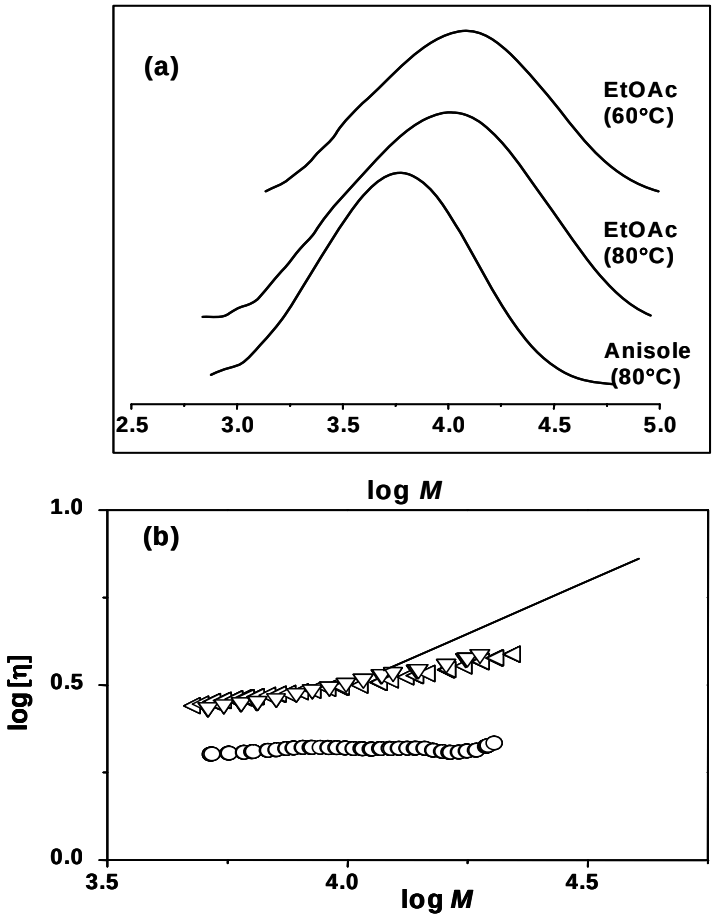

Figure 3. *RI signals (a) and Mark-Houwink plots (b) for the polymers obtained by copolymerizations of BPEA and AIGlc at a constant comonomer ratio, $\gamma = [AIGlc]_0/[BPEA]_0 = 1.5$ in anisole at 80 ºC (○), in ethyl acetate (EtOAc) at 80 ºC (◁), and in ethyl acetate (EtOAc) at 60 ºC (▽). The intrinsic viscosity of linear poly(AIGlc) (−) is given for comparison. See Table 3 for detailed polymerization conditions.*

When the SCVCP of AIGlc with BPEA was carried out in ethyl acetate at 60 ºC, 48 % conversion was reached after 4 h. Almost full conversion was reached only after 24 h, owing to the slow rate of polymerization of AIGlc as discussed earlier. As can be seen from Table 3, $M_{n,\,GPC\text{-}VISCO}$ = 6,600 and M_w/M_n = 1.92 were obtained at almost full conversion. When the reaction was conducted in ethyl acetate at 80 ºC after 24 h, the results are comparable to those obtained at 60 ºC. In both cases, the Mark-Houwink exponents of the branched polymers in THF (α = 0.23-0.24) are significantly lower than that for linear poly(AIGlc) (α = 0.52 ± 0.03). As can be seen in Figure 3b, the absolute intrinsic viscosities of the branched polymers are significantly lower than those of the linear one in the higher molecular weight range ($M > 10^4$), suggesting a more compact architecture with lower intrinsic viscosity. Note that the

viscosity values of the linear polymers are comparable to those of the branched polymers in the low molecular weights range ($M < 10^4$), suggesting that the macroscopic quantities such as intrinsic viscosity and radius of gyration of linear polymers are more or less similar to those of branched ones due to the bulky side groups. However, in the higher molecular weight range, the influence of the bulky side groups is less significant, and the branched structures leads to compact architectures and a decrease in the viscosity. In other words, the bulky side group has significant influence not only on the polymerization rate but also on the solution behavior in low molecular weight area. When the same polymerization was carried out in anisole at 80 ºC, the reaction mixture turned brown after 24 h and there was an apparent lowering of molecular weights ($M_{n,\ GPC\text{-}VISCO}$ = 4,400 and M_w/M_n = 1.68) with lower conversion (58 % even after 24 h). The α value was around 0.08, which is significantly less than that of typical hyperbranched polymers. Moreover, the homopolymerization at 80 º C gave a bimodal GPC curve, as discussed in the previous section. Hence, SCVCP of AIGlc and BPEA with CuBr/PMDETA in ethyl acetate using at 60 º C was selected for our further investigations towards the synthesis of highly branched glycopolymers.

Table 3. Self-Condensing Vinyl Copolymerization of BPEA and AIGlc under Various Conditions [a]

Solvent[b]	Temp (°C)	Time (h)	Conv.[c] (%)	$M_{n,GPC}$ [d] (M_w/M_n)	$M_{n,GPC\text{-}VISCO}$ [e] (M_w/M_n)	α[f]	DB[g]
Ethyl acetate	60	4	48	3,100 (1.54)	4,800 (1.78)	0.19	0.39
Ethyl acetate	60	24	98	5,180 (1.79)	6,600 (1.92)	0.24	0.42
Ethyl acetate	80	24	95	4,800 (1.60)	5,300 (2.21)	0.23	0.42
Anisole	80	24	58	2,900 (1.43)	4,400 (1.68)	0.08	0.41

[a]Copolymerization at a constant comonomer ratio, $\gamma = [AIGlc]_0/[BPEA]_0 = 1.5$, and a constant comonomer-to-catalyst ratio, $\mu = ([AIGlc]_0+[BPEA]_0)/[CuBr]_0 = 100$. [b]Ethyl acetate or anisole (50 wt % to AIGlc) was used as a solvent. [c]Conversion of double bonds as determined by ^{1}H NMR. [d]Determined by GPC using THF as eluent with PtBuA standards. [e]Determined by GPC/viscosity measurement. [f]Mark-Houwink exponent as determined by GPC/viscosity measurement. [g]Degree of branching as determined by ^{1}H NMR using eq 2, before hydrolysis.

Effect of the Comonomer Ratio on the SCVCP of BPEA with AIGlc. The effect of the comonomer ratio on SCVCP of BPEA with AIGlc was investigated with the CuBr/PMDETA system in ethyl acetate. The copolymerization was carried out at 60 ºC at different comonomer ratios, $\gamma = [AIGlc]_0/[BPEA]_0$ between 1 to 10, keeping the comonomer-to-catalyst ratio at a constant value of $\mu = ([AIGlc]_0 + [BPEA]_0)/[CuBr]_0 = 100$. In the case of $\gamma = 1$, almost 90 % conversion was achieved after 4 h. However, in the case of $\gamma = 1.5$ the conversion was 48 % even after 4 h. Hence, the polymerization time was adjusted, depending on the comonomer ratio, γ, because the achievement of almost full conversion is one of important factors to obtain higher molecular weights and degree of branching.[30] Actually the time was prolonged until the reaction mixture became viscous. For γ values ranging from 2.5 to 10, almost full conversion was achieved after 24–120 h, as shown in Table 4. The molecular weights and molecular weight distribution of the copolymers were characterized by GPC/viscosity using universal calibration and conventional GPC. In all cases, the molecular weights determined by GPC-viscosity are higher than the apparent ones obtained by GPC, indicating highly branched structures.

As can be seen in Figure 4, the elution curves shift toward higher molecular weights with increasing comonomer ratio, γ. In general, the number–average molecular weights of branched polymers obtained by SCVCP increase with γ, and such tendency was observed in the SCVCP of *tert*-butyl acrylate with BPEA[38] as well as in the solution polymerization of 2-(diethylamino)ethyl methacrylate with a methacrylate-type inimer.[31] In this study, molecular weights up to $M_{n,GPC\text{-}VISCO} = 13{,}000$ could be obtained at $\gamma = 10$, whereas the polymers obtained at lower γ values ($\gamma = 1.5$, 2.5) had lower molecular weights, which are in accordance with the general tendency. Slight deviation from the tendency (for example, when $\gamma = 1.5$, 2.5, and 5, $M_{n,GPC\text{-}VISCO} = 6600$, 5100, and 11900, respectively) may be related to the difference in the conversion observed at each γ value. According to theory (assuming equal reactivity of active centers[29]), the number-average degree of polymerization increases drastically with conversion of the comonomer, especially at the end of the polymerization. We believe that the relationship between the molecular weights and γ is independent of the polymerization and catalyst systems, and may be attributed to an inherent tendency for the cyclization process in SCVCP. The SCVCP at $\gamma > 10$ is considered to be possible, but a prolonged reaction time or higher catalyst concentration is required to attain higher conversion in the cases of higher γ. This is an inherent character of the system used in this study, which is basically due to the nature of the bulky sugar-carrying acrylate. It must be noted that multimodal GPC traces obtained with $\gamma = 5$ and 10 (Figure 4) indicate the presence

of fractions with different hydrodynamic volumes. The Mark-Houwink plot (Figure 5) of the corresponding polymer, however, is not affected, indicating that the different fractions have similar branched structure.

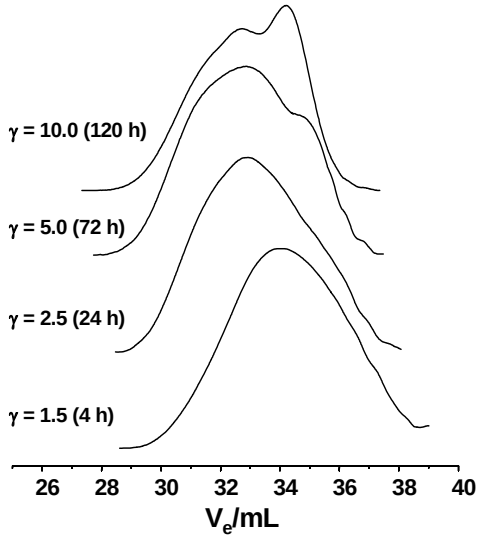

Figure 4. *GPC traces of branched copolymers obtained by SCVCP of BPEA and AIGlc at different comonomer ratios, $\gamma = [AIGlc]_0/[BPEA]_0$. See Table 3 for $\gamma = 1.5$ (4 h) and Table 4 for $\gamma = 1.5$ (24 h), 2.5, 5, 10 for detailed polymerization conditions.*

Mark-Houwink plots and contraction factors,[39] $g' = [\eta]_{branched}/[\eta]_{linear}$, as a function of the molecular weight for representative branched polymers obtained by SCVCP are shown in Figure 5. Relationships between dilute solution viscosity and molecular weight have been determined, and the Mark-Houwink constant typically varies between 0.28 and 0.2, depending on the degree of branching. In contrast, the exponent is typically in the region of 0.6-0.8 for linear homopolymers in a good solvent with a random coil conformation. The Mark-Houwink exponent of the mixture of linear poly(AIGlc)s ($\alpha = 0.52 \pm 0.03$) is lower than that of poly(*tert*-butyl acrylate) ($\alpha = 0.80$), indicating less favorable interaction with the solvent. In both cases, the exponent values are well within the range of linear homopolymers. The contraction factor is another way of expressing the compact structure of a branched polymer. From Figure 5, it is obvious that the viscosities of branched poly(AIGlc)s are significantly lower than those of the linear one and increase with γ. There were only slight differences in the slopes between the branched copolymers, but the values at each molecular weight increase with increasing γ value. The contraction factors for all the branched copolymers decrease with increasing molecular weights. These observations indicate that the differences in the

molecular weights obtained from the GPC/viscosity compared to conventional GPC arises from a systematic decrease in Mark-Houwink exponent, α, and the contraction factor, g′, due to a compact structure resulting polymer from the increased number of branches.

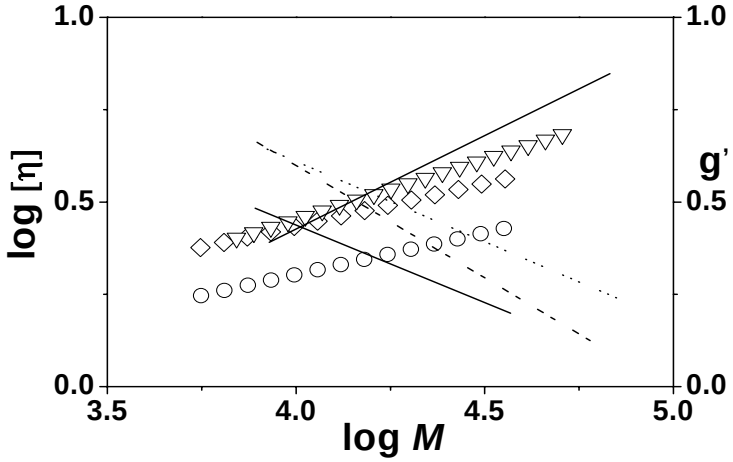

Figure 5. *Mark-Houwink plots for the polymers obtained by copolymerizations of BPEA and AIGlc: γ = 1 (○), 2.5 (◊), 5 (▽). The intrinsic viscosity of a linear poly(AIGlc) (—) is given for comparison. Contraction factors, g′=* $[\eta]_{branched}/[\eta]_{linear}$ *, for the polymers obtained by SCVCP of BPEA and AIGlc: γ = 1 (—), 2.5 (**- -**), 5.0 (····). See Tabe 4 for detailed polymerization conditions.*

Table 4. Self-condensing Vinyl Copolymerization of BPEA and AIGlc at Different Comonomer Ratios γ[a]

γ[b]	Time (h)	Conv.[c] (%)	$M_{n,GPC}$[d] (M_w/M_n)	$M_{n,GPC\text{-}VISCO}$[e] (M_w/M_n)	α[f]	BPEA ratio in polymer		
						Calcd.[g]	Obsd. (NMR)[h]	Obsd. (EA)[i]
1	4	90	7,800 (1.43)	9,200 (2.84)	0.20	0.50	0.41	0.49
1.5	24	98	5,180 (1.79)	6,600 (1.92)	0.24	0.40	0.39	0.46
2.5	24	91	4,900 (1.49)	5,100 (2.13)	0.24	0.28	0.33	0.29
5	72	95	5,500 (1.48)	11,900 (1.59)	0.27	0.16	0.19	0.17
10	120	96	5,400 (1.37)	13,000 (1.95)	0.28	0.09	0.08	0.10

[a]Copolymerization at 60°C with CuBr/PMDETA at a constant comonomer-to-catalyst ratio, μ = ([AIGlc]$_0$+[BPEA)$_0$])/[catalyst]$_0$) = 100 in the presence of ethyl acetate (50 wt % to AIGlc). [b]γ= [AIGlc]$_0$/[BPEA]$_0$. [c]Conversion of double bonds as determined by ^{1}H NMR. [d]Determined by GPC using THF as eluent with PtBuA standards. [e]Determined by GPC/viscosity measurement. [f]Mark-Houwink exponent as determined by GPC/viscosity measurement. [g]Calculated from the composition in feed. [h]Determined by ^{1}H-NMR. [i]Determined from elemental analysis using the bromine content.

The effect of the comonomer ratio, γ, on the Mark-Houwink exponent is shown in Figure 6. In the whole range of γ values, the exponents of the branched polymers are significantly lower (α = 0.20-0.28) compared to that for linear poly(AIGlc) (α = 0.52 ± 0.03). Such a decrease in the Mark-Houwink exponent, α, as well as the contraction factor, g´, provides conclusive evidence for a more compact architecture with increasing number of branches and confirms our earlier observations in SCVCP of other (meth)acrylates.[30,31]

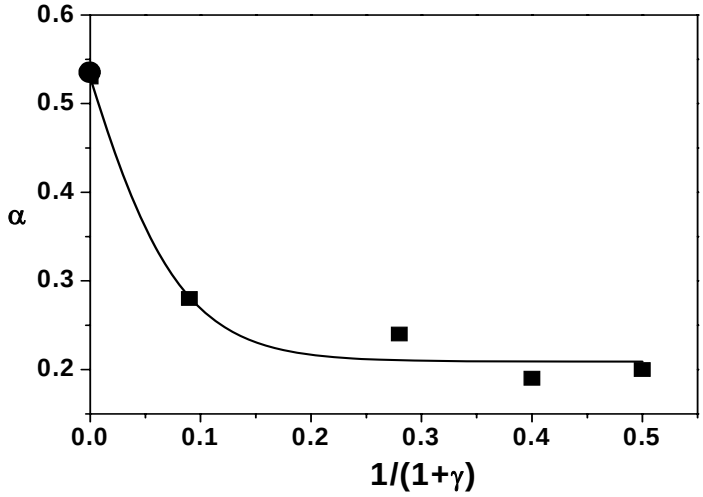

Figure 6. *Dependence of the Mark-Houwink exponent, α, on comonomer ratio, γ (■). (●): Linear poly(AIGlc).*

With ATRP, nearly every chain should contain a halogen atom at its end group, if termination and transfer are essentially absent. In other words, the existence of halogen atom at the chain end can be used as an indicator to confirm that the polymerization proceeds in controlled fashion without termination and transfer reactions. The halogen atom can be also replaced through a variety of reactions leading to end-functional polymers and used as the initiating part for polymerization of a second monomer. In the case of ideal SCVCP via ATRP, the resulting branched polymers carry one bromoester function per inimer unit, and the functionality decreases with comonomer (AIGlc) composition. As shown in Figure 7, the bromine contents of the branched polymers are dependent upon the comonomer composition in the feed and are in fair agreement with the calculated values. This result indicates the existence of reasonable number of bromine atom at the chain end, suggesting that unfavorable termination and transfer reactions are essentially negligible under the condition used in this study, and the number of bromoester end groups can be simply determined by the comonomer ratio, γ, in the feed.

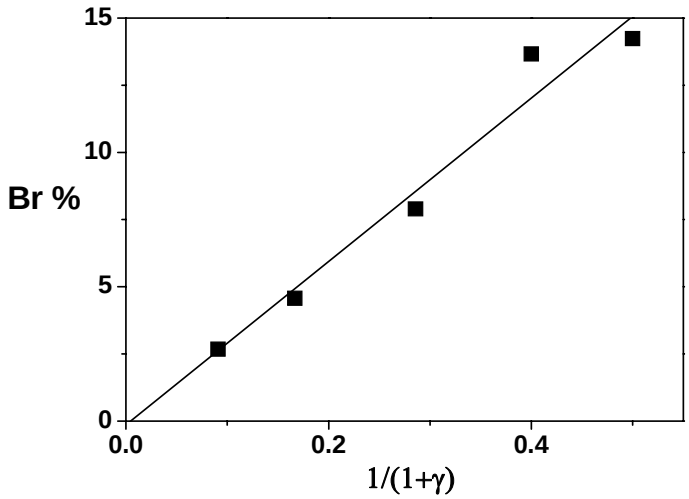

Figure 7. *Dependence of bromine contents on 1/(γ+1). Samples: see Table 4. The calculated value (—) is given for comparison.*

The structure of the linear and branched poly(AIGlc)s was also confirmed by ^{1}H NMR and elemental analysis. Figure 8 shows the respective ^{1}H NMR spectra of the poly(AIGlc)s obtained by ATRP and SCVCP. The characteristic peaks at 1.2-1.4 ppm (isopropylidene protons), 3.9-4.6 and 5.0-5.3 ppm are clearly seen in the linear poly(AIGlc). In the case of the copolymers, besides the signal of poly(AIGlc) segment, the BPEA inimer signals appear at 4.0-4.5 ppm attributed to the protons of the ethylene linkage and the protons which are geminal to bromine in either A*, B*, or M*, all which are derived from BPEA. The latter protons correspond to the end groups. Apart from the peak, a large doublet at 1.85 ppm in the copolymers is assigned to CH_3 of the 2-bromopropionyloxy group, B*, while the peak around 1.1-1.3 ppm is assigned to b, which is formed by addition of the monomer to B*. This peak b is overlapping with the isopropylidene protons of the poly(AIGlc) segment. The BPEA content in the copolymers obtained by SCVCP was determined from the ^{1}H NMR spectra by comparing the peaks at 3.9-4.6 ppm attributed to the sum of five protons (A, B, C, G) of the poly(AIGlc) segment and five protons of the ethylene linkage and that geminal to bromine as mentioned above, and the peak at 5.0-5.3 ppm corresponding to one proton (F) of the poly(AIGlc) segment, as shown in Figure 8. Thus, the comonomer composition can be calculated using the equation (1),

$$\frac{5H(x) + 5H(1-x)}{1H(x)} = \frac{\text{Integral at 3.9 - 4.6 ppm}}{\text{Integral at 5.0 - 5.3 ppm}} \qquad (1)$$

where "x" is the fraction of the monomer, whereas "1-x" is the fraction of the inimer in the polymer. The comonomer fractions calculated from the ratio of these peaks are in good agreement with the comonomer composition in the feed, which corresponds to the γ value, as can be seen in Table 4. The comonomer fractions were also determined by elemental analysis via bromine content, which are also consistent with the theoretical values within experimental error. The agreements suggest complete inimer incorporation.

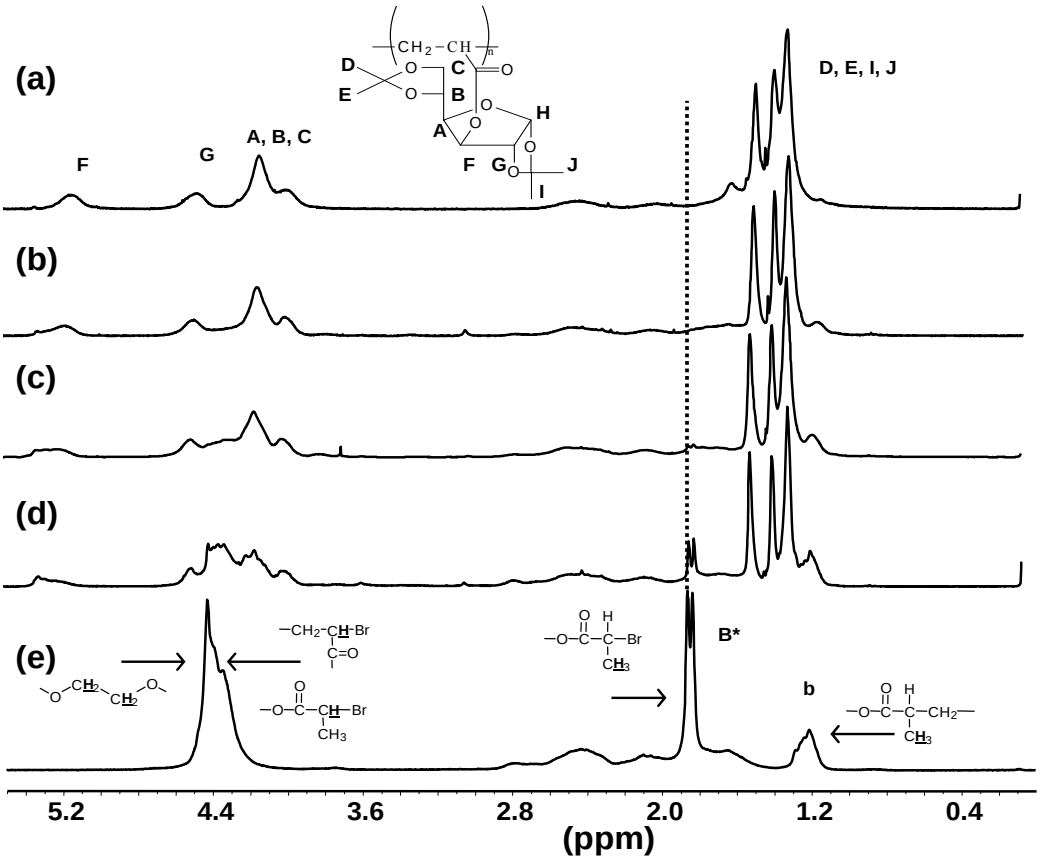

Figure 8. *^{1}H NMR spectra ($CDCl_3$) of the linear (a) and branched poly(AIGlc): γ = 5 (b), 2.5 (c), 1 (d), and poly(BPEA) (e).*[38]

Degree of Branching (DB). Figure 8 shows ^{1}H NMR spectra with the complete assignment of the linear and branched poly(AIGlc)s, as well as poly(BPEA) obtained by a homo-SCVP of BPEA. For poly(BPEA), the proportions of b and B* can be calculated from the broad peak at 1.0-1.3 ppm assigned to b and large doublet at 1.85 ppm assigned to B*. In the cases of the copolymers obtained by SCVCP, these peaks should be related to the degree of branching and the comonomer composition. In our copolymerization system, since the protons of the isopropylidene groups overlap with the b protons, we have indirectly calculated

the proportion of b using ^{1}H NMR. For equal reactivity of active sites, the degree of branching determined by NMR, DB_{NMR}, at full conversion is given as.[29]

$$DB_{NMR} = 2\left(\frac{b}{\gamma+1}\right)\left[1-\left(\frac{b}{\gamma+1}\right)\right] \quad (2)$$

According to the theory of SCVCP, DB_{theo}, at full conversion, can be represented as

$$DB_{theo} = \frac{2\left(1-e^{-(\gamma+1)}\right)\left(\gamma+e^{-(\gamma+1)}\right)}{(\gamma+1)^2} \quad (3)$$

The fraction of b units could be calculated by comparing the peaks at 3.6-4.5 ppm and the large doublet at 1.85 ppm in the copolymers ranging from γ = 1 to 2.5. The peaks at 3.6-4.5 ppm correspond to five protons of poly(AIGlc) segment and five protons of the inimer, as mentioned earlier. The doublet at 1.85 ppm corresponds to 3 protons of methyl group of B* (2-bromopropionyloxy group). Taking into account the inimer (BPEA) composition in the copolymer (see eq. 1), we can calculate the integral of the peak at 1.85 ppm, corresponding to B* + b. On the other hand, the actual ratio of the peaks at 1.85 ppm and 3.6-4.5 ppm determined by ^{1}H NMR provide the value of B* - b. From these approaches, DB_{NMR}= 0.43 and DB_{theo}= 0.49 can be obtained at γ = 1 (b = 0.65). The reliability of the method for the evaluation of b was verified by comparing the value of b after the hydrolysis of the branched and homo poly(AIGlc)s. After the hydrolysis, the isopropylidene groups disappear and the broad peak around 1.0-1.3 is clearly visible (Figure 9), which is then compared with the B* protons for the evaluation of the proportion of b using the equation b = (region at 1.1-1.3 ppm)/(sum of region at 1.85 ppm (B*) and region at 1.1-1.3 ppm (b)). The values of b obtained after the hydrolysis are in good agreement with the values of b obtained by the indirect method, as can be seen in Table 5.

Table 5. Degree of Branching of Copolymers Obtained by SCVCP of AIGlc and BPEA at Different Comonomer Ratios γ

γ^a	b^b	b^c	DB^d	DB^e	$DB_{theo}{}^f$
1.0	0.65	0.60	0.43	0.42	0.49
1.5	0.75	0.67	0.42	0.38	0.47
2.5	0.78	0.68	0.35	0.31	0.40

[a]$\gamma = [AIGlc]_0/[BPEA]_0$. [b]Fraction of reacted B* units as determined by ^{1}H NMR before hydrolysis. [c]Fraction of reacted B* units as determined by ^{1}H NMR after hydrolysis. [d]Degree of branching as determined by ^{1}H NMR using eq 2 before hydrolysis. [e]Degree of branching as determined by ^{1}H NMR using eq 2 after hydrolysis. [f]Theoretical degree of branching as determined using eq 3.

DB_{NMR} decreases with γ, as predicated by calculations. In all the cases, however, the observed values are slightly lower than the calculated ones, which might be attributed to the simplifications made for the calculations i.e. equal reacativity of A*, B*, and M* chain ends. Although NMR experiments afford a conclusive measurement of the degree of branching for lower γ values, the low concentration of branch points in the copolymer at $\gamma > 5$ does not allow the determination of the degree of branching directly by the spectroscopic method, because of low intensities of the peaks in the regions around 1.85 ppm and 1.0-1.3 ppm, as shown in Figure 9. However, for the case of high comonomer ratios, $\gamma >> 1$, the relation between DB_{theo} and γ becomes very simple and does not depend on the reactivity ratios of the various active centres and is represented as $DB_{theo} \approx 2/(\gamma + 1)$.[29] When the reactivities of the various active centres are not equal, the dependences are more complex, and the degree of branching may be higher or lower, depending upon the systems. In this copolymerization system, the rate constant of the sugar-carrying acrylate was comparatively lower than that of the normal acrylates and longer polymerization time was required to attain almost full conversion. Hence, the rate constant of BPEA used as an AB* inimer should be different from that of the comonomer, AIGlc, used in this study. This could also lead to the formation of star-like structures instead of randomly branched architectures. Detailed investigation is now in progress and will be reported elsewhere.

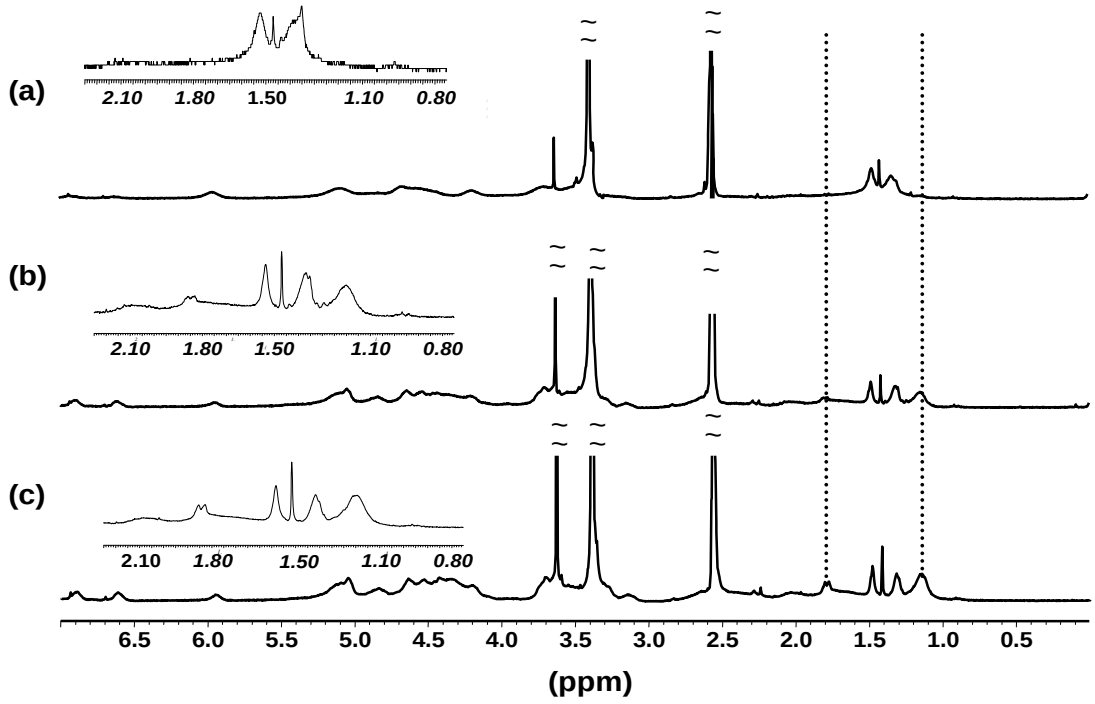

Figure 9. *^{1}H NMR spectra (DMSO-d_6) of the polymers obtained after deprotection of linear poly(AIGlc) (a), and branched poly(AIGlc)s: γ = 2.5 (b), 1.5 (c).*

Deprotection of linear and branched poly(AIGlc)s. The hydrolysis of the isopropylidene groups in the linear and branched poly(AIGlc)s was performed by treating the samples with formic acid.[22] The final product was obtained by freeze-drying from dioxane after the deprotected polymer was dialyzed against water. Figure 9a reveals that the signals of the isopropylidene protons (1.2-1.4 ppm) completely disappear after the hydrolysis of the linear poly(AIGlc) and a broad signal assignable to anomeric hydroxyl groups of the sugar moieties (6.4-7.0 ppm) appear. This proves that the deprotection proceeds quantitatively. The linear deprotected polymers, poly(3-*O*-acryloyl-α,β-D-glucopyranoside), which can be abbreviated as poly(AGlc), are white powders completely soluble in water, methanol and DMSO but insoluble in THF and acetone. For the branched poly(AGlc)s, the solubility of the polymers were dependent upon the comonomer ratios, γ. In the case of γ = 1, the branched poly(AGlc) were partially soluble in water, which is attributed to the 50% of the non-polar inimer segment. From γ = 1.5 onwards, the polymers were completely soluble in water, DMSO and methanol but insoluble in THF and acetone. It is important to note that the unchanged resonance signal of protons of the ethylene linkage and those geminal to bromine at 4.0-4.6

ppm suggests that the BPEA composition in the branched poly(AGlc) is almost the same as that in branched poly(AIGlc). As mentioned in the previous section, the fraction of b units (reacted B* units) and DB_{NMR} after the hydrolysis are in good agreement with those of the branched poly(AIGlc)s. These results also indicate that the branched structure is intact during the complete deprotection of the isopropylidene groups and proceeds selectively to yield characteristic branched poly(AGlc)s.

Figure 10 represents the NMP-phase GPC traces of the linear and branched poly(AGlc)s. The hyperbranched samples show a broad distribution and comparable molecular weights as observed in THF-phase GPC before the hydrolysis. The molecular weights and molecular weight distributions for the hydrolysed branched poly(AGlc)s at γ = 1.0 and 1.5 are M_n = 7,900 (M_w/M_n = 1.91) and M_n = 7,300 (M_w/M_n = 1.40), respectively. These results suggest that the molecular weights and the branched architecture of the hydrolyzed products correspond to those of the branched poly(AIGlc)s. The molecular weight and molecular weight distribution of the hydrolysed homopolymer is M_n = 22,900 (M_w/M_n = 1.16) which is fairly in agreement with $M_{n,calcd.}$ = 23,400 and also with the results, M_n = 24,200 (M_w/M_n = 1.14) obtained before hydrolysis.

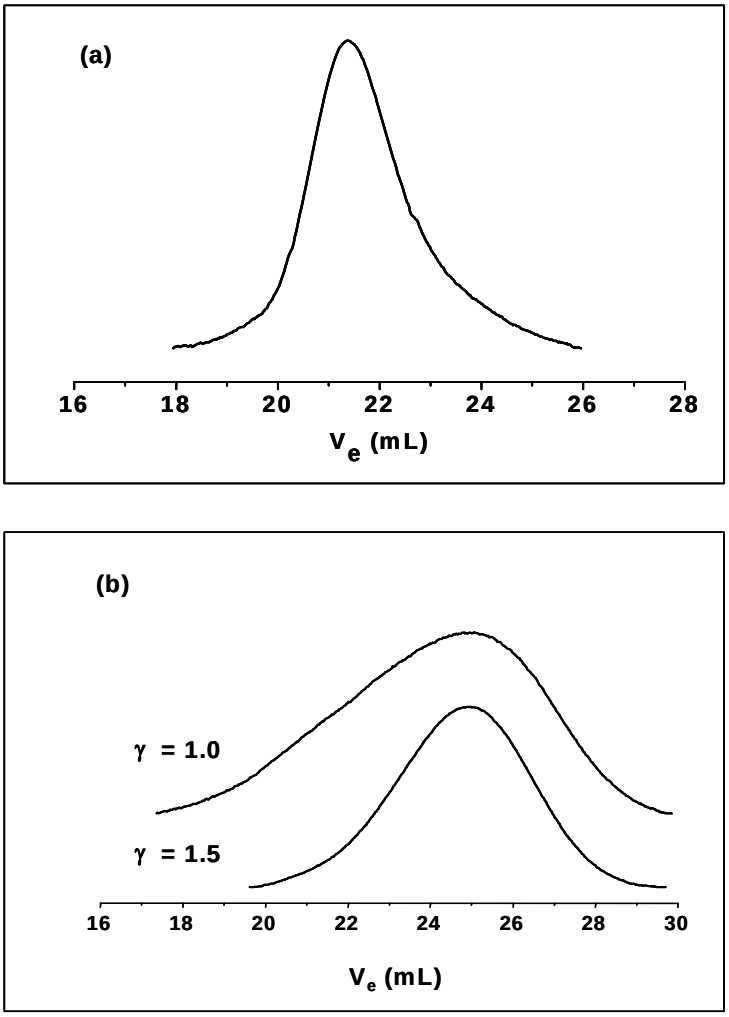

Figure 10. NMP-phase GPC traces of (a) linear poly(AGlc) and (b) branched poly(AGlc)s.

FT-IR spectra of the linear and branched poly(AGlc)s obtained after hydrolysis are shown in Figure S-2 (see supporting information). The absorption bands due to the isoproylidene groups are observed at 3000, 1450, and 1380 cm^{-1} assigned to the C-H stretching and C-H asymmetric and symmetric deformation modes, respectively. The C-O stretching band of the isopropylidene group is also observed in the region between 1200 and 1000 cm^{-1}. After the deprotection, these bands disappear and a strong absorption band around 3500 cm^{-1} is observed due to the hydroxyl group formed by the deprotection. The spectrum of the branched poly(AGlc) at $\gamma = 2.5$ having less branch points is almost same as that of the linear poly(AGlc).

3.4. Conclusions

Self-condensing vinyl copolymerization (SCVCP) of the sugar-carrying acrylate, AIGlc with the acrylic AB* inimer via ATRP provides a straightforward strategy for generating water-soluble hyperbranched glycopolymers and their precursors. Linear poly(AIGlc) with controlled molecular weights and very low polydisperisities ($1.05 < PDI < 1.14$) were obtained in a controlled fashion using CuBr/PMDETA catalyst system. The significant influence of the bulky isopropylidene-protected sugar moiety in AIGlc was observed on the polymerization rate and the macroscopic quantities such as intrinsic viscosity and radius of gyration. It was found that a suitable choice of the polymerization conditions is required to obtain water-soluble glycopolymers with characteristic highly branched architectures, which can then be manipulated for various biological, pharmaceutical, and medical applications. Further studies on this interesting branched glycopolymers for such directions will be reported separately. This work broadens the scope of facile synthesis of branched glycopolymers by a controlled polymerization technique, in which the architecture can be simply manipulated by the nature and composition of sugar-carrying vinyl monomer used as a comonomer. Extension to planar and spherical polymer brushes is also planned.

Acknowledgement. We appreciate S.Wunder for her help during GPC-VISCO measurement.

Supporting Information Available: Figures S-1 and S-2. This material is availabe free of charge via the internet at http://pubs.acs.org.

3.5. References

(1) Lee, Y. C.; Lee, R. T. *Accounts Chem Res* **1995**, *28*, 321-327.

(2) Bovin, N. V.; Gabius, H. J. *Chem Soc Rev* **1995**, *24*, 413.

(3) Capila, I.; Linhardt, R. J. *Angew Chem Int Edit* **2002**, *41*, 391-412.

(4) Klein, J.; Kunz, M.; Kowalczyk, J. *Makromol Chem* **1990**, *191*, 517-528.

(5) Gunay, N. S.; Linhardt, R. J. *Planta Med* **1999**, *65*, 301-306.

(6) Simanek, E. E.; McGarvey, G. J.; Jablonowski, J. A.; Wong, C. H. *Chem Rev* **1998**, *98*, 833-862.

(7) Petronio, M. G.; Mansi, A.; Gallinelli, C.; Pisani, S.; Seganti, L.; Chiarini, F. *Chemotherapy* **1997**, *43*, 211-217.

(8) Ladmiral, V.; Melia, E.; Haddleton, D. M. *Eur Polym J* **2004**, *40*, 431-449.

(9) Wang, Q.; Dordick, J. S.; Linhardt, R. J. *Chem Mater* **2002**, *14*, 3232-3244.

(10) Dordick, J. S.; Linhardt, R. J.; Rethwisch, D. G. *Chemtech* **1994**, *24*, 33-39.

(11) Chen, X. M.; Dordick, J. S.; Rethwisch, D. G. *Macromolecules* **1995**, *28*, 6014-6019.

(12) Zanini, D.; Roy, R. *J Org Chem* **1998**, *63*, 3486-3491.

(13) Dimick, S. M.; Powell, S. C.; McMahon, S. A.; Moothoo, D. N.; Naismith, J. H.; Toone, E. J. *J Am Chem Soc* **1999**, *121*, 10286-10296.

(14) Roy, R.; Pon, R. A.; Tropper, F. D.; Andersson, F. O. *J Chem Soc Chem Comm* **1993**, 264-265.

(15) Aoi, K.; Itoh, K.; Okada, M. *Macromolecules* **1995**, *28*, 5391-5393.

(16) Yamada, K.; Yamaoka, K.; Minoda, M.; Miyamoto, T. *J Polym Sci Pol Chem* **1997**, *35*, 255-261.

(17) Aoi, K.; Tsutsumiuchi, K.; Okada, M. *Macromolecules* **1994**, *27*, 875-877.

(18) Fraser, C.; Grubbs, R. H. *Macromolecules* **1995**, *28*, 7248-7255.

(19) Wulff, G.; Schmid, J.; Venhoff, T. *Macromol Chem Physic* **1996**, *197*, 259-274.

(20) Ohno, K.; Tsujii, Y.; Miyamoto, T.; Fukuda, T.; Goto, M.; Kobayashi, K.; Akaike, T. *Macromolecules* **1998**, *31*, 1064-1069.

(21) Ohno, K.; Tsujii, Y.; Fukuda, T. *J Polym Sci Pol Chem* **1998**, *36*, 2473-2481.

(22) Ohno, K.; Izu, Y.; Yamamoto, S.; Miyamoto, T.; Fukuda, T. *Macromol Chem Physic* **1999**, *200*, 1619-1625.

(23) Gotz, H.; Harth, E.; Schiller, S. M.; Frank, C. W.; Knoll, W.; Hawker, C. J. *J Polym Sci Pol Chem* **2002**, *40*, 3379-3391.

(24) Liang, Y. Z.; Li, Z. C.; Chen, G. Q.; Li, F. M. *Polym Int* **1999**, *48*, 739-742.

(25) Li, Z. C.; Liang, Y. Z.; Chen, G. Q.; Li, F. M. *Macromol Rapid Comm* **2000**, *21*, 375-380.

(26) Ejaz, M.; Ohno, K.; Tsujii, Y.; Fukuda, T. *Macromolecules* **2000**, *33*, 2870-2874.

(27) Narain, R.; Armes, S. P. *Chem Commun* **2002**, 2776-2777.

(28) Narain, R.; Armes, S. P. *Macromolecules* **2003**, *36*, 4675-4678.

(29) Litvinenko, G. I.; Simon, P. F. W.; Müller, A. H. E. *Macromolecules* **1999**, *32*, 2410-2419.

(30) Simon, P. F. W.; Müller, A. H. E. *Macromolecules* **2001**, *34*, 6206-6213.

(31) Mori, H.; Walther, A.; André, X.; Lanzendörfer, M. G.; Müller, A. H. E. *Macromolecules* **2004**, *37*, 2054-2066.

(32) Litvinenko, G. I.; Simon, P. F. W.; Muller, A. H. E. *Macromolecules* **2001**, *34*, 2418-2426.

(33) Mori, H.; Müller, A. H. E. In *Dendrimers V, Topics in Current Chemistry*; Vögtle, F., Ed.; Springer: Heidelberg, 2003; Vol. 228, pp 1-37.

(34) Matyjaszewski, K.; Gaynor, S. G.; Kulfan, A.; Podwika, M. *Macromolecules* **1997**, *30*, 5192-5194.

(35) Mori, H.; Böker, A.; Krausch, G.; Müller, A. H. E. *Macromolecules* **2001**, *34*, 6871-6882.

(36) Ouchi, T.; Jokei, S.; Chikashita, H. *J Heterocyclic Chem* **1982**, *19*, 935-936.

(37) Benoît, H.; Grubisic, Z.; Rempp, P.; Decker, D.; Zilliox, J. G. *J. Chem. Phys.* **1966**, *63*, 1507.

(38) Mori, H.; Chan Seng, D.; Lechner, H.; Zhang, M.; Müller, A. H. E. *Macromolecules* **2002**, *35*, 9270-9281.

(39) Burchard, W. *Adv. Polym. Sci.* **1999**, *143*, 113-194.

3.6. Supporting Information to the paper

Synthesis of Hyperbranched Glycopolymers via Self-Condensing Atom Transfer Radical Copolymerization of a Sugar-Carrying Acrylate

By Sharmila Muthukrishnan, Günter Jutz , Xavier Andre, Hideharu Mori[§], Axel H. E. Müller[*]

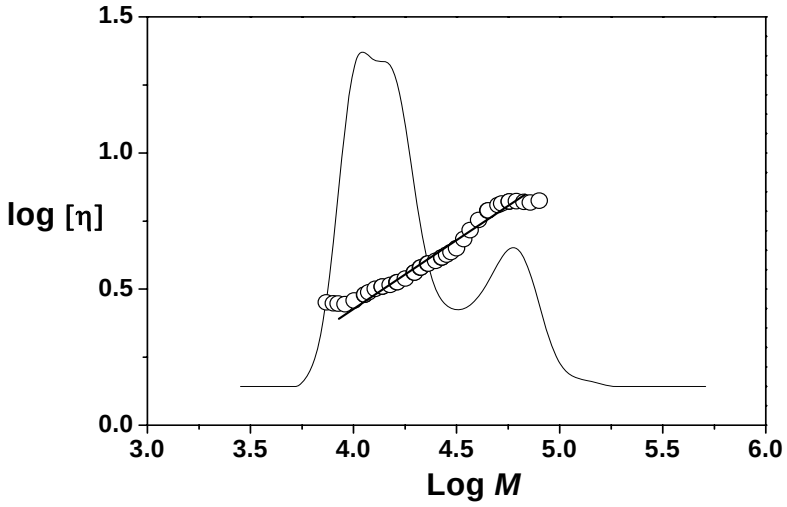

Figure S-1. *Mark-Houwink plot for mixture of linear poly(AIGlc)s. Mark-Houwink exponent,* $\alpha = 0.52 \pm 0.03$.

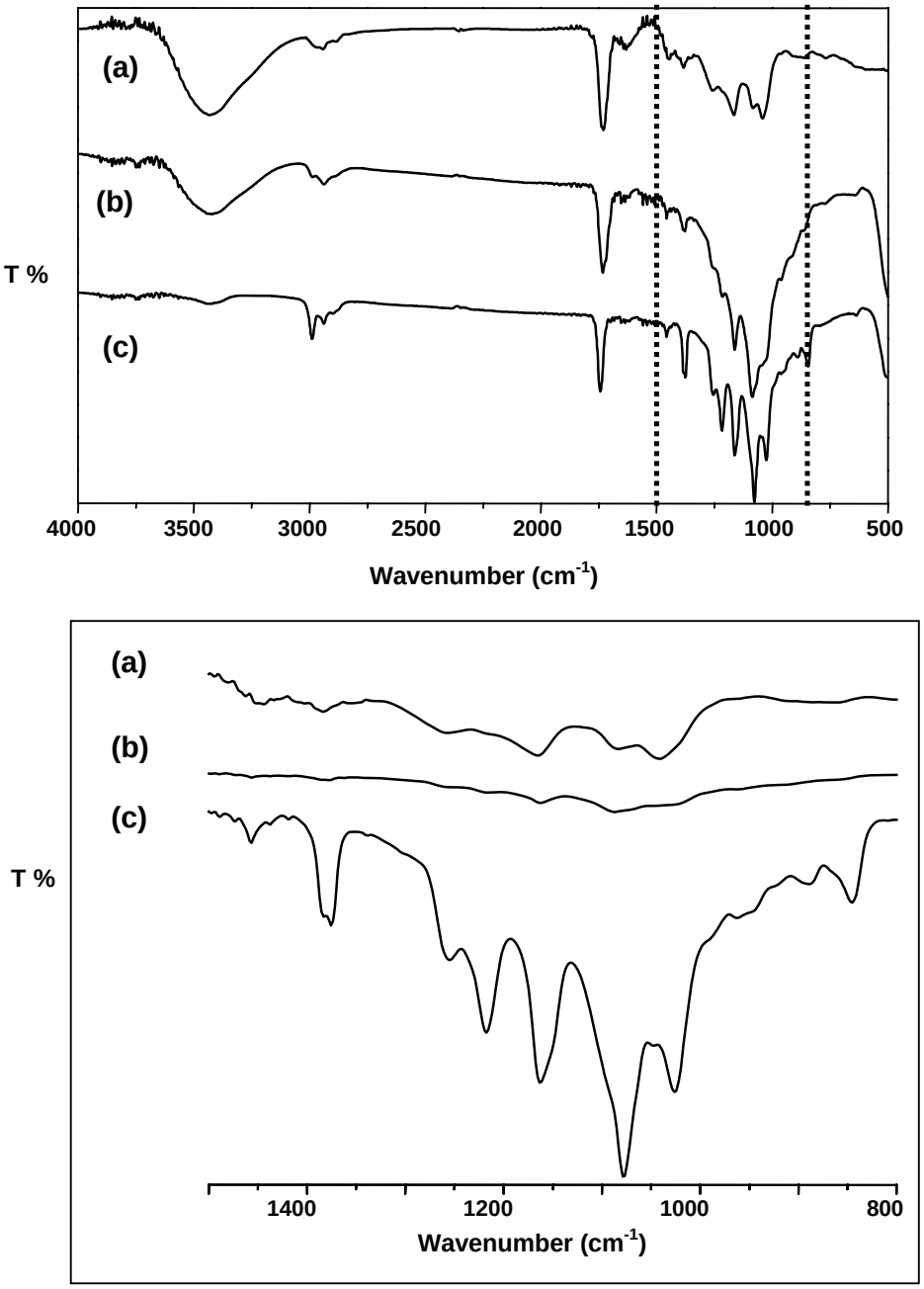

Figure S-2. *FT-IR spectra of (a) branched poly(AGlc) (γ =2.5), (b) linear poly(AGlc), (c) linear poly(AIGlc).*

4. Synthesis and Characterization of Methacrylate-Type Hyperbranched Glycopolymers via Self-Condensing Atom Transfer Radical Copolymerization

Sharmila Muthukrishnan[†], Hideharu Mori[§], Axel H. E. Müller[†,*]

[†] Makromolekulare Chemie II, and Bayreuther Zentrum für Kolloide und Grenzflächen, Universität Bayreuth, D-95440 Bayreuth, Germany

[§] Department of Polymer Science and Engineering, Faculty of Engineering, Yamagata University, 4-3-16, Jonan, Yonezawa, 992-8510, Japan

[*] To whom correspondence should be addressed. e-mail: *Axel.Mueller@uni-bayreuth.de*, Phone:+49 (921) 55-3399, Fax: +49 (921) 55-3393

Published in *Macromolecules* 2005, 38, p. 3108.

Abstract: We report the synthesis of hyperbranched glycopolymers by self-condensing vinyl copolymerization (SCVCP) of the methacrylic AB* inimer, 2-(2-bromoisobutyryloxy)ethyl methacrylate (BIEM) with 3-*O*-methacryloyl-1,2:5,6-di-*O*-isopropylidene-α-D-glucofuranose (MAIGlc) via atom transfer radical polymerization (ATRP), followed by deprotection of the isopropylidene protecting groups. Homopolymerization of MAIGlc with the $(PPh_3)_2NiBr_2$ catalyst system in solution proceeds smoothly, resulting in linear poly(MAIGlc) having controlled molecular weights and narrow molecular weight distribution. The catalyst system could be applied for SCVCP to synthesize hyperbranched poly(MAIGlc)s, as confirmed by GPC, GPC/viscosity analyses, as well as ^{1}H, ^{13}C, and 2D NMR measurements. Depending on the comonomer ratio, $\gamma = [MAIGlc]_0/[BIEM]_0$, branched poly(MAIGlc)s with number-average molecular weights between 17,500 and 29,800 and Mark-Houwink exponents between 0.20 and 0.34 were obtained within reasonable polymerization time (4 h), the polymerization being very much faster than the corresponding glyco-polyacrylates. Deprotection of the isopropylidene protecting groups of the branched poly(MAIGlc)s resulted in water-soluble glycopolymers with randomly branched architectures, which were characterized by elemental analyses, ^{1}H NMR and FT-IR measurements.

4.1. Introduction

During recent years there has been an increasing attention paid to synthetic polymers with pendant saccharide moieties, so called glycopolymers, as biological recognition substances.[1] Since carbohydrate based monomers and polymers confer high hydrophilicity and water-solubility, they are of main interest with respect to very specialized applications in biochemical and biomedical fields, such as molecular recognition processes,[2] drug delivery systems,[3,4] and also as surfactants.[5] They have been used as efficient tools to investigate carbohydrate-based interactions.[6] Glycopolymers at the cell surface are involved in numerous biological functions, adhesion, cell growth regulation, cancer cell metastasis and inflammation.[7] They act as attachment sites for several infectious viruses, toxins, and hormones that result in pathogenesis.[8] In addition to their wide variety of biological applications, glycopolymers are also used as texture-enhancing food additives and reverse osmosis membranes. Due to their unique architectures and monodisperse structures, glycodendrimers have been shown to result in numerous previously unknown or significantly improved physical and chemical properties compared to traditional linear polymers. The polyvalency inherent in carbohydrate-based branched polymers is an important feature, which allows these materials to perform many complicated multivalent processes. They have been used to understand nature´s multivalent processes[9] and as well-defined models of cell surface multiantennary glycoproteins.[10] Glycodendrimers have been tested for bacterial adhesion hemagglutination assays.[11]

The synthesis of sugar-based monomers and polymers has been widely reported in the last decade.[12-14] The synthesis of well-defined glycopolymers from protected sugar-carrying monomers has been achieved using both ionic polymerization[15] and controlled radical polymerization.[16-18] The tolerance of atom transfer radical polymerization (ATRP) towards hydroxyl groups has enabled the direct synthesis of sugar-carrying polymers without protecting chemistry.[19,20] ATRP has been used for the synthesis of many sugar-carrying block[21,22] and graft polymers[16]. Controlled/″Living″ radical polymerization has thus proved to be a very facile approach for the well-defined and controlled synthesis of glycopolymers.

We have very recently reported the synthesis of randomly branched glycopolymers using self-condensing vinyl copolymerization (SCVCP) of a glyco-acrylate, 3-*O*-acryloyl-1,2:5,6-di-*O*-isopropylidene-α-D-glucofuranoside (AIGlc) via atom transfer radical polymerization (ATRP).[23] Water-soluble glycopolymers with characteristic highly branched architectures was obtained using this approach. A significant influence of the bulky isopropylidene-protected sugar moiety in AIGlc was observed on the polymerization rate. It was also found that a suitable choice of the polymerization conditions (CuBr/N,N,N',N'',N''-

pentamethyldiethylenetriamine (PMDETA) at 60 ºC in ethyl acetate) was required to obtain glycopolymers with well-defined branched architectures. However, the system has several drawbacks, including limited molecular weights and extremely low polymerization rate; for example branched poly(AIGlc) with number-average molecular weight of 13,000 at a comonomer ratio, $\gamma = 10$ was obtained after 120 h. These difficulties may lead to limitations of the hyperbranched glyocopolymers to be employed for various biological, pharmaceutical, and medical applications. In addition, the purification of the glyco-acrylate monomer is quite difficult. These drawbacks motivated us to investigate the corresponding methacrylates.

This paper reports the synthesis of highly branched glycopolymers using a methacrylic AB* inimer, 2-(2-bromoisobutyryloxy)ethyl methacrylate (BIEM) with a sugar-carrying methacrylate, 3-*O*-methacryloyl-1,2:5,6-di-*O*-isopropylidene-α-D-glucofuranoside (MAIGlc). The synthetic route to highly branched glycopolymers is given in Scheme 1. The curved lines represent polymer chains. A*, B*, and M* are active units, whereas a, b, and m are reacted ones. A is methacryloyl group. M and m stand for MAIGlc units at the chain end and in the linear segment, respectively. For an ideal SCVCP process, living polymerization systems are required to avoid crosslinking reactions and gelation due to chain transfer or recombination reactions. Hence the important step is to find suitable conditions where both homopolymerization of MAIGlc and homo-SCVP of the inimer (BIEM) can proceed in controlled/"living" fashion. In this study, we have used the $(PPh_3)_2NiBr_2$ catalyst system to prepare well-defined and monodisperse linear poly(MAIGlc)s. The effect of different catalyst systems was investigated. Highly branched poly(MAIGlc)s having different molecular weights and degree of branching were synthesized by SCVCP with different comonomer ratios, γ.

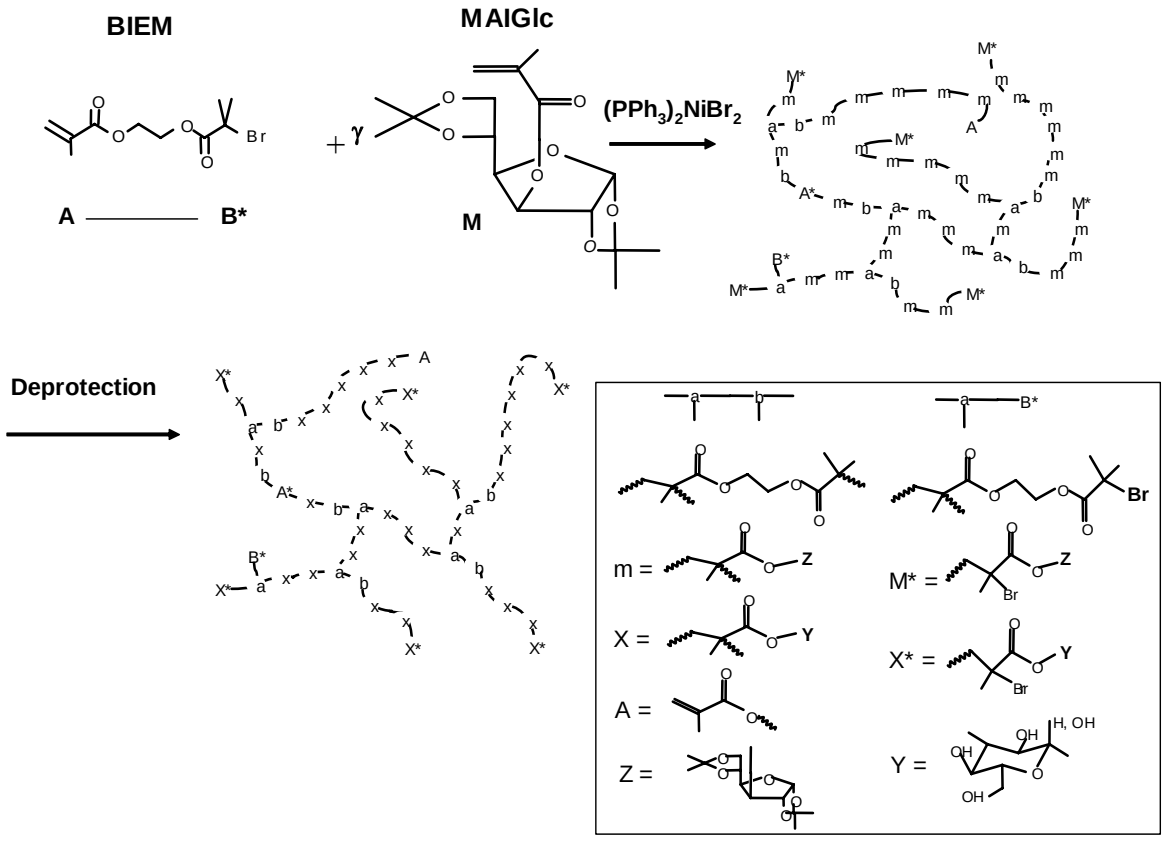

Scheme 1. *General route to branched glycopolymers via self-condensing vinyl copolymerization, followed by deprotection of isopropylidene protecting groups.*

4.2. Experimental Section

Materials. CuBr (95%, Aldrich) was purified by stirring overnight in acetic acid. After filtration, it was washed with ethanol, ether, and then dried. N,N,N',N'',N''-Pentamethyldiethylenetriamine (PMDETA, 99 %, Aldrich) and ethyl 2-bromoisobutyrate (98%, Aldrich) were distilled and degassed. Bis(triphenylphosphine)nickel(II) bromide ($(PPh_3)_2NiBr_2$, 99%, Aldrich) was used as received. 1,1,4,7,10,10-Hexamethyltriethylenetetramine (HMTETA, 97 %, Aldrich) and other reagents were commercially obtained and used without further purification. 3-*O*-Methacryloyl-1,2:5,6-di-*O*-isopropylidene-D-glucofuranose (MAIGlc) was synthesized by the reaction of 1,2:5,6-di-*O*-isopropylidene-D-glucofuranose and methacrylic anhydride in pyridine and purified by vacuum distillation as reported by Klein et al.[24] Synthesis of a methacrylic AB* inimer, 2-(2-

bromoisobutyryloxy)ethyl methacrylate (BIEM), was conducted by the reaction of 2-bromo-isobutyryl bromide with 2-hydroxyethyl methacrylate in the presence of pyridine as reported previously.[25,26] The inimer was degassed by three freeze-thaw cycles.

Polymerization. All polymerizations were carried out in a round bottom flask sealed with a plastic cap. A representative example for copolymerization ($\gamma = [MAIGlc]_0/[BIEM]_0 = 5$), is as follows: BIEM (0.169 g, 0.608 mmol) was added to a round bottom flask containing $(PPh_3)_2NiBr_2$ (0.0271 g, 0.0365mmol), MAIGlc (1.0 g, 3.04 mmol), and ethyl acetate (1.0 g, 50 wt% to MAIGlc). After BIEM was added to the mixture, the flask was placed in an oil bath at 100 ºC for 3.0 h. Almost full conversion of the double bonds (> 95%) was confirmed by ^{1}H NMR. The content was dissolved in THF, and was subsequently passed through a silica column, the polymer was precipitated from THF into methanol. Then the product was freeze-dried from dioxane and finally dried under vacuum at room temperature. The polymer had M_n = 10100 and M_w/M_n = 1.51 according to conventional GPC and M_n = 21000 and M_w/M_n = 1.55 according to GPC/viscosity using universal calibration. The resulting polymer was soluble in chloroform, THF, and acetone, but insoluble in methanol, hexane and water.

A representative example of homopolymerization of MAIGlc is as follows: Ethyl 2-bromoisobutyrate (0.0034 g, 0.0152 mmol) was added to a round bottom flask containing $(PPh_3)_2NiBr_2$ (0.0113 g, 0.0152 mmol) and MAIGlc (0.50 g, 1.522 mmol) in ethyl acetate (0.50 g, 50 wt% to MAIGlc). Then the flask was placed in an oil bath at 100 ºC for 1.5 h. Conversion of the double bonds, as detected by ^{1}H NMR, was 70 %. The viscous content of the flask was dissolved in THF. The solution was passed through a silica column, and the polymer was precipitated from THF into methanol. Finally the product was freeze dried from dioxane and dried under vacuum at room temperature. The polymer had M_n = 21,200 and M_w/M_n = 1.18 according to conventional GPC, and M_n = 28900 and M_w/M_n = 1.29 according to GPC/viscocity using universal calibration, and M_n = 26100 and M_w/M_n = 1.12 according to MALDI-TOF MS measurement.

A mixture of linear poly(MAIGlc)s with various molecular weights was used as comparison in the solution viscosity studies. Molecular weight for this sample is M_n = 44,400 and M_w/M_n = 1.33 (determined by GPC/viscosity using universal calibration). See Figure S-1 (supporting information).

Deprotection. The transformation of linear poly(MAIGlc) into water soluble polymer poly (3-*O*-methacryloyl-α,β-D-glucopyranose) (MAGlc) was achieved under mild acidic condition.[17] The linear poly(MAIGlc) (100 mg) was dissolved in 80 % formic acid (12 ml) and stirred for 48 h at room temperature. Then 5 ml of water was added and it was stirred for

another 3 h. The solution was dialysed using Spectra/Por^R (MWCO: 1000) against Millipore water for 2 days. The resulting polymer was freeze-dried and then dried under vacuum. The deprotected polymer was obtained as white powder in a quantitative yield (65 mg, yield = 85 %), which was soluble in water, methanol, and DMSO, but insoluble in THF and acetone. The deprotection was done in a similar way in the case of randomly branched poly(MAIGlc), which resulted in water-soluble branched glycopolymers.

Characterization. The linear and branched polymers obtained from MAIGlc were characterized by conventional GPC and GPC with viscosity detector using THF as eluent at a flow rate of 1.0 ml/min at room temperature. A conventional THF-phase GPC system was used to obtain apparent molecular weights. GPC system I; column set: 5μm PSS SDV gel, 10^2, 10^3, 10^4, 10^5 Å, 30 cm each; detectors: Waters 410 differential refractometer and Waters photodiode array detector operated at 254 nm. Narrow poly(*tert*-butyl methacrylate) standards (PSS, Mainz) were used for the calibration of column set I. Molecular weights of the branched polymers were determined by the universal calibration principle[27] using the viscosity module of the PSS-WinGPC scientific V 6.1 software package. Linear PMMA standards (PSS, Mainz) were used to construct the universal calibration curve. GPC system II; column set: 5μ PSS SDV gel, 10^3 Å, 10^5 Å and 10^6 Å, 30cm each; detectors: Shodex RI-71 refractive index detector; Jasco Uvidec-100-III UV detector (λ = 254 nm); Viscotek viscosity detector H 502B.

A 1-methyl-2-pyrrolidone (NMP)/LiBr-phase GPC system was used to obtain apparent molecular weights of the hydrolyzed polymers. GPC system III; column set: two PSS GRAM 7μm, 1000 and 100 Å columns thermostated at 70 °C; detectors: Waters 486 UV detector (γ = 270 nm), and Bischoff RI detector 8110. 50 μL of the sample diluted in NMP (0.05 M LiBr) were injected at a flow rate of 1 mL/min. Linear PS standards were used for calibration.

MALDI-TOF mass spectrometry was performed on a Bruker Reflex III instrument equipped with a 337 nm N_2 laser in the reflector mode and 20 kV acceleration voltage. 2,5-Dihydroxy benzoic acid (Aldrich, 97%) was used as a matrix. Samples were prepared from THF solution by mixing matrix (20 mg/mL) and polymer (10 mg/mL) in a ratio of 4:1. The number-average molecular weights, of the polymers were determined in the linear mode.

^{1}H and ^{13}C NMR spectra were recorded with a Bruker AC-250 spectrometer. ^{1}H-^{13}C 2D (heteronuclear single quantum correlation) spectra were recorded with a Bruker Avance-360 spectrometer (360.13 MHz for ^{1}H and 90.56 MHz for ^{13}C under *J* mode). FT-IR spectra were recorded on a Bruker Equinox 55 spectrometer. The elemental analyses were performed by

Ilse Beetz Mikroanalytisches Laboratorium (Kulmbach) and by using Elementaranalysator Vario EL III (Anorganische Chemie II, University of Bayreuth).

4.3. Results and Discussion

Effect of Catalyst System on the Homopolymerization of MAIGlc. In order to find a suitable catalyst system for the synthesis of highly branched glycopolymers by SCVCP via ATRP, we initially investigated the influence of the catalyst system (Cu- and Ni-based catalysts) on the homopolymerization of MAIGlc. In a previous paper, we have demonstrated that the synthesis of randomly branched polymers by SCVCP of methyl methacrylate with 2-(2-bromoisobutyryloxy)ethyl methacrylate (BIEM) was achieved using $(PPh_3)_2NiBr_2$.[25] In contrast CuBr/hexamethyltriethylenetetramine (HTMTETA) was a suitable catalyst system for the SCVCP of 2-(diethylamino)ethyl methacrylate with BIEM.[28] We have also employed the CuBr/ N,N,N',N",N"-pentamethyldiethylenetriamine (PMDETA) catalyst system for the SCVCP of AIGlc (an acrylate type sugar-carrying monomer) with an acrylic-type inimer.[23] Based on these results, the solution polymerization of MAIGlc was conducted using three different catalyst systems with ethyl 2-bromoisobutyrate (EBIB), which has a same initiating group as in a methacrylic inimer (BIEM). The results are summarized in Table 1 and Figure 1. When MAIGlc was polymerized using $(PPh_3)_2NiBr_2$ with EBIB at 100 ºC in ethyl acetate, the conversion reached 70% (as determined by ^1H NMR) after 1.5 h. The number-average molecular weight of poly(MAIGlc) as determined by conventional GPC using PtBuMA standands was M_n = 21,200, which is almost comparable to the theoretical value (M_n = 22,900), and the polydisperity index was M_w/M_n = 1.18. For the polymerization with CuBr/HMTETA at 60 ºC, full conversion was obtained after 3 h, and the number-average molecular weight of the polymer was M_n = 32,700, which is almost the same as the theoretical value (32,800), and the polydispersity index was M_w/M_n = 1.19. In contrast, the polymer obtained using CuBr/PMDETA has a broader molecular weight distribution than in the cases of CuBr/HMTETA and $(PPh_3)_2NiBr_2$, as shown in Figure 1. Hence the possibility of using CuBr/PMDETA system for the synthesis of highly branched glycopolymethacrylates was ruled out.

The solution polymerization of MAIGlc has been reported by Ohno et al.[17] using the CuBr/4,4'-di(n-heptyl)-2,2'-bipyridine (dHbipy) catalyst system, and the resulting polymers had slightly broader molecular weight distributions ranging from 1.27 to 1.82, depending on the $[M]_0/[I]_0$ ratio. Thus, the $(PPh_3)_2NiBr_2$ and CuBr/HMTETA catalyst systems lead to polymers with significantly lower polydispersity. Another important issue is the difference in the polymerization rate between the glycomethacrylate, MAIGlc, and its acrylate analog. In

our previous paper, it was found that the solution polymerization of a glycoacrylate, AIGlc,[23] is extremely slow, which was attributed to the bulkiness of the side group. A long reaction time (120 h) was required to obtain higher molecular weight polymers (M_n = 30,000) using the CuBr/PMDETA system at $[M]_0/[I]_0$ = 100. On the other hand, the bulky side group has no significant influence on the polymerization rate in the case of solution polymerization of the glycomethacrylate, MAIGlc. Almost full conversion was obtained in 3 h using CuBr/HMTETA system at $[M]_0/[I]_0$ = 100.

Table 1. Homopolymerization of 3-*O*-Methacryloyl-1,2:5,6-di-*O*-isopropylidene-D-glucofuranoside (MAIGlc) in Ethyl Acetate (50 wt%)[a]

Catalyst/Ligand	Temp (°C)	Time (h)	Conv.[b] (%)	$M_{n,calc}$[c]	$M_{n,GPC}$[d] (M_w/M_n)
$(PPh_3)_2NiBr_2$	100	1.5	70	22,900	21,200 (1.18)
CuBr/HMTETA	60	3.0	100	32,800	32,700 (1.19)
CuBr/PMDETA	60	1.5	95	31,100	33,400 (1.51)

[a]Solution polymerization with ethyl 2-bromoisobutyrate; $[M]_0 : [I]_0 : [Cat]_0 : [Lig]_0$ = 100 : 1 : 1 : 1. [b]Monomer conversion as determined by ^{1}H-NMR. [c]Theoretical number-average molecular weight as calculated from the monomer conversion. [d]Determined by GPC using THF as eluent with PtBMA standards.

In this study as can be seen later, the linear and branched polymers obtained from MAIGlc were characterized by conventional GPC and GPC with viscosity detector (using universal calibration), as the relation between molecular weight and hydrodynamic volume of branched polymers differs substantially from the linear ones. In addition, the bulky side group in poly(MAIGlc) may lead to a different hydrodynamic volume compared to that of standard PtBuMA. In order to clarify these points, a linear poly(MAIGlc) obtained by $(PPh_3)_2NiBr_2$ was characterized by GPC/viscosity using universal calibration and MALDI-TOF mass spectrometry (MS). As can be seen in Figure 2, the GPC trace and MALDI-TOF mass spectrum show unimodal peak with low polydispersity, and the molecular weights and molecular weight distributions obtained from MALDI-TOF MS (M_n = 26,100, M_w/M_n = 1.12) and GPC/viscosity (M_n = 28,900, M_w/M_n = 1.29) are in agreement with those obtained from

the conventional GPC using PtBuMA standards and with the theoretical values. MALDI-TOF MS underestimates the polydispersity of polymers with moderate or wide MWD.[29]

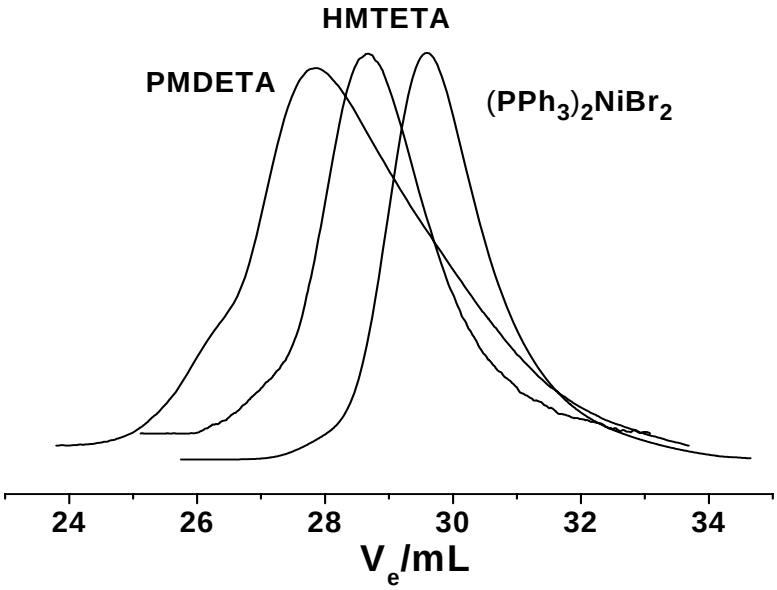

Figure 1. *GPC traces of linear poly(MAIGlc)s prepared with various catalyst systems. See Table 1 for detailed polymerization conditions.*

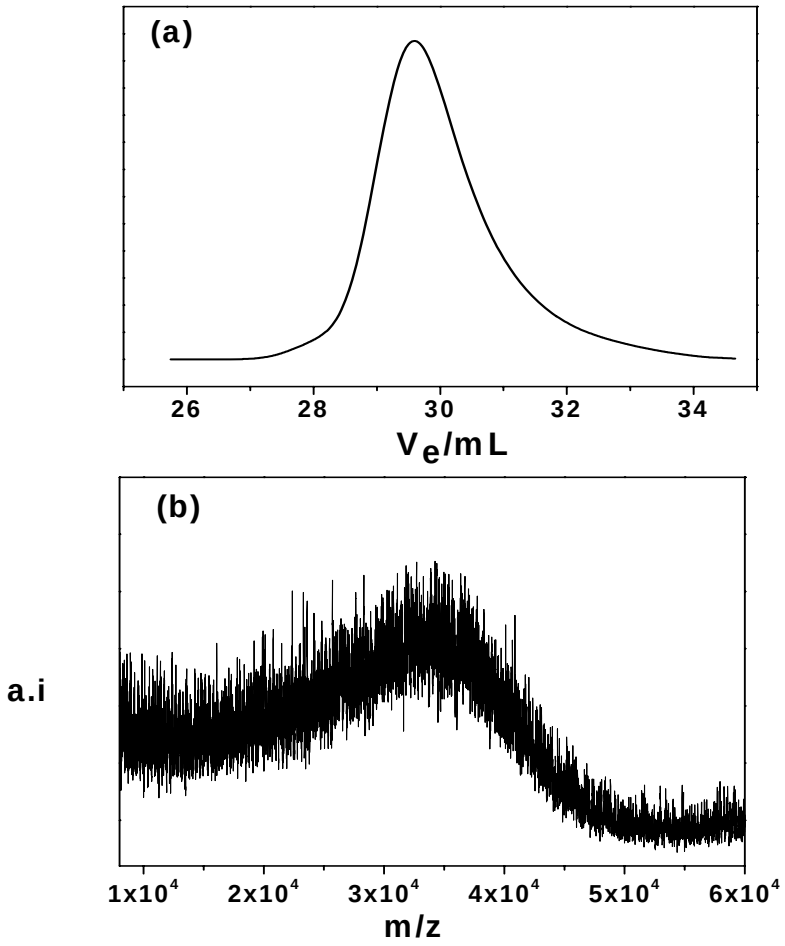

Figure 2. *(a) GPC trace (RI signal) and (b) MALDI-TOF mass spectrum (linear mode) of linear poly(MAIGlc) obtained by $(PPh_3)_2NiBr_2$ at $[M]_0/[I]_0 = 100$. See Table 1 for detailed polymerization conditions.*

Effect of Polymerization Conditions on SCVCP of BIEM with MAIGlc. To compare the catalyst systems CuBr/HMTETA and $(PPh_3)_2NiBr_2$, copolymerizations were conducted at a constant comonomer ratio, $\gamma = [MAIGlc]_0/[BIEM]_0 = 1.5$, and a constant comonomer-to-catalyst ratio, $\mu = ([MAIGlc]_0 + [BIEM]_0)/[(Cat]_0 = 100$ where $[MAIGlc]_0$, $[BIEM]_0$, and $[Cat]_0$ represent the initial concentrations of comonomer, inimer, and catalyst, respectively. The results are summarized in Table 2. When SCVCP of MAIGlc with BIEM was carried out in ethyl acetate at 100 ºC using $(PPh_3)_2NiBr_2$, almost full conversion was reached after 2 h. The viscous reaction mixture was soluble in THF at ambient temperature. The polymer obtained after precipitation into methanol had $M_n = 17{,}600$ and $M_w/M_n = 2.12$ (as determined

by GPC/viscosity using universal calibration), compared to M_n = 7,900 and M_w/M_n = 1.94 (as determined by conventional GPC). The higher molecular weights determined by GPC-viscosity compared with apparent ones obtained by GPC indicate branched structures. The Mark-Houwink exponent of the branched polymers is apparently lower (α = 0.22) compared to that for linear poly(MAIGlc) ($\alpha = 0.51 \pm 0.03$). When the copolymerization was conducted at 60 ºC using CuBr/HMTETA system, 83% conversion was reached after 4 h. As can be seen in Figure 3b, the intrinsic viscosity of the branched polymer obtained by the CuBr/HMTETA system is higher at a given molecular weight than that of the polymer obtained using $(PPh_3)_2NiBr_2$, indicating a less compact structure. Further, the branched polymer obtained by CuBr/HMTETA system has a higher Mark-Houwink exponent (α = 0.25) and a lower degree of branching (DB = 0.37), determined from ^{1}H NMR (see Figure S-2 in Supporting Information). Hence, SCVCP of MAIGlc and BIEM with $(PPh_3)_2NiBr_2$ in ethyl acetate at 100 ºC was selected for our further investigations towards the synthesis of highly branched glycopolymers having higher molecular weight within reasonable polymerization time.

In our previous paper, we demonstrated that the polymerization rate of the sugar-carrying acrylate, AIGlc, was apparently lower than that of conventional acrylates, which eventually led to longer polymerization time to attain almost full conversion in SCVCP of AIGlc with an acrylate-type inimer.[23] On the other hand, homopolymerization of MAIGlc and SCVCP of MAIGlc and BIEM proceeded smoothly with $(PPh_3)_2NiBr_2$. In this copolymerization system, BIEM used as an AB* inimer contains the methacryl and bromoisobutyryloxy groups both of which form tertiary halides. MAIGlc used as a comonomer also generates a tertiary radical. In general, the tertiary halides are known to produce a higher concentration of radicals than secondary active sites.[30] Hence, it can be presumed that the difference in the polymerization rate between the sugar-carrying acrylate and methacrylate is due to the different reactivity of secondary and tertiary halides.

The efficiency of the catalyst system and the nature of ligand used to complex metal ions were found to play an important role in the determination of the activity, molecular weights, molecular weight distribution, and branched architectures of the polymers obtained by homopolymerization of MAIGlc, and SCVCP of BIEM and MAIGlc. For a successful SCV(C)P via ATRP, a sufficient proportion of dormant species should be maintained throughout the polymerization in order to keep a low concentration of monomeric and polymeric radicals. The behavior is mainly related to the activation and deactivation rate constants in the ATRP equilibrium. In our copolymerization system, the difference in the reactivity between the catalyst systems, CuBr/HMTETA and $(PPh_3)_2NiBr_2$, is basically

related to the equilibrium between the active and dormant species in the system. In this system, the tertiary α-bromoester dormant species (A* and M*) formed during the reaction should have a reactivity similar to the bromoisobutyryloxy group (B*) found on the AB* inimer.

Table 2. Self-Condensing Vinyl Copolymerization of BIEM and MAIGlc under Various Conditions in Ethyl Acetate (50 wt % to AIGlc)[a]

Catalyst/Ligand	Temp (°C)	Time (h)	Conv.[c] (%)	$M_{n,GPC}$[d] (M_w/M_n)	$M_{n,GPC\text{-}VISCO}$[e] (M_w/M_n)	α[f]	DB[g]
$(PPh_3)_2NiBr_2$	100	2.0	97	7,900 (1.94)	17,600 (2.12)	0.22	0.42
CuBr/HMTETA	60	4.0	83	9,800 (1.64)	13,700 (1.50)	0.25	0.37

[a]Copolymerization at a constant comonomer ratio, $\gamma = [MAIGlc]_0/[BIEM]_0 = 1.5$, and a constant comonomer-to-catalyst ratio, $\mu = (MAIGlc]_0+[BIEM]_0)/[Cat]_0 = 100$. [c]Conversion of double bonds as determined by ^1H NMR. [d]Determined by GPC using THF as eluent with PtBMA standards. [e]Determined by GPC/viscosity measurement. [f]Mark-Houwink exponent as determined by GPC/viscosity measurement. [g]Degree of branching as determined by ^1H NMR using eq 2.

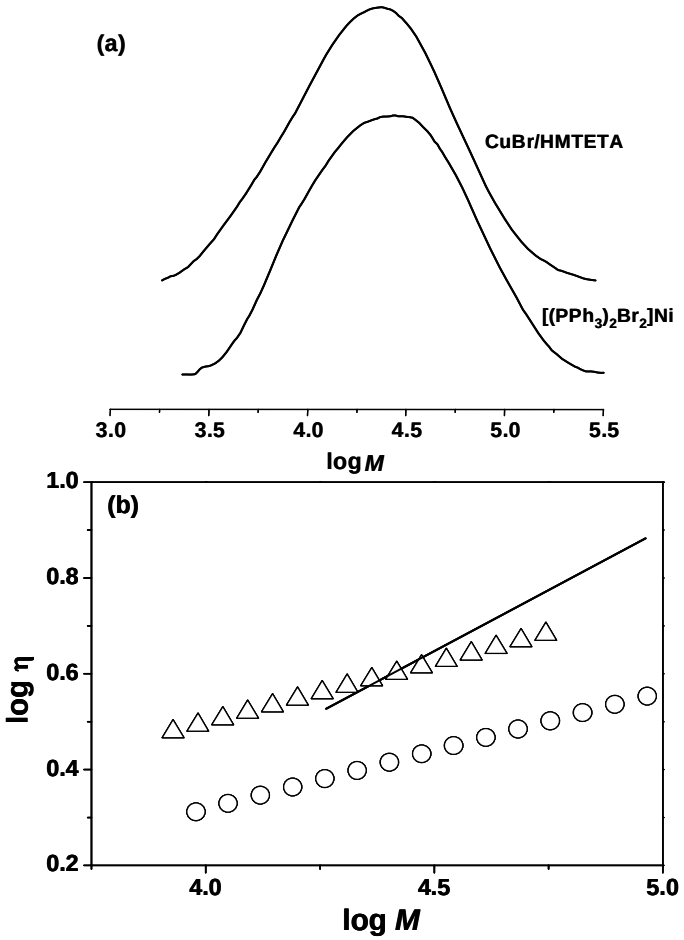

Figure 3. *RI signals (a) and Mark-Houwink plots (b) for the polymers obtained by copolymerizations of BIEM and MAIGlc at a constant comonomer ratio, γ = [MAIGlc]$_0$/[BIEM]$_0$ = 1.5 using $(PPh_3)_2NiBr_2$ at 100 ºC (○), CuBr/HMTETA at 60 ºC (△). The intrinsic viscosity of linear poly(MAIGlc) (−) is given for comparison. See Table 2 for detailed polymerization conditions.*

Effect of the Comonomer Ratio on SCVCP of BIEM with MAIGlc. The influence of the comonomer ratio on SCVCP of BIEM with MAIGlc was investigated with $(PPh_3)_2NiBr_2$ in ethyl acetate. The polymerization was conducted at 100 °C at different comonomer ratios, $\gamma = [MAIGlc]_0/[BIEM]_0$ between 1 and 25, keeping the comonomer-to-catalyst ratio at a constant value of $\mu = ([MAIGlc]_0 + [BIEM]_0)/[(PPh_3)_2NiBr_2]_0 = 100$. Under that condition, almost full conversion was reached within 5 h for $\gamma > 10$. The tendency is markedly different from the case of AIGlc (sugar-carrying acrylate), where ca. 120 h were required to reach full conversion at $\gamma = 10$.[23] This is an indication that the bulky isopropylidene-protected glucofuranoside side group in MAIGlc is not a crucial factor to retard the polymerization rate

as in the case of AIGlc. The molecular weights and molecular weight distribution of the copolymers were characterized by GPC/viscosity using universal calibration and conventional GPC in THF and NMP. The results are given in Table 3. In all samples, the molecular weights determined by GPC-viscosity are higher than the apparent ones obtained by GPC, indicating highly branched structures. The ratios of $M_{n,GPC\text{-}VISCO}$ to $M_{n,GPC\text{-}THF}$ of the copolymers are 2.35-1.92, suggesting that that a suitable amount of AB* inimer, BIEM, in the feed leads to a considerably compact structure, and the difference in the amount has an influence on the molecular weights and compact structure in solution. All samples show relatively low polydispersities.

As can be seen in Figure 4, the elution curves shift toward higher molecular weights with increasing comonomer ratio, γ. Number-average molecular weights of the copolymers consistently increase with γ, Molecular weights up to $M_{n,GPC\text{-}VISCO}$ = 29,800 could be obtained at γ = 25. The same tendency was observed in SCVCP of *tert*-butyl acrylate with an acrylate-type inimer via ATRP[31] as well as SCVCP of methyl methacrylate with a methacrylate-type inimer having a silylketene acetal group via group transfer polymerization[32] and also with the solution polymerization of 2-(diethylamino)ethyl methacrylate with a methacrylate-type inimer.[28] These results suggest that the relationship between the molecular weights and γ is independent on the polymerization and catalyst systems, and may be attributed to an inherent tendency for cyclization in SCVCP process.

Table 3. Self-Condensing Vinyl Copolymerization of BIEM and MAIGlc at Different Comonomer Ratios γ[a]

γ[b]	$M_{n,GPC-THF}$[c] (M_w/M_n)	$M_{n,GPC-NMP}$[d] (M_w/M_n)	$M_{n,GPC-VISCO}$[e] (M_w/M_n)	α[f]	DB_{NMR}[g]	DB_{theo}[h]	BIEM ratio in polymer		
							Calcd.[i]	Obsd. (NMR)[j]	Obsd. (EA)[k]
1	9,300 (1.81)	6,300 (1.45)	17,500 (2.01)	0.20	0.47	0.49	0.50	0.60	0.48
1.5	7,900 (1.94)	-	17,600 (2.12)	0.22	0.42	0.47	0.40	0.40	0.36
2.5	9,500 (1.75)	-	18,000 (1.85)	0.26	0.32	0.40	0.29	0.33	0.29
5	10,100 (1.51)	6,700 (1.53)	21,000 (1.55)	0.30	0.24	0.24	0.17	0.19	0.18
10	11,100 (1.53)	7,700 (1.43)	23,300 (1.57)	0.34	0.12	0.17	0.09	0.10	0.10
25	15,400 (1.44)	-	29,800 (1.71)	0.28		0.08	0.04	0.06	0.08

[a]Copolymerization at 100°C with $(PPh_3)_2NiBr_2$ at a constant comonomer-to-catalyst ratio, μ = ([MAIGlc]$_0$+[BIEM)$_0$])/[catalyst]$_0$) = 100 in the presence of ethyl acetate (50 wt % to MAIGlc). Almost full conversion was reached after 2-5 h. [b]γ= [MAIGlc]$_0$/[BIEM]$_0$. [c]Determined by GPC using THF as eluent with PtBMA standards. [d]Determined by NMP-phase GPC using PS standards. [e]Determined by GPC/viscosity measurement. [f]Mark-Houwink exponent as determined by GPC/viscosity measurement. [g] Degree of Branching as determined by ^{1}H NMR using eq 2. [h] Theoretical degree of branching as determined using eq 3. [i]Calculated from the composition in feed. [j]Determined by ^{1}H-NMR. [k]Determined from elemental analysis using the bromine content.

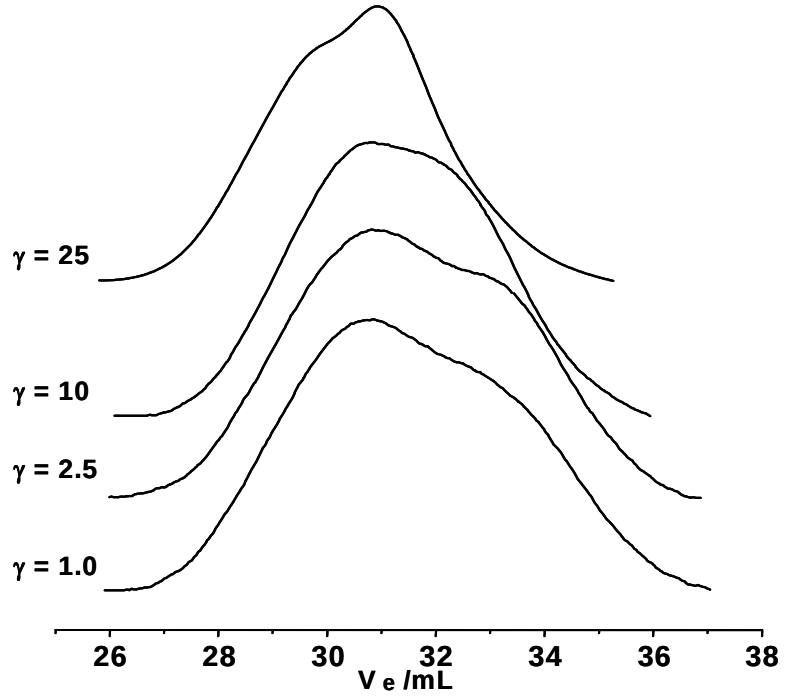

Figure 4. *GPC traces of branched copolymers obtained by SCVCP of BIEM and MAIGlc at different comonomer ratios, γ = $[MAIGlc]_0/[BIEM]_0$. See Table 3 for detailed polymerization conditions.*

Mark-Houwink plots and contraction factors,[33] g'=$[\eta]_{branched}/[\eta]_{linear}$, as a function of the molecular weight for representative branched polymers obtained by SCVCP are shown in Figures 5a and 5b. Relationships between solution viscosity and molecular weight have been determined, and the Mark-Houwink constant typically varies between 0.34 and 0.20, depending on the degree of branching. In contrast, the exponent is typically in the region of 0.6-0.8 for linear homopolymers in a good solvent with a random coil conformation. The Mark-Houwink exponent of the mixture of linear poly(MAIGlc)s is 0.51 ± 0.03, which is similar to that of linear poly(AIGlc)s (α = 0.52 ± 0.03).[23] This result suggests that the relatively lower exponent values of the sugar-carrying polymers are mainly due to bulky isopropylidene-protected glucofuranoside side chains, resulting in less favorable interactions with the solvent. As shown in Figure 5a, the intrinsic viscosities of the branched polymers are significantly lower than those of the linear one in the higher molecular weight range ([M] > 10^4), suggesting a more compact architecture. Figure 5b shows that the contraction factors for all the branched polymers decrease with increasing molecular weights. The GPC/viscosity measurements of branched poly(methyl methacrylate),[32] poly(*tert*-butyl

acrylate)s[31,34], poly[2-(diethylamino)ethyl methacrylate],[28] and poly(AIGlc)s[23] obtained by SCVCP with a (meth)acrylic-type inimer showed the similar tendency, suggesting the feasibility of the viscosity improvement by the inimer incorporation, regardless of the nature of inimer and comonomer. In other words, the bulky side groups in MAIGlc and AIGlc have no significant influence on the general tendency of macroscopic quantities in branched polymers, in which intrinsic viscosity and radius of gyration can be controlled by the branched architecture. These observations indicate that the differences in the molecular weights obtained from the GPC/viscosity compared to conventional GPC arises from a systematic decrease in Mark-Houwink exponent, α, and the contraction factor, g', due to a compact structure resulting from the increased number of branches. It must be noted that multimodal GPC traces obtained with γ = 2.5, 10, and 25 (Figure 4) indicate the presence of fractions with different hydrodynamic volumes. The Mark-Houwink plots (Figure 5a) of the corresponding polymers, however, are not affected, indicating that the different fractions have similar structure.

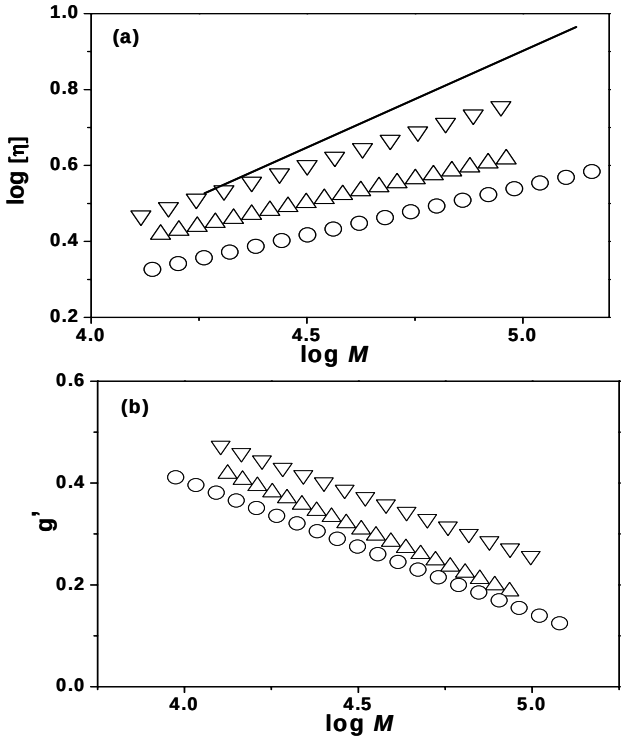

Figure 5. *Mark-Houwink plots (a) and contraction factors, g'=$[\eta]_{branched}/[\eta]_{linear}$ (b) for the polymers obtained by SCVCP of BIEM and MAIGlc: γ = 1.5 (○), 5.0 (△), 10 (▽). The intrinsic viscosity of a linear poly(MAIGlc) (—) is given for comparison.*

The influence of the (theoretical) fraction of branchpoints in the polymers, 1/(1+γ), on the Mark-Houwink exponent is shown in Figure 6. In the whole range of γ values, the exponents of the branched polymers are significantly lower (α = 0.2-0.34) compared to that for linear poly(MAIGlc) (α = 0.51 ± 0.03). Such systematic decrease in the Mark-Houwink exponent, α, as well as the contraction factor, g', provides conclusive evidence for a more compact architecture with an increased number of branches.

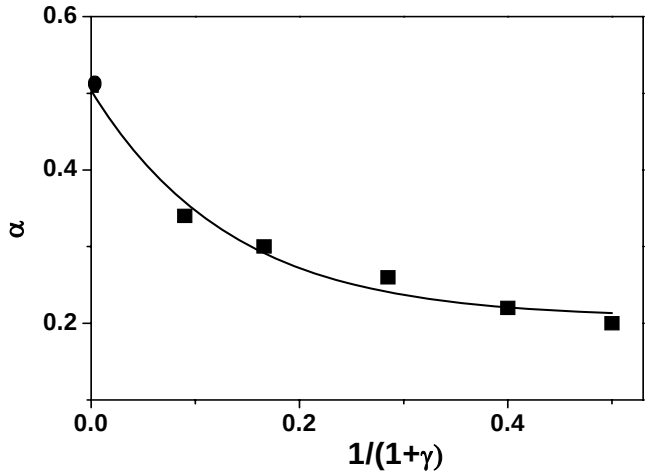

Figure 6. *Dependence of the Mark-Houwink exponent, α, on the fraction of branchpoints (■). (●): Linear poly(MAIGlc).*

In the case of ideal SCVCP via ATRP, the resulting branched polymers carry one bromoester function per inimer unit, and the functionality decreases with comonomer (MAIGlc) composition. As can be seen in Figure 7, the bromine content of the branched polymers is dependent upon the comonomer composition in the feed and is in fair agreement with the calculated values. This is an indication that unfavorable termination and transfer reactions are essentially negligible under the condition used in this study, and the number of bromoester end groups can be simply determined by the comonomer ratio, γ, in the feed. This result also indicates the feasibility to use the bromoester end groups for further modifications and as the initiating part for polymerization of a second monomer.

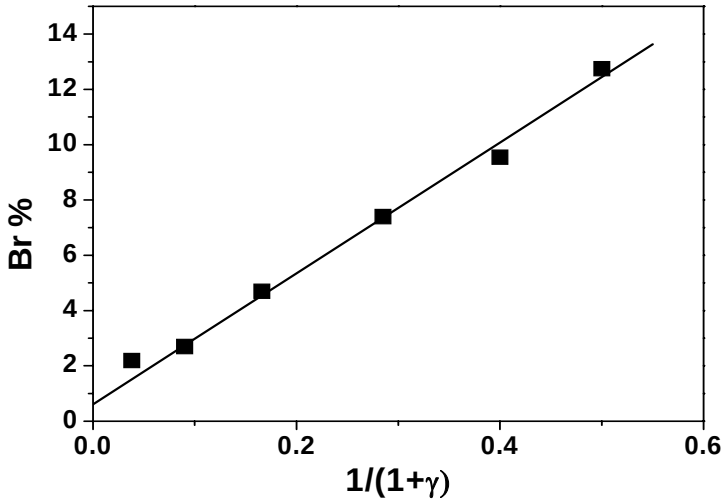

Figure 7. *Dependence of bromine content on the fraction of branching units. Samples: see Table 3. The calculated values (—) are given for comparison.*

The structures of the linear and branched poly(MAIGlc)s were also confirmed by ^{1}H NMR. Figure 8 shows ^{1}H NMR spectra with the complete assignment of the linear and branched poly(MAIGlc)s, as well as poly(BIEM) obtained by a homo-SCVP of BIEM. The characteristic peaks at 1.2-1.4 ppm (isopropylidene protons), 3.8-5.0 and 5.7-6.0 ppm are clearly seen in the linear poly(MAIGlc). In the case of the copolymers, besides the signal of poly(MAIGlc) segment, the BIEM inimer signals appear at 4.1-4.5 and 1.9-2.0 ppm which correspond to the protons of the ethylene linkage of BIEM and methyl protons adjacent to a bromine atom (A* and M* in the polymer chain end and B* in the 2-bromoisobutyryloxy group), respectively. Apart from these peaks, a peak around 0.8-1.4, which is formed by addition of the monomer to B* and is assigned to b, should exist. However, this peak b is invisible, because it is overlapping not only with the isopropylidene protons of the poly(MAIGlc) segment, but also with the methyl protons of the polymer backbone. The BIEM content in the copolymers obtained by SCVCP was determined from the ^{1}H NMR spectra by comparing the peaks at 3.8-5.0 ppm attributed to the sum of six protons (A, B, C, F, G) of the poly(MAIGlc) segment and four protons of the ethylene linkage as mentioned above, and the peak at 5.7-6.0 ppm corresponding to one proton (H) of the poly(MAIGlc) segment, as shown in Figure 8. Thus, the comonomer composition can be calculated using the equation 1,

$$\frac{6H(x) + 4H(1 - x)}{1H(x)} = \frac{\text{Integral at } 3.8 - 5.0 \text{ ppm}}{\text{Integral at } 5.7 - 6.0 \text{ ppm}} \quad (1)$$

where *x* is the fraction of the monomer and 1-*x* is the fraction of the inimer in the polymer. The comonomer fractions calculated from the ratio of these peaks are in good agreement with the comonomer composition in the feed, which corresponds to the γ value, as can be seen in Table 3. The comonomer fractions were also determined by elemental analysis via bromine content, which are also consistent with the theoretical values within experimental error. The agreements suggest complete inimer incorporation.

^{13}C NMR measurements were used for the characterization of the resulting branched architectures. Figure 9a shows characteristic peaks at 176.3 (d), 171.7 (g), 63.5 (e), 62.9 (f), 55.9 (h), 45.1 (b), 31.1 (i), and 17.6 (c) ppm for poly(2-(2-bromoisobutyryloxy)ethyl methacrylate), which is a perfectly linear analogue of poly(BIEM) and was prepared by ATRP of 2-hydroxyethyl methacrylate, followed by esterification with α-bromoisobutyryl bromide.[28,35] In the case of the linear poly(MAIGlc), characteristic peaks at 177.5 (N), 110.0 (L), 107.6 (M), 24,6, 24.1, 23.4 (D, E, I, J) ppm can be seen (Figure 9c). In addition to these peaks, a quaternary carbon peak at 40.6 ppm (h´) is clearly observed in the copolymer obtained by SCVCP of BIEM and MAIGlc (Figure 9b), which is attributed to the branching point.

In order to get further insight regarding the branched architectures, ^{1}H-^{13}C two dimensional (heteronuclear single quantum correlation) measurements were also used, in which ^{13}C measurements were done under *J* mode to distinguish between different types of carbon in the polymers. In Figure 10a, the 2D NMR of linear poly(MAIGlc) shows well-separated and sharp peaks. The tertiary carbon (-CH_3) and methine carbon (-CH) have peaks in the same direction, whereas methylene (–CH_2) and quaternary carbon show peaks in the opposite direction. Figure 10a depicts clearly the ^{1}H-^{13}C correlation peaks characteristic for linear poy(MAIGlc). In addition to these peaks, a quaternary carbon peak at 40.6 ppm (h`), which has no corresponding peak in the $^{1}H$ NMR, is observed in the polymer obtained by SCVCP of MAIGlc and BIEM (Figure 10b). This peak (h`) is assigned to b formed by activation of the 2-bromoisobutyryloxy moieties (B*) and subsequent addition of MAIGlc, which is attributed to the branching points.

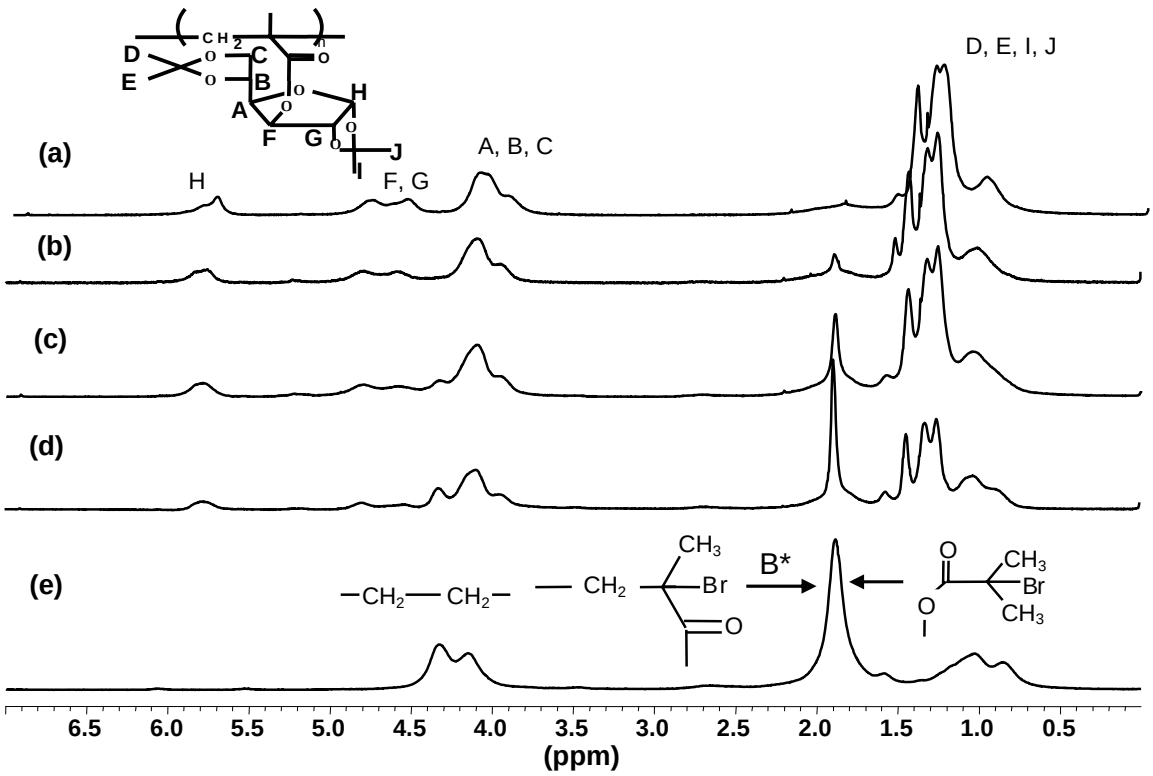

Figure 8. *^{1}H NMR spectra ($CDCl_3$) of the linear (a) and branched poly(MAIGc): γ = 10 (b), 2.5 (c), 1.0 (d), and poly(BIEM) (e).*

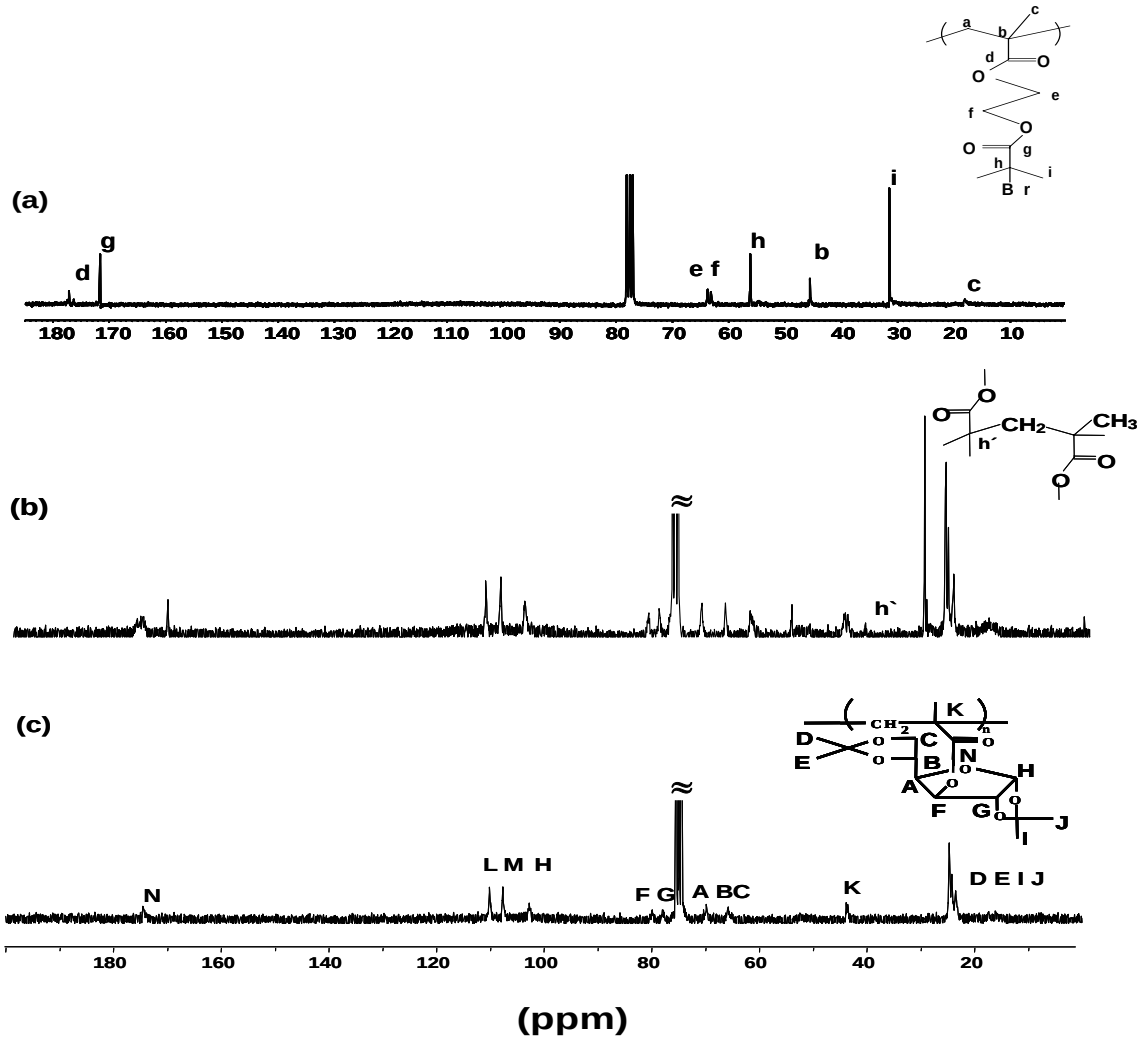

Figure 9. *^{13}C NMR spectra ($CDCl_3$) of the linear poly(2-(2-bromoisobutyryloxy)ethyl methacrylate) (a), the polymer obtained by SCVCP of BIEM and MAIGlc at γ = 1.5 (b), and linear poly(MAIGlc) (c).*

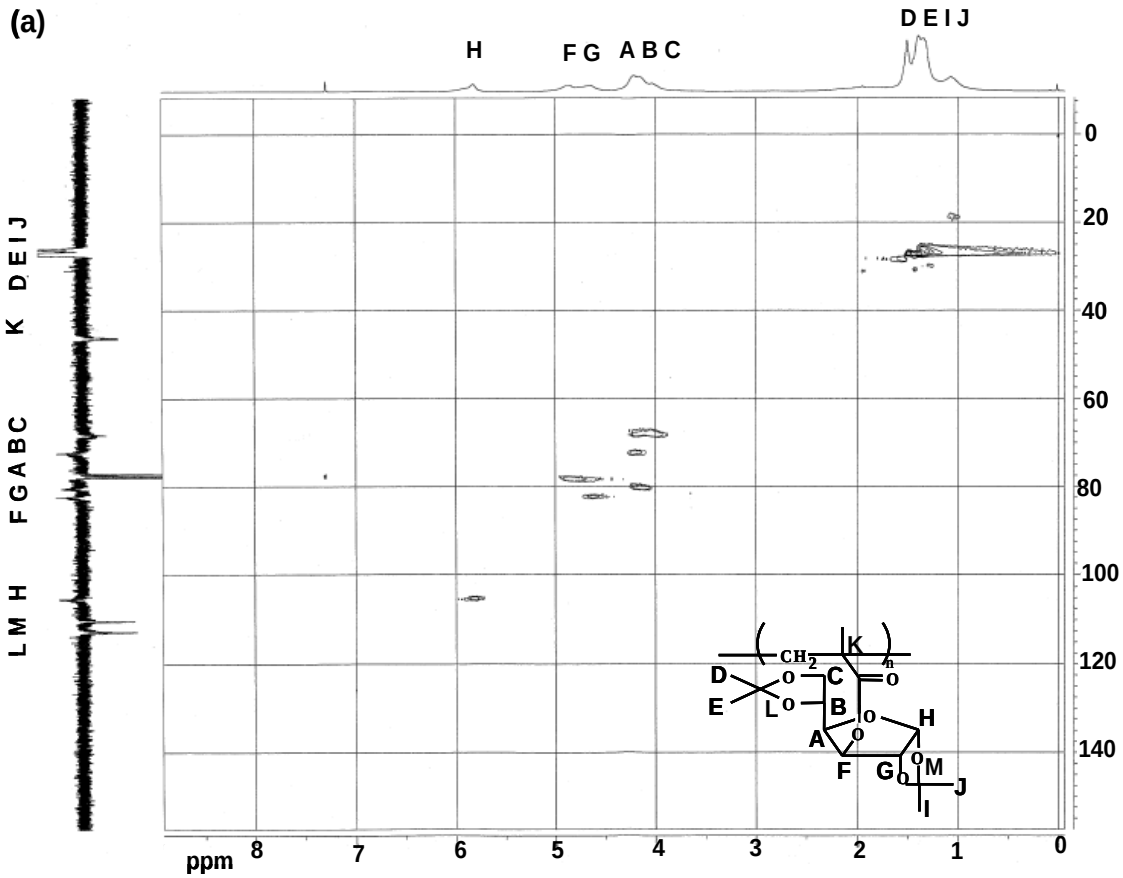
(a)
H
FG ABC
DEIJ
K DEIJ
FGABC
LMH
ppm
8
7
6
5
4
3
2
1
0
0
20
40
60
80
100
120
140
K
CH2
n
D
O
C
O
E
L
O
B
O
H
A
O
F
G
O
M
O
J
I

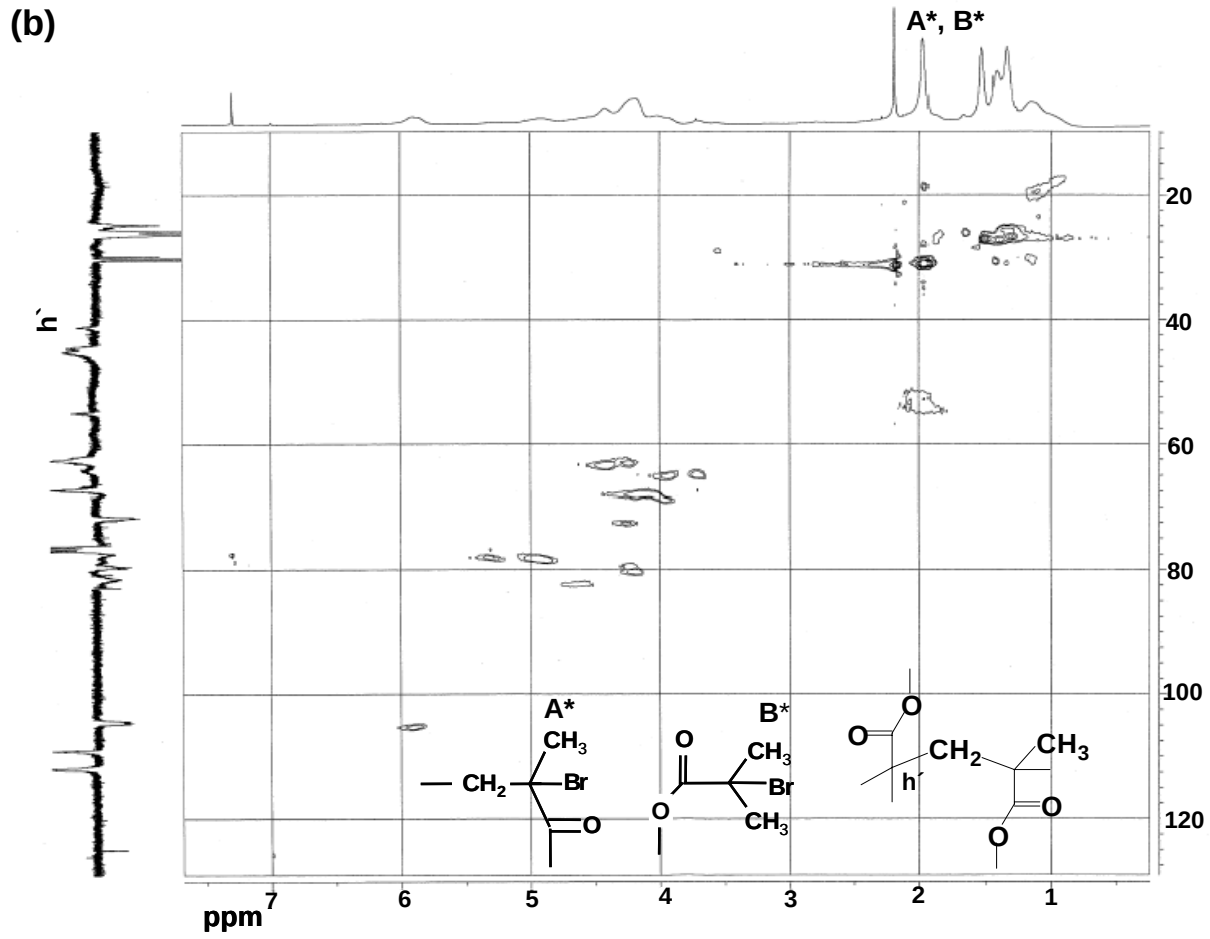

Figure 10. *^{1}H -^{13}C Heteronuclear single quantum correlation of linear poly(MAIGc) (a), and the copolymer obtained by SCVCP of BIEM and MAIGlc at γ = 1.5 (b).*

Degree of Branching (DB). The direct determination of DB for hyperbranched methacrylates obtained by SCVP of methacrylate-type inimers via ATRP was reported to be impossible, although NMR experiments afforded a conclusive measurement of DB in the cases of hyperbranched acrylates.[23,31] For poly(BIEM), the proportion of B* and b can not be determined directly, because of the overlapping signals of the methyl protons in the polymer backbone with the methyl protons from the B* and b groups.[30] In case of the copolymers obtained by SCVCP, these peaks (B* and b) should be related to the degree of branching and the comonomer composition. In our copolymerization system, we have indirectly calculated the proportion of b using ^{1}H NMR. For equal reactivity of active sites, the degree of branching determined by NMR, DB_{NMR}, at full conversion is given as.[36]

$$DB_{NMR} = 2\left(\frac{b}{\gamma+1}\right)\left[1-\left(\frac{b}{\gamma+1}\right)\right] \qquad (2)$$

According to the theory of SCVCP, DB_{theo}, at full conversion, can be represented as

$$DB_{theo} = \frac{2\left(1 - e^{-(\gamma+1)}\right)\left(\gamma + e^{-(\gamma+1)}\right)}{(\gamma+1)^2} \qquad (3)$$

The fraction of b units could be calculated by comparing the peaks at 3.8-5.0 ppm and peak around 1.9-2.0 ppm in the copolymers ranging from γ = 1 to 10. The peaks at 3.8-5.0 ppm correspond to six protons of poly(MAIGlc) segment and four protons of the inimer, as mentioned earlier. The peak at 1.9-2.0 ppm correspond to methyl protons adjacent to a bromine atom (A* and M* in the polymer chain end and B* in the 2-bromoisobutyryloxy group), respectively. Although B* in BIEM is consumed during the copolymerization, for every B* consumed one A* or M* is formed and consequently, original B* = B^*_{left} + A* + M*. B^*_{left} corresponds to 6 protons, whereas A* + M* has three protons. Once the fractions of the monomer *x* and the inimer 1-*x* in the polymer are known (see eq. 1), we can indirectly calculate the value of B* using the eq. 4. Once B* is known, using the relation B*+ b = 1, b can be evaluated. From these approaches, DB_{NMR} = 0.42 and DB_{theo}= 0.47 can be obtained at γ = 1.5 (b = 0.74). The reliability of this method has already being verified and reported for the branched poly(AIGlc)s.[23]

$$\frac{6H(x) + 4H(1-x)}{6H(B^*) + 3H(1-x)} = \frac{\text{Integral at } 3.8 - 5.0 \text{ ppm}}{\text{Integral at } 1.9 - 2.0 \text{ ppm}} \qquad (4)$$

DB_{NMR} decreases with γ, as predicated by calculations In all the cases, however, the observed values are slightly lower than the calculated ones, which might be attributed to the simplifications made for the calculations i.e. equal reactivity of A*, B*, and M* chain ends. Although NMR experiments afford a conclusive measurement of the degree of branching for lower γ values, the low concentration of branchpoints in the copolymer at γ > 10 does not allow the determination of the degree of branching directly because of low intensities of the peaks in the regions around 1.9-2.0 ppm, as shown in Figure 8. However, for the case of high comonomer ratios, γ >>1, the relation between DB_{theo} and γ becomes very simple and does not depend on the reactivity ratios of the various active centers and is represented as $DB_{theo} \approx 2/\gamma$.

Table 4. Characterization of Branched Poly(MAGlc)s Obtained after Deprotection

γ[a]	$M_{n,GPC}$[b] (M_w/M_n)	$M_{n,calcd}$[c] (M_w/M_n)[f]	BIEM ratio in the polymer	
			Obsd. (EA)[d]	Obsd. (EA)[e]
1	8,100 (1.36)	15,100 (1.45)	0.34	0.48
5	8,900 (1.30)	17,200 (1.53)	0.08	0.18
10	9,500 (1.32)	18,000 (1.43)	0.04	0.10

[a]γ= $[MAIGlc]_0/[BIEM]_0$. [b]Determined by NMP-phase GPC using linear PS standards after hydrolysis. [c]Calculated from $M_{n,GPC\text{-}VISCO}$ of the precursors according to eq. 5. [d]Determined from elemental analysis using the bromine content after hydrolysis. [e]Determined from elemental analysis using the bromine content before hydrolysis. [f]Polydispersity of precursor, from NMP-phase GPC using PS standards (see Table 3).

Deprotection of Linear and Branched Poly(MAIGlc)s. The hydrolysis of the isopropylidene groups in the linear and branched poly(MAIGlc)s was performed by treating the samples with formic acid.[17,23] The final product was obtained by freeze-drying from dioxane after the deprotected polymer was dialyzed against water. The ^{1}H NMR spectra of the linear and branched poly(3-*O*-methacryloyl-α,β-D-glucopyranoside)s, which can be abbreviated as poly(MAGlc)s, are shown in Figure 11. Figure 11a shows that the signals of the isopropylidene protons (1.2-1.4 ppm) completely disappear after the deprotection, and a broad signal attributed to anomeric hydroxyl groups of the sugar moieties (6.4-7.0 ppm) appear. This indicates the quantitative deprotection of the isopropylidene protecting groups. The linear poly(MAGlc)s are white powders completely soluble in water, methanol, and DMSO, but insoluble in THF and acetone. In the case of the branched poly(MAGlc)s, the solubility were dependent upon the comonomer ratios, γ. In the case of γ = 1, the branched poly(MAGlc)s were partially soluble in water, which is due to the 50% of the non-polar inimer segment. For γ > 1.5, the polymers were soluble in water, DMSO, and methanol, but insoluble in THF and acetone. Note that the unchanged resonance signal of protons of the ethylene linkage at 4.0-4.6 ppm (Figure 11) suggests that the branched structure is intact during the complete deprotection of the isopropylidene groups and the BIEM compostition in poly(MAGlc)s is almost same as that before deprotection.

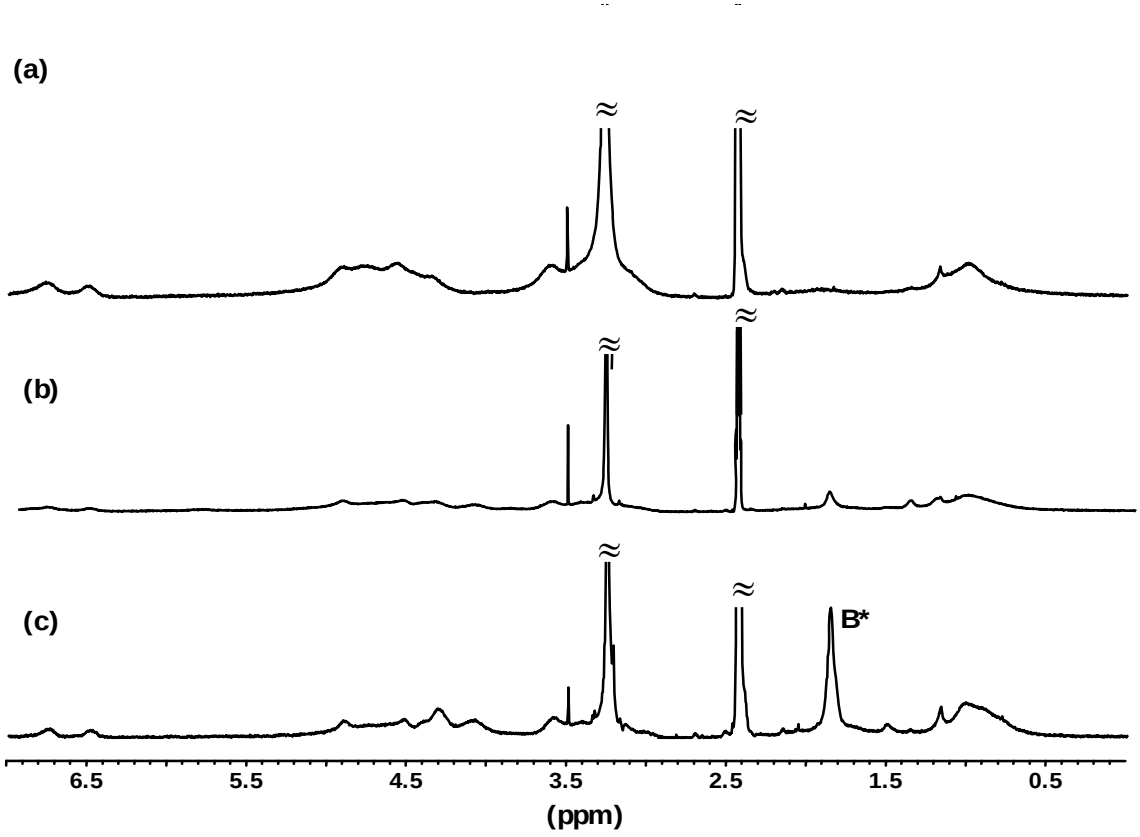

Figure 11. *^{1}H NMR spectra (DMSO-d_6) of the polymers obtained after deprotection of linear poly(MAIGlc) (a), and branched poly(MAIGlc)s: γ = 10 (b), γ = 1.0 (c).*

FT-IR spectra of the linear and branched poly(MAGlc)s obtained after hydrolysis are shown in Figure S-3 (see Supporting Information). Before deprotection, the absorption bands due to the isoproylidene groups are observed at 3000, 1450, and 1380 cm^{-1} assigned to the C-H stretching and C-H asymmetric and symmetric deformation modes, respectively. After the deprotection, these bands disappear and a strong absorption band around 3500 cm^{-1} is observed due to the hydroxyl group formed by the deprotection. The spectrum of the branched poly(MAGlc) at γ = 5 having less branching points is almost same as that of the linear poly(MAGlc).

Figure 12 represents the NMP-phase GPC traces of the branched poly(MAGlc)s. The results are summarized in Table 4. The expected molecular weights of the branched poly(MAGlc)s, $M_{n,calc}$, can be approximately calculated as

$$M_{n,calc} = M_{n,GPC\text{-}VISCO} \text{ of poly(MAIGlc) x } \frac{m_{MAGlc}\gamma + m_{BIEM}}{m_{MAIGlc} + m_{BIEM}} \qquad (5)$$

where m_{MAIGlc}, m_{MAGlc}, and m_{BIEM} are the molar masses of the monomer and inimer, respectively. As can be seen from Table 4, the calculated number-average molecular weights are higher than the apparent values determined by NMP-phase GPC using PS standards. The number-average molecular weights and molecular weight distributions of poly(MAIGlc)s determined by NMP-phase GPC using PS standards are also different from those obtained using THF-phase GPC using PtBMA standards (see Table 3 and Table 4). Obviously, these molecular weights are not accurate, due to the linear samples of a different polymer used as calibration standards. The molecular weight and molecular weight distribution of the linear poly(MAGlc) is M_n = 18,200 (M_w/M_n = 1.22) which is fairly in agreement with $M_{n,calcd.}$ = 17,400. Nevertheless, there is no significant difference in the molecular weight between the samples before and after the deprotection, suggesting that the hydrolysis proceeds smoothly without destruction of the branched branching architectures. However, the somewhat lower polydispersity indices suggest that the low molecular weight part of the polymers was removed in the dialysis process.

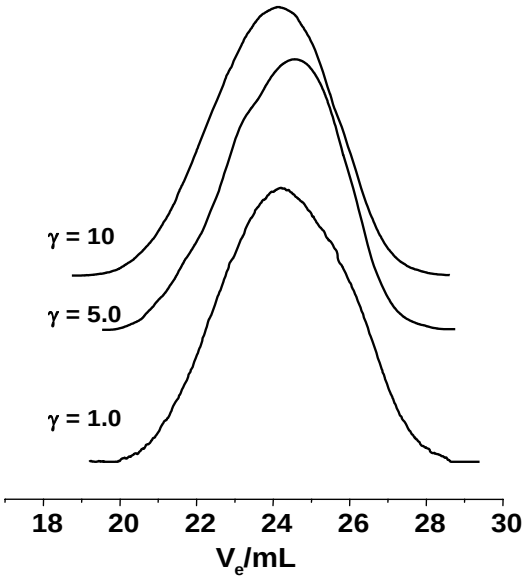

Figure 12. *NMP-phase GPC traces of branched poly(MAGlc)s*

The bromine contents of the representative branched poly(MAGlc)s obtained by elemental analysis were 10.51 %, 2.66 %, and 1.27 % for γ = 1.0, 5.0 and 10, repectively (Calcd: 15.61 %, 5.2 %, and 2.89 %, respectively), while the values of the same samples before the hydrolysis were 12.75 % 4.70 % , and 2.70 %. The reasonable bromine content of the

hydrolyzed product indicates that most of the terminal bromester groups are kept without any modification during the hydrolysis reaction and can be used for further modifications. The carbon and hydrogen contents of the branched and homo poly(MAGlc)s were also determined using elemental analysis. For instance, the atomic composition of the hydrolyzed homopolymer was C, 43.89; H, 6.8 (Calcd: C, 43.5; H, 5.6) while the value of the same sample before the hydrolysis was C, 59.05; H, 7.6 (Calcd: C, 54.8; H, 6.7). For the hydrolyzed branched copolymer (γ =1), the atomic composition was C, 45.6; H, 6.1(Calcd: C, 42.96; H, 5.51) while values of the same sample before hydrolysis were C, 52.1; H, 6.6 (Calcd: C, 49.5; H, 6.1). These results indicate that the deprotection of the isopropylidene groups in the branched and linear poly(MAIGlc)s proceeds selectively to yield the desired branched and linear poly(MAGlc)s.

4.4. Conclusions

We have demonstrated that the $(PPh_3)_2NiBr_2$ catalyst system could be successfully employed for the homopolymerization of MAIGlc and SCVCP of BIEM and MAIGlc, which resulted in the synthesis of monodisperse linear poly(MAIGlc)s and randomly branched poly(MAIGlc)s with relatively high molecular weights, respectively. The bulky isopropylidene-protected sugar moiety in MAIGlc had no significant influence on the polymerization rate as in the case of AIGlc, and both the homopolymerization and SCVCP proceeded smoothly within reasonable polymerization time. The deprotection of the isopropylidene protecting groups resulted in water-soluble linear and branched poly(MAGlc)s, which can be employed as effective tools for various biological and medicinal applications. This work substantially broadens and extends the scope of facile and straightforward strategy for generating water-soluble glycopolymers and their precursors by a controlled polymerization technique.

Acknowledgement. We appreciate S.Wunder for her help during GPC-VISCO measurement. We would like to thank Daniel Varon and Meloni Schanobel for the 2D NMR measurement. Günter Jutz and Anna Dietel are acknowledged for MALDI-TOF MS and elemental analysis measurements, respectively.

Supporting Information Available: Figures S-1, S-2 and S-3. This material is available free of charge via the internet at http://pubs.acs.org.

4.5. References

(1) Lee, Y. C.; Lee, R. T. *Accounts of Chemical Research* **1995**, *28*, 321-327.

(2) Wassarman, P. M. *Science* **1987**, *235*, 553-560.

(3) Chen, X. M.; Dordick, J. S.; Rethwisch, D. G. *Macromolecules* **1995**, *28*, 6014-6019.

(4) Dordick, J. S.; Linhardt, R. J.; Rethwisch, D. G. *Chemtech* **1994**, *24*, 33-39.

(5) Klein, J.; Kunz, M.; Kowalczyk, J. *Makromolekulare Chemie-Macromolecular Chemistry and Physics* **1990**, *191*, 517-528.

(6) Bovin, N. V.; Gabius, H. J. *Chemical Society Reviews* **1995**, *24*, 413-&.

(7) Dwek, R. A. *Chemical Reviews* **1996**, *96*, 683-720.

(8) Varki, A. *Glycobiology* **1993**, *3*, 97-130.

(9) Zanini, D.; Roy, R. *Journal of Organic Chemistry* **1998**, *63*, 3486-3491.

(10) Aoi, K.; Itoh, K.; Okada, M. *Macromolecules* **1995**, *28*, 5391-5393.

(11) Roy, R.; Pon, R. A.; Tropper, F. D.; Andersson, F. O. *Journal of the Chemical Society-Chemical Communications* **1993**, 264-265.

(12) Wulff, G.; Schmid, J.; Venhoff, T. *Macromolecular Chemistry and Physics* **1996**, *197*, 259-274.

(13) Ladmiral, V.; Melia, E.; Haddleton, D. M. *European Polymer Journal* **2004**, *40*, 431-449.

(14) Narain, R.; Jhurry, D.; Wulff, G. *European Polymer Journal* **2002**, *38*, 273-280.

(15) Labeau, M. P.; Cramail, H.; Deffieux, A. *Macromolecular Chemistry and Physics* **1998**, *199*, 335-342.

(16) Ejaz, M.; Ohno, K.; Tsujii, Y.; Fukuda, T. *Macromolecules* **2000**, *33*, 2870-2874.

(17) Ohno, K.; Tsujii, Y.; Fukuda, T. *Journal of Polymer Science Part a-Polymer Chemistry* **1998**, *36*, 2473-2481.

(18) Ohno, K.; Tsujii, Y.; Miyamoto, T.; Fukuda, T.; Goto, M.; Kobayashi, K.; Akaike, T. *Macromolecules* **1998**, *31*, 1064-1069.

(19) Narain, R.; Armes, S. P. *Chemical Communications* **2002**, 2776-2777.

(20) Narain, R.; Armes, S. P. *Macromolecules* **2003**, *36*, 4675-4678.

(21) Li, Z. C.; Liang, Y. Z.; Chen, G. Q.; Li, F. M. *Macromolecular Rapid Communications* **2000**, *21*, 375-380.

(22) Liang, Y. Z.; Li, Z. C.; Chen, G. Q.; Li, F. M. *Polymer International* **1999**, *48*, 739-742.

(23) Muthukrishnan, S.; Jutz, G.; André, X.; Mori, H.; Müller, A. H. E. *Macromolecules* **2005**, *38*, 9-18.

(24) Klein, J.; Herzog, D.; Hajibegli, A. *Makromolekulare Chemie-Rapid Communications* **1985**, *6*, 675-678.

(25) Mori, H.; Böker, A.; Krausch, G.; Müller, A. H. E. *Macromolecules* **2001**, *34*, 6871-6882.

(26) Matyjaszewski, K.; Gaynor, S. G.; Kulfan, A.; Podwika, M. *Macromolecules* **1997**, *30*, 5192-5194.

(27) Benoît, H.; Grubisic, Z.; Rempp, P.; Decker, D.; Zilliox, J. G. *J. Chem. Phys.* **1966**, *63*, 1507.

(28) Mori, H.; Walther, A.; André, X.; Lanzendörfer, M. G.; Müller, A. H. E. *Macromolecules* **2004**, *37*, 2054-2066.

(29) Spickermann, J.; Martin, K.; Raeder, H. J.; Muellen, K.; Schlaad, H.; Müller, A. H. E.; Krueger, R. P. *European Mass Spectrometry* **1996**, *2*, 161-165.

(30) Matyjaszewski, K.; Pyun, J.; Gaynor, S. G. *Macromolecular Rapid Communications* **1998**, *19*, 665-670.

(31) Mori, H.; Seng, D. C.; Lechner, H.; Zhang, M. F.; Müller, A. H. E. *Macromolecules* **2002**, *35*, 9270-9281.

(32) Simon, P. F. W.; Müller, A. H. E. *Macromolecules* **2001**, *34*, 6206-6213.

(33) Burchard, W. *Adv. Polym. Sci.* **1999**, *143*, 113-194.

(34) Mori, H.; Müller, A. H. E. *Dendrimers V: Functional and Hyperbranched Building Blocks, Photophysical Properties, Applications in Materials and Life Sciences* **2003**, *228*, 1-37.

(35) Zhang, M.; Breiner, T.; Mori, H.; Müller, A. H. E. *Polymer* **2003**, *44*, 1449-1458.

(36) Litvinenko, G. I.; Simon, P. F. W.; Müller, A. H. E. *Macromolecules* **1999**, *32*, 2410-2419.

4.6. Supporting Information to the paper

Synthesis and Characterization of Methacrylate-Type Hyperbranched Glycopolymers via Self-Condensing Atom Transfer Radical Copolymerization

By Sharmila Muthukrishnan[†], Hideharu Mori[§], Axel H. E. Müller[†,*]

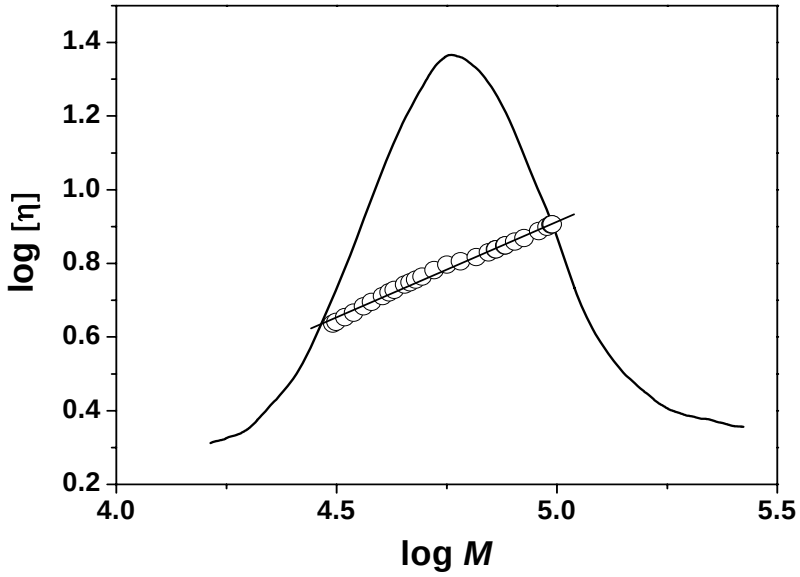

Figure S-1. *Mark-Houwink plot for mixture of linear poly(MAIGlc)s. Mark-Houwink exponent,* $\alpha = 0.51 \pm 0.03$.

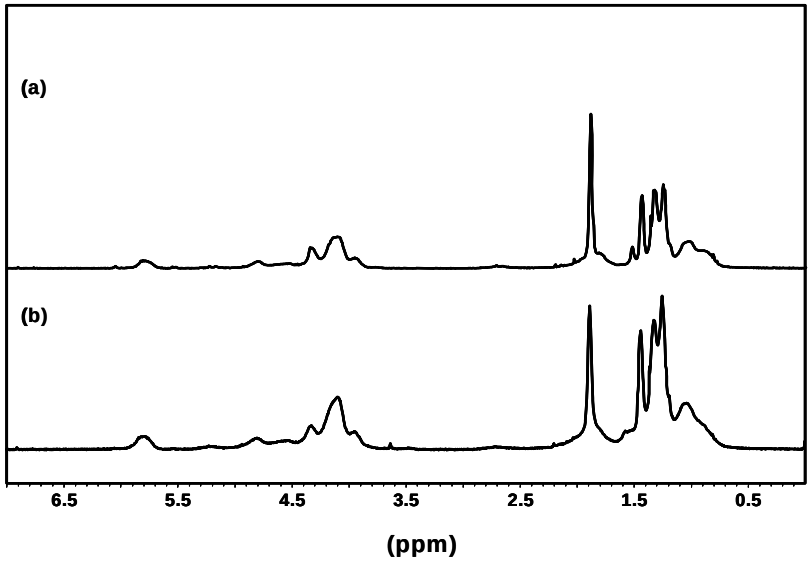

Figure S-2. *^{1}H NMR spectra ($CDCl_3$) of the polymers obtained by SCVCP of MAIGlc and BIEM obtained at γ = 1.5 using CuBr/HMTETA at 60 ºC (a) and $(PPh_3)_2NiBr_2$ at 100 ºC (b)*

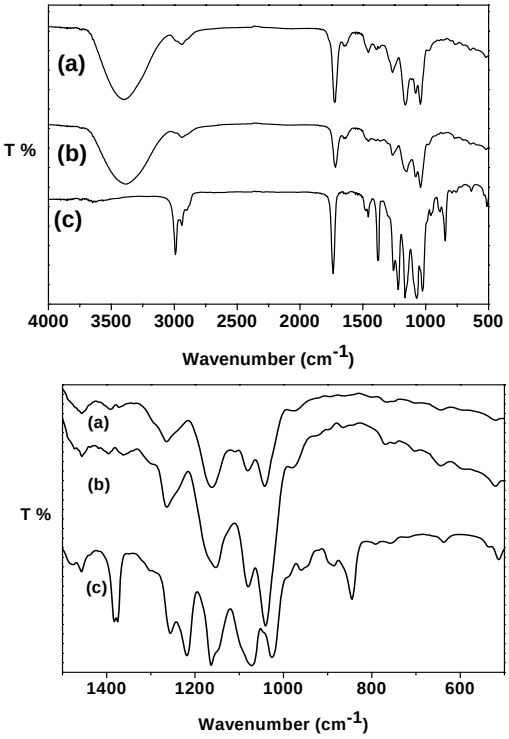

Figure S-3. *FT-IR spectra of (a) branched poly(MAGlc) (γ = 5.0), (b) linear poly(MAGlc), (c) linear poly((MAIGlc).*

5. Synthesis and Characterization of Surface-Grafted Hyperbranched Glycomethacrylates

Sharmila Muthukrishnan[†], Dominik P. Erhard[†], Hideharu Mori[§], Axel H. E. Müller[†,*]

[†]Makromolekulare Chemie II, and Bayreuther Zentrum für Kolloide und Grenzflächen, Universität Bayreuth, D-95440 Bayreuth, Germany

[§] Department of Polymer Science and Engineering, Faculty of Engineering, Yamagata University, 4-3-16, Jonan, Yonezawa, 992-8510, Japan

[*] To whom correspondence should be addressed. e-mail: *Axel.Mueller@uni-bayreuth.de*, Phone:+49 (921) 55-3399, Fax: +49 (921) 55-3393

Submitted to *Macromolecules*

Abstract: Hyperbranched glycopolymers are grafted from a silicon wafer with a covalently attached initiator layer of α-bromoester fragments using self-condensing vinyl copolymerization (SCVCP) of the methacrylic AB* inimer, 2-(2-bromoisobutyryloxy)ethyl methacrylate (BIEM) and a sugar-carrying monomer, 3-*O*-methacryloyl-1,2:5,6-di-*O*-isopropylidene-α-D-glucofuranose (MAIGlc) via atom transfer radical polymerization (ATRP). The film thickness and characteristic surface morphology were determined using ellipsometry and scanning force microscopy (SFM), respectively. The thickness and roughness of the resulting surfaces depend on the catalyst amount and the comonomer ratio, $\gamma = [MAIGlc]_0/[BIEM]_0$. A linear polymer brush of MAIGlc was also obtained in the presence of a sacrificial initiator via ATRP. Deprotection of the isopropylidene groups of the branched and linear polymer brushes resulted in hydrophilic surfaces as investigated by contact angle measurements. The quantitative deprotection was also confirmed by diffuse-reflectance infrared spectroscopy (DRIFT-IR). X-ray photoelectron spectroscopy (XPS) was further used to determine the surface chemical composition before and after deprotection.

5.1. Introduction

The surface properties of inorganic materials can be easily tailored by the preparation of ultrathin films from a variety of polymers. Polymer brushes with desired thickness grafted to or from solid substrates are very useful for a wide range of applications like protective coatings,[1] to enhance the biocompatibility of materials,[2] and the fabrication of electronic devices.[3] Polymer brushes can serve as smart materials, since they may collectively react to environmental stimuli such changes of the pH or ionic strength, temperature, solvent quality, or mechanical forces.[4,5] Polymer brushes have been prepared from block copolymers where one block is strongly adsorbed to the surface with the other block forming the brush layer.[6] The non-covalent nature of this method can result in low surface coverage and desorption of the brushes from the surface. In order to circumvent these problems, an increasing amount of interest has been devoted to the covalent attachment of the polymer chains to surfaces so called "grafting to" approach which was limited by crowding of the chains at the surface hindering the diffusion of chain ends to surface for further attachment.[7,8] The best strategy for the synthesis of high-density and well-controlled polymeric brushes is the "grafting from" approach, where the functionalized initiators are covalently attached to the solid substrate and then linear chains are grown from the surface to give the covalently attached polymer chains by using free-radical polymerization.[9,10] Controlled/"living" radical polymerization has gained considerable attention in recent years and is being increasingly employed for the well-defined synthesis of polymer brushes of high grafting density. [11-19]

We have previously demonstrated a novel synthetic approach for the preparation of the hyperbranched (meth)acrylates on a planar solid substrate, in which a silicon wafer grafted with an initiator layer composed of an α-bromoester fragment was used for a self-condensing vinyl polymerization (SCVP) via atom transfer radical polyemerization (ATRP).[20,21] Here, we have adopted the similar strategy towards the one pot synthesis of hyperbranched glycomethacrylates at the surface of a silicon wafer.

Recently, there has been an increasing attention paid to synthetic polymers with pendant saccharide moieties, so called glycopolymers, as biological recognition substances.[22] Since carbohydrate-based monomers and polymers confer high hydrophilicity and water-solubility, they are of main interest with respect to very specialized applications in biochemical and biomedical fields. Glycopolymers can serve as a model system to study the specific molecular recognition functions of saccharides and to investigate carbohydrate-based interactions.[23-26] Glycopolymers at the cell surface are involved in numerous biological functions: adhesion, cell growth regulation, cancer cell metastasis and inflammation.[26] They

have been used to understand nature´s multivalent processes[27] and as well-defined models of cell surface multiantennary glycoproteins.[28] Glycodendrimers have been tested for bacterial adhesion hemagglutination assays.[29]

Here, we report on the synthesis and characterization of surface-initiated self-condensing vinyl copolymerization of a methacrylic AB* monomer (inimer) with the sugar-carrying methacrylate monomer, 3-*O*-methacryloyl-1,2:5,6-di-*O*-isopropylidene-α-D-glucofuranoside (MAIGlc) using a silicon wafer functionalized with covalently attached monolayers of initiators for ATRP to synthesize highly branched glycomethacrylates at the surface. Such a chemically sensitive surface with a high density of functional groups can be employed for several technological applications like chemical sensing, cellular engineering and can also be used as support materials for combinatorial chemistry. The molecular recognition abilities of these surfaces composed of glycopolymers can be conveniently estimated by measuring the strength of their interactions with appropriate proteins and are useful in the field of surface glycoengineering.[30] Hence, such interfaces can be considered as useful tools for understanding the protein-carbohydrate interactions in terms of molecular and cell recognition abilities of saccharides.

Fukuda et al. reported the grafting of MAIGlc by immobilizing the initiator, 2-(4-chlorosulfonylphenyl)ethyltrimethoxysilane on to a silicon wafer using the Langmuir-Blodgett technique and then used ATRP to obtain surface-grafted linear poly(MAIGlc)s.[15] We have recently reported the synthesis of water-soluble hyperbranched glycopolymer films of sugar-carrying acrylate and methacrylate in solution by self-condensing vinyl copolymerization (SCVCP) via ATRP in the presence of CuBr/PMDETA and $(PPh_3)_2NiBr_2$ catalyst systems.[31,32] As a part of our continuous efforts to prepare glycopolymers of different architectures, involving randomly branched, star and cylindrical brush structures.[31-34] here we report on one-step self-condensing ATRP towards the synthesis of branched glycopolymers of MAIGlc, bearing a bulky side group. In this study, we discuss on the grafting density, surface morphology, wettability and chemical composition of the resulting surfaces depending on the catalyst amount and the comonomer ratio, $\gamma = [MAIGlc]_0/[BIEM]_0$. Deprotection of the bulky isopropylidene groups result in hydrophilic surfaces which were further investigated by SFM, ellipsometry and contact angle measurements. Linear poly(MAIGlc) was also grafted from the surface and characterized thoroughly.

The synthetic approach to hyperbranched glycopolymers grafted from a planar surface is shown in Scheme 1. A silicon wafer grafted with an initiator, B*, for controlled/"living" radical polymerization is used for SCVCP. The inimer is denoted AB* where A is the

methacryloyl group and B* the initiating α-bromoester group of the molecule. The surface initiated polymerization can be initiated in two ways (Scheme 1): (i) the addition of the active B* group of the functionalized silicon wafer to the vinyl group A of the AB* inimer forming dimer with two active sites, A* and B*, and (ii) the addition of a B* group to the vinyl group of monomer M forming a dimer with one active site, M*. Both the initiating B* group and the newly created propagating centers A* and M* can react with any vinyl group in the system. Thus, there are three different types of active centers, A*, B*, and M* on the silicon surface, which can react with double bonds A (inimer and macromolecules; each macromolecule contains strictly one double bond) and M (monomer). A*, B*, M* are active radicals and a, b, m are respective reacted units. Simultaneously, the B* moieties of the AB* inimer can add to the double bonds in solution, i.e. double bonds of another inimer or of the monomer, M, leading to soluble hyperbranched polymer. A part of this polymer can later add to active centers of surface-grafted polymer. This one-pot self-condensing ATRP is versatile and can be regarded as a convenient approach towards the preparation of smart surfaces.

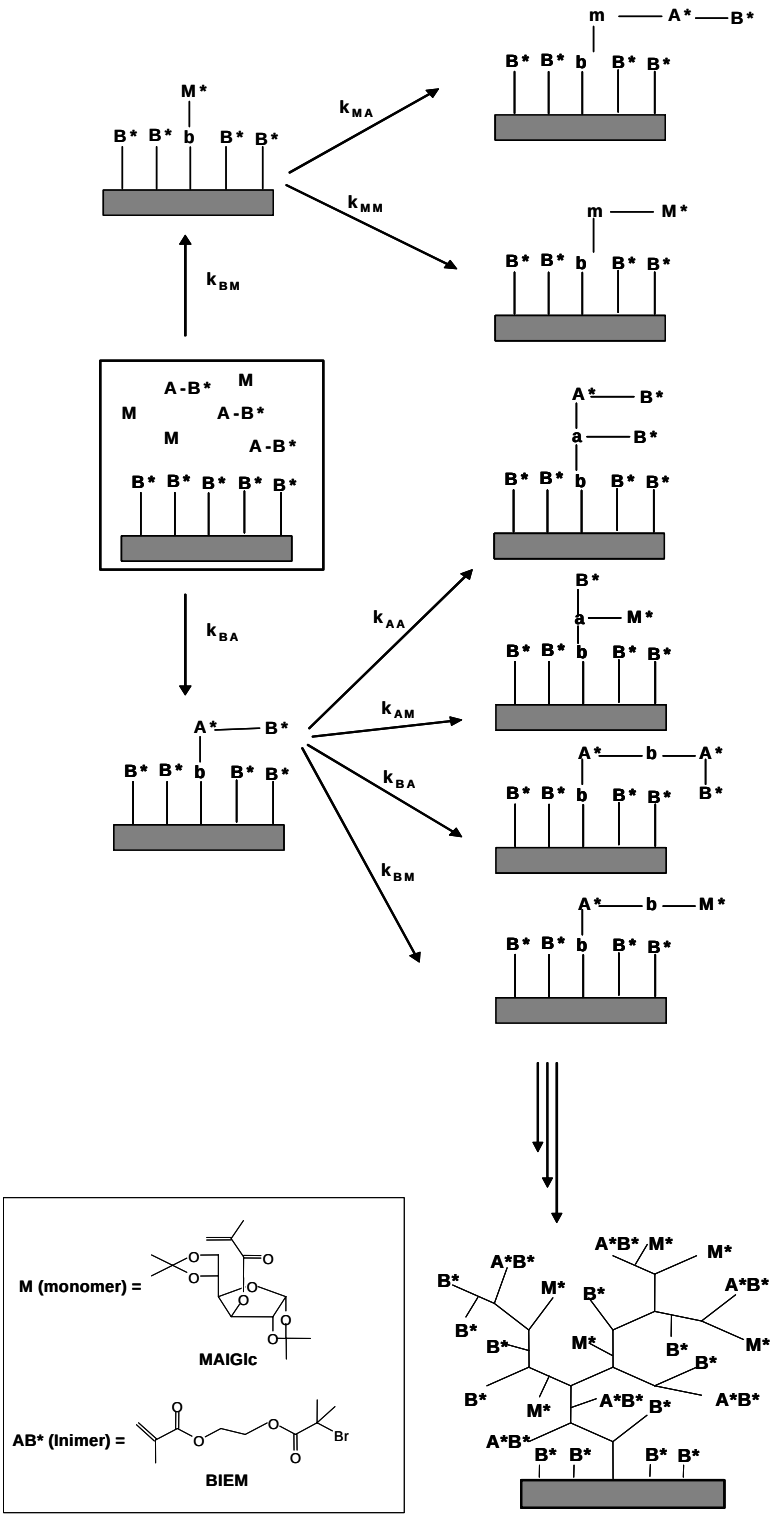

Scheme 1. *General route to the synthesis of surface-grafted hyperbranched glycomethacrylates.*

5.2. Experimental Section

Materials. Bis(triphenylphosphine)nickel(II) bromide ($(PPh_3)_2NiBr_2$, 99%, Aldrich) and trichlorosilane (Cl_3SiH, 99.9% Fluka) were used as received. Ethyl 2-bromoisobutyrate (EBIB, 98%, Aldrich) was distilled and degassed. 3-*O*-Methacryloyl-1,2:5,6-di-*O*-isopropylidene-D-glucofuranose (MAIGlc) was synthesized by the reaction of 1,2:5,6-di-*O*-isopropylidene-D-glucofuranose and methacrylic anhydride in pyridine and purified by vacuum distillation as reported by Klein et al.[35] Synthesis of a methacrylic AB* inimer, 2-(2-bromoisobutyryloxy)ethyl methacrylate (BIEM), was conducted by the reaction of 2-bromo-isobutyryl bromide with 2-hydroxyethyl methacrylate in the presence of pyridine as reported previously.[21,36] The inimer was degassed by three freeze-thaw cycles. Other reagents were commercially obtained from Aldrich and used without further purification. The silicon wafers (100) used in this study were 1.2 × 1.6 cm² in size and were thoroughly cleaned before use as described before.[21] The preparation of the α-bromoester initiator attached to a silicon wafer was conducted by reaction of (5′-trichlorosilylpentyl) 2-bromo-2-methylpropionate with a silicon wafer as reported by Husseman et al.[16] The trichlorosilyl α-bromoester, which has reactive species capable of bonding to the surface and a latent α-bromoester, was prepared by reaction of hex-5-enol with 2-bromoisobutyryl bromide, followed by the hydrosilylation reaction with trichlorosilane. The functionalized silicon wafers were stored at room temperature in a drybox and thereafter used for polymerizations.

Polymerization. All polymerizations were carried out in a round-bottom flask sealed with a plastic cap in the glove-box. A representative example, ($\gamma = 1$) is as follows: distilled and degassed BIEM (0.424 g, 1.52 mmol) was added to a round-bottom flask containing the functionalized silicon wafer, $Ni(PPh_3)_2Br_2$ (12.7 mg, 0.0171 mmol) and MAIGlc (0.5 g, 1.52 mmol) in ethyl acetate (50 wt % to MAIGlc). The covered flask was placed in an oil bath at 100 °C. After 1.5 h, the content was very viscous and the polymerization was stopped by cooling. Conversion of the double bonds as detected by ^1H NMR of the ungrafted material was 95%. Then the mixture was dissolved in THF and was passed through an alumina column. The soluble polymer had M_n = 8,500 and M_w/M_n = 3.30 (as determined by GPC/viscosity using universal calibration). Then the wafer was removed from the mixture and rinsed with THF several times followed by dichloromethane. Finally, any adsorbed polymer was removed from the wafer by Soxhlet extraction in THF for 2 days. Then the wafer was dried under nitrogen and stored at room temperature in air.

A typical experiment for homopolymerization of MAIGlc is as follows: ethyl 2-bromoisobutyrate (EBIB; 11.8 mg, 0.0609 mmol) was added to a round bottom flask containing the functionalized silicon wafer, $Ni(PPh_3)_2Br_2$ (45.0 mg, 0.0609 mmol) and MAIGlc (2.0 g, 6.09 mmol) in ethyl acetate (50 wt % to MAIGlc)). The covered flask was then placed in an oil bath at 100 °C for 1.5 h. Conversion of monomer as detected by ^1H NMR of the ungrafted material was 75%. The soluble polymer had M_n = 30,200 and M_w/M_n = 1.29 (as determined by GPC/viscosity using universal calibration). The ungrafted material was removed in a manner similar to that described above for copolymerization.

Deprotection. The deprotection of the isopropylidene groups of the linear and branched poly(MAIGlc) grafts was performed by dipping the substrates in 80% formic acid for 48 h at room temperature.[15] Then they were washed several times with water and dried in a nitrogen stream. Finally, they were dried at room temperature under vacuum for 24 h.

Characterization. The polymers formed in solution were characterized by GPC using using THF as eluent at a flow rate of 1.0 ml/min at room temperature. Molecular weights of the branched polymers were determined by the universal calibration principle[37] using the viscosity module of the PSS-WinGPC scientific V 6.1 software package. Linear PMMA standards (PSS, Mainz) were used to construct the universal calibration curve. GPC system I; column set: 5μ PSS SDV gel, 10^3 Å, 10^5 Å and 10^6 Å, 30 cm each; detectors: Shodex RI-71 refractive index detector; Jasco Uvidec-100-III UV detector (λ = 254 nm); Viscotek viscosity detector H 502B. The polymers bound loosely to the surface were washed with THF and passed through a neutral alumina column to remove the catalyst residues. ^1H NMR spectra were recorded with a Bruker AC-250 spectrometer. Topographic images of the grafted substrates were observed by Scanning Force Microscopy (SFM), using a Digital Instruments Dimension 3100 microscope operated in Tapping Mode (free amplitude of the cantilever ≈ 30 nm, set point ratio ≈ 0.98). Average surface root-mean-square roughness, (R_{RMS}), of the grafted substrates were evaluated using the roughness analysis tool in the Nanoscope III software.

The thickness of the grafted layer was estimated by Sentec 850 ellipsometer which can determine the ellipsometric angles Ψ and Δ for the whole visible range simultaneously. The measurements were typically performed in the range between 350 and 850 nm and at angles of 40°, 50°, 60°, and 70°. The refractive index of the graft layers used for the evaluation was found by spin-coating a thick layer of the corresponding soluble polymers on the silicon wafer. For the linear polymer brush, a refractive index of 1.429 was obtained. For branched polymers depending upon the comonomer ratio,γ it varied from 1.543 (γ =1) to 1.437 (γ =

10). The thickness was evaluated based on a three layer model (silicon, oxide layer and polymer layer). Surface coverage, Γ (mg/m²), and grafting density, Σ (chains/nm²), were calculated by equations 1 and 2, respectively:

$$\Gamma = h\rho \tag{1}$$

$$\Sigma = \frac{\Gamma \cdot N_A}{M_n} \tag{2}$$

where h is the layer thickness, $\rho = 1.1$ g/cm is the mass density of PMMA, N_A is Avogadro's number and M_n is the number-average molecular weight.

In order to estimate the thickness of the swollen polymer layers, spectroscopic ellipsometry was performed by means of a Spectroscopic ellipsometer M-2000VI (Woolam Inc., USA). The angle of incidence could be set continuously in the range from 45 to 90°. The light source used was a 50-W QHT lamp. M-2000VI measured 500 wavelengths simultaneously covering the spectral range from 370 – 1700 nm. Accurate measurements over the full Δ and Ψ range could be acquired (Δ= 0° - 360°; Ψ= 0° - 90°). Typical measurement times were in the range between 1 to 5 seconds. A cell for liquid media with de-ionized water was used for the measurements of the swollen layers.

Diffuse-reflectance infrared Fourier-transform (DRIFT) spectra were recorded on a Bruker IFS 66V at a resolution of 2 cm^{-1} and 256 scans were taken for all the samples. A well-cleaned bare silicon wafer was used as reference in all the cases. Contact-angle measurements were carried out in air by a sessile droplet technique on a Dataphysics OCA 15 plus instrument (Dataphysics Instruments, GmbH, Germany). The results were evaluated using ellipse fitting.

X-ray photoelectron spectra (XPS) were measured using a Perkin Elmer PHI 5600 ESCA spectrometer with a monochromatic Mg-K X-ray source (E_{exc} = 1253.6 eV). The survey spectra (0-1000 eV) were recorded at an analyzer pass energy of 187.85 eV (step width, 800 meV; step time, 20 ms). For detail spectra, the step width of 25 meV and step time of 100 ms were used. All the spectra were recorded at a takeoff angle of 45°.

5.3. Results and Discussion

Synthesis of Surface-Grafted Hyperbranched Glycopolymers. We have previously reported the synthesis and extensive characterization of silicon wafers with surface-functionalized initiators containing an α-bromoester group capable of initiating self-condensing ATRP of AB* inimers.[21] In this study, we have adopted the similar procedure for the functionalization

of the silicon wafer towards the synthesis of hyperbranched glycopolymers using SCVCP via ATRP. For the synthesis of the surface-grafted hyperbranched glycopolymers with characteristic structure and properties, it is important to adjust the comonomer-to-catalyst ratio, μ = ([MAIGlc]$_0$ + [BIEM]$_0$)/[$(PPh_3)_2NiBr_2$]$_0$, and the comonomer ratio, γ = [MAIGlc]$_0$/[BIEM]$_0$, because these two parameters affect significantly the degree of branching, molecular weights, and polydispersity of the branched polymers obtained by SCVCP. The influence of comonomer ratio, γ are discussed. The effect of the comonomer-to-catalyst ratio, μ, on the thickness, morphology and grafting density of the grafted polymers is described in the Supporting Information (see also Table 1).

Surface topography. Surface topography. The surface topography of the grafted hyperbranched glycopolymers obtained after Soxhlet extraction in THF for 2 days was investigated using tapping mode SFM. Three to four scans were taken at different spots on the sample. Table 1 represents the properties of the soluble as well as grafted polymers obtained. When the copolymerization was carried out with BIEM inimer and MAIGlc monomer at μ = 200 and comonomer ratio, γ = [MAIGlc]$_0$/[BIEM]$_0$, = 1 at 100 °C, a viscous polymer was obtained after 1.5 h. The soluble polymer had M_n = 9,400 and M_w/M_n = 3.23 as determined by GPC/viscosity using universal calibration. Theoretical calculations have shown that the molecular weights and molecular weight distributions of the surface-grafted hyperbranched polymers formed by SCVCP are comparable to those formed in the solution.[38] However, we cannot exclude that a hyperbranched polymer molecule formed in solution attaches with its double bond to one of the active centers of a polymer molecule bound to the surface, increasing its molecular weight. This effect is limited by the disappearance of double bonds due to the intramolecular cyclization reaction. Consequently, the molecular weights of the polymers formed in solution can be regarded as lower limits of those formed on the surface and we do not believe that the difference is extreme.

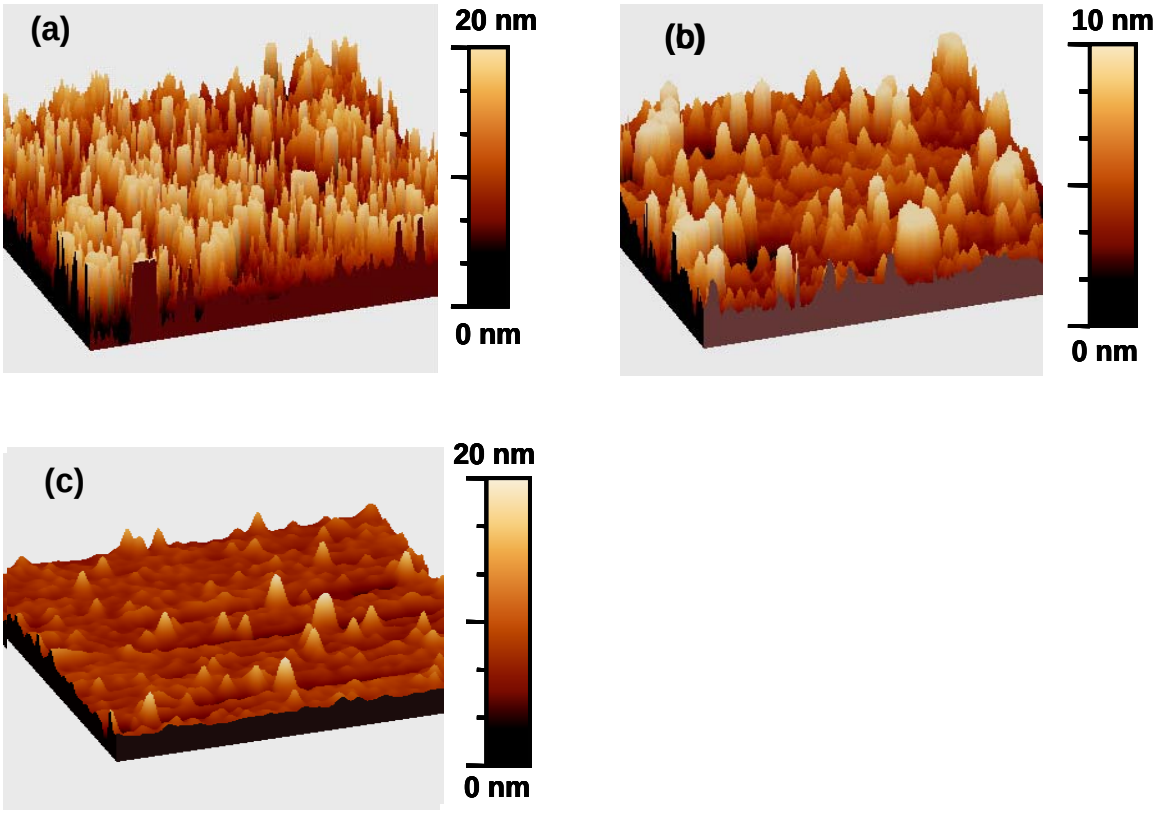

Figure 1. *Three-dimensional height images of the grafted polymers obtained from SCVCP of BIEM and MAIGlc at* $\mu = 200$ *and (a)* $\gamma = 1$*, (b)* $\gamma = 10$*, and (c)* $\gamma = \infty$ *(homopolymerization of MAIGlc). The X, Y scale is 5 µm.*

Table 1. Synthesis and Characterization of Surface-Grafted Highly Branched and Linear Glycomethacrylates and Properties of Soluble Polymers[a]

γ[b]	μ[d]	$M_{n,\ GPC/VISCO}$[e]	M_w/M_n[e]	mean film thickness[f] (nm)	mean roughness[g] (nm)	surface coverage[h], Γ (mg/m^2)	grafting density[i], Σ ($chains/nm^2$)	DB_{theo}[j]	Contact angle[k] (deg)
1[a]	100	8,500	3.30	3.0	2.08	3.30	0.23	0.49	-
1[a]	200	9,400	3.23	6.7	3.58	7.37	0.47	0.49	80.3
5[a]	200	10,500	2.92	6.5	3.15	7.15	0.41	0.29	73.4
10[a]	200	28,000	1.51	6.0	2.12	6.60	0.14	0.09	67.7
∞[c]	-	30,200	1.29	12.0	1.79	13.20	0.26	0	78.0

[a]Copolymerization at 100 °C with $(PPh_3)_2NiBr_2$ in the presence of ethyl acetate (50 wt% to MAIGlc). Almost full conversion was reached after 1.5-3 h. [b]$\gamma = [MAIGlc]_0/[BIEM]_0$. [c]Homopolymerization of MAIGlc (50 wt% to ethyl acetate) with ethyl 2-bromoisobutyrate (equimolar to catalyst) as a controlling initiator at 100 °C with $(PPh_3)_2NiBr_2$. [d]$\mu = ([MAIGlc]_0+[BIEM]_0)/[(PPh_3)_2NiBr_2]_0$. [e]As determined by GPC/viscosity measurement. [f]Determined by ellipsometry. [g]Determined by SFM. [h]According to eq.1. [i]According to eq.2. [j]Theoretical degree of branching. [k]Obtained by sessile drop method using ellipse fitting.

In order to clarify the influence of the comonomer ratio, γ, on the grafting behaviour, SCVCP of BIEM and MAIGlc was carried out at different comonomer ratios, γ = 1, 5 and 10, keeping the comonomer-to-catalyst ratio at a constant value of μ = 200. Table 1 summarizes the results of the soluble and grafted polymers obtained by SCVCP. As can be seen from Table 1, the absolute molecular weights of the soluble polymers increase with the increasing comonomer ratio, γ which confirms to earlier reports on SCVCP.[32,39,40] The mean thickness of the resulting polymer films after Soxhlet extraction slightly decreases with increasing comonomer ratio, γ. At γ = 1 it is 6.7 nm whereas at γ = 10 is 6.0 nm respectively. As can be seen from Figures 1a and c, the protrusions are irregularly distributed throughout the copolymer surface. The roughness of the resulting copolymer surfaces also decreases with the increasing comonomer ratio. The copolymer surface at γ = 1 (Figure 1a) has smaller but more protrusions when compared to the surface at γ = 10 (Figure 1b). The increase in the size in the case of γ = 10 can be due to the accumulation of a higher number of polymer chains. This can also be explained on the basis of the fact that with the increase in the comonomer ratio, γ, the degree of branching decreases. This implies that the copolymer surface at γ = 10, has higher R_g and has larger protrusions. Since $R_g \sim DB^{-1/4} M^{0.4}$,[41] this effect cannot be very large but can still contribute to some extent for the increase in the size of the protrusion compared to the copolymer surface at γ = 1. While decrease in the number of protrusions can be either due to the overlap with the neighbouring protrusions or due to the lower efficiency of the initiating sites on the surface.

A lower efficiency of the initiating sites can be the result of the bulkiness of the monomer, MAIGlc used in this study. With the increase in the comonomer ratio, the monomer content, MAIGlc increases in the system and this can lead to enhanced steric crowding resulting in the decrease of the grafting density as can be seen from Table 1. We have reported a grafting density of 0.39 chains/nm^2 for highly branched PMMA obtained by SCVCP of BIEM and MMA at a comonomer ratio, γ = 10 under similar conditions using the same silicon functionalized initiator whereas in this study, a grafting density of 0.13 chains/nm^2 is obtained for branched poly(MAIGlc) at γ = 10 indicating the strong influence of the bulkiness and geometry of the monomer, MAIGlc used here. The grafting density decreases drastically from 0.47 chains/nm^2 to 0.14 chains/nm^2 depending upon the comonomer ratio, which again indicates that with the increase in the content of MAIGlc in the system, the grafting density decreases due to the enhanced steric crowding. Another possible explanation is that the rigidity of the glycomonomer in the copolymer with high MAIGlc content is related to the

apparent decrease in the grafting density. The significant impact of the bulkiness of the monomer, MAIGlc in reducing the initiating efficiency has already being observed in the case of glycocylindrical brushes and glycostars, respectively.[33,34]

The homopolymerization of MAIGlc was performed from a functionalized silicon wafer using EBIB as a controlling initiator at $[MAIGlc]_0$:$[EBIB]_0$:$[(PPh_3)_2NiBr_2]_0$ ratio of 100:1:1 at 100 °C. After 1.5 h, the monomer conversion (as determined by ^1H NMR) was 75 % resulting in a viscous polymer. The linear poly(MAIGlc) has M_n = 30,200 ($DP_{n,exp.} \approx 80$) and M_w/M_n = 1.29 (as determined by GPC/viscosity using universal calibration), which is fairly in agreement with $M_{n,calcd}$ = 24,600. In living polymerizations of conventional monomers from surface-grafted initiators, the molecular weight and molecular weight distribution of the grafted polymers is often assumed to be almost equal to that of polymer initiated by added soluble initiators.[16,42] The film thickness obtained after Soxhlet extraction for 2 days is 12.5 nm as determined by ellipsometry. This value is in between the diameter of a random coil ($2Rg \approx 2x\ 0.25\ nm\ x\ DP^{1/2} \approx 5$ nm) and that of a fully extended chain ($L_c = 0.25\ nm\ x\ DP_n \approx$ 20 nm), indicating a brush-like structure below the maximum brush density ($\sum_{max}$ = 0.7 chains/nm^2 for linear PMMA brushes as reported by Fukuda et al.[13]). The film thickness should be around 20 nm ($0.25\ nm\ x\ DP_n$) if the backbone of the polymer was fully extended. In our study the measured thickness is much less than the expected value which indicates that the polymer film does not consist of fully extended chains. Such observations have already been reported in literature even if the measured thickness increases with the reaction time, there are certain discrepancies between the calculated and observed values.[19] The SFM height image (Figure 1c) of this surface-grafted poly(MAIGlc) revealed a relatively uniform and smooth surface with a mean roughness of 1.79 nm. The grafting density of the polymer brushes obtained by homopolymerization of MAIGlc is found to be 0.26 chains/nm^2, which is higher than the value of 0.1 chain/nm^2 as obtained by Fukuda et al. for the synthesis linear poly(MAIGlc) brushes by Cu based ATRP from a silicon surface functionalized with 2-(4-chlorosulfonylphenyl) ethyltrimethoxysilane.[15]

Surface Composition. X-ray photoelectron spectroscopy (XPS) was employed to determine the composition of the branched and linear glycopolymer brushes. The survey scan spectra of the branched copolymer surfaces at γ = 1, 5 and the linear polymer brush are shown in Figure S-2 (Supporting Information). The survey scan spectrum of the branched copolymer surface at γ = 1, shows the presence of three elements: oxygen (533 eV), carbon (285 eV), and silicon (150 and 99 eV). Additionally, the bromine peaks assigned to Br_{3d} (70 eV), $Br_{3p1/2}$ (184 eV) and Br_{3s} (278 eV) are also visible. But there are still silicon peaks

indicating that the thickness of the layer is smaller than the photoelectron escape depth of about 11 nm.[43] These results are quite comparable to the thickness and surface topography observed by SFM. The atomic composition (45% C and 42% O) of this branched copolymer brush is fairly in agreement with the calculated value (51% C) indicating the successful formation of the branched polymer on the surface. Since the branched copolymer surface at $\gamma = 1$ has a higher degree of branching and thus more end groups, this results in enhancement and enrichment of bromine groups at the surface which is also clearly confirmed by XPS.

Figures S-2b and c depict the The spectra of the branched copolymer at $\gamma = 5$ and the linear polymer brush show again C, O and Si peaks, but in the case of the linear polymer brush, the signal for Si is very weak since the thickness is comparatively higher. For the copolymer surface at $\gamma = 5$, the bromine peak is seen additionally but the intensity is not as high as in the case of $\gamma = 1$ owing to its lower degree of branching. In case of the linear polymer brush obtained by ATRP, there is no significant peak for bromine. Such observations were also reported for branched poly(*tert*-butyl acrylate)s where significant difference in the Br content at the surfaces of the branched and linear polymers was confirmed by XPS.[21]

Deprotection of MAIGlc to MAGlc Units. The deprotection of the isopropylidene groups on the grafted substrates was performed by treatment with 80% formic acid for 48 h at room temperature.[15,32] The thickness of the graft layer after deprotection for a branched copolymer surface at $\gamma = 10$ decreased from 6.0 to 4.6 nm whereas for the linear polymer brush, it decreased from 12 to 11 nm, respectively. The slight decrease in the thickness after deprotection could be due to the decrease in the volume of the polymer, associated with the removal of the bulky isopropylidene groups which may be partially is compensated by hydration.

The surface topography was again visualized using SFM. Figure 2 depicts the SFM images obtained after deprotection of the grafted substrates at $\gamma = 10$ and for the linear polymer brush. In case of $\gamma = 10$, the protrusions are randomly distributed throughout and the roughness is 1.59 nm, (34% of thickness) which is much smaller than that before hydrolysis (2.12 nm, corresponding to 38% of thickness), but has the same *relative* value (34% of thickness). In the case of the linear polymer brush, the surface roughness is 1.50 (13.5% of thickness) which is comparable to that before hydrolysis (1.79, corresponding to 14% of thickness).

In order to inverstigate the swelling behaviour of the grafted polymer layers in water after deprotection, the ellipsometry measurements in water using a cell for liquid media was performed. As can be seen from Table 2, for the branched copolymer surface at $\gamma = 10$, the thickness of the polymer film increased from 4.6 nm (dry state) to 29.9 nm under water indicating that there is a significant amount of swelling. In the case of linear brush, the thickness increased from 11 nm (dry state) to 19 nm under water indicating that the chains are almost completely strectched under water which is close to its maximum contour length, L_c = 20 nm (0.25 x DP_n).

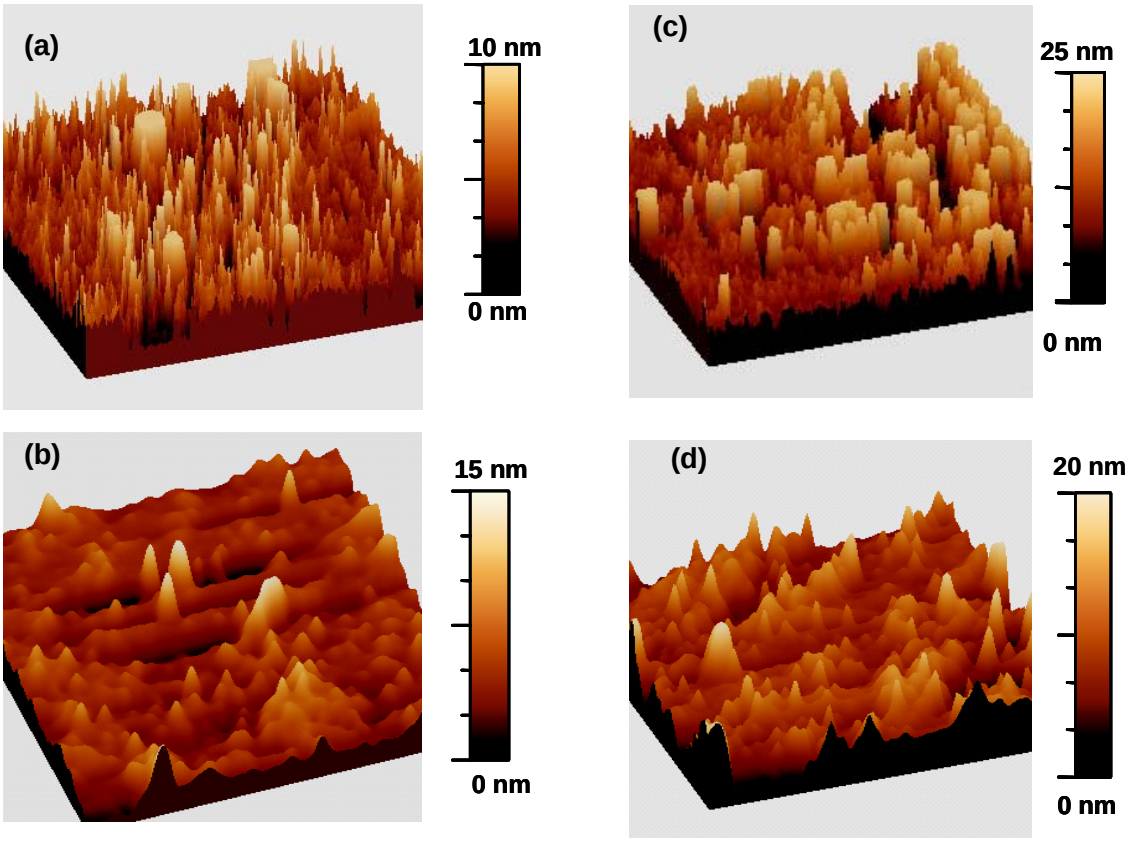

Figure 2. *Three-dimensional height images of the grafted polymers obtained after deprotection in the dry state (a, b) and under water (c, d): (a,c) branched copolymer surface at* $\gamma = 10$ *and (b,d) linear polymer brush. The (X, Y) scale is 5 µm.*

In order to get further insights about the swelling behaviour of these brushes, preliminary measurements were performed using SFM in water. The SFM image in water of the deprotected copolymer surface at $\gamma = 10$ showed a significant increase in the height of the protrusions and are broader than in the dry state as can be seen from Figure 2c and the roughness also increased from 1.59 nm to 4.61 nm, indicating the swelling of the polymer layer in water. In the case of linear polymer brush (Figure 2d) compared to that in dry state, the roughness changed from 1.50 nm to 2.4 nm, respectively. These results indicate that in case of the linear polymer brush, the chains are probably more stretched than the branched copolymer surface in the dry state so the extent of swelling in water is not that significant compared to the branched copolymer surface.

In order to ensure quantitative deprotection, diffuse-reflectance infrared Fourier transform (DRIFT) spectra were measured on the grafted wafers. Figures 3a and b represent DRIFT

spectra for the grafted linear polymer brushes after and before deprotection. Before deprotection, the absorption bands due to the isopropylidene groups are observed at 1450 and 1380 cm^{-1} assigned to the C-H asymmetric and symmetric deformation modes, respectively, as indicated by arrows in Figure 3b. The C-O stretching band of the isopropylidene group is overlapping with the SiO_2 layer which is also detected in the region between 1200 and 1000 cm^{-1}. After the deprotection, these bands disappear and a strong absorption band around 3500 cm^{-1} is observed due to the hydroxyl group formed by the deprotection. The decrease in the intensity of the carbonyl group after deprotection can be due to the decrease in the film thickness. The DRIFT spectrum of the deprotected branched copolymer surface at $\gamma = 10$ is shown in Figure S-3 (Supporting Information). The intensities of the hydroxyl and carbonyl peaks are very weak owing to its very low thickness (4.6 nm). Nevertheless, the absence of the peaks attributed to the isopropylidene groups and presence of the hydroxyl groups around 3500 cm^{-1} are clearly visible, indicating the successful deprotection.

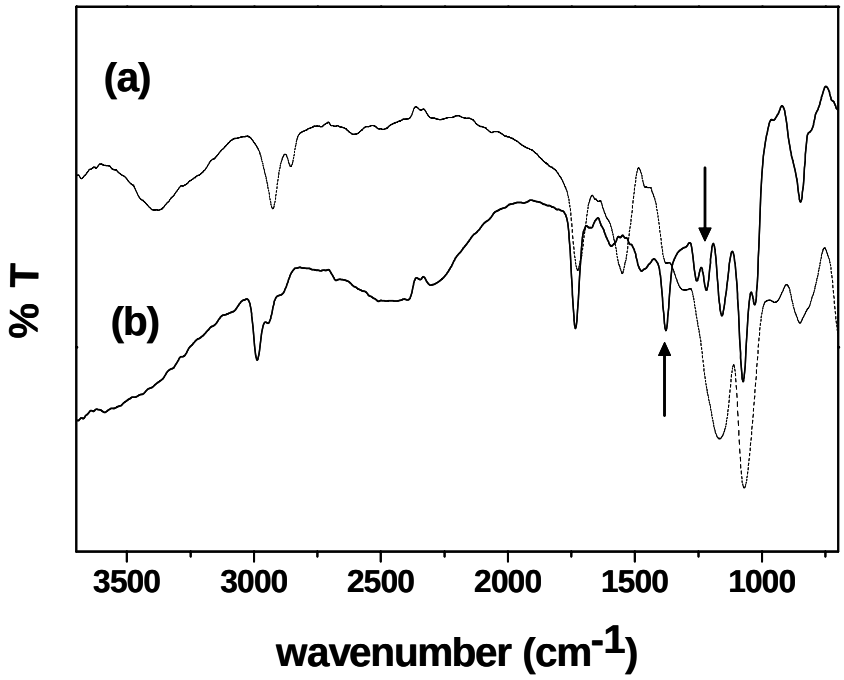

Figure 3. *Diffuse-reflectance infrared fourier transform (DRIFT) spectra of surface-grafted (a) linear poly(MAIGlc) brush after deprotection (b) linear poly(MAIGlc) brush..*

The deprotected substrates were further investigated by XPS in order to determine the surface composition of the resulting surfaces. Figure 4a depicts the XPS survey spectrum of the deprotected branched copolymer surface at $\gamma = 10$. Three elements: oxygen (533 eV), carbon (285 eV), and silicon (150 and 99 eV), are clearly seen similar to that before hydrolysis. The bromine peaks assigned to Br_{3d} (70 eV), $Br_{3p1/2}$ (184 eV) and Br_{3s} (278 eV) are also visible, which shows that a sufficient amount of α-bromoester groups remains, which can be further modified or used to initiate "hyperstars". The atomic composition (48% C and 38% O) is in good agreement with the calculated values (47.0 % C and 42.7% O) of the deprotected branched copolymer surface indicating the successful deprotection of the isopropylidene groups at the surface.

Figure 4b depicts the XPS survey spectrum of deprotected linear poly(MAIGlc) brush. The atomic compositions of 74% C and 25% O (Calcd: O, 28%) are obtained for the linear poly(MAIGlc) brush before deprotection whereas after deprotection the compositions are 67.8% and 31.5% (Calcd: O, 33%), which clearly indicates that after deprotection there is an increase in the oxygen content at the surface due to the presence of the hydroxyl groups and decrease in the carbon content.

Table 2. Characterization of Surface-Grafted Highly Branched and Linear Glycomethacrylates Obtained after Deprotection

γ[a]	$M_{n,calcd}$	mean film thickness[c] (nm)	mean film thickness[d] (nm)	mean roughness[e] (nm)	surface coverage[f], Γ (mg/m^2)	grafting density[g], Σ ($chains/nm^2$)	contact angle[h] (deg)
1	8,100[b]	5.0	-	-	5.5	0.40	58
10	21,700[b]	4.6	29.9	1.59	5.06	0.14	49
∞	21,000	11.0	19.0	1.50	12.1	0.34	39

[a]$\gamma = [MAIGlc]_0/[BIEM]_0$. [b] $M_{n,calcd} = M_{n,GPC\text{-}VISCO}$ of poly(MAIGlc) x $(m_{MAGlc}\gamma + m_{BIEM})/(m_{MAIGlc}\gamma + m_{BIEM})$. [c]As determined by ellipsometry. [d]As determined by ellipsometry under water. [e]As determined by SFM. [f]According to eq.1. [g]According to eq.2. [h]Obtained by sessile drop method using ellipse fitting.

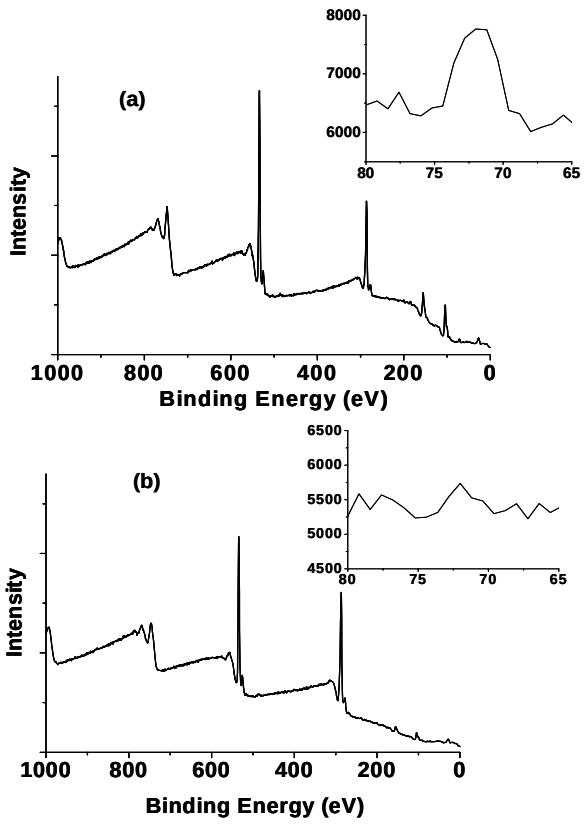

Figure 4. *XPS survey spectra of the grafted polymers obtained after deprotection of (a) branched copolymer brush at* $\gamma = [MAIGlc]_0:[BIEM]_0 = 10$*, (b) linear poly(MAIGlc) brush. Insets: region associated with the peak derived from bromine.*

Tuning Surface Properties. Tables1 and 2 show the water contact angles of series of copolymer surfaces obtained by SCVCP and linear polymer brush obtained via ATRP before and after deprotection of isopropylidene groups, respectively. The copolymer surface of thickness 7.0 nm at $\gamma = 1$ and $\mu = 200$ shows a contact angle of 80.3°. This indicates that the copolymer surface at $\gamma = 1$ is hydrophobic and the hydrophobicity decreases with the increase in the comonomer ratio, γ which could be attributed to the decrease in the roughness and grafting density with the increase in the comonomer ratio. The linear polymer brush with relatively thick and uniform layer of 12.5 nm shows a water contact angle of 78°. These hydrophobic surfaces were transformed into hydrophilic surfaces via deprotection of the isopropylidene groups and further confirmed by contact angle measurements.

As can be seen from Table 2, the deprotected branched copolymer surfaces at $\gamma = 1$ and $\gamma = 10$ have water contact angles of 59° and 49°, repectively, and for linear polymer brush it is

39°. The contact angles in the case of branched copolymer surfaces (γ = 1 and 10) are higher due to the presence of the hydrophobic inimer units when compared to linear poly(MAIGlc) brush. The significant decrease in the contact angles compared to those before deprotection confirms that the substrates are completely hydrophilic due to the presence of hydroxyl groups at the surface. These results indicate the versatility of this approach to prepare surfaces of desired properties and the ease in employing SCVCP via ATRP to achieve this goal. The grafting density of the branched and linear polymer brushes after hydrolysis (table 2) is comparable to that before deprotection (Table 1) indicating that there is no significant degrafting occured during the course of hydrolysis. Such surfaces can be further modified and employed for understanding carbohydrate-protein interactions and as models for understanding complicated nature ´s multivalent processes.

5.4. Conclusions

We present the facile one-pot self-condensing ATRP for the synthesis of surface-grafted hyperbranched glycopolymers. The randomly branched copolymer surfaces possess characteristic architecture, topography and surface tuning properties. To compare the difference in the topography and surface characteristics, linear poly(MAIGlc) brush was also synthesized via ATRP. The linear polymer brush has a relatively smooth and homogenous layer compared to the branched copolymer surfaces. The significant difference in Br content between linear and branched polymers brushes was observed by XPS demonstrates the feasibility to control and modify the surface chemical functionality. Deprotection of the bulky isopropylidene groups results in hydrophilic surfaces and the successful deprotection was confirmed by DRIFT, XPS and contact angle measurements. There were significant differences in the wettability between the randomly branched and linear polymer brushes. Due to the α-bromoeseter terminal units, such surfaces can be further modified and can be employed for several biological applications.

Acknowlegement. Dr. Helmut Hänsel (Physikalische Chemie II), Dieter Will (Anorganische Chemie II) and Daniela Mössner (IMTEK, Freiburg) are acknowledged for ellipsometric, DRIFT-IR and XPS measurements, respectivley. We thank Dr. Oswald Prucker (IMTEK, Freiburg) for valuable suggestions. Roland Schulze (IPF, Dresden) is also greatly acknowledged for the ellipsometric measurements in water.

5.5. References

(1) Israelachvili, J. *Intermolecular and Surface Forces*; Academic Press: New York, 1992.

(2) Dumitriu, S. *Polymeric Biomaterials*; Marcel Dekker: New York, 1994.

(3) Badwen, M. J.; Turner, S. R. *In Electronic and Photonic Applications of Polymers*; Advance in Chemistry Series 218; American Chemical Society: Washington, DC, 1988.

(4) Israels, R.; Gersappe, D.; Fasolka, M.; Roberts, V. A.; Balazs, A. C. *Macromolecules* **1994**, *27*, 6679-6682.

(5) Sevick, E. M.; Williams, D. R. M. *Macromolecules* **1994**, *27*, 5285-5290.

(6) Dan, N.; Tirrell, M. *Macromolecules* **1993**, *26*, 4310-4315.

(7) Bridger, K.; Vincent, B. *European Polymer Journal* **1980**, *16*, 1017-1021.

(8) Benouada, H.; Hommel, H.; Legrand, A. P.; Balard, H.; Papirer, E. *Journal of Colloid and Interface Science* **1988**, *122*, 441-449.

(9) Prucker, O.; Rühe, J. *Macromolecules* **1998**, *31*, 592-601.

(10) Prucker, O.; Rühe, J. *Macromolecules* **1998**, *31*, 602-613.

(11) Rühe, J. *Macromol. Symp.* **1997**, *126*, 215.

(12) Ejaz, M.; Yamamoto, S.; Ohno, K.; Tsujii, Y.; Fukuda, T. *Macromolecules* **1998**, *31*, 5934-5936.

(13) Yamamoto, S.; Ejaz, M.; Tsujii, Y.; Matsumoto, M.; Fukuda, T. *Macromolecules* **2000**, *33*, 5602-5607.

(14) Yamamoto, S.; Ejaz, M.; Tsujii, Y.; Fukuda, T. *Macromolecules* **2000**, *33*, 5608-5612.

(15) Ejaz, M.; Ohno, K.; Tsujii, Y.; Fukuda, T. *Macromolecules* **2000**, *33*, 2870-2874.

(16) Husseman, M.; Malmstrom, E. E.; McNamara, M.; Mate, M.; Mecerreyes, D.; Benoit, D. G.; Hedrick, J. L.; Mansky, P.; Huang, E.; Russell, T. P.; Hawker, C. J. *Macromolecules* **1999**, *32*, 1424-1431.

(17) Advincula, R. C.; Brittain, W. J.; Caster, K. C.; Rühe, J. *Polymer Brushes*; Wiley VCH: Weinheim, 2004.

(18) Matyjaszewski, K.; Pietrasik, J.; Bombalski, L.; Cusick, B.; Kowalewski, T.; Pyun, J. *Polymer Preprints (American Chemical Society, Division of Polymer Chemistry)* **2005**, *46*, 498-499.

(19) Matyjaszewski, K.; Miller, P. J.; Shukla, N.; Immaraporn, B.; Gelman, A.; Luokala, B. B.; Siclovan, T. M.; Kickelbick, G.; Vallant, T.; Hoffmann, H.; Pakula, T. *Macromolecules* **1999**, *32*, 8716-8724.

(20) Mori, H.; Müller, A. H. E. *Dendrimers V: Functional and Hyperbranched Building Blocks, Photophysical Properties, Applications in Materials and Life Sciences* **2003**, *228*, 1-37.

(21) Mori, H.; Böker, A.; Krausch, G.; Müller, A. H. E. *Macromolecules* **2001**, *34*, 6871-6882.

(22) Lee, Y. C.; Lee, R. T. *Accounts of Chemical Research* **1995**, *28*, 321-327.

(23) Bovin, N. V.; Gabius, H. J. *Chemical Society Reviews* **1995**, *24*, 413.

(24) Bliss, T. V. P.; Collingridge, G. L. *Nature* **1993**, *361*, 31.

(25) Wassarman, P. M. *Science* **1987**, *235*, 553-560.

(26) Dwek, R. A. *Chemical Reviews* **1996**, *96*, 683-720.

(27) Zanini, D.; Roy, R. *Journal of Organic Chemistry* **1998**, *63*, 3486-3491.

(28) Aoi, K.; Itoh, K.; Okada, M. *Macromolecules* **1995**, *28*, 5391-5393.

(29) Roy, R.; Pon, R. A.; Tropper, F. D.; Andersson, F. O. *Journal of the Chemical Society-Chemical Communications* **1993**, 264-265.

(30) Sun, X.-L.; Faucher, K. M.; Houston, M.; Grande, D.; Chaikof, E. L. *Journal of the American Chemical Society* **2002**, *124*, 7258-7259.

(31) Muthukrishnan, S.; Jutz, G.; André, X.; Mori, H.; Müller, A. H. E. *Macromolecules* **2005**, *38*, 9-18.

(32) Muthukrishnan, S.; Mori, H.; Müller, A. H. E. *Macromolecules* **2005**, *38*, 3108-3119.

(33) Muthukrishnan, S.; Zhang, M.; Burkhardt, M.; Drechsler, M.; Mori, H.; Müller, A. H. E. *Macromolecules* **2005**, *38*, 7926-7934.

(34) Muthukrishnan, S.; Plamper, F.; Mori, H.; Müller, A. H. E. *Macromolecules* **2005**, *ASAP*.

(35) Klein, J.; Herzog, D.; Hajibegli, A. *Makromolekulare Chemie-Rapid Communications* **1985**, *6*, 675-678.

(36) Matyjaszewski, K.; Gaynor, S. G.; Kulfan, A.; Podwika, M. *Macromolecules* **1997**, *30*, 5192-5194.

(37) Benoît, H.; Grubisic, Z.; Rempp, P.; Decker, D.; Zilliox, J. G. *J. Chem. Phys.* **1966**, *63*, 1507.

(38) Litvinenko, G. I.; Muller, A. H. E. *Macromolecules* **2002**, *35*, 4577-4583.

(39) Simon, P. F. W.; Müller, A. H. E. *Macromolecules* **2001**, *34*, 6206-6213.

(40) Mori, H.; Walther, A.; André, X.; Lanzendörfer, M. G.; Müller, A. H. E. *Macromolecules* **2004**, *37*, 2054-2066.

(41) Zhulina, E. B.; Vilgis, T. A. *Macromolecules* **1995**, *28*, 1008.

(42) Huang, X.; Wirth, M. J. *Macromolecules* **1999**, *32*, 1694-1696.

(43) Chen, X.; Gardella, J. A.; Kumler, P. L. *Macromolecules* **1993**, *26*, 3778-3783.

5.6. Supporting Information to the paper

Synthesis and Characterization of Surface-Grafted Hyperbranched Glycomethacrylates

By Sharmila Muthukrishnan[†], Dominik P. Erhard[†], Hideharu Mori[§], and Axel H. E. Müller[†],*

Effect of Comonomer-to-Catalyst Ratio, μ, on Film Thickness and Grafting Density. The mean thickness of the polymer layer as determined by ellipsometry obtained from the SCVCP of MAIGlc and BIEM at a constant comonomer ratio, $\gamma = 1$, increases from 3.0 nm to 6.7 nm when increasing the comonomer-to-catalyst ratio, μ, from 100 to 200. The surface roughness also increases with the increasing ratio. As can be seen from Figure S-1, the polymer film obtained at $\mu = 200$ shows densely packed protrusions distributed throughout the copolymer surface, whereas in the case of $\mu = 100$, the copolymer surface has lower grafting density and film thickness. The variation in the film thickness with the comonomer-to-catalyst ratio, μ, can be attributed to the fact that in the case of a higher ratio, more initiating sites are activated on the surface due to the high solubility of the catalyst in the inimer as well as the monomer and different number of polymer chains are attached to the surface. Since there is no significant difference in the number-average molecular weights between these soluble polymers, the size of the protrusion basically depends on different numbers of polymer chains enclosed in it. The size of the protrusions also seems to increase slightly with the catalyst ratio, indicating that higher catalyst ratio induces an increase in the size of the protrusions by accumulating more number of polymer chains. These results indicate that by changing the comonomer to catalyst ratio, the film thickness and surface topography of the surface-grafted hyperbranched glycopolymers can be easily controlled.

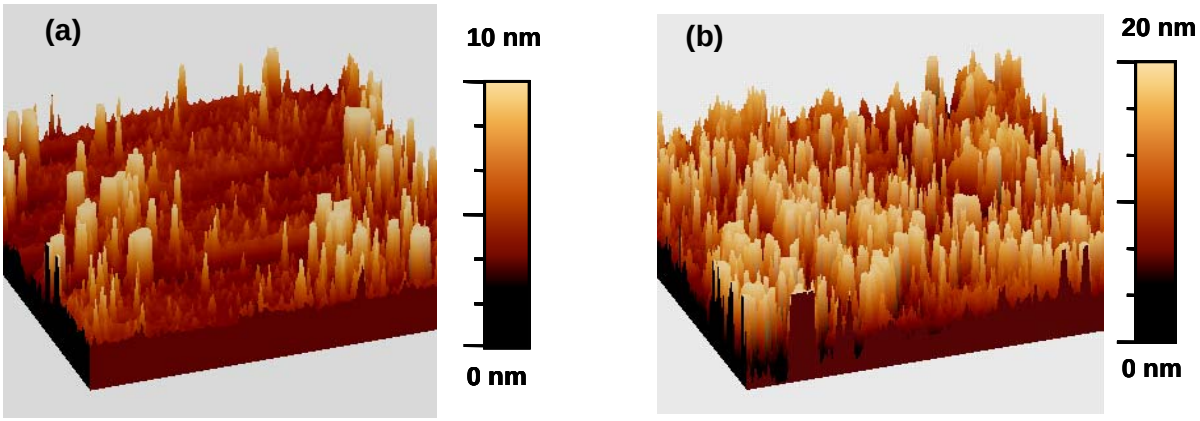

Figure S-1. *Three-dimensional height images of the grafted polymers obtained from SCVCP of BIEM and MAIGlc at a constant comonomer ratio,* $\gamma = 1$ *(a)* $\mu = 100$*, (b)* $\mu = 200$*.*

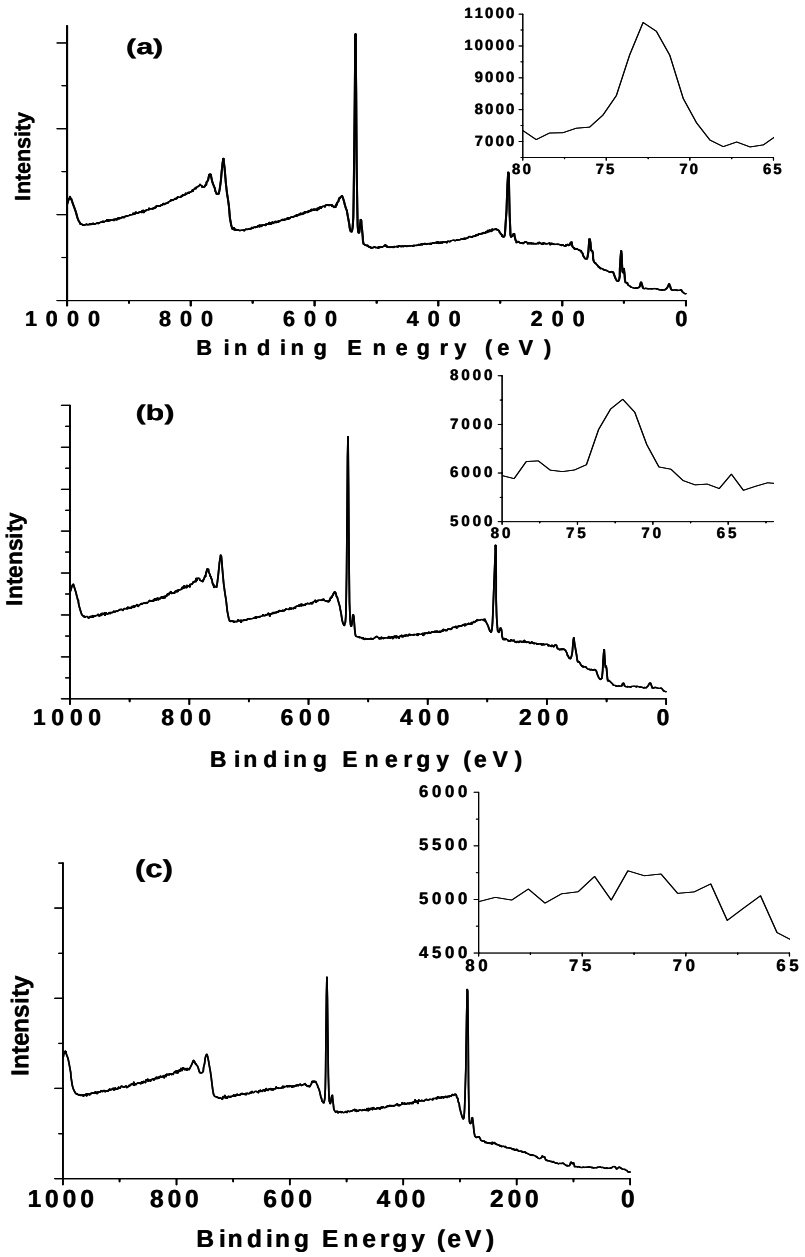

Figure S-2. *XPS survey spectra of the grafted polymers obtained from SCVCP of BIEM and MAIGlc at γ = [MAIGlc]0:[BIEM]0 = 1 (a) and 5 (b), and (c) homopolymerization of MAIGlc. Insets: region associated with the peak derived from bromine.*

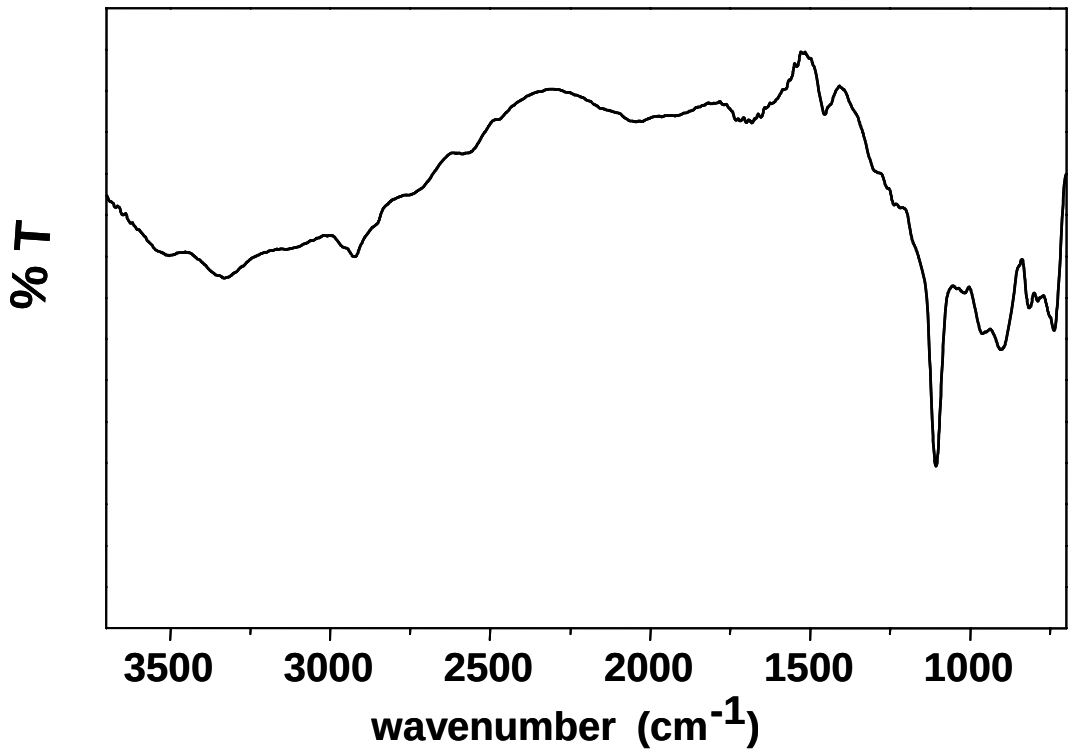

Figure S-3. *Diffuse-reflectance infrared fourier transform (DRIFT) spectra of surface-grafted branched copolymer brush at $\gamma = 10$ obtained after deprotection.*

6. Molecular Sugar Sticks: Cylindrical Glycopolymer Brushes

Sharmila Muthukrishnan[†], Mingfu Zhang[†,$], Markus Burkhardt[†], Markus Drechsler[†], Hideharu Mori[§], Axel H. E. Müller[†,*]

[†]Makromolekulare Chemie II and Bayreuther Zentrum für Kolloide und Grenzflächen, Universität Bayreuth, D-95440 Bayreuth, Germany

[§] Department of Polymer Science and Engineering, Faculty of Engineering, Yamagata University, 4-3-16, Jonan, Yonezawa, 992-8510, Japan

[*] To whom correspondence should be addressed. e-mail:axel.mueller@uni-bayreuth.de, fax: +49 (921) 55-3393

[$] Present address: Polymer Science and Engineering, University of Massachusetts, Amherst, MA 01003, USA

Published in *Macromolecules* 2005, 38, p. 7926

Abstract: We report the synthesis of glycocylindrical brushes ("molecular sugar sticks") with poly(3-*O*-methacryloyl-α,β-D-glucopyranose), (PMAGlc) side chains, using the 'grafting from' approach via atom transfer radical polymerization (ATRP) of the protected monomer, 3-*O*-methacryloyl-1,2:5,6-di-*O*-isopropylidene-D-glucofuranose (MAIGlc). The formation of well-defined brushes with narrow length distribution was confirmed by GPC-MALS and ^{1}H NMR. The initiating efficency of the initiating sites of the polyinitiator, poly(2-(2-bromoisobutyryloxy)ethyl methacrylate) were determined to be in the range of $0.23 < f < 0.38$ by cleaving the side chains from the backbone. The cleaved side chains were analyzed using ^{1}H NMR, GPC/viscosity and GPC-MALS measurements. In spite of the rather low initiating efficiency, the the glycocylindrical brushes show the characteristic worm-like structure, as visualized by SFM. The deprotection of the isopropylidene groups of the PMAIGlc side chains resulted in water-soluble glycocylindrical brushes. SFM measurements, cryogenic transmission electron microscopy and dynamic light scattering show a stretched, worm-like structure.

6.1. Introduction

Regular comblike polymers exhibit the structure of cylindrical brushes if the side chains are densely grafted, i.e., every monomer unit of the main chain carries a side chain, and the main chain is longer than the side chains. In the past, three routes for preparing cylindrical brushes have been used, i.e., "grafting through", "grafting onto", and "grafting from" approaches. The first method, the conventional radical polymerization of macromonomers ("grafting through")[1,2] typically results in a broad chain length distribution of the resulting polymer and incomplete macromonomer conversion. The 'grafting onto' technique[3,4] allows the use of well-defined main chain and side chains, but has often suffered from insufficient grafting efficiency. Finally, in the 'grafting from' approach side chains of the brush have been formed via atom transfer radical polymerization (ATRP) initiated by pendant initiating groups on the backbone.[5-7] This method resulted in well-defined polymer brushes with high grafting density and narrow length distributions of the backbone. The purification of the resulting cylindrical brushes was much simpler compared to other two methods.

Using ATRP in the 'grafting from' approach, we have recently reported the synthesis of the cylindrical polymer brushes with polystyrene (PS), poly(*n*-butyl acrylate) (P*n*BA), poly(*t*-butyl acrylate) (P*t*BA), and poly(acrylic acid) (PAA) side chains, as well as of core-shell brushes with amphiphilic block copolymer side chains, e.g. PAA-*b*-PS or PAA-*b*-P*n*BA.[6,8] The ability of the hydrophilic PAA core of the amphiphilic core-shell brushes to coordinate with different metal cations was used for the synthesis of novel organic/inorganic hybrid nanocylinders.[9-11]

Here we report on the synthesis and characterization of cylindrical polymer brushes comprising of poly(3-*O*-methacryloyl-1,2:5,6-di-*O*-isopropylidene-α-D-glucofuranoside), (PMAIGlc) side chains, using the 'grafting from' approach via ATRP. After deprotection, the water-soluble cylindrical glycopolymer brush poly(3-*O*-methacryloyl-α,β-D-glucopyranose) (PMAGlc) was obtained.

Recently, considerable attention has been paid for the design of biofunctional materials carrying the ligand on synthetic polymers. Synthetic carbohydrate polymers with biocompatible and biodegradable properties can be used for investigating carbohydrate-based interactions.[12] Carbohydrate based monomers and polymers confer high hydrophilicity and water-solubility due to which they are of main interest with respect to very specialized applications in basic biochemical and biomedical research such as molecular recognition processes,[13] drug delivery systems,[14,15] and also as surfactants.[16]

ATRP has been used for the synthesis of many sugar-carrying block,[17,18] graft[19] and hyperbranched polymers.[20,21] In this paper, we have employed ATRP for the synthesis of glycocylindrical brushes using a bulky sugar-carrying methacrylate monomer, 3-*O*-methacryloyl-1,2:5,6-di-*O*-isopropylidene-α-D-glucofuranoside (MAIGlc), via 'grafting from' approach. Cylindrical glycopolymer brushes are architecturally interesting, because of the possibility to form extended chain conformations, based on the intramolecular excluded-volume interactions between bulky side chains densely grafted to the backbone. The synthetic route leading to the glycopolymer brushes is outlined in Scheme 1.

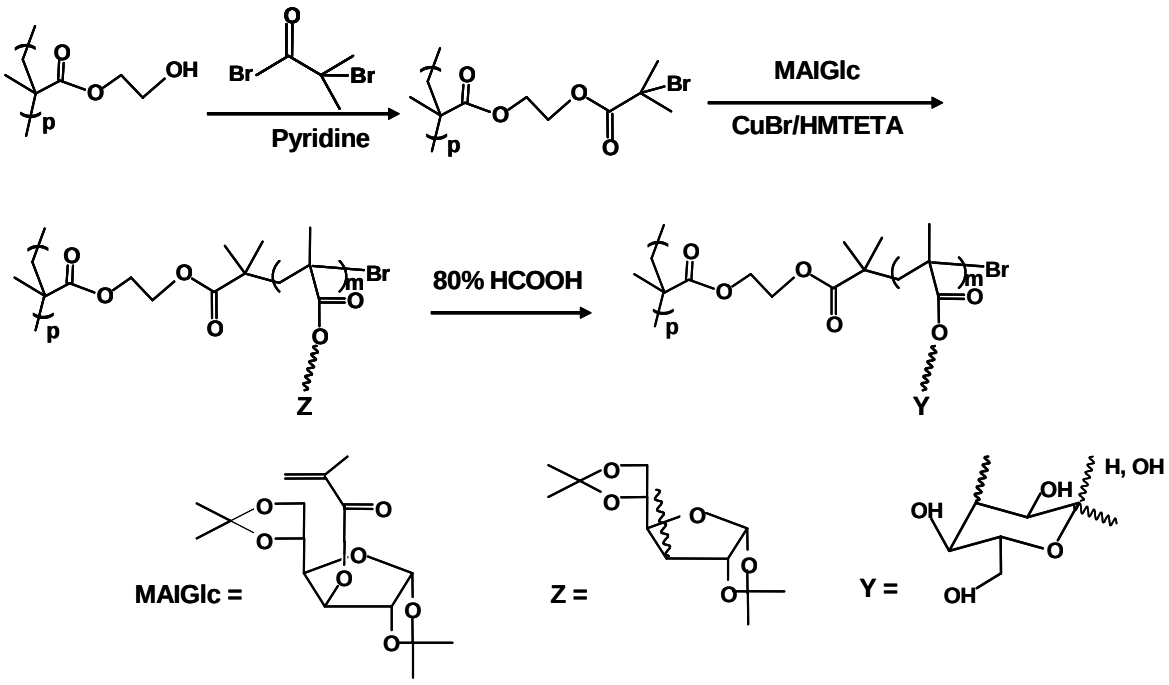

Scheme 1. *General route to the synthesis of glycocylindrical brushes ("Sugar sticks")*

6.2. Experimental Section

Materials. CuBr (95%, Aldrich) was purified by stirring overnight in acetic acid. After filtration, it was washed with ethanol, ether, and then dried. 1,1,4,7,10,10-Hexamethyltriethylenetetramine (HMTETA, 97 %, Aldrich) was distilled and degassed before use. Sodium methoxide (25 % in methanol, Aldrich) was used as received. 3-O-Methacryloyl-1,2:5,6-di-O-isopropylidene-D-glucofuranose (MAIGlc) was synthesized by the reaction of 1,2:5,6-di-O-isopropylidene-D-glucofuranose and methacrylic anhydride in pyridine and purified by vaccum distillation as reported by us recently.[21] The synthesis and characterization of the two polyinitiators, poly(2-(2-bromoisobutyryloxy)ethyl methacrylate)

(PBIEM-I and PBIEM-II), employed for the synthesis of the polymer brushes was described in an earlier publication.[6,8] PBIEM-I was prepared by the reaction of bromoisobutyryl bromide with poly(2-hydroxyethyl methacrylate) (PHEMA) obtained by ATRP. PBIEM-II was synthesized from PHEMA obtained via anionic polymerization of trimethylsilyl-protected HEMA. 1H NMR (CDCl3): δ = 4.37, 4.21 (-CH2-OCO-), 2.20-1.40 (-CH2-C), 1.97 [-C(Br)(CH3)2], 1.30-0.70 (-CH3) ppm.

Polymerizations. All polymerizations were carried out in a round bottom flask sealed with a plastic cap. A representative example for the synthesis of a cylindrical brush is as follows: To a round bottom flask containing CuBr (2.7 mg, 0.0190 mmol), MAIGlc (2.5 g, 7.62 mmol) in ethyl acetate (2.5 g, 50 wt %) was added the polyinitiator, PBIEM-II (10.6 mg, 0.0381 mmol of initiating α-bromoester group) (See Table 1) and stirred for 10 min to dissolve the polyinitiator completely. Then HMTETA (4.3 mg, 0.0190 mmol) was added to this mixture and the color changed to green indicating the start of polymerization. The flask was then placed in an oil bath at 60 ºC for 25 min. Monomer conversion as detected by ^{1}H NMR, was 10 %. The contents of the flask, which were very viscous even at such a low conversion, were then dissolved in THF. The solution was passed through a silica column, and the polymer was precipitated from THF into methanol two times. Then it was then precipitated in petroleum ether twice to remove the unreacted monomer completely. Finally the product was freeze-dried from dioxane and dried under vacuum at room temperature. The polymer had M_n = 58.6 x 10^4 and M_w/M_n = 1.07 according to conventional GPC using PS calibration and M_n = 1120 x 10^4 and M_w/M_n = 1.09) as determined by GPC-MALS measurement. The polymer was soluble in THF and chloroform but insoluble in methanol, acetone and water.

Deprotection. The transformation of sugar sticks containing poly(MAIGlc) side chains into water soluble polymer with poly(3-*O*-methacryloyl-α,β-D-glucopyranose) (MAGlc) side chains was achieved under mild acidic condition.[21] The polymer (100 mg) was dissolved in 80 % formic acid (12 mL) and stirred for 48 h at room temperature. Then 5 mL of water were added and it was stirred for another 3 h. The solution was dialysed using a Spectra/Por^R dialysis tube (MWCO: 1000) against Millipore water for 2 days. The resulting polymer was freeze-dried from water and dried under vacuum. The deprotected polymer was obtained as white powder which was soluble in water, methanol but insoluble in THF and acetone.

Solvolysis of the glycocylindrical brushes. The solvolysis of the brushes was achieved via base catalyzed transesterification in methanol.[22] The polymer (20 mg) was dissolved in THF in a capped vial. Methanol was added until the polymer was precipitated, and then sodium methoxide (25 % in Methanol, 4-5 drops) was added. The capped vial was then placed in an

oil bath and kept at 90 ºC for 7 days. Then, the solution was cooled and stirred for 2 h in the presence of cationic ion-exchange resin (Dowex MSC-1). The solution was decanted and evaporated. The molecular weight of the resulting product was analyzed using conventional GPC, GPC/viscosity and GPC-MALS measurements.

Characterization. The apparent molecular weights of the brushes and cleaved side chains were characterized by conventional *GPC* using THF as eluent at a flow rate of 1.0 mL/min at room temperature. Column set: 5µm PSS SDV gel, 10^2, 10^3, 10^4, 10^5 Å, 30 cm each; detectors: Waters 410 differential refractometer and Waters photodiode array detector operated at 254 nm. Narrow PS and PMMA standards (PSS, Mainz) were used for the calibration of the column set. GPC with a multi-angle light scattering detector (GPC-MALS) and a Viscotek viscosity detector H 502B (GPC/viscosity) were used to determine the absolute molecular weights of the brushes and of the side chains cleaved by solvolysis. THF was used as eluent at a flow rate of 1.0 mL/min. column set: 5µ PSS SDV gel, 10^3 Å, 10^5 Å and 10^6 Å, 30 cm each; detectors: Shodex RI-71 refractive index detector, and Wyatt DAWN DSP-F MALS detector equipped with a 632.8 nm He-Ne laser. The refractive index increment in THF solution of the glycocylindrical brush at 25 ºC was determined to be dn/dc = 0.0723 mL/mg using a Chromatix KM-16 laser differential refractometer. The refractive index increment in THF solution of the detached side chains at 25 ºC was determined to be dn/dc = 0.065 mL/mg using a PSS DnDc-2010/620 differential refractometer. For GPC/viscosity the universal calibration principle was used. Linear PMMA standards (PSS, Mainz) were used to construct the universal calibration curve. *^{1}H NMR* was recorded with a Bruker AC-250 instrument at room temperature.

Dynamic light scattering (DLS) was performed on an ALV DLS/SLS-SP 5022F compact goniometer system with an ALV 5000/E correlator and a He-Ne laser (λ = 632.8 nm). Prior to the light scattering measurements the sample solutions were filtered using Millipore Teflon filters with a pore size of 0.45 µm. The measured intensity correlation functions were subjected to CONTIN analysis. Apparent hydrodynamic radii of the glycocylindrical brushes were calculated according to the Strokes-Einstein equation.

The samples for *scanning force miscroscopy* (SFM) measurements were prepared either by dip-coating from dilute solutions of brushes in tetrahydrofuran or dioxane/water mixtures, with concentration of 1 mg/L, onto freshly cleaved mica surface or by spin casting onto a carbon-coated mica surface. Carbon-coated mica substrates were prepared using the mini-deposition system Balzers MED 010 to deposit carbon of approximately 5 nm thickness by evaporation. The SFM images were taken with a Digital Instruments Dimension 3100

microscope operated in Tapping Mode (free amplitude of the cantilever ≈ 30 nm, set point ratio ≈ 0.98).

For *cryogenic transmission electron microscopy* (cryo-TEM) studies, a drop of the sample was put on an untreated bare copper transmission electron microscopy (TEM) grid (600 mesh, Science Services, München, Germany), where most of the liquid was removed with blotting paper leaving a thin film stretched over the grid holes. The specimens were instantly shock frozen by rapid immersion into liquid ethane and cooled to approximately 90 K by liquid nitrogen in a temperature-controlled freezing unit (Zeiss Cryobox, Zeiss NTS GmbH, Oberkochen, Germany). The temperature was monitored and kept constant in the chamber during all the sample preparation steps. After freezing the specimens, the remaining ethane was removed using blotting paper. The specimen was inserted into a cryo-transfer holder (CT3500, Gatan, München, Germany) and transferred to a Zeiss EM922 EF-TEM. Examinations were carried out at temperatures around 90 K. The TEM was operated at an acceleration voltage of 200 kV. Zero-loss filtered images (ΔE = 0 eV) were taken under reduced dose conditions (100 – 1000 e/nm^2). All images were registered digitally by a bottom mounted CCD camera system (Ultrascan 1000, Gatan) combined and processed with a digital imaging processing system (Gatan Digital Micrograph 3.9 for GMS 1.4).

6.3. Results and Discussion

6. 3.1. Synthesis and Molecular Characterization of Glycocylindrical Brushes

Synthesis of Protected Cylindrical Brushes. We have previously reported the synthesis of the polyinitiator poly(2-(2-bromoisobutyryloxy)ethyl methacrylate), (PBIEM), where the precursor, poly(2-hydroxyethyl methacrylate), (PHEMA), was made via ATRP as well as anionic polymerization.[8] Whereas ATRP led to moderately narrow molecular weight distributions of the backbone ($1.16 < M_w/M_n < 1.24$),[6,8] anionic polymerization led to nearly monodisperse main chains (M_w/M_n = 1.08) with high molecular weight.[8] The number-average molecular weights of the two polyinitiators PBIEM-I and PBIEM-II are 6.68 x 10^4 and 41.8 x 10^4, respectively, corresponding to number-average degrees of polymerization DP_n = 240 and 1,500, respectively. By using these polyinitiators, glycopolymer cylindrical brushes with different backbone lengths were obtained.

We recently reported that CuBr/HMTETA and $(PPh_3)_2NiBr_2$ are among the best catalyst systems for the homopolymerization of MAIGlc to obtain linear poy(MAIGlc)s with narrow molecular weight distribution (MWD).[21] In this work, we chose CuBr/HMTETA for the synthesis of glycocylindrical brushes.

Table 1. Synthesis and characterization of short and long glycocylindrical brushes via ATRP[a]

Brush	Initiator	$[M]_0/[I]_0$	Time (min)	Conv.[b] (%)	10^{-4} x $M_{n,\ GPC}$[c]	PDI[c]	10^{-4} x $M_{n,\ MALS}$	$DP_{n,\ side\ chain}$ (calc)[d]	R_g (nm)
1	PBIEM-I	100	10	11.0	6.63	1.19	59	6.6	25.6 ± 0.4
2	PBIEM-I	300	20	9.3	8.91	1.18	150	19	27.1 ± 0.5
3	PBIEM-I	400	40	10.0	17.8	1.25	180	22	31.2 ± 0.4
4	PBIEM-II	300	30	5	40.8	1.19	900	18	41.5 ± 0.1
5	PBIEM-II	200	25	10	58.6	1.07	1120	22	59.5 ± 0.3

[a]Solution polymerization in ethylacetate (50 wt% to MAIGlc) at 60 °C at constant $[I]_0 : [CuBr]_0 : [HMTETA]_0 = 1 : 0.5 : 0.5$. [b]Determined by ^{1}H-NMR. [c]Determined by GPC using THF as eluent with PS standards. [d]Calculated from $M_{n,MALS,}$ assuming 100 % initiation efficiency according to $DP_{sc,\ calc} = (M_{n,\ brush} - M_{n,\ backbone})/(nM_0)$, where n = degree of polymerization of the backbone and $M_{0,}$ monomer molecular weight, respectively.

Table 1 represents the results of the synthesis of glycocylindrical brushes by using CuBr/HMTETA as the catalyst system, MAIGlc as monomer and PBIEM-I and PBIEM-II as polyinitiators. It should be noted that the polyinitiator with higher molecular weight (PBIEM-II) dissolves in the reaction mixture much slower than PBIEM-I. The time of stirring before the addition of ligand should be long enough to ensure the complete dissolution of polyinitiator. Otherwise a broad molecular weight distribution of the final product will result. As can be seen from Table 1, very low conversions are maintained in all cases in order to obtain well-defined glycocylindrical brushes. Even at such low conversions, the reaction mixture becomes very viscous owing to the very high molecular weights of the resulting brushes. The obtained cylindrical brushes with MAIGlc side chains show monomodal GPC eluograms (Figures 1 and 2) and their molecular weight distributions are quite narrow (PDI <1.25), indicating that intermacromolecular coupling reactions are negligible. Hence, without adding Cu(II) salts,[5] a high ratio of monomer to initiator and a low conversion are sufficient to suppress undesirable side reactions, and to obtain the desired glycocylindrical brushes.

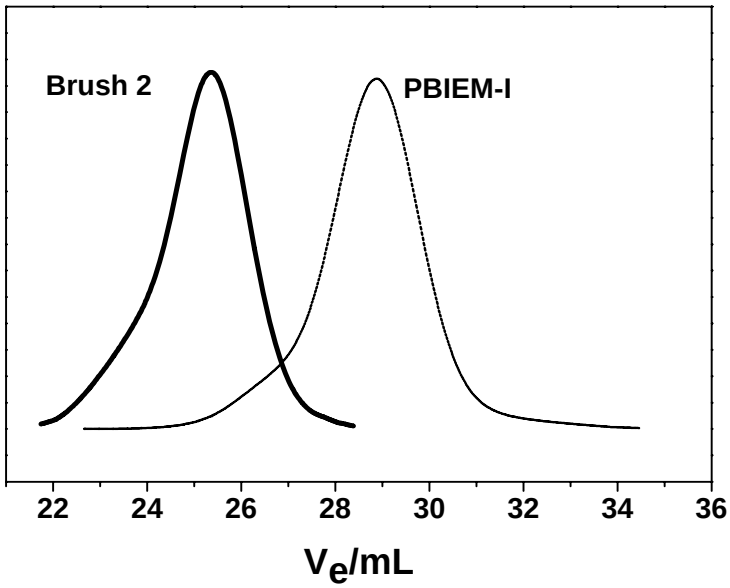

Figure 1. GPC traces of PBIEM-I (DP = 240) and the corresponding short glycocylindrical Brush 2 in THF.

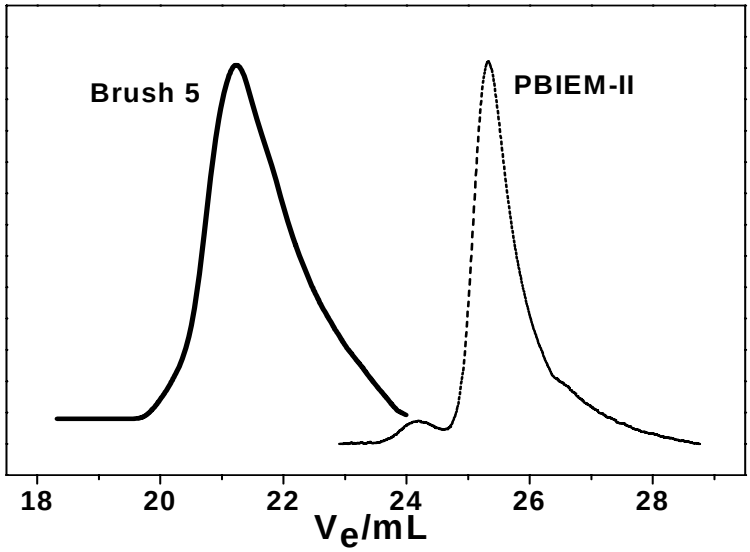

Figure 2. GPC traces of PBIEM-II (DP = 1,500) and the corresponding long glycocylindical Brush 5 in THF.

The molecular weights of these brushes obtained from GPC using linear PS standards are just the apparent ones. Hence, the true molecular weights of these brushes as well as the radii of gyration, R_g, in THF were determined by GPC-MALS. As can be seen from Table 1, for the same backbone, R_g of the brushes increases with the side chain lengths. The main chain stiffness of the polymer brush increases with increasing side chain length, because the overcrowding of longer side chains forces the otherwise flexible main chain into a more stretched conformation. In addition, at a given DP of side chain (DP_{sc}) a larger R_g was observed for brushes with poly(MAIGlc) side chains compared to brushes with P*t*BA side chains with the same backbone. For instance, in the case of brushes with poly(MAIGlc) side chains, R_g = 31.2 nm was obtained at DP_{sc} = 22 for Brush 3, whereas R_g = 11.6 nm at DP_{sc} = 28, was observed for P*t*BA synthesized from the same polyinitiator.[8] This could be attributed to the bulky sugar moiety of the monomer (MAIGlc) under study, leading to a stronger stretching of the backbone. The molar masses obtained by light scattering are significantly higher than those obtained by GPC. This is due to the compact nature of the brushes.

Figure 3 represents the ^{1}H NMR spectra of linear poly(MAIGlc), polyinitiator and the glycocylindrical brushes. In Figure 3c, there are two typical peaks at 4.21 and 4.37 ppm (*a* and *a´*), which represent the methylene protons between two ester groups of the polyinitiator. After the formation of the brush with poly(MAIGlc) side chains, the characteristic peaks at 1.2-1.4 ppm (isopropylidene protons), 3.8-5.0 and 5.7-6.0 ppm are clearly seen in Figure 3b.

This indicates the successful formation of glycocylindrical brushes with poly(MAIGlc) side chains.

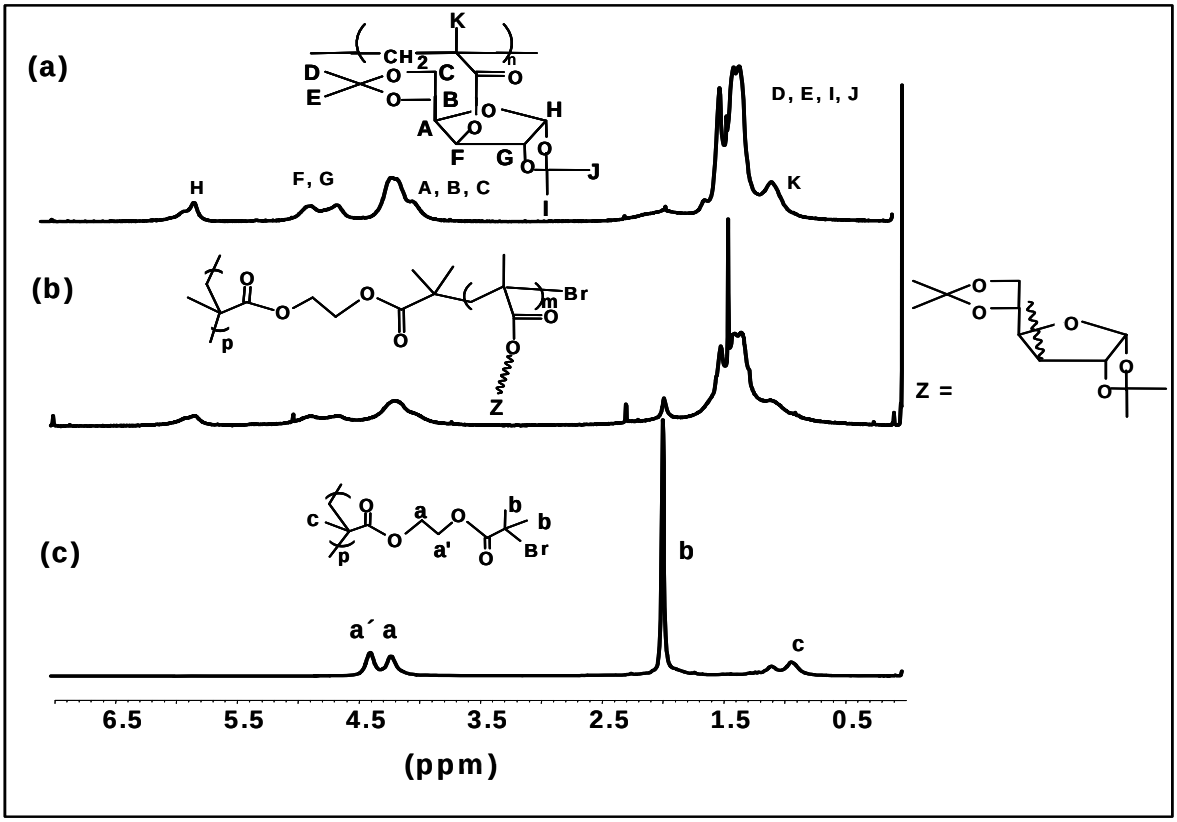

Figure 3. ^{1}H NMR spectra ($CDCl_3$) of (a) linear poly(MAIGlc), (b) cylindrical brush with poly(MAIGlc) side chains (Brush 3), and (c) the polyinitiator (PBIEM-I).

Solvolysis of the Glycocylindrical brushes. In order to determine the exact side chain length, and thus the initiation site efficiency, the side chains were cleaved from the backbone via base-catalyzed trans-esterification in methanol. ^{1}H NMR spectra of the resulting products. (cf. Figure 4) revealed that solvolysis with sodium methoxide resulted in side chains consisting of a statistical copolymer of 17 % MMA and 83 % MAIGlc units. The comonomer composition was determined by comparing the peaks at 3.59 ppm attributed to the methyl ester protons ($-OCH_3$) of the MMA units and at 5.8-6.0 ppm attributed to the single ring proton of MAIGlc units. Similar results were obtained for Brush 4 and Brush 5. In order to calculate the DP of the side chains, the molecular weights of the side chains (see below) were divided by an average molecular weight of the comonomers, M_0 = 290 g/mol.

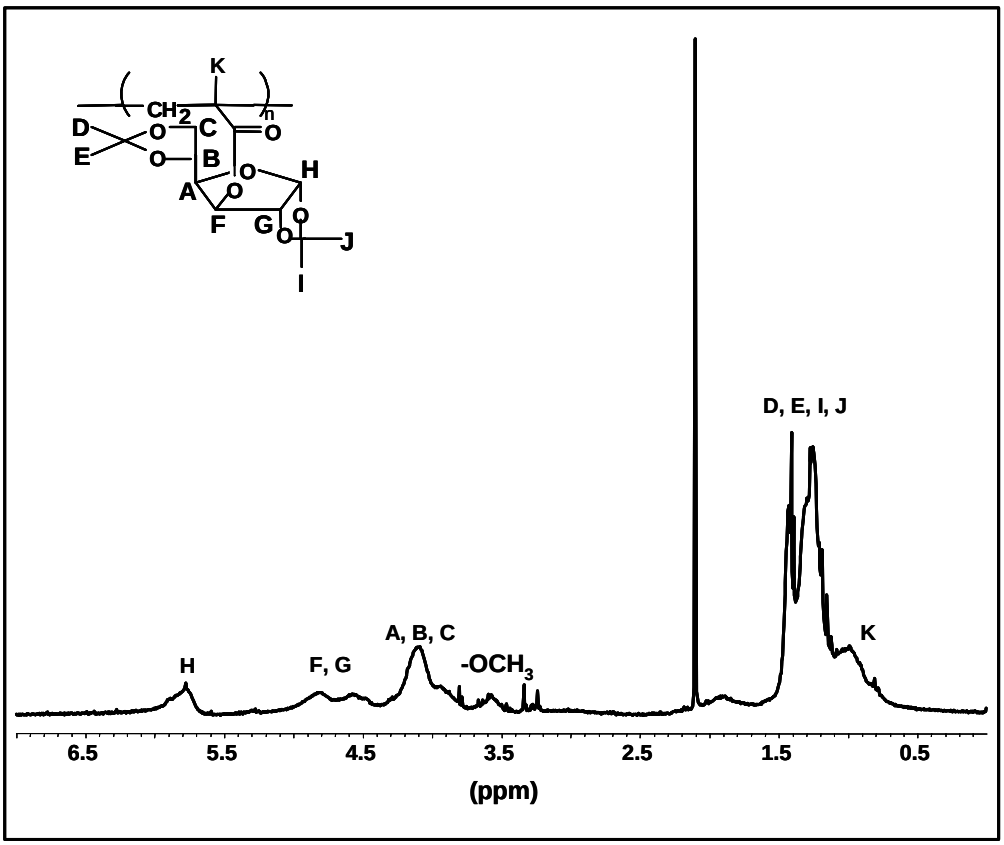

Figure 4. *^{1}H NMR spectra ($CDCl_3$) of the detached side chains of Brush 3.*

Table 2 summarizes the detailed characterization of the side chains cleaved by solvolysis and the corresponding initiation efficiencies, *f*. The GPC traces of Brush 3 and the cleaved side chains are given in Figure 5. The monomodal character of the detached side chains shows the absence of the inter- and intramolecular coupling reactions. The absolute molecular weights of the cleaved side chains were determined by using GPC/viscosity and GPC-MALS measurements which allows the accurate evaluation of the initiation efficiencies. The polydispersity index of the cleaved arms is $M_w / M_n \cong 1.3$ as can be seen from Table 2, which is a typical value for polymer obtained by slow initiation (limiting $M_w / M_n = 1.33$ for $k_p >> k_i$ in the Gold distribution[23]). Under these conditions all monomer is consumed before complete initiation. The initiating efficiency of Brush 3 was found to be only 28 % as shown in Table 2. The initiating efficiencies of the PMAIGlc brushes investigated are in the range of 23 - 38 %. This value is much smaller that that obtained for the polymerizatgion of styrene using the same polyinitiator, PBIEM.[6] Recently, Matyjaszewski et al.[22] have demonstrated that the initiating efficiency is limited to approximately 50 % for the polymerization of MMA using PBIEM. In our study, the increased bulkiness of the monomer, MAIGlc, could

contribute to the low initiation efficiency of the brushes. In spite of the low grafting efficiency, the bulky sugar moiety of the monomer (MAIGlc), leads to the stronger stretching of the backbone resulting in extended worm-like conformations, as will be discussed below.

Table 2. Characterization of cleaved side chains of PMAIGlc Brushes and of initiation site efficiencies, f [a)]

Brush	$M_{n,\,GPC}$ [b]	M_w/M_n [b]	$M_{n,\,GPC\text{-}VISCO}$ [c]	M_w/M_n [c]	$M_{n,\,GPC\text{-}MALS}$ [d]	DP_n [e]	f [e] (%)	DP_{bb}/DP_{sc}
3	22300	1.34	23900	1.38	23200	81.2	27	2.9
4	9000	1.34	13600	1.40	-	46.8	38.4	32
5	19100	1.26	27400	1.35	28100	95.6	23.0	15.6

a) $f = DP_{n,\,calc}/DP_{n,\,exp.}$ [b]Determined by GPC using THF as eluent with PMMA standards. [c]Determined by GPC/viscosity measurement. [d]Determined by GPC-MALS measurement. [e]Average of GPC/viscosity and GPC-MALS measurements.

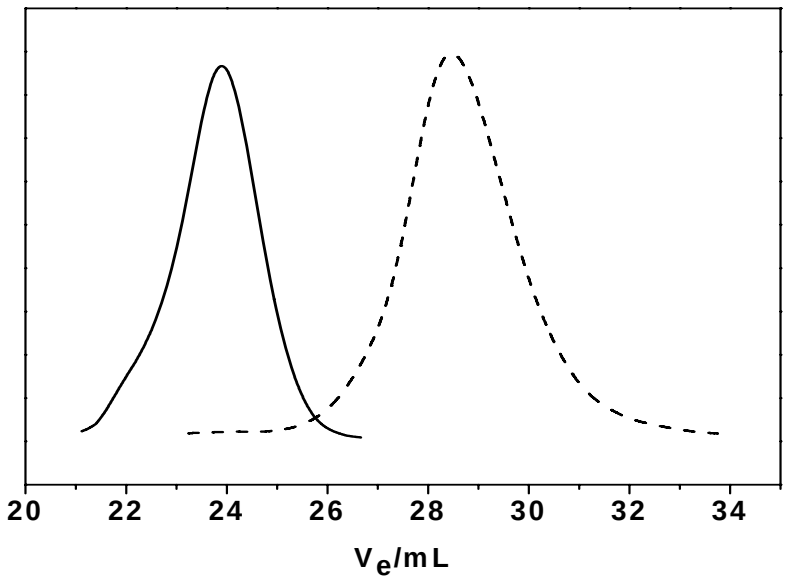

Figure 5. *GPC traces of Brush 3 (—) and cleaved side chains (**--**) after solvolysis.*

Deprotection of the Cylindrical Brushes. The hydrolysis of the isopropylidene groups of the glycocylindrical brushes was performed by treating the samples with formic acid at room temperature.[21,24] The final product was obtained by dialysis against water and freeze-drying. The ^{1}H NMR spectrum of the glycocylindrical brush with poly(3-*O*-methacryloyl-α,β-D-

glucopyranoside)s side chains, abbreviated as poly(MAGlc), is shown in Figure 6a. The signals of the isopropylidene protons (1.2-1.4 ppm) completely disappear after the deprotection and a broad signal attributed to anomeric hydroxyl groups of the sugar moieties (6.4-7.0 ppm) appear. This shows the quantitative deprotection of the isopropylidene protecting groups. The deprotected short glycocylindrical brushes are white powders, completely soluble in water and methanol, but insoluble in THF, chloroform, and acetone (similar to linear poly(MAGlc)). However, the long brushes are only partially soluble in methanol, but completely soluble in water and water/dioxane (1/1) mixtures.

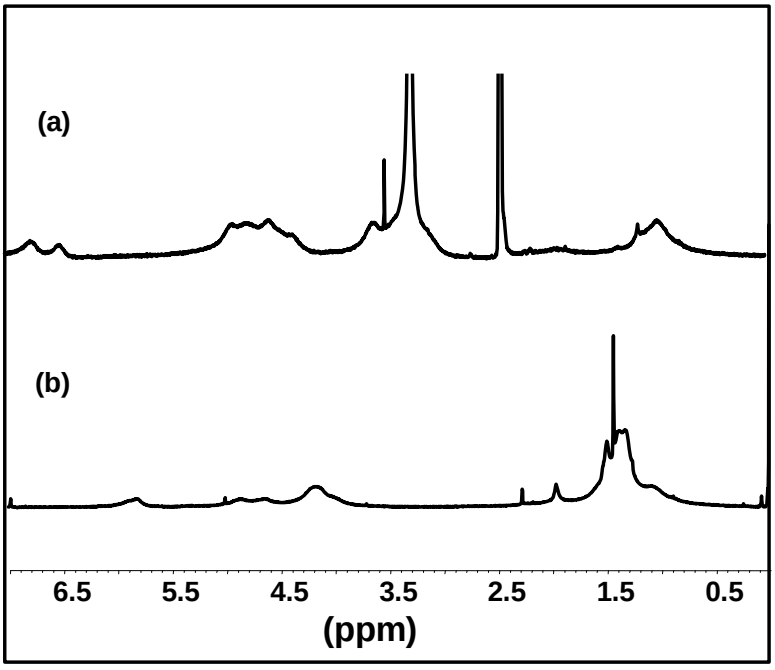

Figure 6. *^{1}H NMR spectra of of the deprotected Brush 3 with MAGlc side chains (a, d_6-DMSO), and glycocylindrical brush with MAIGlc side chains (b, $CDCl_3$).*

6.3.2. Solution Properties of the Cylindrical Brushes

Protected Cylindrical Brushes. Dynamic light scattering (DLS) was also used to characterize the glycocylindrical brushes in THF solution. Figure 7a shows the normalized intensity correlation functions of the glycocylindrical Brush 4 at different scattering angles. The normalized intensity functions were subjected to CONTIN analysis. The angular dependence of R_h for Brush 4 is shown in Figure 7b. A very strong angular dependence is observed indicating the worm-like nature of the glycocylindrical brushes with very high

aspect ratio (ratio between the backbone and the side chains lengths).[25] In contrast to Brush 4, the angular dependence for the short Brush 2 (Figure 8) is much weaker owing to its low aspect ratio. In order to obtain polymers exhibiting cylindrical shape, a high aspect ratio is necessary.

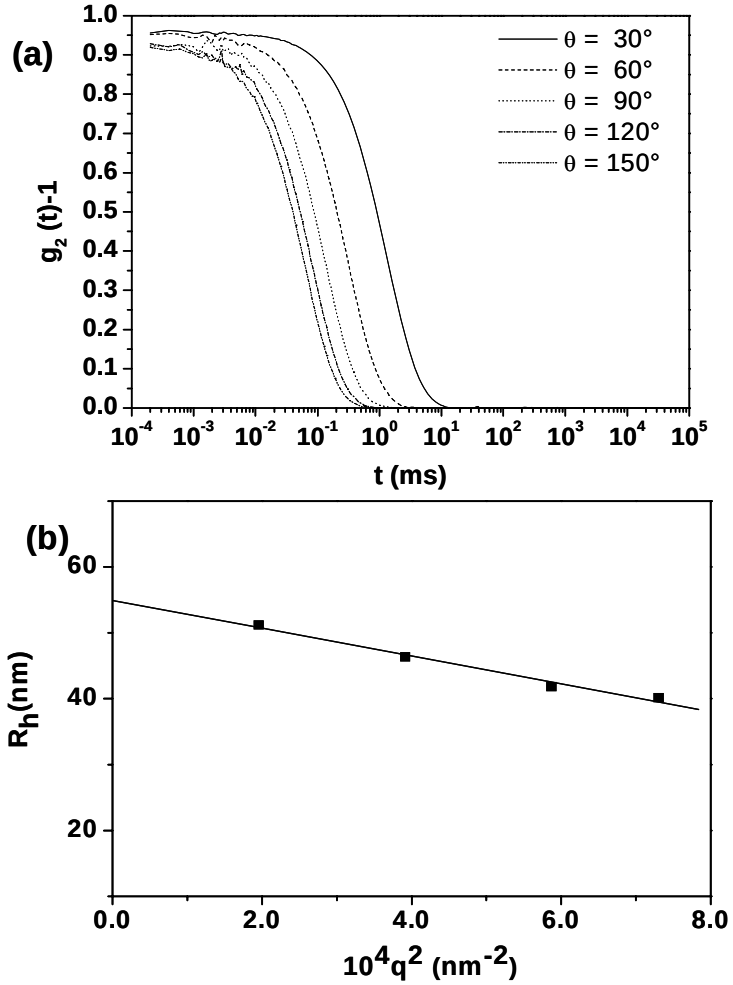

Figure 7. *(a) Normalized intensity correlation functions at different scattering angles, and (b) dependence of R_h on the square scattering vector for glycocylindrical Brush 4 in THF.*

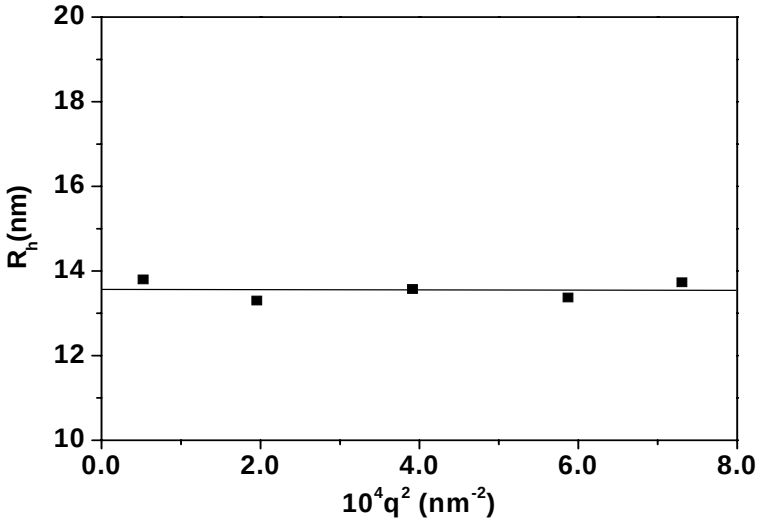

Figure 8. *Angular dependence of R_h for short glycocylindrical Brush 2 in THF.*

Deprotected Cylindrical Brushes. DLS was performed for the deprotected Brush 4 in water with a concentration of 0.4 g/L at room temperature (Figure 9). The CONTIN analysis of the autocorrelation functions show a monomodal hydrodynamic radius distribution at all scattering angles. The hydrodynamic radius distribution of this brush at scattering angle of 90º in water is shown in Figure 9b. The z-average hydrodynamic radius of this brush at 90º is 63.3 nm. The angular dependence plot of this brush is shown in Figure 9c. Again the angular dependence of R_h is very strong indicating its stretched worm-like nature. After extrapolation of q^2 to zero, the hydrodynamic radius of this brush in water is 72.9 nm which is significantly higher than the extrapolated hydrodynamic radius, R_h = 54.9 nm, for the same brush in THF before hydrolysis. This indicates that after hydrolysis, the brushes in water are more stretched owing to the hydration of the sugar moieties. These results are further supported by SFM and cryo-TEM measurements.

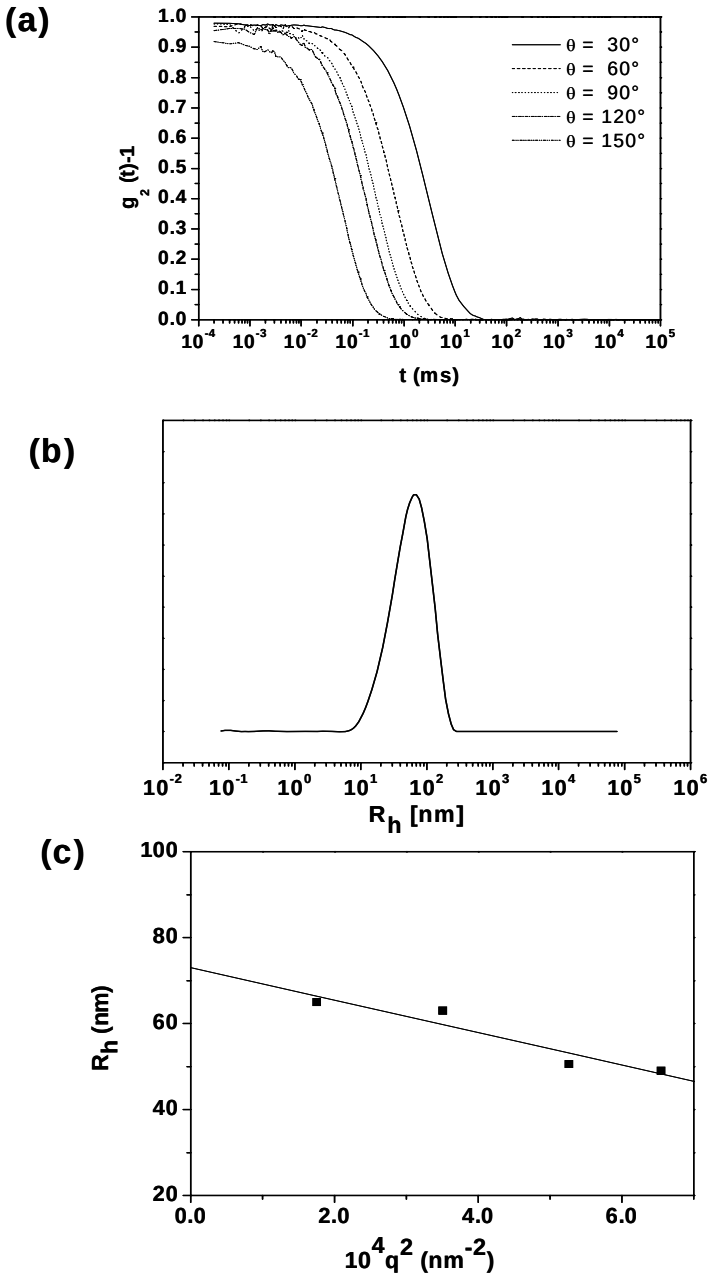

Figure 9. *(a) Normalized intensity correlation functions at different scattering angles, (b) the corresponding hydrodynamic radius distribution at scattering angle of 90º, and (c) dependence of R_h on the square scattering vector for deprotected glycocylindrical Brush 4 in water.*

6.3.3. Visualization of the Cylindrical Brushes by SFM and cryo-TEM

Scanning Force Microscopy of the Protected Cylindrical Brushes. The glycocylindrical brushes were then further characterized by scanning force microscopy (SFM). The protected samples were prepared either by dip-coating from dilution THF solutions using freshly cleaved mica as substrate or by spin-coating from dilute solutions onto carbon-coated mica.

Figure 10a displays an image of the long glycocylindrical brush, Brush 5 dip-coated from THF on mica. When the polyinitiator synthesized via anionic polymerization (PBIEM-II) was used, long cylindrical brushes with narrow backbone length distribution were obtained. The high uniformity as well as the regular cylindrical shape enables us to perform a statistical analysis. The number-average and weight-average lengths of 160 cylinders are L_n = 138 nm and L_w = 147 nm, respectively, with a polydispersity L_w/L_n = 1.06 which agrees well with the polydispersity of the backbone (M_w/M_n = 1.08). The number-average brush length of 138 nm corresponds to the length per main chain monomer unit of 0.09 nm, which is much smaller than the maximum value of 0.25 nm, indicating that the main chain is not completely stretched out but locally coiled. This could be due to the low grafting efficency (f = 23 %) of the brush as discussed earlier.

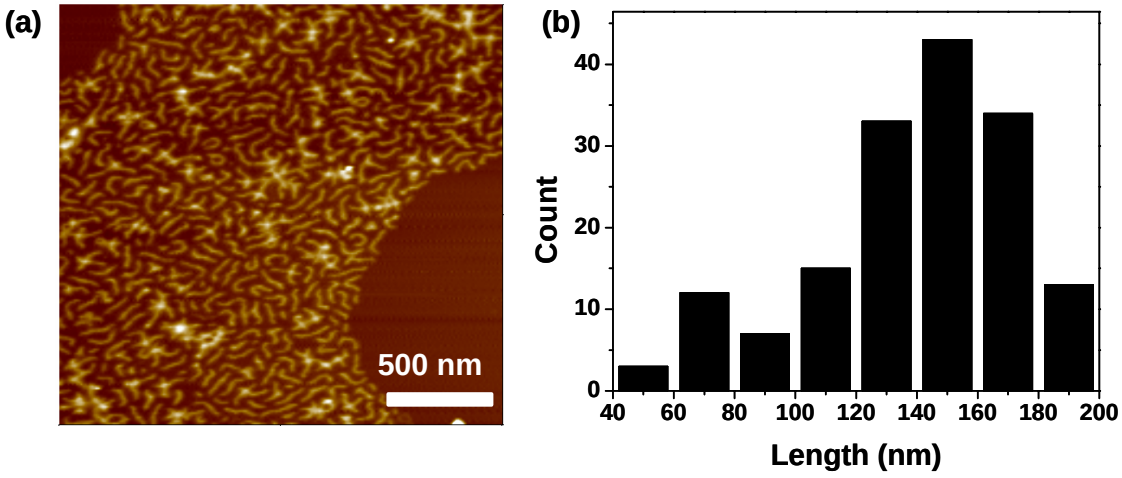

Figure 10. *(a) SFM Tapping Mode height image of Brush 5, dip-coated from dilute THF solution on mica, (z-range: 15 nm) and (b) histogram of the contour length for 160 molecules.*

Figure 11a represents the SFM image of the long Brush 4, spin-coated from THF onto carbon-coated mica. Carbon-coated mica was chosen in order to avoid problems associated with aggregation and dewetting. Single worm-like macromolecules can be visualized directly. The number-average and weight-average lengths of 20 individual cylinders in

Figure 11a are L_n = 110 nm and L_w = 114 nm, respectively, with a polydispersity L_w/L_n = 1.04. These brushes are somewhat shorter than Brush 5, possibly due to the shorter side chains (DP = 47 vs 96), although their grafting density is higher than that of Brush 5 (*f* = 38 % vs 23 %).

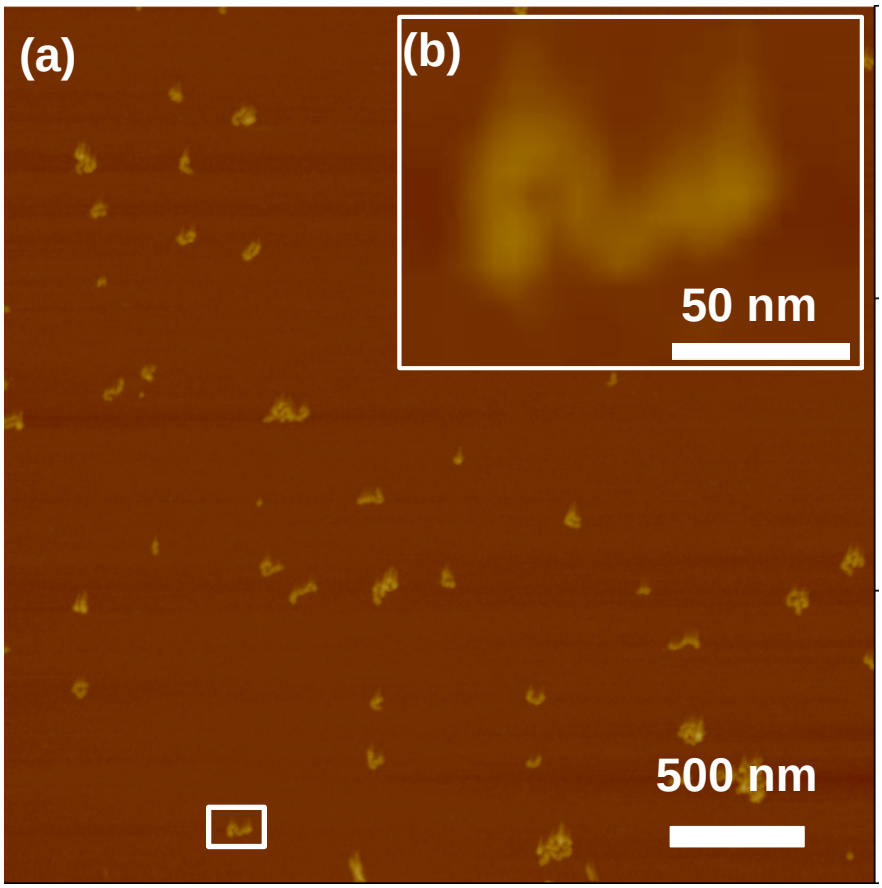

Figure 11. *(a) SFM Tapping Mode height image of the Brush 4, spin-coated from dilute solution on carbon-coated mica, (z-range: 20 nm) and (b) 5x magnification of the single cylinder marked by a rectangle in (a).*

SFM of the Deprotected Brushes. Figure 12 shows the SFM image of the deprotected long Brush 4, spin-coated from dioxane-water mixture (volume ratio of 1/1) onto mica. Worm-like macromolecules could be visualized indicating that the structure is preserved during deprotection. The number and weight-average lengths of 40 cylinders are L_n = 130 nm and L_w = 134 nm, respectively, with a polydispersity, L_w/L_n = 1.03. The cylinders appear to be more stretched than those before hydrolysis (L_n = 110 nm). The cylinders are still much

shorter than the maximum contour length of cylinders in the fully stretched state. These results are quite compatible to the results obtained from DLS measurements for Brush 4 in water (R_h ($q^2 \rightarrow 0$) = 72.9 nm). The curvature of the brushes is higher than expected. In order to check whether this is due to the interaction of the molecule with the substrate, cryo-TEM measurements in water were performed as discussed in the next section.

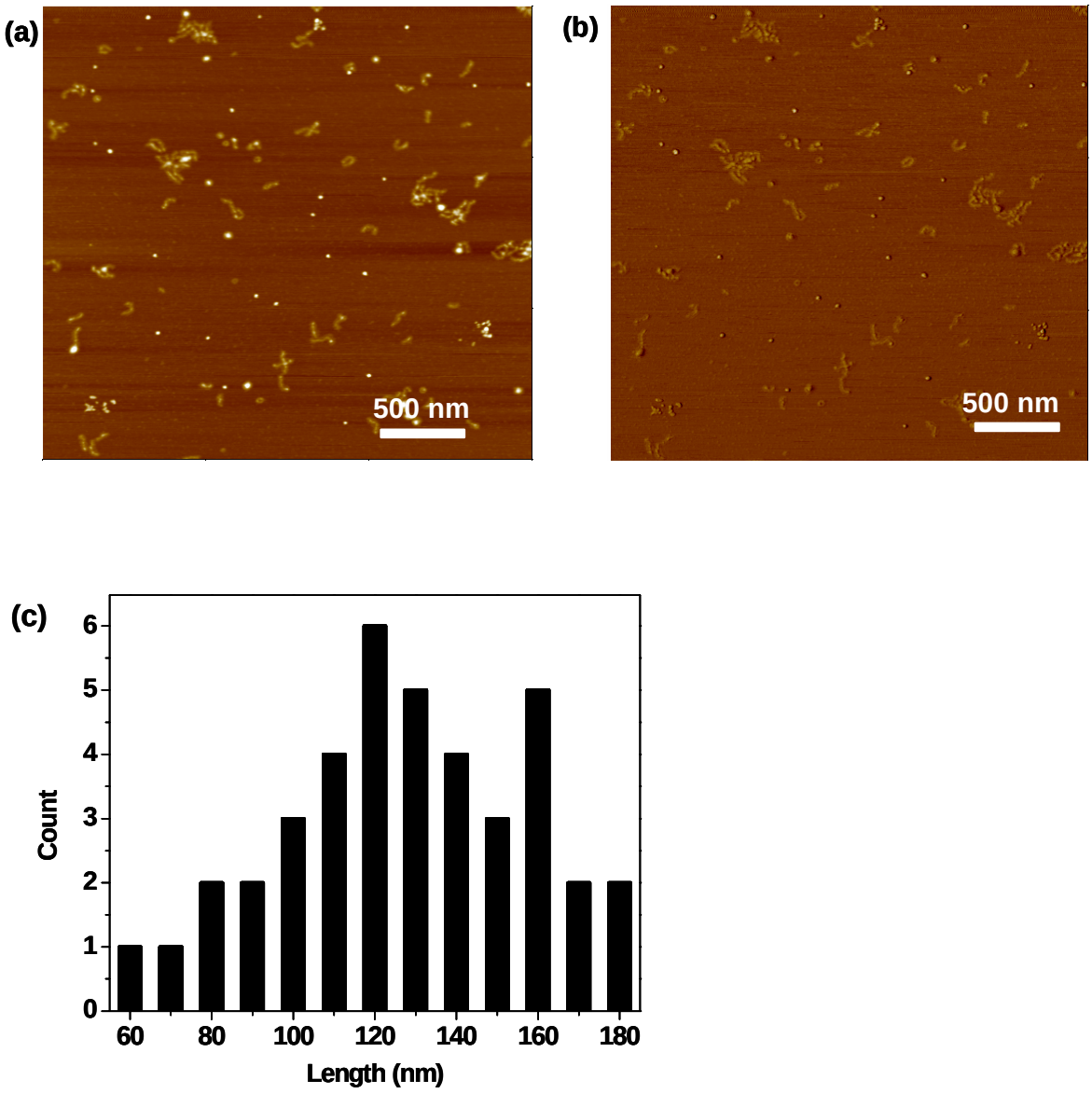

Figure 12. *SFM Tapping Mode images of the deprotected Brush 4, spin-coated from dilute water/dioxane (1/1) solution on mica, (a) height image (z-range: 10 nm), (b) phase image (range: 40°), and (c) histogram of the contour length for 40 molecules.*

Cryogenic Transmission Electron Microscopy (cryo-TEM) Characterization of Deprotected Glycocylindrical Brushes. The structure of the deprotected glycocylindrical Brush 4 in aqueous solution was characterized using cryo-TEM. This tool allows to directly image the original shape and size of the polymers in solution, since the sample is vitrified before the measurement. The cryo-TEM image of the deprotected Brush 4 (Figure 13), shows worm-like cylinders. The magnification of a single cylinder is also shown as an insert and the length of that single cylinder is found to be 130 nm which agrees very well with the length of the deprotected Brush 4 obtained by SFM measured in the dry state.

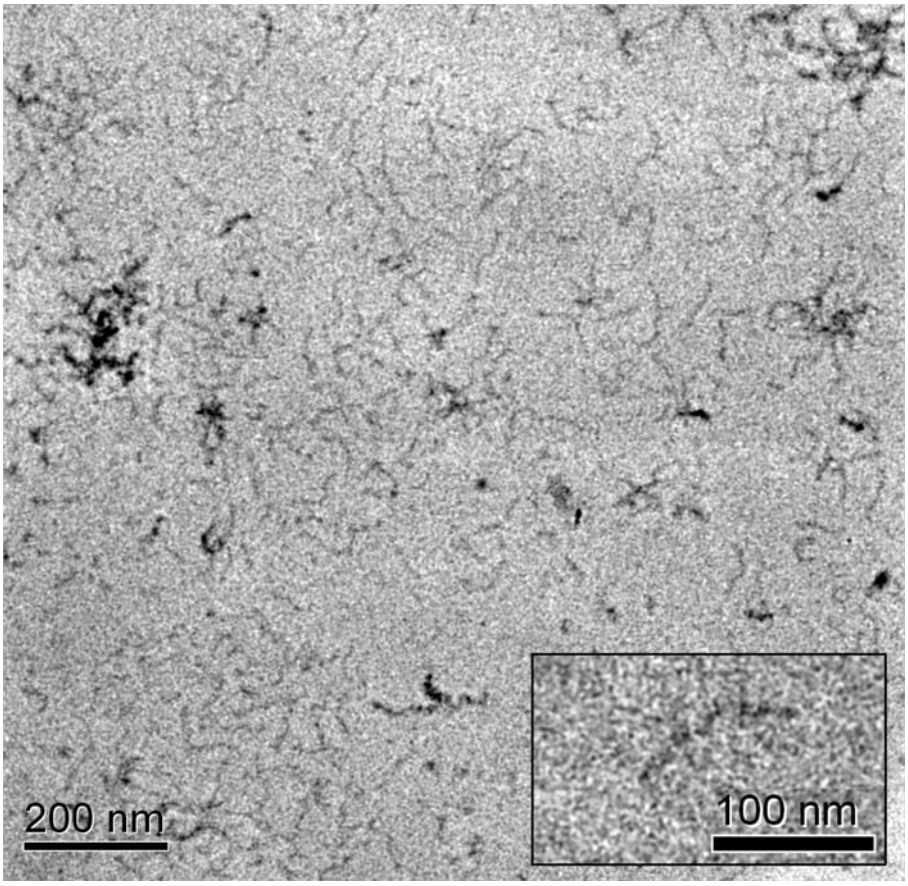

Figure 13. *Cryo-TEM image of the deprotected, long Brush 4.*

6.4. Conclusions

We have demonstrated that the CuBr/HMTETA catalyst system could be successfully employed for the homopolymerization of MAIGlc in the "grafting from" process, leading to well-defined glycocylindrical brushes or "sugar sticks". The deprotection of the isopropylidene protecting groups resulted in water-soluble glycocylindrical brushes. The extensive characterization of the water-soluble brushes by DLS, SFM, and cryo-TEM confirms their stretched, worm-like structure. Analysis of the side chains detached by basic solvolysis indicated that the grafting efficiency was approximately $0.20 < f < 0.40$. Thus, although the side chains are not as densely spaced as for some PS or polyacrylate brushes, their behaviour is typical rather for cylindrical brushes than comb-shaped polymers. Such brushes with carbohydrate moieties in the side chains can be manipulated for various biological and medicinal applications. Such investigations are in progress.

Acknowledgement. This work was supported by the Deutsche Forschungsgemeinschaft (grant no. Mu 896/14). We wish to thank Prof. Werner Köhler for his useful suggestions regarding DLS measurements. Clarrisa Abetz is acknowledged for the preparation of carbon-coated mica substrate. We also very much appreciate the constructive comments of the reviewers.

6.5. References

(1) Tsukahara, Y.; Mizuno, K.; Segawa, A.; Yamashita, Y. *Macromolecules* **1989**, *22*, 1546-1552.

(2) Djalali, R.; Hugenberg, N.; Fischer, K.; Schmidt, M. *Macromolecular Rapid Communications* **1999**, *20*, 444-449.

(3) Schappacher, M.; Billaud, C.; Paulo, C.; Deffieux, A. *Macromolecular Chemistry and Physics* **1999**, *200*, 2377-2386.

(4) Ryu, S. W.; Hirao, A. *Macromolecules* **2000**, *33*, 4765-4771.

(5) Beers, K. L.; Gaynor, S. G.; Matyjaszewski, K.; Sheiko, S. S.; Möller, M. *Macromolecules* **1998**, *31*, 9413-9415.

(6) Cheng, G.; Böker, A.; Zhang, M.; Krausch, G.; Müller, A. H. E. *Macromolecules* **2001**, *34*, 6883-6888.

(7) Li, C.; Gunari, N.; Fischer, K.; Janshoff, A.; Schmidt, M. *Angewandte Chemie, International Edition* **2004**, *43*, 1101-1104.

(8) Zhang, M.; Breiner, T.; Mori, H.; Müller, A. H. E. *Polymer* **2003**, *44*, 1449-1458.

(9) Zhang, M.; Drechsler, M.; Müller, A. H. E. *Chemistry of Materials* **2004**, *16*, 537-543.

(10) Zhang, M.; Teissier, P.; Krekhova, M.; Cabuil, V.; Müller, A. H. E. *Progress in Colloid & Polymer Science* **2004**, *126*, 35-39.

(11) Zhang, M.; Estournes, C.; Bietsch, W.; Müller, A. H. E. *Advanced Functional Materials* **2004**, *14*, 871-882.

(12) Lee, Y. C.; Lee, R. T. *Accounts of Chemical Research* **1995**, *28*, 321-327.

(13) Wassarman, P. M. *Science* **1987**, *235*, 553-560.

(14) Chen, X. M.; Dordick, J. S.; Rethwisch, D. G. *Macromolecules* **1995**, *28*, 6014-6019.

(15) Dordick, J. S.; Linhardt, R. J.; Rethwisch, D. G. *Chemtech* **1994**, *24*, 33-39.

(16) Klein, J.; Kunz, M.; Kowalczyk, J. *Makromolekulare Chemie-Macromolecular Chemistry and Physics* **1990**, *191*, 517-528.

(17) Li, Z. C.; Liang, Y. Z.; Chen, G. Q.; Li, F. M. *Macromolecular Rapid Communications* **2000**, *21*, 375-380.

(18) Liang, Y. Z.; Li, Z. C.; Chen, G. Q.; Li, F. M. *Polymer International* **1999**, *48*, 739-742.

(19) Ejaz, M.; Ohno, K.; Tsujii, Y.; Fukuda, T. *Macromolecules* **2000**, *33*, 2870-2874.

(20) Muthukrishnan, S.; Jutz, G.; André, X.; Mori, H.; Müller, A. H. E. *Macromolecules* **2005**, *38*, 9-18.

(21) Muthukrishnan, S.; Mori, H.; Müller, A. H. E. *Macromolecules* **2005**, *38*, 3108-3119.

(22) Neugebauer, D.; Sumerlin, B. S.; Matyjaszewski, K.; Goodhart, B.; Sheiko, S. S. *Polymer* **2004**, *45*, 8173-8179.

(23) Gold, L. *J. Chem. Phys.* **1958**, *28*, 91.

(24) Ohno, K.; Tsujii, Y.; Fukuda, T. *Journal of Polymer Science Part a-Polymer Chemistry* **1998**, *36*, 2473-2481.

(25) Dentini, M.; Coviello, T.; Burchard, W.; Crescenzi, V. *Macromolecules* **1988**, *21*, 3312-3320.

7. Synthesis and Characterization of Glycomethacrylate Hybrid Stars from Silsesquioxane Nanoparticles

Sharmila Muthukrishnan[†], Felix Plamper[†], Hideharu Mori[§], Axel H. E. Müller[†,*]

[†]Makromolekulare Chemie II, and Bayreuther Zentrum für Kolloide und Grenzflächen, Universität Bayreuth, D-95440 Bayreuth, Germany

[§] Department of Polymer Science and Engineering, Faculty of Engineering, Yamagata University, 4-3-16, Jonan, Yonezawa, 992-8510, Japan

[*] To whom correspondence should be addressed. e-mail: *Axel.Mueller@uni-bayreuth.de*, Phone:+49 (921) 55-3399, Fax: +49 (921) 55-3393

Published in *Macromolecules* 2005, 38, p. 10631.

Abstract: A silsesquioxane nanoparticle-based macroinitiator of ca. 58 functions was synthesized and characterized using ^{1}H NMR, MALDI-TOF MS and elemental analysis. The macroinitiator was used to synthesize glycomethacrylate stars with approximately 25 arms of different lengths using 3-O-Methacryloyl-1,2:5,6-di-O-isopropylidene-α-D-glucofuranose (MAIGlc) as the monomer via atom transfer radical polymerization (ATRP). Well-defined glycostars could be synthesized by restricting the polymerization to low conversion. The molecular weights of the star polymers were determined using GPC with viscosity and multi-angle light scattering (MALS) detectors. In order to determine the efficiency of the initiating sites, the arms were cleaved off from the core by solvolysis with sodium methoxide and thoroughly characterized; indicating that ca. 25 arms per star had been synthesized. The morphology of the glycostars was visualized using scanning force microscopy (SFM) and field emission scanning electron microscopy (FE-SEM). Deprotection of the isopropylidene groups resulted in water-soluble stars which were characterized using SFM, SEM, asymmetric-flow field flow fractionation (AF-FFF), dynamic light scattering (DLS), cryogenic transmission electron microscopy (cryo-TEM) and bright field transmission electron microscopy (TEM).

7.1. Introduction

Branched structures have been the subject of continuing interest in polymer chemistry. Branched polymers in comparison to their linear analogues with identical molecular weights offer lower melt and solution viscosities.[1,2] They possess different hydrodynamic properties and higher degrees of chain end functionality compared to linear polymers of similar composition. Precise architectural control in polymers is essential because it affects their properties and morphology. Among the branched structures, star polymers are architecturally interesting since each molecule has only one branch point. The synthesis of well-defined stars has always been a challenging task. There are two main methods to obtain star polymers: either by linking a given number of linear chains to a central core ("arm-first" method)[3,4] or by growing branches from an active core ("core-first" method).[5,6] In order to obtain stars with a precise number of arms by using the core-first methodology, it is essential to use structurally well-defined plurifunctional initiators.

In order to obtain well-defined stars, it is essential that a controlled polymerization technique be used that maintains chain functionality. There are different techniques like living anionic,[7,8] cationic,[9] and group transfer metathesis polymerization[10,11] to obtain well-defined stars, but all require strenuous methods of reagent purification and are only useful for a limited range of monomers. The development of controlled/"living" radical polymerization has opened up a potentially wide path to well-defined macromolecules.[12-14] Among the various controlled/"living" radical polymerization techniques, atom transfer radical polymerization (ATRP) provides control over chain length and chain functionality by maintaining a very low steady-state concentration of active growing chains which are in dynamic equilibrium with the so-called dormant species. There are several reports on ATRP-based synthesis of stars of different arm numbers using organic initiators and different transition metal catalysts.[15-19] There has been growing attention and interest towards the synthesis of star polymers initiated by inorganic cores.[18] Recently, the successful synthesis of organic/inorganic hybrid stars from an octafunctional cubic silsesquioxane via ATRP of methyl methacrylate has been reported.[20] This is due to the general interest of combining potential application of hybrid materials with the facility with which branched polymers can be processed.[21]

Here, we demonstrate the use of a novel silsesquioxane nanoparticle-based macroinitiator for ATRP with approximately 58 initiating functions to initiate the polymerization of a bulky sugar-carrying methacrylate monomer, 3-*O*-methacryloyl-1,2:5,6-di-*O*-isopropylidene-α-D-glucofuranose (MAIGlc) and describe the conditions best suited towards the synthesis of

well-defined glycostars. During recent years there has been an increasing attention paid to the synthesis of glycopolymers due to their high hydrophilicity and water-solubility. They can be used as efficient tools to investigate carbohydrate-based interactions and to understand nature´s multivalent processes.[22] They are of main interest with respect to very specialized applications in biochemical and biomedical fields, such as molecular recognition processes,[23] drug delivery systems[24] etc.

Controlled/"living" radical polymerization has proved to be a very facile approach for well-defined and controlled synthesis of glycopolymers.[25-27] As a part of our continuous efforts to develop branched glycopolymers having controlled architectures, here, we report on the synthesis of well-defined glycostars using "core first" approach via ATRP. We have very recently reported the synthesis and structural characterization of functional silsesquioxane-based nanoparticles.[28,29] In this report, these silsesquioxane nanoparticles are modified into ATRP macroinitiators with approximately 58 functions and used for the synthesis of glycopolymer/nanoparticle hybrids. Such organic-inorganic hybrid nanoparticles have attracted a great deal of attention due to their wide range of applications in optics, engineering and biosciences. To the best of our knowledge, this is the first report on employing silsesquioxane nanoparticle-based macroinitiators for the synthesis of well-defined glycopolymer-inorganic hybrid stars. The synthetic route leading to glycostars is shown in scheme 1.

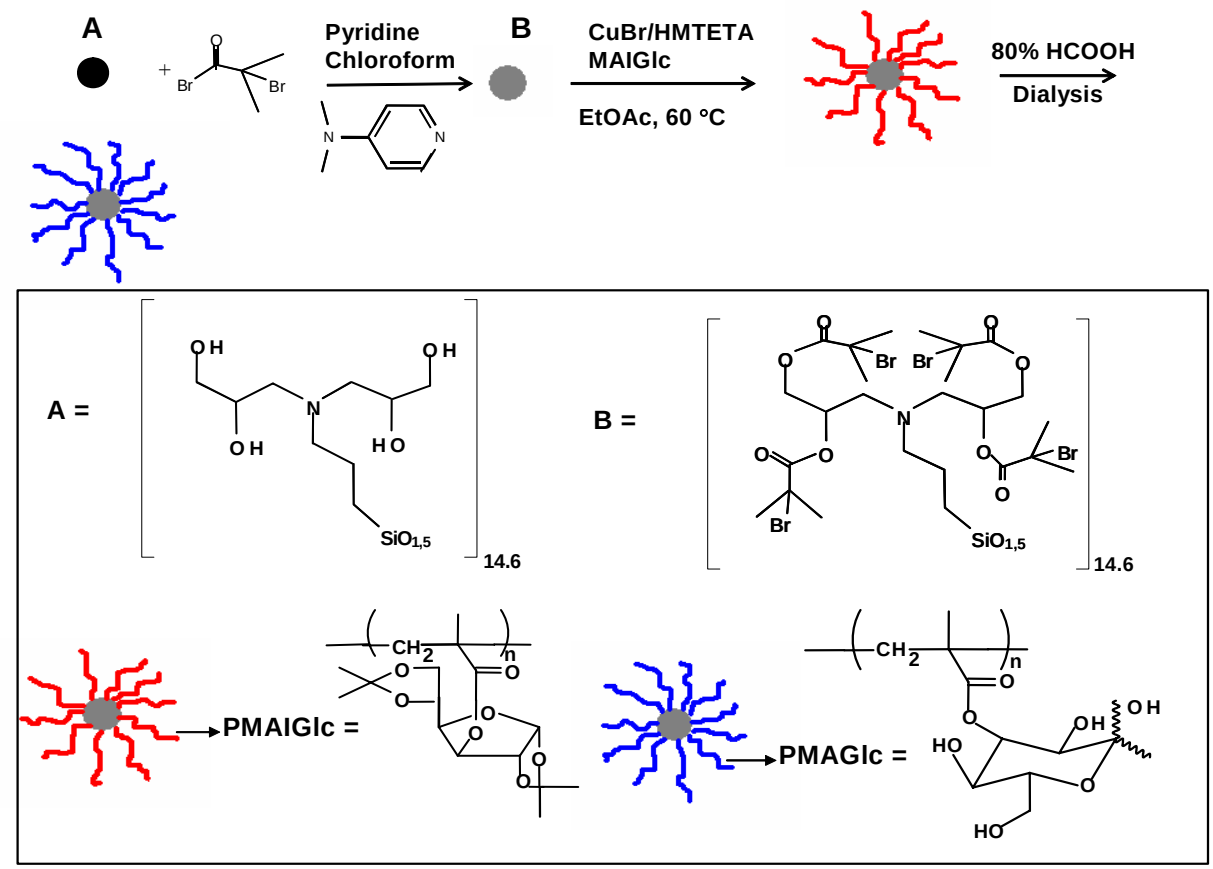

Scheme 1. *General route to the synthesis of glycopolymer/silsesquioxane hybrid stars.*

7.2. Experimental Section

Materials. CuBr (95%, Aldrich) was purified by stirring overnight in acetic acid. After filtration, it was washed with ethanol, ether, and then dried. 1,1,4,7,10,10-Hexamethyltriethylenetetramine (HMTETA, 97 %, Aldrich) was distilled and degassed before use. 3-*O*-Methacryloyl-1,2:5,6-di-*O*-isopropylidene-D-glucofuranose (MAIGlc) was synthesized by the reaction of 1,2:5,6-di-*O*-isopropylidene-D-glucofuranose and methacrylic anhydride in pyridine and purified by vaccum distillation as reported by us recently.[30] 2-Bromo-2-methylpropionyl bromide (98%, Aldrich) and 4-(N,N-dimethylamino) pyridine (99%, Aldrich) were used as received without further purification. The synthesis of the functional silsesquioxane nanoparticles with 3-bis(2,3-dihydroxypropyl)aminopropyl functions by acidic condensation of the corresponding triethoxysilane was described earlier.[28,29]

Synthesis of the Silsesquioxane-Based Macroinitiator: The functional silsesquioxane nanoparticles (10 g; 0.155 mol hydroxy groups) were dried thoroughly in a vacuum oven at

80°C for 3 h before use. Pyridine (60 ml) and chloroform (100 ml) were added to a round-bottom flask containing nanoparticles. To the above solution was added one spatula of 4-(N,N-dimethylamino) pyridine and then it was cooled with ice. 2-Bromo-2-methylpropionyl bromide (41 g; 0.178 mol; 22 ml) was added dropwise slowly until the mixture changed to yellow. The mixture was stirred for 2 days. Then the brown suspension was diluted with diethyl ether (two liquid phases) and extracted twice with cold water. The yellow organic phase was washed twice with 5 wt % NaOH. Finally, the organic layer was dried with $MgSO_4$ and the solvent was removed under reduced pressure. The product was then freeze-dried from dioxane (17 g; yield 51 %). It was further purified by dialysis from THF (Spectra Pore; MWCO: 1000 Da). After two days the solution was concentrated, freeze dried from dioxane and dried in the vacuum oven (40°C; 4h). ^{1}H NMR ($CDCl_3$): 0.3-0.8 (-CH_2 in the α position to the silicon atom), 1.3-1.7 (-CH_2 in the β position to the silicon atom), 1.8-2.0 (-CH_3 adjacent to the bromine atom), 2.2-3.0 (-CH_2 in the α position to the N atom), and 3.9-5.3 (-CH_2 and -CH in the α position to the O atom). The molecular weight and polydispersity index (PDI) for the modified nanoparticles as determined by MALDI-TOF MS were M_n = 10,500 and M_w/M_n = 1.25, respectively.

Elemental Analysis: 37.44 wt.% Br (expected: 37.41); 1.70 wt.% N (expected: 1.64); 3.38 wt.% Si (expected: 3.29).

Polymerizations. All polymerizations were carried out in a round bottom flask sealed with a plastic cap. A representative example for the synthesis of glycostars is as follows: To a round bottom flask containing CuBr (3.5 mg, 0.025 mmol), MAIGlc (5.0 g, 15.24 mmol) in ethyl acetate (5.0 g, 50 wt %) was added the silsesquioxane-based macroinitiator, (10.1 mg, 0.050 mmol) (See Table 1) and stirred for 5 min to dissolve the macroinitiator completely. Then HMTETA (5.6 mg, 0.025 mmol) was added to this mixture and the color changed to green indicating the start of the polymerization. The flask was then placed in an oil bath at

60 °C for 25 min. Monomer conversion as detected by ^{1}H NMR, was 8 %. The content in the flask was viscous even at such a low conversion which was then dissolved in THF. The solution was passed through a silica column, and the polymer was precipitated from THF into methanol two times. Then it was again precipitated in petroleum ether twice to remove the unreacted monomer completely. Finally the product was freeze-dried from dioxane and dried under vacuum at room temperature. The polymer had $M_n = 16.0 \times 10^4$ and $M_w/M_n = 1.12$ according to conventional GPC using PtBMA calibration, and $M_n = 41.6 \times 10^4$ and M_w/M_n = 1.17 according to GPC/viscosity using universal calibration, and $M_n = 43.6 \times 10^4$ and M_w/M_n

= 1.20 according to GPC/MALS measurement. The resulting polymer was completely soluble in THF, chloroform, and dioxane but insoluble in methanol, acetone and water.

Solvolysis of the Glycostars. Arm cleavage was achieved via base-catalyzed transesterification in methanol similar to that adopted for the solvolysis of glycocylindrical brushes.[31,32] The polymer (10 mg) was dissolved in THF in a capped vial. Methanol was added until the polymer was precipitated, and then sodium methoxide (25 % in Methanol, 4-5 drops) was added. The capped vial was then placed in an oil bath and kept at 90 ºC for 3 days. Then, the solution was cooled and stirred for 2 h in the presence of cationic ion-exchange resin (Dowex MSC-1). The solution was decanted and evaporated to yield cleaved arms. The molecular weight of the resulting product was analyzed using conventional GPC and GPC-MALS measurements.

Deprotection. The transformation of protected glycostars into water-soluble ones with poly(3-*O*-methacryloyl-α,β-D-glucopyranose) (MAGlc) arms was achieved under mild acidic condition.[30] The polymer (50 mg) was dissolved in 80 % formic acid (12 mL) and stirred for 48 h at room temperature. Then 5 mL of water were added and it was stirred for another 3 h. The solution was dialysed using a Spectra/Por^R dialysis tube (MWCO: 1000) against Millipore water for 2 days. The resulting polymer was freeze-dried from water and dried under vacuum. The deprotected polymer was obtained as white powder which was soluble in water and methanol, but insoluble in THF and acetone.

Characterization. The apparent molecular weights of the stars and cleaved arms were characterized by conventional *GPC* using THF as eluent at a flow rate of 1.0 mL/min at room temperature. Column set: 5μm PSS SDV gel, 10^2, 10^3, 10^4, 10^5 Å, 30 cm each; detectors: Waters 410 differential refractometer and Waters photodiode array detector operated at 254 nm. Narrow PtBMA and PMMA standards (PSS, Mainz) were used for the calibration of the column set. GPC with a multi-angle light scattering detector (GPC/MALS) and a Viscotek viscosity detector H 502B (GPC/viscosity) were used to determine the absolute molecular weights of the stars and of the arms cleaved by solvolysis. THF was used as eluent at a flow rate of 1.0 mL/min. column set: 5μ PSS SDV gel, 10^3 Å, 10^5 Å and 10^6 Å, 30 cm each; detectors: Shodex RI-71 refractive index detector, and Wyatt DAWN DSP-F MALS detector equipped with a 632.8 nm He-Ne laser. The refractive index increment in THF solution of the glycostar and cleaved arms at 25 ºC were determined to be dn/dc = 0.066 mL/mg and 0.065 mL/mg, respectively using a PSS DnDc-2010/620 differential refractometer. The refractive index increment in water solution of the deprotected glycostar at 25 °C was determined to be 0.146 mL/mg. For GPC/viscosity the universal calibration principle was used. Linear PMMA

standards (PSS, Mainz) were used to construct the universal calibration curve. *^{1}H NMR* was recorded with a Bruker AC-250 instrument at room temperature. *Fourier transform infrared* (FT-IR) spectra were recorded on a Bruker Equinox 55 spectrometer. The elemental analyses were performed by IIse Beetz Mikroanalytisches Laboratorium (Kulmbach).

MALDI-TOF mass spectrometry was performed on a Bruker Reflex III instrument equipped with a 337 nm N_2 laser in the reflector mode and 20 kV acceleration voltage. 2,5-Dihydroxy benzoic acid (Aldrich, 97%) was used as a matrix for molecular weight determination of the silsesquioxane initiator (mass ratio DHB : initiator 10 : 1; linear mode). Overlap with signals of matrix or low molecular compounds was resolved by Lorentzian fit in the undisturbed region, as a Gaussian fit showed to be less suitable for proper alignment with the measured signal.

Asymmetric flow field-flow fractionation (AF-FFF) was accomplished for the deprotected glycostar on a Postnova HRFFF-10000 system equippted with RI, UV and multiangle light scattering (Wyatt DAWN EOS, λ = 632.8 nm) detectors: dimension of the channel, 0.35 mm; cutoff molecular weight of the membrane 5KDa; injection volume, 20 μL; constant cross–flow gradient, 1.5 mL/min within 30 min; laminar flow out, 0.6 mL/min; eluent, water with 25 mM of sodium nitrate and 200 ppm of sodium azide; sample concentration, 0.5 g/L.

Dynamic light scattering (DLS) was performed on an ALV DLS/SLS-SP 5022F compact goniometer system with an ALV 5000/E correlator and a He-Ne laser (λ = 632.8 nm). Prior to the light scattering measurements the sample solutions were filtered using Millipore Teflon filters with a pore size of 0.45 μm. The measured intensity correlation functions were subjected to CONTIN analysis. Apparent hydrodynamic radii of the glycostars were calculated according to the Strokes-Einstein equation.

The samples for *scanning force miscroscopy* (SFM) measurements were prepared either by spin-coating from dilute (8 mg/L) solutions of glycostars in tetrahydrofuran or methanol/water (1/1, volume ratio) mixtures, onto freshly cleaved mica surface. The SFM images were taken with a Digital Instruments Dimension 3100 microscope operated in Tapping Mode (free amplitude of the cantilever ≈ 30 nm, set point ratio ≈ 0.98, tip radius ~ 20 nm).

The samples for *field emission scanning electron microscopy* (FE-SEM) measurements were prepared either by spin-coating from dilute (8 mg/L) solutions of glycostars in tetrahydrofuran or methanol/water (1/1, volume ratio) mixtures, onto polished silicon wafers. These samples were directly characterized by using a LEO 1530 Gemini microscope (acceleration voltage, 1.0 kV).

Bright field *transmission electron microscopy* (TEM) was performed using a Zeiss electron microscope (CEM 902) operated at 80 kV. The samples were prepared by negative staining with uranyl acetate on carbon-coated Cu grids from dilute (10 mg/L) water solutions according to the standard procedure.[33] For *cryogenic transmission electron microscopy* (cryo-TEM) studies, a drop of the sample was put on an untreated bare copper TEM grid (600 mesh, Science Services, München, Germany), where most of the liquid was removed with blotting paper leaving a thin film stretched over the grid holes. The specimens were instantly shock frozen by rapid immersion into liquid ethane and cooled to approximately 90 K by liquid nitrogen in a temperature-controlled freezing unit (Zeiss Cryobox, Zeiss NTS GmbH, Oberkochen, Germany). The temperature was monitored and kept constant in the chamber during all the sample preparation steps. After freezing the specimens, the remaining ethane was removed using blotting paper. The specimen was inserted into a cryo-transfer holder (CT3500, Gatan, München, Germany) and transferred to a Zeiss EM922 EF-TEM. Examinations were carried out at temperatures around 90 K at an acceleration voltage of 200 kV. Zero-loss filtered images ($\Delta E = 0$ eV) were taken under reduced dose conditions (100 – 1000 e/nm^2). All images were registered digitally by a bottom mounted CCD camera system (Ultrascan 1000, Gatan) combined and processed with a digital imaging processing system (Gatan Digital Micrograph 3.9 for GMS 1.4).

7.3. Results and Discussion

7.3.1. Synthesis and Characterization of the Silsesquioxane Nanoparticle-Based Macroinitiator. We have very recently reported the synthesis and structural determination of functional silsesquioxane nanoparticles (see Scheme 1).[28,29] The molecular weight and PDI of the nanoparticles are Mn = 3,760 and Mw/Mn = 1.21 as determined by MALDI-TOF MS. These nanoparticles were found to consist of complete and incomplete cage-like structures with Si-O-Si and Si-O-C bonds.28 The average particle size is 2.7 nm as determined by TEM. Since the molecular weight of a unit with one Si atom is 258.3 the particles contain approximately 14.6 Si atoms or 58 hydroxyl functions. The standard deviation of the MALDI-TOF MS distribution (Figure 1) is 31 %, thus the particles have 58 ± 18 hydroxyl functions.

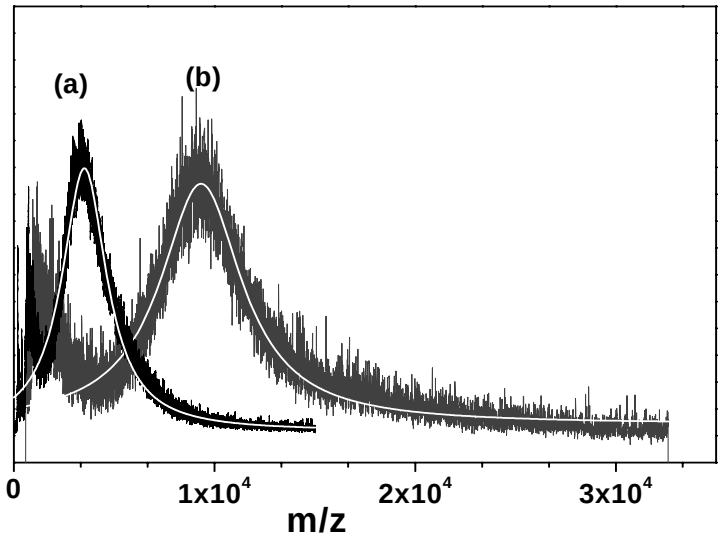

Figure 1. *MALDI-TOF mass spectra of (a) silsesquioxane nanoparticles and (b) silsesquioxane-based macroinitiator. The lines represent Lorentzian fits.*

These silsesquioxane nanoparticles were transformed to ATRP macroinitiators with approximately 58 initiating functions by the esterfication reaction with 2-bromo isobutyryl bromide. Figure 2 represents the ^{1}H NMR spectra of the silsesquioxane-based nanoparticles and macroinitiator. The characteristics peaks of the macroinitiator are clearly seen at 0.3-0.8 (*CH*$_2$ in the α position to the silicon atom), 1.3-1.7 (*CH*$_2$ in the β position to the silicon atom), 1.8-2.0 (-*CH*$_3$ adjacent to the bromine atom), 2.2-3.0 (*CH*$_2$ in the α position to the N atom), and 3.9-5.3 (*CH*$_2$ and *CH* in the α position to the O atom), respectively indicating the successful synthesis of the macroinitiator.

Figure 3 shows the FT-IR spectra of the nanoparticles and the macroinitiator. In the case of nanoparticles, there is a broad absorption band for the hydroxyl functionality from 3000 to 3800 cm^{-1} with a maximum at 3400 cm^{-1}. In addition, a sharp peak between 2840 and 2940 cm^{-1} is seen, which is due to the C-H stretching vibration in the alkyl chain on the nanoparticles and also a strong absorption band around 1030-1150 cm^{-1} resulting from Si-O-Si stretching is observed. In the case of the silsesquioxane-based macroinitiator, the disappearance of the broad absorption band of OH functionality at around 3000-3800 cm^{-1}

and also the appearance of a sharp peak at 1740 cm^{-1} resulting from the carbonyl functionality indicates the successful synthesis of the macroinitiator.

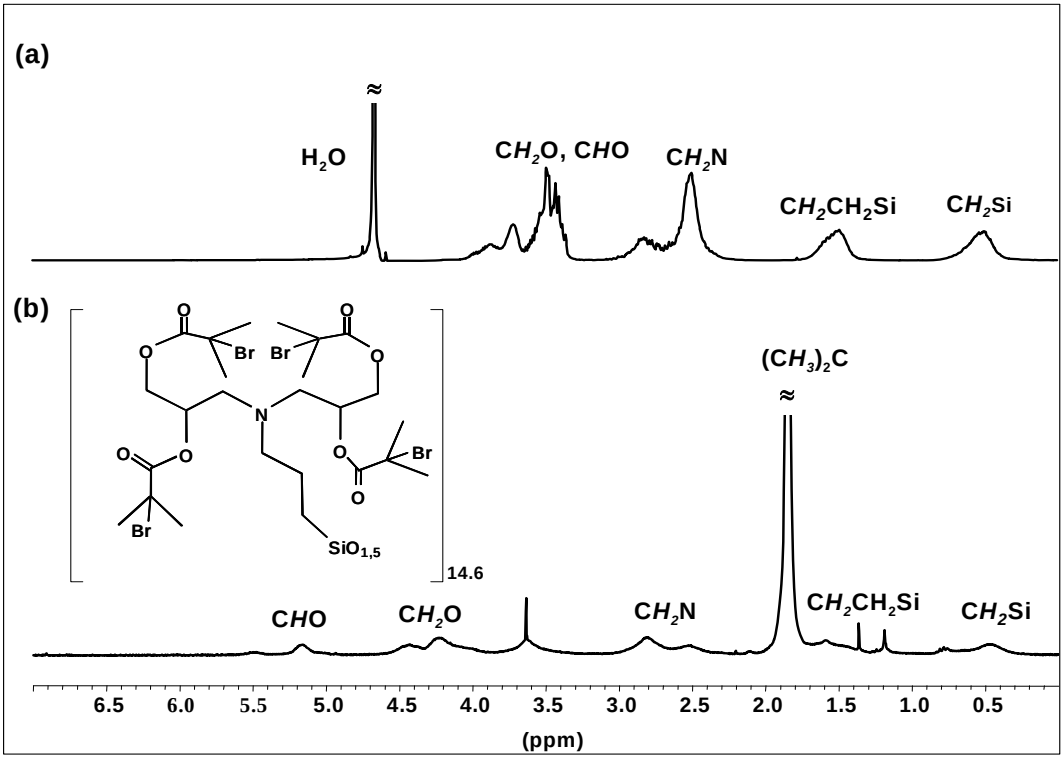

Figure 2. *^1H NMR spectra of (a) silsesquioxane-based nanoparticles (D_2O) and (b) silsesquioxane-based macroinitiator ($CDCl_3$).*

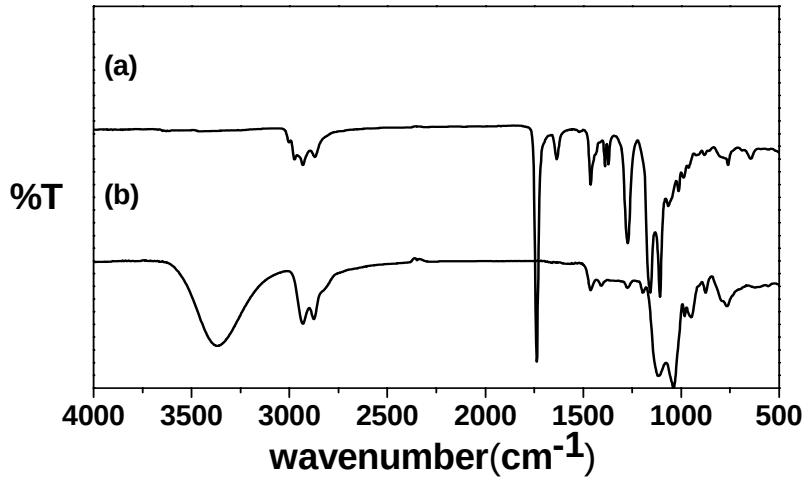

Figure 3. *FT-IR spectra of (a) silsesquioxane-based macroinitiator, and (b) silsesquioxane nanoparticles.*

The macroinitiator was further investigated by MALDI-TOF MS and elemental analysis. The molecular weight and PDI of the modified nanoparticles are M_n = 10,200 and M_w/M_n = 1.25 (Figure 1). The molecular weight is lower than the calculated one ($M_{n,cald}$ = 12,500) Since FT-IR indicates full conversion of hydroxyl functions to α-bromoesters, we attribute the difference to the loss of HBr molecules in the ionization procedure, which is a common observation for bromoesters[19]. The atomic composition of the silsesquioxane-based macroinitiator determined by elemental analysis are Br, 37.44; N, 1.70; Si, 3.38 (Calcd: Br, 37.41; N, 1.64; Si, 3.29), respectively. The agreement between experimental and calculated values indicates the successful synthesis of the silsesquioxane-based macroinitiator of approximately 58 functions.

7.3.2. Synthesis and Characterization of Glycomethacrylate Stars. We have recently reported that CuBr/HMTETA is one of the best catalyst systems for the hompolymerization of MAIGlc to obtain linear poly(MAIGlc)s with narrow molecular weight distribution (MWD).[30] Therefore, we chose this catalyst system in order to obtain well-defined glycostars. Table 1 represents the results of the synthesis of glycostars using the silsesquioxane-based macroinitiator and MAIGlc as the monomer. The aim of our study was to obtain well-defined glycostars of different arm lengths. Hence the polymerization was restricted to low conversions in order to avoid inter-macromolecular coupling reactions. As can be seen from Table 1, a high ratio of monomer to initiator and a low conversion were found to be sufficient to suppress undesirable side reactions. It has also been reported by Laine et al., that well-defined eight-arm PMMA stars could be synthesized using octafunctional cubic silsesquioxanes only at very low conversions.[20]

Table 1. Synthesis and characterization of silsesquioxane-based glycomethacrylate stars via ATRP[a]

Glycostar	$[M]_0/[I]_0$	Time (min)	Conv.[b] (%)	10^{-4} x $M_{n,cald.}$[c]	10^{-4} x $M_{n,\ GPC}$[d] (PDI)	10^{-4} x $M_{n,\ GPC\text{-}VISCO}$[e] (PDI)	10^{-4} x $M_{n,GPC\text{-}MALS}$[f] (PDI)	$DP_{n,arm,cald.}$[g]
1	100	10	16.0	30.4	11.8 (1.09)	24.5 (1.25)	24.9 (1.12)	13
2	300	15	5.0	28.5	9.2 (1.08)	25.6 (1.25)	26.4 (1.12)	14
3	300	25	8.0	45.7	16.0 (1.12)	41.6 (1.17)	43.6 (1.20)	23
4	600	25	6.0	68.4	23.2 (1.12)	60.1 (1.26)	66.0 (1.12)	35

[a]Solution polymerization in ethyl acetate (50 wt% to MAIGlc) at 60 °C at constant $[I]_0 : [CuBr]_0 : [HMTETA]_0 = 1 : 0.5 : 0.5$. [b]Determined by ^{1}H-NMR. [c]Calculated assuming 100 % initiation site efficiency of the silsesquioxane-based macroinitiator. [d]Determined by GPC using THF as eluent with PtBMA standards. [e]Determined by GPC/viscosity measurement. [f] Determined by GPC-MALS measurement. [g]Calculated from $M_{n,\ GPC\text{-}MALS}$ assuming 100 % initiation site efficiency.

Figure 4 represents the ^{1}H NMR of the glycostar poly(MAIGlc). As it can be seen from Figure 4, after the formation of the star with the silsesquioxane core, the characteristic peaks at 1.2-1.4 ppm (isopropylidene protons), 3.8-5.0 and 5.7-6.0 ppm are clearly seen indicating the successful formation of the glycostars with silsesquioxane core.

The molecular weights of the resulting glycostars were first estimated by conventional GPC using PtBMA calibration. The GPC traces show monomodal distributions indicating the well-defined and controlled synthesis of the required glycostars as shown in Figure S-1 (Supporting Information). The polydispersities of the polymer samples measured in this study remain low ($M_w/M_n \leq 1.25$, Table 1). The molecular weights obtained by conventional GPC using PtBMA calibration are just apparent ones due to the compact nature of the branched macromolecules and the lack of suitable standards. Hence, GPC/viscosity and GPC/MALS techniques were further used to estimate the true molecular weights of the glycostars.

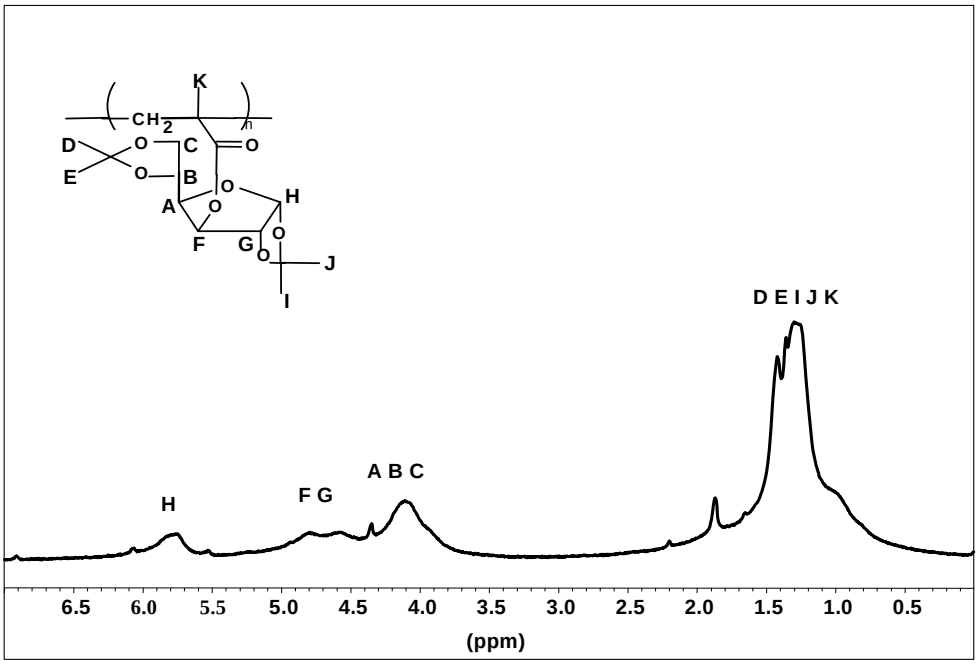

Figure 4. *^{1}H NMR spectra ($CDCl_3$) of Glycostar 4, poly(MAIGlc).*

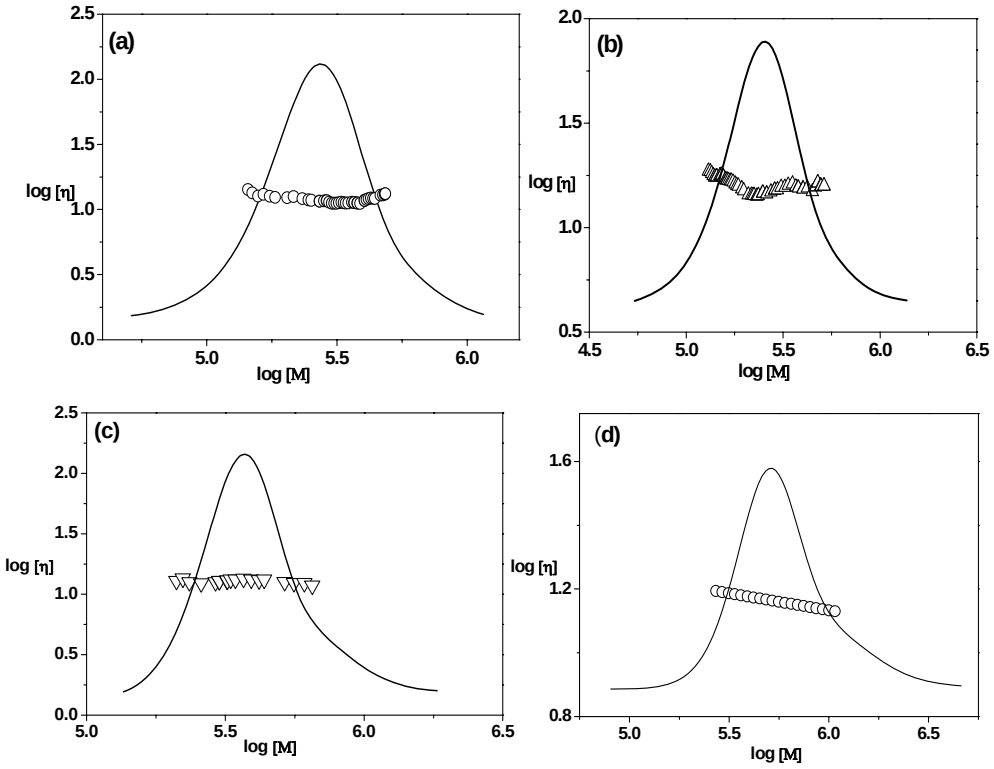

Figure 5. *Molecular weight distributions (RI signal) and intrinsic viscosities of (a) Glycostar 1, (b) Glycostar 2, (c) Glycostar 3, and (d) Glycostar 4.*

GPC coupled with an online viscometer (GPC/viscosity) was used to determine the absolute molecular weights as well as the Mark-Houwink exponent for the relationship between intrinsic viscosity and molecular weight of the glycostars. The GPC/viscosity traces exhibit monomodal distributions as can be seen from Figure 5. The molecular weights obtained by GPC/viscosity are higher than those obtained by conventional GPC using PtBMA calibration indicating their compact nature (Table 1). The Mark-Houwink exponents will be discussed further below.

The glycostars were further characterized by GPC with a multiangle light scattering detector (GPC/MALS) in order to obtain the absolute molecular weights and the radii of gyration of the stars. As can be seen from Table 1, the molecular weights are in agreement with those obtained by GPC/viscosity and the calculated ones. The peaks also show monomodal distribution indicating the well-defined nature of the glycostars . The radii of gyration will be discussed further below.

7.3.3. Arm cleavage of the Glycostars. In order to determine the exact initiation site efficiencies, solvolysis of the glycostars with sodium methoxide was performed to cleave the arms from the silsesquioxane core. ^{1}H NMR spectra of the resulting products (cf. Figure 6) revealed that solvolysis of Glycostar 4 with sodium methoxide resulted in side chains consisting of a statistical copolymer of 17 % MMA and 83 % MAIGlc units similar to that observed in the case of the solvolysis of glycocylindrical brushes.[31] The comonomer composition was determined by comparing the peaks at 3.59 ppm attributed to the methyl ester protons (OCH_3) of the MMA units and at 5.8-6.0 ppm attributed to the single ring proton of MAIGlc units. Similar results were obtained for Glycostar 3. In order to calculate the DP of the side chains, the molecular weights of the arms were divided by an average molecular weight of the comonomers, M_0 = 290 g/mol.

Table 2. Characterization of cleaved arms of PMAIGlc Glycostars and initiation site efficiencies, f [a)]

Glycostar	10^3 $M_{n,\ GPC}$ [b]	M_w/M_n [b]	10^3 $M_{n,\ GPC\text{-}MALS}$ [c]	$DP_{n,cald.}$ [d]	$DP_{n,exp.}$ [e]	f (%)
3	20.0	1.28	16.0	23	55.2	42.6
4	27.6	1.38	23.0	35	79.3	44.1

[a] $f = DP_{n,calc}/DP_{n,exp.}$ [b]Determined by GPC using THF as eluent with PS standards. [c]Determined by GPC-MALS measurement. [d]Calculated from $M_{n,\ GPC\text{-}MALS}$ assuming 100 % initiation site efficiency. [e]Determined by the GPC-MALS measurement of cleaved arms after solvolysis.

Table 2 summarizes the detailed characterization of the arms cleaved by solvolysis and the corresponding initiation efficiencies, f. The GPC traces of Glycostar 4 and of the cleaved arms are given in Figure 7. The monomodal character of the detached arms shows the absence of inter- and intramolecular coupling reactions. The absolute molecular weights of the cleaved arms were determined by using GPC-MALS measurements. The polydispersity index of the cleaved arms is $M_w/M_n \cong 1.3$ (Table 2), which is a typical value for polymers obtained by slow initiation (limiting $M_w/M_n = 1.33$ for $k_p >> k_i$ in the Gold distribution[34]). The initiating efficiencies of Glycostars 3 and 4 were found to be 42.6 and 44.1 % (Table 2), which are attributed to the steric hindrance exerted by the bulky sugar-carrying monomer used in this study. This implies that approximately 25 ± 8 arms have been initiated instead of 58. Correspondingly, the arms of Glycostars 1 and 2 are longer than calculated by a factor of 1/0.43 = 2.3, respectively. Even in the case of a less bulkier monomer, like *tert*-butyl acrylate, the initiating site efficiency using this silsesquioxane-based macroinitiator is in the

range of 60-70%[35] indicating that not only the steric hindrance of the monomer plays a role. To some extent the structure of the silsesquioxane-based macroinitiator itself could contribute to the lowering of the initiating efficiency due to the enhanced steric crowding as the chain grows, making some of the initiating sites inaccessible.

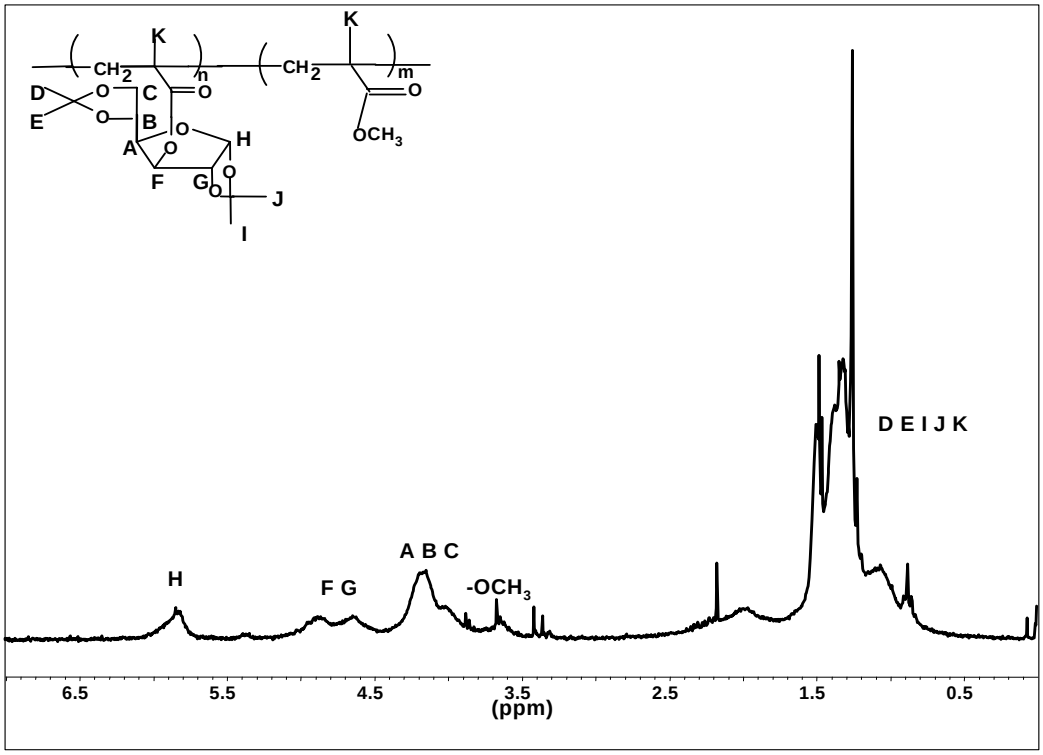

Figure 6. *^1H NMR spectrum ($CDCl_3$) of the cleaved arms of Glycostar 4.*

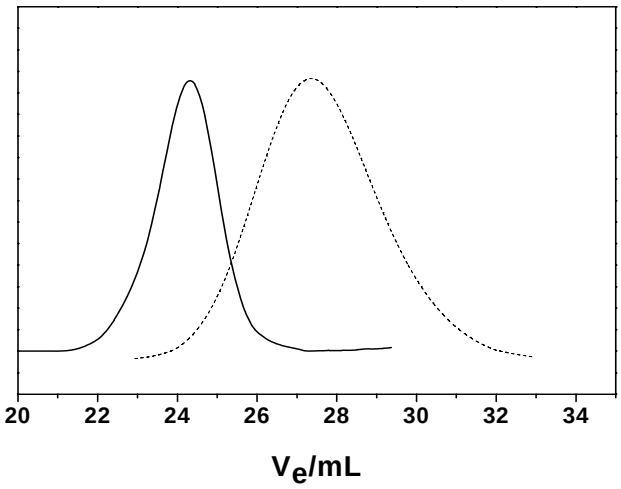

Figure 7. *GPC traces of Glycostar 4 (—) and cleaved arms (····) after solvolysis.*

7.3.4. Solution Properties of Protected Glycostars. The solution properties of glycostars were characterized using GPC/viscosity, GPC/MALS and DLS measurements. Compared to their linear analogues with the same molecular weight star polymers have smaller dimensions leading to a lower intrinsic viscosity. This effect becomes more pronounced with increasing number of arms. For stars with the same arm number but with different arm lengths, the Mark-Houwink exponent of the relation between intrinsic viscosity and molecular weight, $[\eta] = K[M]^{\alpha}$, is the same as for a linear polymer.[36] On the other hand, if the arm length is constant and the arm number varies, the Mark-Houwink exponent can become negative.[37] As can be seen from Table 3 and Figure 5, the α values for the four protected glycostars in THF are found to be slightly negative. On one hand, this could result merely from the hydrodynamic broadening in the columns due to the rather low polydispersities of the polymers. On the other hand, it could also result from a polydispersity in arm numbers. In order to clarify these points, a mixture of glycostars was injected to get a broader molecular weight distribution which is more given by a polydispersity of arm lengths in this case. The number-average molecular weight and PDI for the mixture of star polymers are $M_n = 28.3 \times 10^4$ and $M_w/M_n = 1.33$, respectively (Figure 8). The observed Mark-Houwink exponent, $\alpha = 0.42 \pm 0.01$ is close to that ($\alpha = 0.51 \pm 0.03$) for the mixture of linear poly(MAIGlc)s.[30] The slightly lower α value in our study compared to the linear poly(MAIGlc)s is attributed to the combined effects of the polydispersity in both the arm number and the arm length in the mixture of glycostars.

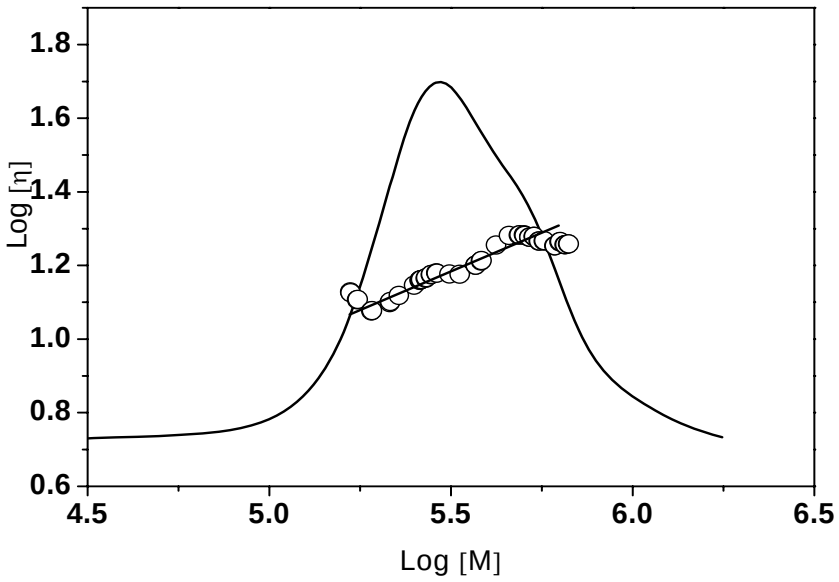

Figure 8. *Molecular weight distribution and and Mark-Houwink plot for mixture of glycostars 1-4; $\alpha = 0.42 \pm 0.01$.*

The radii of gyration of the glycostars are quite low (Table 3) and increase slightly with the arm length. The Zimm plots are shown are shown in Figure S-2 (Supporting Information). According to Daoud and Cotton,[38] $R_g \sim N^{0.2} \cdot M_{arm}^{0.5}$, the exponent for the relationship between the molecular weight and radius of gyration, α_s for the star polymer with constant number of arms is close to that of the corresponding linear polymer. In our study, determination of α_s was impossible owing to the very low radii of gyration (≤ 15 nm) of the glycostars. Nevertheless, further information was obtained from the combination of GPC/MALS and dynamic light scattering (DLS) data as described below.

Dynamic light scattering (DLS) was used to determine the hydrodynamic radii of the glycostars in THF solution. Figure 9a shows the normalized intensity correlation functions of Glycostar 4 at different angles. The autocorrelation functions were subjected to CONTIN analysis. The hydrodynamic radius distribution of this brush at scattering angle of 90° in THF is shown in Figure 9b. Table 3 shows the z-average hydrodynamic radius of all glycostars at 90°. The angular dependence of the hydrodynamic radii is very low, as expected for spherical structures. A structure-sensitive parameter is obtained from the ratio, $\rho = R_g/R_h$. As can be seen from Table 3, this parameter is close to unity. It has been calculated by Burchard et al.[2] that for star molecules with monodisperse arms and $f >> 1$, $\rho = 1.079$ under θ-conditions.

Table 3. Solution properties of silsesquioxane-based glycostars before and after deprotection in THF and water, respectively.

Glycostar	α^a	R_g^b	R_h^c	$\rho = R_g/R_h$
1	-0.210		8.7 ± 0.7	
2	-0.094		9.9 ± 0.4	
3	-0.049	10.7 ± 1.3	10.8 ± 0.8	0.99 ± 0.14
4	-0.090	14.6 ± 0.7	14.0 ± 0.7	1.04 ± 0.06
4[d]	-	14.4 ± 1.3	11.5 ± 0.6	1.25 ± 0.13

[a]Mark-Houwink exponent as determined by GPC/viscosity measurement. [b]Radius of gyration as determined by GPC-MALS. [c]z-average hydrodymic radius at 90° as determined by DLS measurements. [d]after depotection, characterized in water.

Figure 10 shows the molar mass dependence of the hydrodynamic radius (the radii of gyration of stars 1 and 2 were too low to allow for a reliable measurement but the ratio R_g/R_h apparently is constant). As mentioned earlier, for the star polymer with constant number of arms, the exponent should be close to that of the corresponding linear polymer. In our study, the value of $\nu_h = 0.42 \pm 0.08$ is slightly lower than 0.5 but close to the observed Mark-Houwink exponent, $\alpha = 0.42 \pm 0.01$ for mixture of star polymers. This lower value again indicates the slight polydispersity in both the arm number and the arm length.

The structure of these glycostars were further visualized using scanning force microscopy (SFM) and scanning electron microscopy (SEM) (see below).

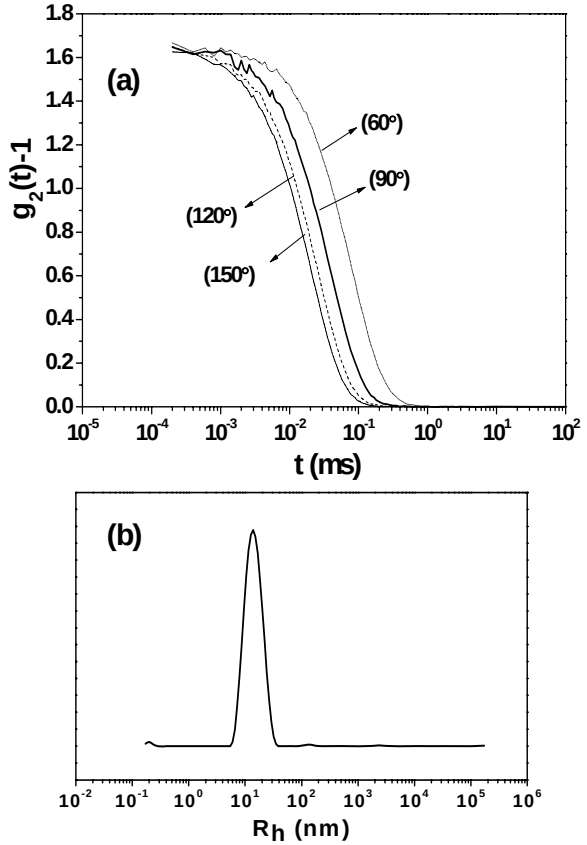

Figure 9. *(a) Normalized intensity correlation functions of Glycostar 4 in THF at different scattering angles, and (b) the corresponding intensity-weighted hydrodynamic radius distribution at scattering angle of 90º,* $<R_h>_z$ *= 14.0 nm.*

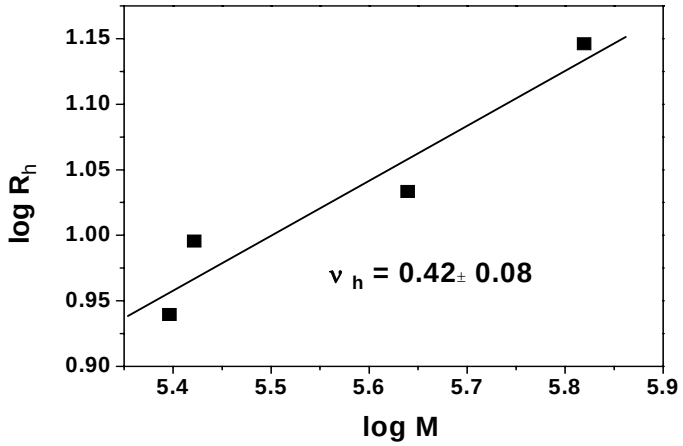

Figure 10. *Dependence of the hydrodynamic radius on molecular weight of the glycostars.*

7.3.5. Deprotection and Solution Properties of Deprotected Glycostars. Water-soluble glycostars were obtained by deprotection of the isopropylidene groups by treating the samples with formic acid at room temperature.[30] Figure 11a represents the ^{1}H NMR spectrum of the deprotected Glycostar 4. The signals of the isopropylidene protons (1.2-1.4 ppm) completely disappear and a broad signal due to the anomeric hydroxyl groups of the sugar moieties (6.4-7.0 ppm) appear indicating the quantitative deprotection of the isopropylidene groups. These stars are completely soluble in water and methanol, but insoluble in THF, chloroform and hexane.

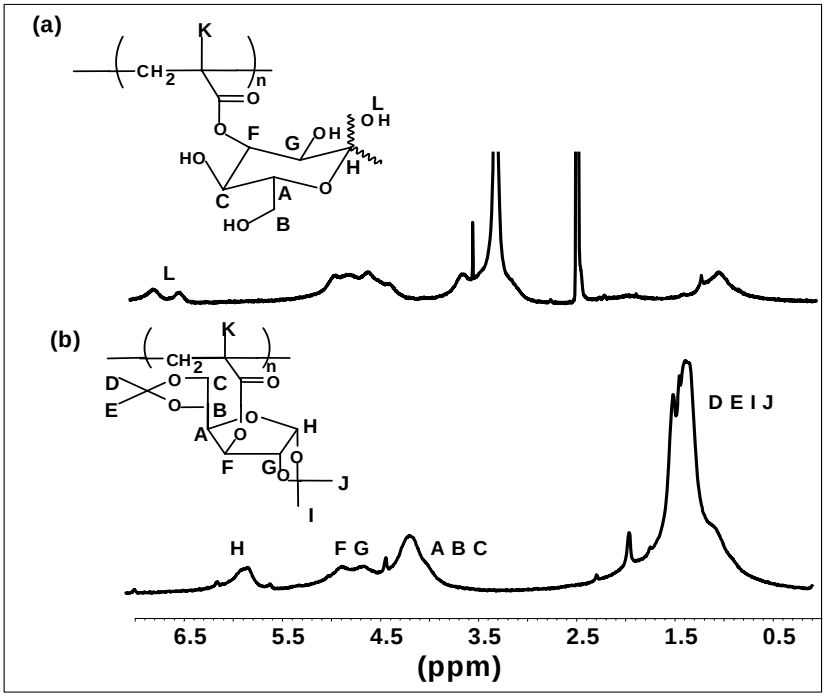

Figure 11. *^{1}H NMR spectra of (a) the deprotected Glycostar 4 with MAGlc arms (DMSO-d_6), and (b) Glycostar 4 with MAIGlc arms ($CDCl_3$).*

DLS was performed to study the solution properties of the deprotected Glycostar 4 in water. The CONTIN analysis of the autocorrelation functions showed a bimodal hydrodynamic radius distribution with R_h = 11.5 nm and 88 nm, respectively. The hydrodynamic radius distribution at a scattering angle of 90° in water is shown in Figure 12. The values of R_h for the smaller species are independent of the scattering angle, whereas those for the larger species show a pronounced angular dependence, indicating the formation of polydisperse aggregates which could be due to hydrogen-bonding interactions between the hydroxyl groups. Although these large species give considerable contribution to the intensity of the

scattered light, their weight or even mole fraction seems to be vanishing (less than a few percent by weight) and hence their presence in the system may be neglected.

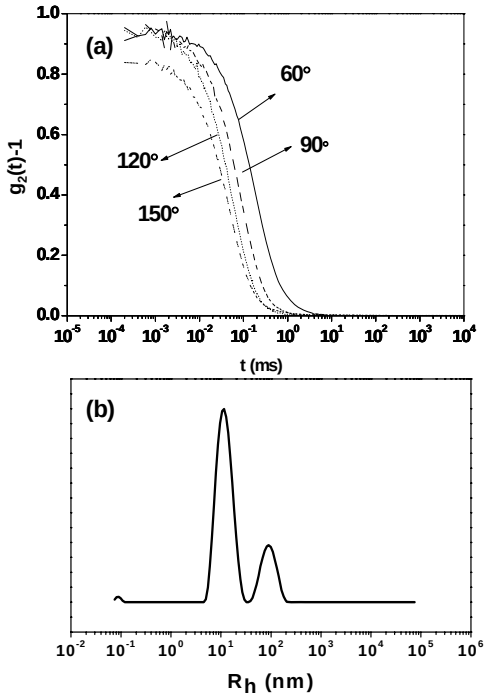

Figure 12. *(a) Normalized intensity correlation functions at different scattering angles, and (b) the corresponding intensity weighted hydrodynamic radius distribution at scattering angle of 90º of deprotected Glycostar 4 in water (0.5 g/L).*

The deprotected Glycostar 4 was further charcterized by asymmetric flow field-flow fractionation (AF-FFF) with a MALS detector in water with 25 mM of $NaNO_3$, which is added to minimize the interaction of the polymer with the membrane. As can be seen from Figure 13, there are two species separated by the cross-flow under the conditions used for elution. The amount of the first species is very low as can be seen from the concentration signal and is almost absent in the MALS signal. The molecular weight and PDI for the first species (area I in Figure 13) is found to be $M_n \sim 29 \times 10^4$ and $M_w/M_n = 1.22$ which could to due to a small population of stars with smaller arm lengths (DP ~ 47) or lower arm number (~ 15). The radius of gyration is too low to be determined for the first species. The molecular weight and PDI of the second species (area II) which is the required deprotected Glycostar 4 is determined to be $M_n = 53.5 \times 10^4$ ($M_{n,cald.} = 49.2 \times 10^4$) and $M_w/M_n = 1.16$, respectively. The radius of gyration is ~ 14 nm which is quite comparable to that before hydrolysis (14.6 nm). The zimm plot for the deprotected Glycostar 4 is shown in Figure S-3 (Supporting

Information). The structure-sensitive parameter, ρ, for the deprotected Glycostar 4 is found to be ρ = 1.25 ± 0.13, which is slightly but not significantly higher than the value obtained before hydrolysis. The increase in the ρ value after hydrolysis might be attributed to excluded volume interactions which have been predicted to increase the ρ values by around 13-17 % in simulations.[39-41] There is no significant peak for aggregates as was seen in by DLS, which shows that the presence of aggregates in our system may be neglected.

The deprotected Glycostar 4 was further visualized by SFM and FE-SEM as decscribed in the next section.

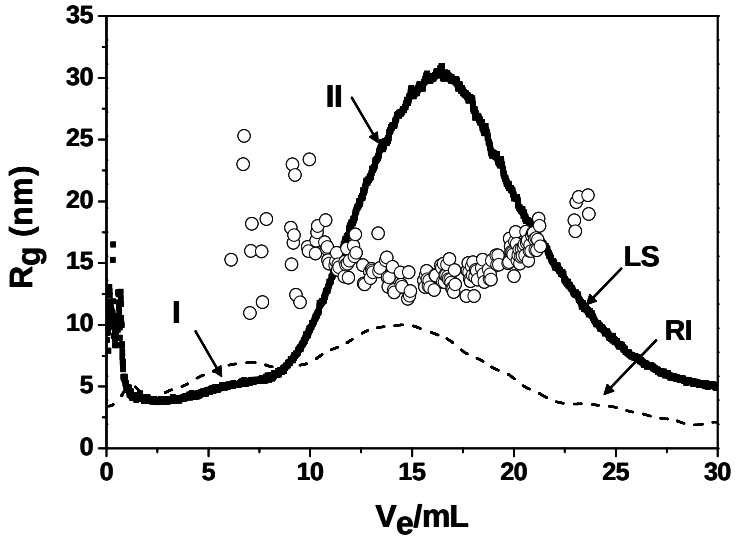

Figure 13. *Asymmetric flow field-flow fractionation (AF-FFF-MALS) traces of deprotected Glycostar 4 in water (0.5 g/L) with 25 mM $NaNO_3$, and (○) radius of gyration at a scattering angle of 90°.*

7.3.6. Visualization of the Glycostar/Silsesquioxane hybrids by Scanning Force and Electron Microscopies.

Protected Glycostars. In order to obtain further insight into the morphology of these hybrid glycostars, they were characterized by scanning force microscopy (SFM) by spin-coating a very dilute THF solution (8 mg/L) onto a freshly cleaved mica sheet. Figure 14 displays an image of Glycostar 4. Spherical isolated particles are clearly seen indicating the uniform and well-defined formation of hybrid stars. The diameter of the particle marked by a rectangle in Figure 14a is 46 nm (non-corrected for the tip radius) and the height is ~ 5 nm (see Figure S-4, Supporting Information) which is somewhat higher than the diameter of the

starting silsesquioxane nanopartilces (~ 3 nm). The polymer-silsesquioxane hybrids are much larger in diameter than the starting material, but very flat, indicating the collapsed structure of the hybrids on mica. Since the diameter obtained by SFM is always too high due to the tip size convolution, field emission scanning electron microscopy (FE-SEM) measurements were performed to obtain the exact size of the resulting glycostar hybrids.

Figure 15 displays the FE-SEM image of Glycostar 4, prepared by spin-coating from a dilute THF solution (8 mg/L) onto a silicon wafer. Well-defined and isolated particles can be clearly seen. The average diameter of these glycostars varies between 28 nm to 31 nm. This value is quite comparable to the results obtained by GPC-MALS and DLS (R_g = 14.6 nm and R_h = 14 nm, respectively). Hence these results confirm the successful formation of glycopolymer/silsesquioxane hybrid stars.

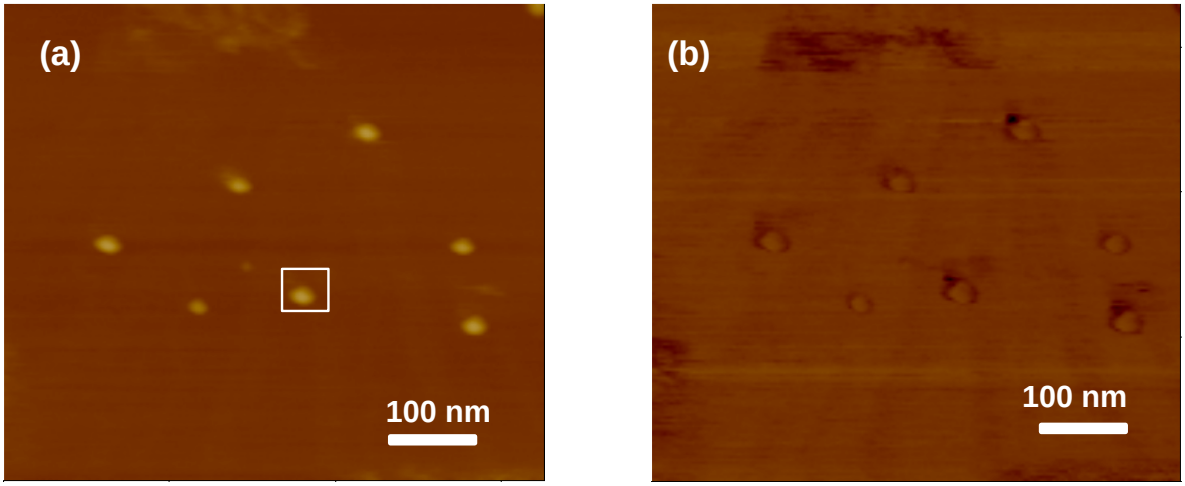

Figure 14. *SFM Tapping Mode images of Glycostar 4, spin-coated from dilute THF solution on to mica, (a) height image (z-range: 20 nm), (b) phase image (range: 45º).*

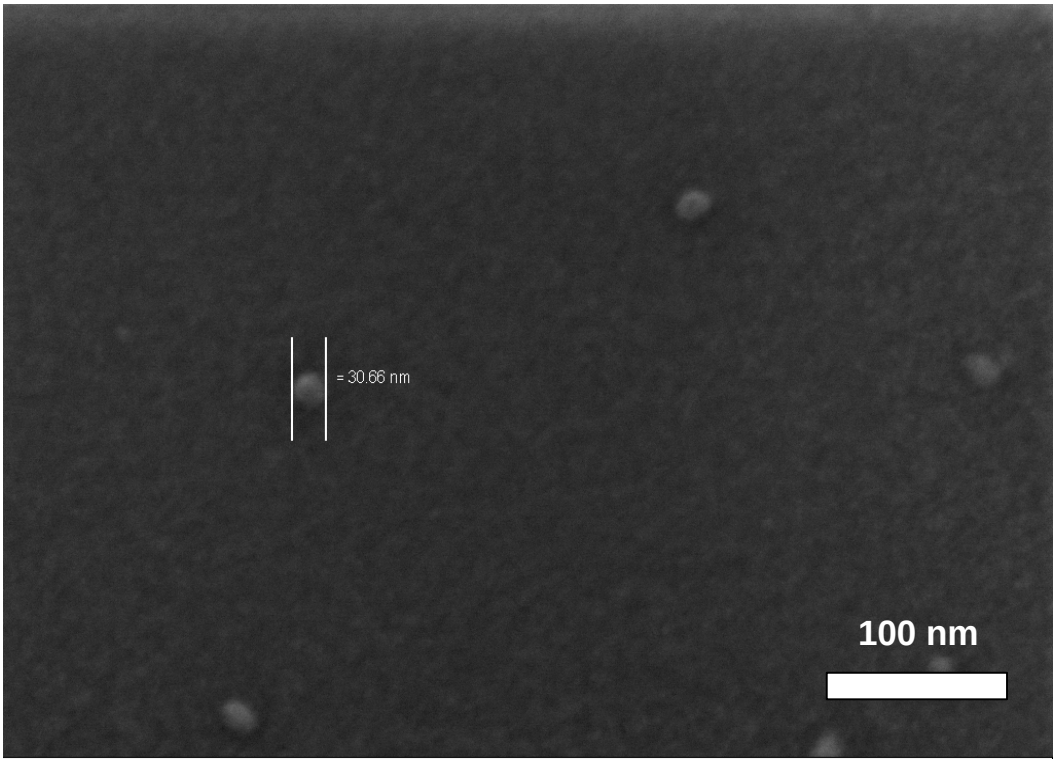

Figure 15. *Representative FE-SEM image of Glycostar 4, spin-coated from dilute THF solution onto a silicon wafer* .

Deprotected Glycostars. Figure 16 shows an SFM image of the deprotected Glycostar 4, spin-coated from a water-methanol mixture (volume ratio of 1/1) onto a freshly cleaved mica sheet. Spherical isolated particles are seen like those before hydrolysis indicating that the structure of the glycostars are retained during hydrolysis. The cross section of the particle marked in Figure 16b is shown in Figure S-5 (Supporting Information) and the diameter is found to be 40 nm. The height is ca. 3 nm, similar to the starting nanoparticles, indicating an even more collapsed structure. The diameters vary between 35 and 40 nm, but these values again suffer from convolution with the tip size.

FE-SEM images were taken of deprotected Glycostar 4 after spin-coating the sample from water-methanol mixture (volume ratio of 1/1) onto a silicon wafer. As it can be seen from Figure 17, there are isolated spherical objects of sizes ranging from 30 to 40 nm. Unlike the SFM images, some huge aggregates of approximately 100 nm in diameter are seen. This mainly could be due to the different substrates used for SFM and FE-SEM in the present study. In the case of silicon substrate, probably the interaction between the deprotected stars is much stronger than with the substrate resulting in the formation of aggregates during drying. The aggregates appear to have formed by the combination of several isolated

particles. Nevertheless, the size of the deprotected Glycostar 4 (diameter = 30-40 nm) is quite comparable to that obtained by AFFF and DLS measurements (R_g = 14.4 nm, R_h = 11.5 nm, respectively).

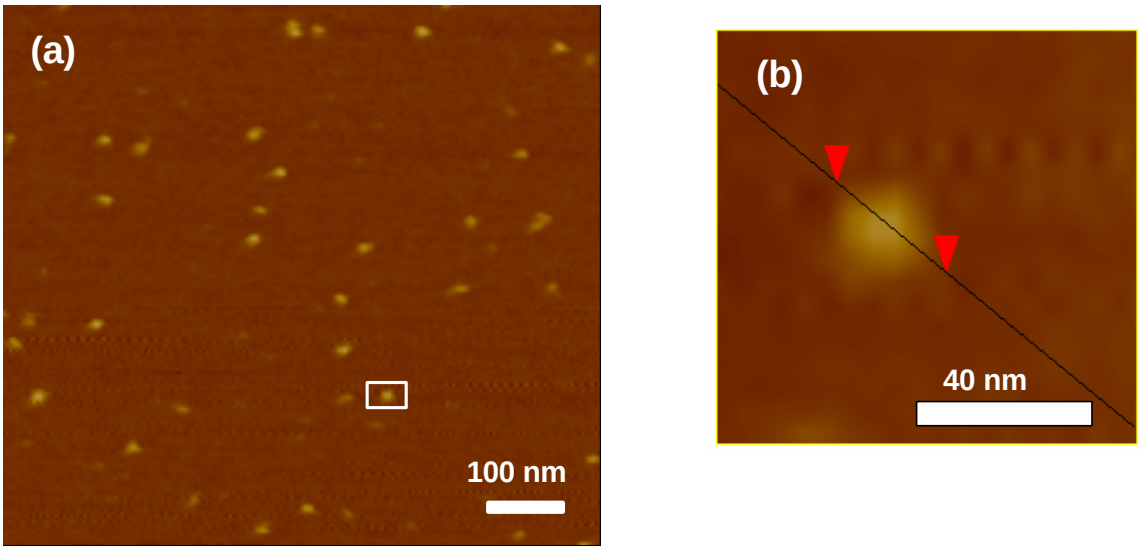

Figure 16. *SFM Tapping Mode images of the deprotected Glycostar 4, spin-coated from dilute water/methanol (1/1) solution onto mica, (a) height image (z-range: 10 nm), and (b) higher magnification of a single particle marked by a rectangle in (a).*

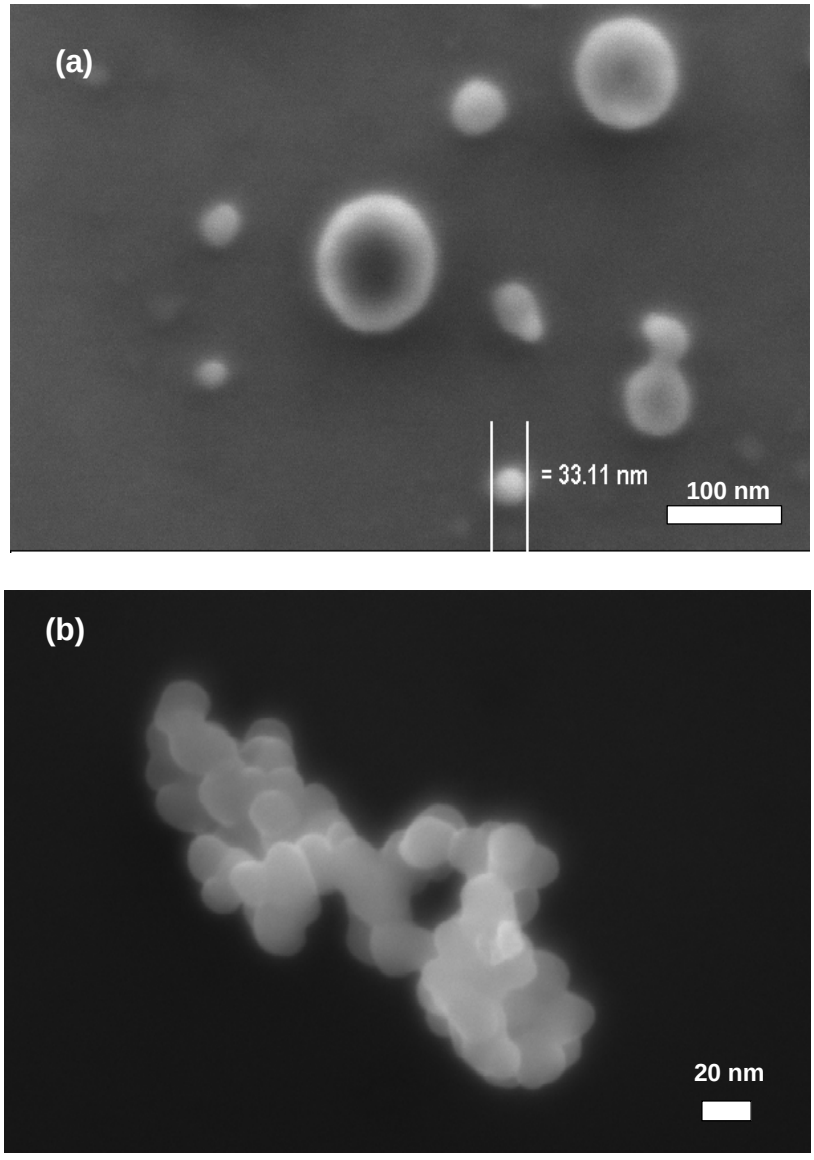

Figure 17. *Representative FE-SEM images of (a) deprotected Glycostar 4, and (b) aggregate formation, spin-coated from dilute water/methanol (1/1) solution onto mica.*

The structure of the deprotected Glycostar 4 was further characterized using cryo-TEM and TEM (negative staining using uranyl acetate) in aqeuous solution. Cryo-TEM allows to directly image the original shape and size of the polymers in solution, since the sample is vitrified before the measurement. As can be seen from Figure 18, cryo-TEM shows small dots which denotes only the silsesquioxane-based core of the stars and the diameter is approximately 5±2 nm. The shell is not seen in the cryo-TEM image due its very low contrast against water. In order to get further insights, TEM images were recorded using negative staining with uranyl acetate which is shown as an insert in Figure 18. Now, the contrast mechanism is different and spherical objects are observed similar to those seen from FE-SEM

and SFM images. The particle size varies between 25-45 nm, respectively and the shell is seen without a distinct core unlike in the case of cryo-TEM.

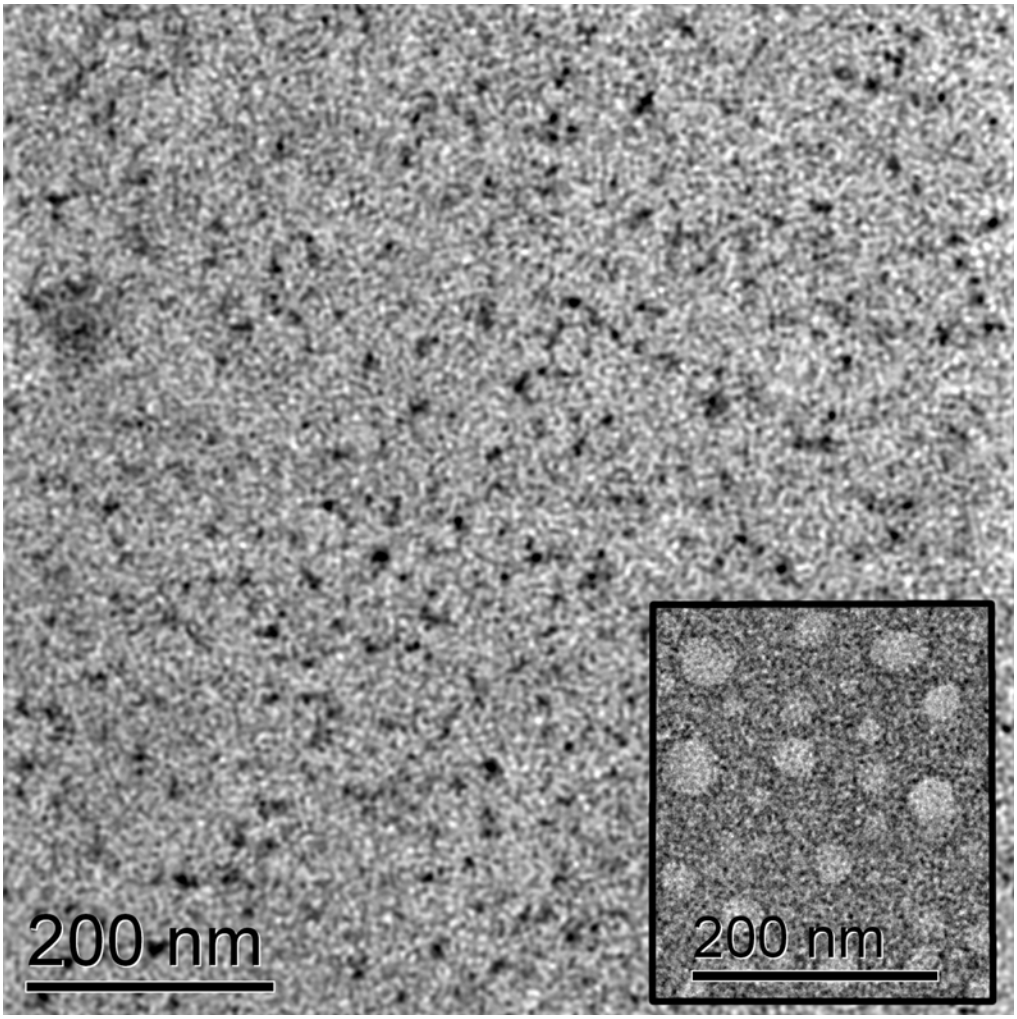

Figure 18. *Cryo-TEM image of the deprotected Glycostar 4, (Insert- TEM image obtained by negative staining).*

7.4. Conclusions

Functional silsesquioxane nanoparticles could be transformed into a macroinitiator of approximately 58 functions suitable for the successful synthesis of well-defined glycopolymer/silsesquioxane hybrid stars. Analysis of the arms cleaved by basic solvolysis indicated the initiation site efficiency of the silsesquioxane-based macroinitiator is about 44 % which could be due to bulkiness of the monomer, MAIGlc as well as the influence of the structure of the macroinitiator, some functions possibly being less accessible than others. The absence of inter- or intramolecular coupling reactions was also shown by the unimodal

character of the cleaved arms. Both the proteced and deprotected glycostars have a spherical structure in THF and water solution, respectively. However, both in DLS and SEM a tendency for aggregation for the water-soluble glycostars is seen, indicating hydrogen-bonding interactions between the stars.

Acknowledgement. This work was supported by the Deutsche Forschungsgemeinschaft (grant no. Mu 896/14). We wish to thank Clarrisa Abetz and Dr. Markus Drechsler for SEM and TEM measurements as well as Sabine Wunder and Evis Penott-Chang for AF-FFF measurements.

Supporting Information Available: Figures S-1, S-2, S-3, S-4 and S-5. This material is available free of charge via the internet at http://pubs.acs.org.

7.5. References

(1) Roovers, J. *Encycl. Polym. Sci. Eng.* **1985**, *2*, 478-499.

(2) Burchard, W. *Adv. Polym. Sci.* **1999**, *143*, 113-194.

(3) Hadjichristidis, N.; Guyot, A.; Fetters, L. J. *Macromolecules* **1978**, *11*, 668-672.

(4) Morton, M.; Helminiak, T. E.; Gadkary, S. D.; Bueche, F. *Journal of Polymer Science* **1962**, *57*, 471-482.

(5) Schappacher, M.; Deffieux, A. *Macromolecules* **1992**, *25*, 6744-6751.

(6) Angot, S.; Murthy, K. S.; Taton, D.; Gnanou, Y. *Macromolecules* **1998**, *31*, 7218-7225.

(7) Sawamoto, M. *Plastics Engineering (New York)* **1996**, *35*, 381-436.

(8) Sawamoto, M. *Cationic Polymerizations*, Matyjaszewski, K. ed.; Marcel Dekker: New York, 1996, p 381.

(9) Hsieh, H. L.; Quirk, R. P. *Anionic Polyemrization*; Marcel Dekker: New York, 1996.

(10) Risse, W.; Wheeler, D. R.; Cannizzo, L. F.; Grubbs, R. H. *Macromolecules* **1989**, *22*, 3205-3210.

(11) Simms, J. A. *Rubber Chemistry and Technology* **1991**, *64*, 139-151.

(12) Wang, J.-S.; Greszta, D.; Matyjaszewski, K. *Polymeric Materials Science and Engineering* **1995**, *73*, 416-417.

(13) Wang, J.-S.; Matyjaszewski, K. *J Am Chem Soc* **1995**, *117*, 5614-5615.

(14) Xia, J.; Zhang, X.; Matyjaszewski, K. *Macromolecules* **1999**, *32*, 4482-4484.

(15) Ohno, K.; Wong, B.; Haddleton, D. M. *Journal of Polymer Science, Part A: Polymer Chemistry* **2001**, *39*, 2206-2214.

(16) Heise, A.; Hedrick, J. L.; Trollss, M.; Miller, R. D.; Frank, C. W. *Macromolecules* **1999**, *32*, 231-235.

(17) Ueda, J.; Kamigaito, M.; Sawamoto, M. *Macromolecules* **1998**, *31*, 6762-6768.

(18) Matyjaszewski, K.; Miller, P. J.; Pyun, J.; Kickelbick, G.; Diamanti, S. *Macromolecules* **1999**, *32*, 6526-6535.

(19) Plamper, F.; Becker, H.; Lanzendörfer, M.; Patel, M.; Wittemann, A.; Ballauff, M.; Müller, A. H. E. *Macromol. Chem. Phys.,* **2005**, *206*, 1813-1825.

(20) Costa, R. O. R.; Vasconcelos, W. L.; Tamaki, R.; Laine, R. M. *Macromolecules* **2001**, *34*, 5398-5407.

(21) Matyjaszewski, K.; Miller, P. J.; Fossum, E.; Nakagawa, Y. *Applied Organometallic Chemistry* **1998**, *12*, 667-673.

(22) Zanini, D.; Roy, R. *J Org Chem* **1998**, *63*, 3486-3491.

(23) Bovin, N. V.; Gabius, H. J. *Chem Soc Rev* **1995**, *24*, 413-&.

(24) Dordick, J. S.; Linhardt, R. J.; Rethwisch, D. G. *Chemtech* **1994**, *24*, 33-39.

(25) Muthukrishnan, S.; Jutz, G.; André, X.; Mori, H.; Müller, A. H. E. *Macromolecules* **2005**, *38*, 9-18.

(26) Narain, R.; Armes, S. P. *Chem Commun* **2002**, 2776-2777.

(27) Ohno, K.; Tsujii, Y.; Fukuda, T. *Journal of Polymer Science Part A-Polymer Chemistry* **1998**, *36*, 2473-2481.

(28) Mori, H.; Lanzendoerfer, M. G.; Müller, A. H. E.; Klee, J. E. *Macromolecules* **2004**, *37*, 5228-5238.

(29) Mori, H.; Müller, A. H. E.; Klee, J. E. *J Am Chem Soc* **2003**, *125*, 3712-3713.

(30) Muthukrishnan, S.; Mori, H.; Müller, A. H. E. *Macromolecules* **2005**, *38*, 3108-3119.

(31) Muthukrishnan, S.; Zhang, M.; Burkhardt, M.; Drechsler, M.; Mori, H.; Müller, A. H. E. *Macromolecules* **2005**, *38*, 7926-7934.

(32) Neugebauer, D.; Sumerlin, B. S.; Matyjaszewski, K.; Goodhart, B.; Sheiko, S. S. *Polymer* **2004**, *45*, 8173-8179.

(33) Harris, J. R.; Horne, R. W. *Micron* **1994**, *25*, 5-13.

(34) Gold, L. *J. Chem. Phys.* **1958**, *28*, 91.

(35) Plamper, F.; Müller, A. H. E. *unpublished results*.

(36) Roovers, J.; Zhou, L. L.; Toporowski, P. M.; Vanderzwan, M.; Iatrou, H.; Hadjichristidis, N. *Macromolecules* **1993**, *26*, 4324-4331.

(37) Held, D.; Müller, A. H. E. *Macromol. Symp.* **2000**, *157*, 225-237.

(38) Daoud, M.; Cotton, J. P. *Journal De Physique* **1982**, *43*, 531-538.

(39) Rey, A.; Freire, J. J.; de la Torre, J. G. *Macromolecules* **1987**, *20*, 342.

(40) Freire, J. J.; Rey, A.; Delatorre, J. G. *Macromolecules* **1986**, *19*, 457-462.

(41) Freire, J. J.; Pla, J.; Rey, A.; Prats, R. *Macromolecules* **1986**, *19*, 452-457.

7.6. Supporting Information to the paper

Synthesis and Characterization of Glycomethacrylate Hybrid Stars from Silsesquioxane Nanoparticles

By Sharmila Muthukrishnan[†], Felix Plamper[†], Hideharu Mori[§], Axel H. E. Müller[†,*]

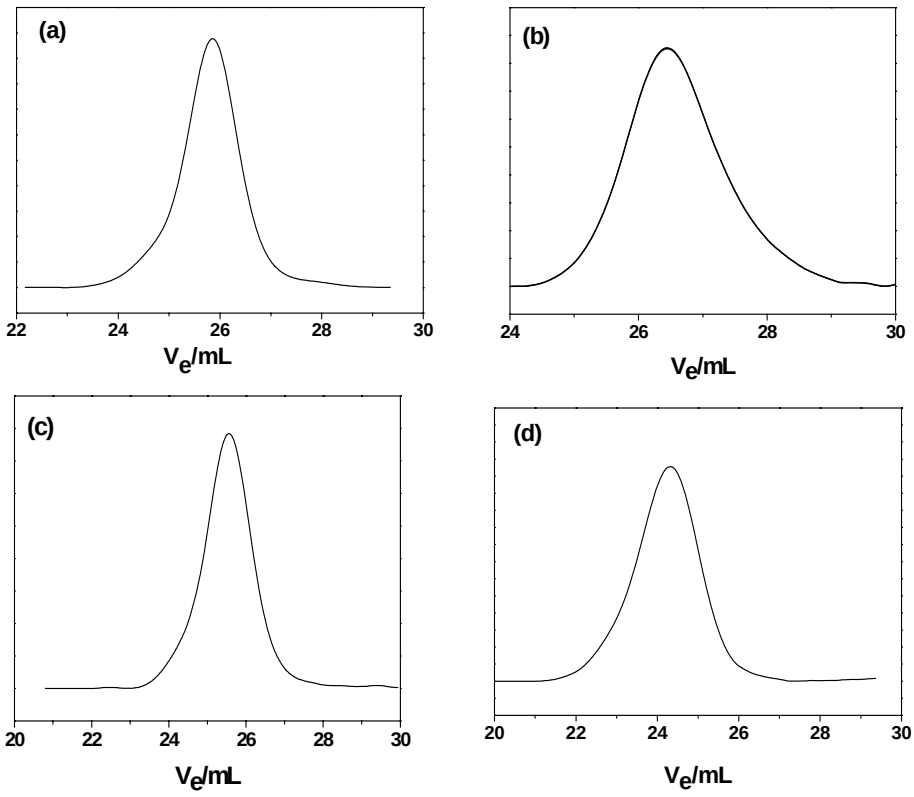

Figure S-1. *GPC traces (RI signal) of (a) Glycostar 1, (b) Glycostar 2, (c) Glycostar 3, and (d) Glycostar 4, respectively.*

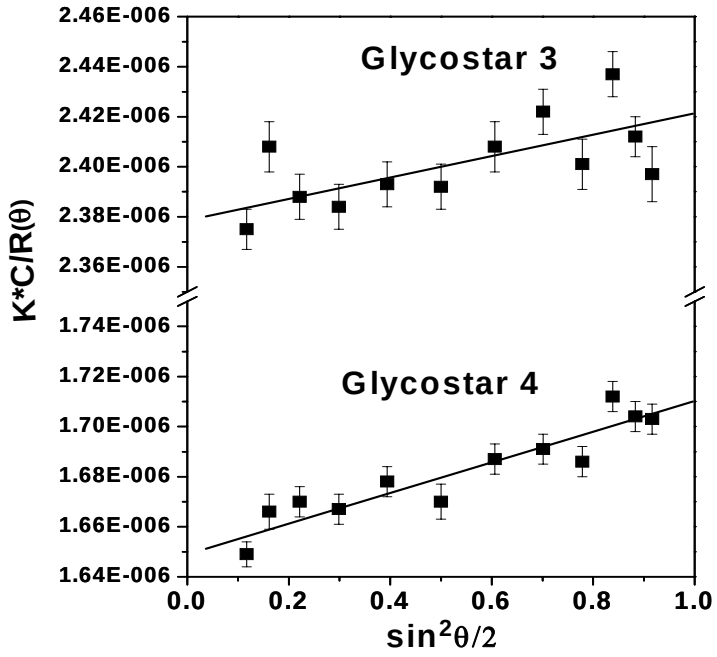

Figure S-2. *Zimm plots for Glycostars 3 and 4 in THF solution.*

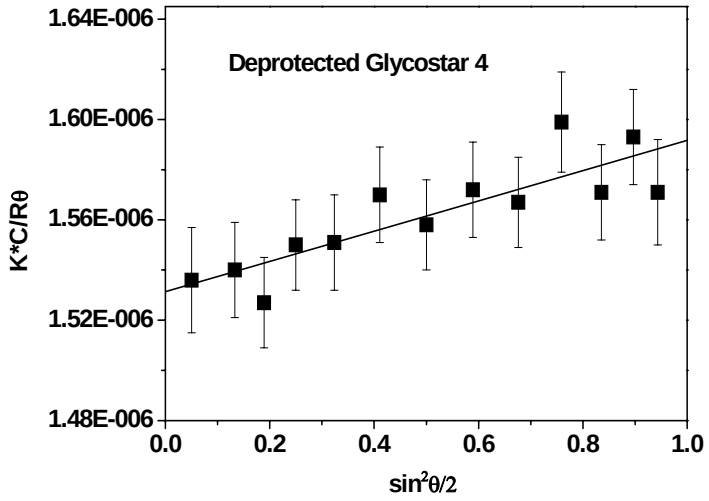

Figure S-3. *Zimm plot for deprotected Glycostar 4.*

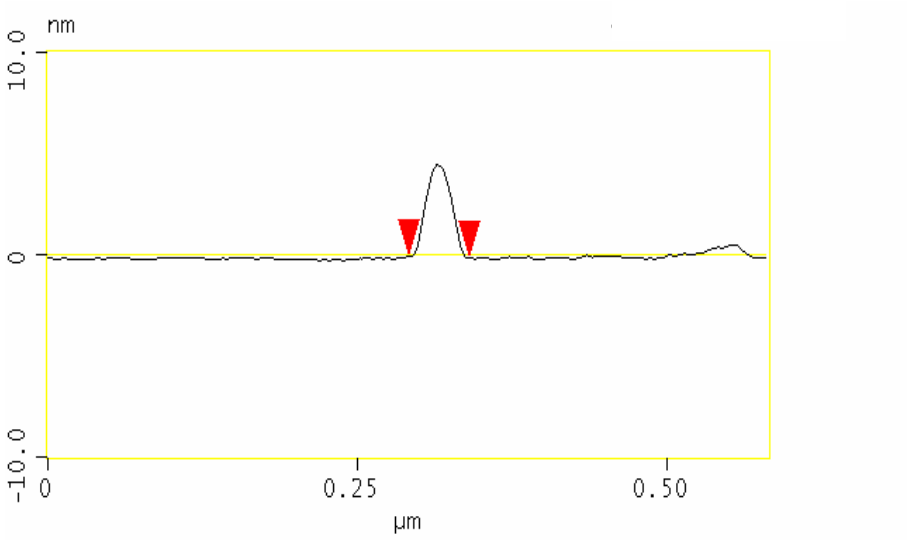

Figure S-4. *Cross-section analysis of a single particle of Glycostar 4.*

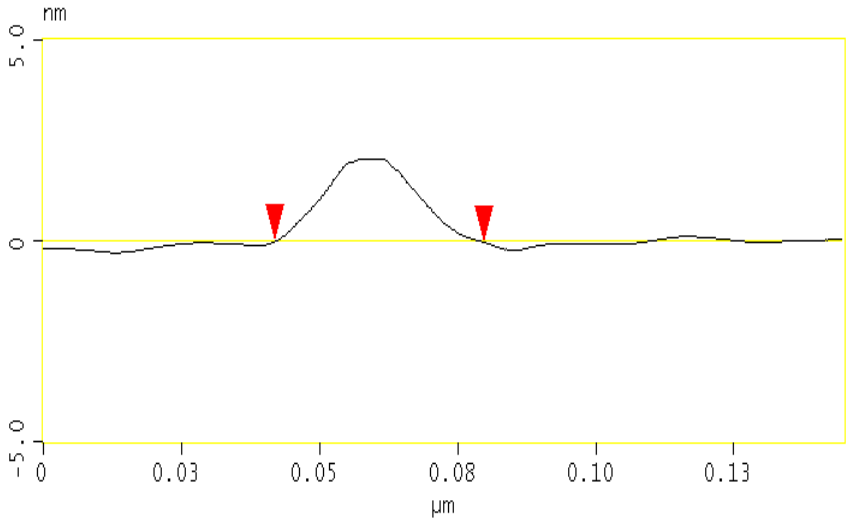

Figure S-5. *Cross-section analysis of a single particle of deprotected Glycostar 4.*

8. Summary

Linear and branched glycopolymers of a sugar-carrying acrylate monomer, 3-*O*-acryloyl-1,2:5,6-di-*O*-isopropylidene-α-D-glucofuranose (AIGlc), were synthesized via atom transfer radical polymerization (ATRP). Self-condensing vinyl copolymerization (SCVCP) via ATRP was employed for the synthesis of highly branched glycoacrylates. The successful synthesis of linear and branched glycoacrylates were confirmed by ^{1}H NMR, GPC/viscosity and MALDI-TOF mass spectrometry. Relationships between dilute solution viscosity and molecular weight were determined, and the Mark-Houwink exponent for branched poly(AIGlc)s typically varied between 0.28 and 0.20, depending on the degree of branching. The degree of branching (DB), evaluated by ^{1}H NMR, are in good agreement with the calculated values, providing the facile and successful synthesis of branched glycopolymers using SCVCP. The linear and branched polymers were converted into water-soluble ones by the deprotection of the isopropylidene groups. The complete deprotection was confirmed by ^{1}H NMR, FT-IR and GPC, respectively.

The sugar-carrying methacrylate monomer, 3-*O*-methacryloyl-1,2:5,6-di-*O*-isopropylidene-α-D-glucofuranose (MAIGlc) was used to synthesize linear and branched glycomethacrylates via ATRP. Homopolymerization resulted in linear poly(MAIGlc) of controlled molecular weight and molecular weight distribution. Randomly branched poly(MAIGlc)s were synthesized using a methacrylic inimer, 2-(2-bromoisobutyryloxy)ethyl methacrylate (BIEM) via SCVCP. The successful synthesis of linear and branched poly(MAIGlc)s were confirmed by GPC, GPC/viscosity analyses, as well as ^{1}H, ^{13}C, and 2D NMR measurements. Mark-Houwink exponents between 0.20 and 0.34 were obtained within reasonable polymerization time (4 h), which was very much faster than the corresponding glyco-polyacrylates. Linear and branched poly(MAIGlc)s were finally deprotected to yield water-soluble glycomethacrylates.

Then, the facile one-pot self-condensing ATRP was utilized to synthesize surface-grafted branched glycopolymers. The hyperbranched glycomethacrylates were grafted from a silicon wafer consisting of a covalently attached initiator layer of α-bromoester fragments by using SCVCP of a methacrylic inimer, BIEM and sugar-carrying methacrylate monomer, MAIGlc. The thickness and roughness of the resulting surfaces were estimated using ellipsometry and scanning force microscopy (SFM) and found to depend on the catalyst amount and the comonomer ratio, γ. In the case of a linear polymer brush, the surface was relatively smooth and uniform. Deprotection of the isopropylidene groups of the branched and linear polymer

brushes resulted in hydrophilic surfaces as investigated by contact angle measurements and DRIFT-IR. A significant difference in Br content between linear and branched polymers brushes was observed by X-ray photoelectron spectroscopy (XPS) which demonstrates the feasibility to control and modify the surface chemical functionality. Due to the presence of the α-bromoester terminal units, such surfaces can be further modified and can be employed in future for several biological applications.

Then, the synthesis of glycocylindrical brushes ("molecular sugar sticks") with poly(3-*O*-methacryloyl-α,β-D-glucopyranose), (PMAGlc) side chains, was achieved using the 'grafting from' approach via atom transfer radical polymerization (ATRP) of the monomer, MAIGlc. The formation of well-defined brushes with narrow length distribution was confirmed by GPC with a multi-angle light scattering detector (MALS) and ^{1}H NMR. The worm-like nature of the glycocylindical brushes was visualized using SFM. The initiating efficency of the initiating sites of the polyinitiator, poly(2-(2-bromoisobutyryloxy)ethyl methacrylate) were determined to be in the range of $0.23 < f < 0.38$ by cleaving the side chains from the backbone by basic solvolysis. After deprotection of the isopropylidene groups of PMAIGlc side chains, SFM measurements, cryogenic transmission electron microscopy and dynamic light scattering showed a stretched, worm-like structure due to the hydration of the sugar moieties.

Finally, glycomethacrylate hybrid stars were synthesized using a silsesquioxane nanoparticles-based macroinitiator of ca. 58 initiator functions and MAIGlc as monomer via ATRP using the "core first" approach. Well-defined glycostars could be synthesized by restricting the polymerization to low conversion. The molecular weights of the star polymers were determined using GPC with viscosity and multi-angle light scattering (MALS) detectors. Analysis of the arms cleaved by basic solvolysis indicated the initiation site efficiency of the silsesquioxane-based macroinitiator is about 44 % which could be due to bulkiness of the monomer, MAIGlc as well as the influence of the structure of the macroinitiator, some functions possibly being less accessible than others. The morphology of the protected as well as deprotected stars were visualized using SFM and scanning electron microscopy (SEM) and found to be spherical in THF and water solution, respectively.

Such glycopolymers of different branched architectures synthesized via ATRP, have very high density of sugar moieties which can be in future manipulated to understand nature ´s multivalent processess, their interactions with proteins, in drug delivery etc due to their enhanced biocompatibility and hydrophilicity.

Zusammenfassung

Lineare und verzweigte Glykopolymere eines zuckerhaltigen Acrylats , 3-*O*-acryloyl-1,2:5,6-di-*O*-isopropylidene-α-D-glucofuranose (AIGlc), wurden durch Atom Transfer Radical Polymerization (ATRP) synthetisiert. Selbstkondensierende Vinylcopolymerisation (SCVCP) mit Hilfe von ATRP wurde für die Synthese von hochverzweigten Glykoacrylaten verwendet. Die erfolgreiche Synthese von linearen und verzweigten Glykoacrylaten wurde mit Hilfe von ^{1}H-NMR, GPC/Viskosität and MALDI-TOF Massenspektroskopie bewiesen. Die Beziehungen zwischen der Viskosität der verdünnten Lösungen und dem Molekulargewicht wurden bestimmt. Der Mark-Houwink-Exponent für verzweigte Poly(AIGlc)s variiert je nach Verzweigungsgrad typischerweise zwischen 0.28 und 0.20. Die Verzweigungsgrade (degree of branching, DB) wurden durch ^{1}H-NMR bestimmt und stimmen gut mit den berechneten Werten überein, was die einfache und erfolgreiche Synthese von verzweigten Glykopolymeren mit Hilfe von SCVCP beweist. Die linearen und verzweigten Polymere wurden durch Entfernung der Isopropylidenschutzgruppen in wasserlösliche Polymere überführt. Die vollständige Umsetzung wurde mit ^{1}H-NMR, FT-IR und GPC überprüft.

Das zuckerhaltige Methacrylat 3-*O*-methacryloyl-1,2:5,6-di-*O*-isopropylidene-α-D-glucofuranose (MAIGlc) wurde verwendet um mit Hilfe von ATRP lineare und verzweigte Glykomethacrylate darzustellen. Die Homopolymerisation ergab lineare Poly(MAIGlc)s mit kontrolliertem Molekulargewicht und Molekulargewichtsverteilung. Statistisch verzweigte Poly(MAIGlc)s wurden mit dem methacrylischen Inimer 2-(2-bromoisobutyryloxy)ethyl methacrylat (BIEM) durch SCVCP synthetisiert. Die erfolgreiche Synthese von linearem und verzweigten Poly(MAIGlc)s wurde durch GPC und GPC/Viskositätsanalysen, als auch durch ^{1}H-, ^{13}C-, und 2D-NMR Messungen bewiesen. Mark-Houwink-Exponenten zwischen 0.20 und 0.34 wurden innerhalb von relativ kurzen Polymerisationszeiten (4 Stunden) erhalten, was deutlich schneller ist als für die entsprechenden Glyko-polyacrylate. Die linearen und verzweigten Poly(MAIGlc)s wurden schließlich entschützt, um wasserlösliche Glykomethacrylate zu erhalten.

Die einfache Eintopf selbstkondensierende ATRP wurde benutzt, um oberflächengepfropfte verzweigte Glykopolymere zu synthetisieren. Die hyperverzweigten Glykomethacrylate wurden ausgehend von einem Siliconwafer, der eine kovalent gebundene α-Bromoester-Initiatorschicht besaß, mit Hilfe von SCVCP des methacrylischen Inimers BIEM und des zuckerhaltigen methacrylischen Monomers MAIGlc aufgepfropft. Die Schichtdicke und die Oberflächenrauigkeit der so geschaffenen Oberflächen wurde durch Ellipsometrie und

Rasterkraftmikroskopie (SFM) abgeschätzt. Beides hängt von der Katalysatormenge und dem Comonomerverhältnis, γ, ab. Im Falle der linearen Polymerbürste war die Oberfläche relativ eben und einheitlich. Die Entfernung der Isopropylidenschutzgruppen der verzweigten und der linearen Polymerbürsten ergab hydrophile Oberflächen, die mit Kontaktwinkelmessungen und DRIFT-IR untersucht wurden. Ein erheblicher Unterschied im Bromgehalt zwischen den linearen und den verzweigten Polymerbürsten wurde mit Röntgen-Photoelektronen-Spektroskopie (XPS) beobachtet. Dies demonstriert die Möglichkeit der Kontrolle und der Veränderung der chemischen Funktionalität der Oberfläche. Aufgrund der vorhandenen α-Bromoesterendgruppen können solche Oberflächen verändert werden und können in Zukunft für verschiedene biologische Anwendungen Verwendung finden.

Die Synthese von glykozylindrischen Bürsten („molekulare Zuckerstäbe“) mit Poly(3-*O*-methacryloyl-α,β-D-glucopyranose)-, (PMAGlc-) Seitenketten wurde durch die „grafting from“ Methode mit Hilfe der Atom Transfer Radical Polymerization (ATRP) des Monomers MAIGlc erhalten. Die Bildung von gut-definierten Bürsten mit enger Längenverteilung wurde durch GPC mit einen Lichtstreudetektor (MALS) and ^{1}H-NMR nachgewiesen. Die wurmähnliche Natur der glykozylindrischen Bürsten wurde durch SFM sichtbar gemacht. Die Initiatoreffektivität der initiierenden Seiten des Polyinitiators, Poly(2-(2-bromoisobutyryloxy)ethyl methacrylat) wurde durch die Abspaltung der Seitenarme vom Rückgrat durch basische Solvolyse als im Bereich von $0.23 < f < 0.38$ bestimmt. Nach der Abspaltung der Isopropylidenschutzgruppen der PMAIGlc-Seitenketten zeigen SFM-, dynamische Lichtstreumessungen und Cryogene Transmissionselektronenmikroskopie aufgrund der Hydration der Zuckereinheiten eine gestreckte, wurmähnliche Struktur.

Schließlich wurden Glykomethacrylat-Hybridsterne unter Verwendung eines Makroinitiators auf Basis von Silsesquioxan-Nanopartikeln mit etwa 58 Initiatorfunktionen und MAIGlc als Monomer mit Hilfe von ATRP mit der „Core-first“-Methode synthetisiert. Wohldefinierte Glykosterne konnten durch die Beschränkung der Polymerisation auf geringe Umsätze synthetisiert werden. Die Molekulargewichte der Sternpolymere wurden durch GPC mit Viskositäts- und Lichtstreudetektoren bestimmt. Die Analyse der durch basische Solvolyse abgespaltenen Arme zeigt eine Initiatoreffektivität von 44% des silsesquioxan-basierenden Makroinitiators. Dies könnte auf die Sperrigkeit des Monomers MAIGIc als auch auf den strukturellen Einfluss des Makroinitiators zurückzuführen sein, d.h. dass manche Funktionalitäten einfacher zugänglich sind als andere. Die sphärische Morphologie der geschützten als auch der entschützten Sterne wurde durch SFM und Rasterelektronenmikroskopie (SEM) sichtbar gemacht.

Solche durch ATRP dargestellten Glykopolymere mit verschiedenen verzweigten Architekturen haben eine sehr hohe Dichte an Zuckereinheiten, welche in Zukunft verändert werden können, um die multivalenten Prozesse der Natur, ihre Wechselwirkungen mit Proteinen, die Pharmakotherapie usw. aufgrund ihrer erhöhten Biokompatibilität und Hydrophilie zu untersuchen.

9. List of publications

During the course of this thesis the following papers have been published (or accepted/submitted/to be submitted):

- Muthukrishnan, S.; Jutz, G.; André, X.; Mori, H.; Müller, A. H. E. "Synthesis of Hyperbranched Glycopolymers via Self-Condensing Atom Transfer Radical Copolymerization of Sugar-Carrying Acrylate" *Macromolecules*, **2005**, 38, 9.

- Muthukrishnan, S.; Mori, H.; Müller, A. H. E. **"**Synthesis of Novel Hyperbranched Glycopolymers" Proceedings of 40th IUPAC Symposium on Macromolecules , MACRO **2004**, Paris, July (**2004**).

- Muthukrishnan, S.; Mori, H.; Müller, A. H. E. "Synthesis and Characterization of Methacrylate-Type Hyperbranched Glycopolymers via Self-Condensing Atom Transfer Radical Copolymerization" *Macromolecules*, **2005**, 38, 3108.

- Muthukrishnan, S.; Zhang, M.; Burkhardt, M.; Drechsler, M.; Mori, H.; Müller, A.H.E. "Molecular Sugar Sticks: Cylindrical Glycopolymer Brushes" *Macromolecules*, **2005**, 38, 7926.
- Muthukrishnan, S.; Drechsler, M.; Mori, H.; Müller, A. H. E. "Glycopolymers with Branched Architectures: Sugar Balls and Sugar Sticks" *Polym. Prepr. (Am. Chem. Soc., Div. Polym. Chem.)*, 46(2), 247, (**2005**).

- Muthukrishnan, S.; Plamper, F.; Mori, H.; Müller, A. H. E. "Synthesis and Characterization of Glycomethacrylate Hybrid Stars from Silsesquioxane Nanoparticles" *Macromolecules*, **2005**, 38, 10631.

- Muthukrishnan, S.; Dominik, P. E.; Mori, H.; Müller, A. H. E. "Synthesis and Characterization of Surface-Grafted Hyperbranched Glycomethacrylates" *Macromolecules*, (Submitted).

- Muthukrishnan, S.; Dominik, P. E.; Mori, H.; Müller, A. H. E. "Synthesis and Characterization of Surface-Grafted Hyperbranched Glycomethacrylates" *Polymeric Materials: Science & Engineering*, **2006** (in press).

- Muthukrishnan, S.; Mori, H.; Müller, A. H. E. "Synthesis and Characterization of Glycopolymers of different topologies using a sugar-carrying methacrylate" *in* K. Matyjaszewski, Ed.: ACS Symp. Ser., Controlled/LivingRadical Polymerization, **2006** (in press).

Acknowledgements

At this juncture, I would like to extend my gratitude to all the people who have contributed to my work in one way or the other during the course of my Ph.D. programme.

I take this opportunity to thank Prof. Dr. Axel H. E. Müller for his fruitful suggestions, constant encouragement, supervision and patience. I am greatly indebted to him for having given me an opportunity to work in a very interesting topic and healthy atmosphere. I indeed consider it to be a pride to have such a noble and outstanding person as my "Doctorvater".

Then, its my turn to express my immense gratitude to Dr. Hideharu Mori, who introduced me to the world of ATRP and glycopolymers. From the day one, he has been constantly encouraging and motivating me towards my project. His motivation and inspiration has always triggered me to work hard and just harder. He has always being very patient in teaching even very minute things which has definitely helped me a lot to learn the nuances of research work. Without this opportunity, I would not have got a chance to assess my research abilities.

I am thankful to Dr. Mingfu Zhang, Günter Jutz and Andreas Walther for showing lot of care and patience during my start which helped me a lot to settle down in the new lab. Special thanks to Dr. Mingfu Zhang for several useful discussions and suggestions.

Thanks to Dr. Markus Drechsler and Astrid Göpfert for their great help during TEM measurements. Clarissa Abtez is greatly acknowledged for SEM measurements.

I would like to thank the whole crew of PC II who have always being kind enough in allowing me to use their instruments. I am particularly thankful to Dr. Helmut Hänsel and Dr. Frank Schubert for their zeal and spirit in helping me whenever I dropped into their office. Markus Hund and Kristin Schmidt are greatly acknowledged for introducing me to AFM technique.

I am grateful to Youyong Xu, Xavier Andre and Sabine Wunder for GPC measurements. Again, thanks to Sabine Wunder for a nice collaboration during GPC/viscosity and MALS measurements. Dominik Erhardt is specially acknowledged for a wonderful collaboration during the course of his advanced practical course in MC II.

Now, its my turn to thank all the members of MC II- Dr. Yanfei Liu, Harald Becker, Dr. Holger Schmalz, Markus Burkhardt, Adriana Boschetti, Felix Plamper, Markus Ruppel, Jiayin Yuan, Sergey Nosov, Chi-Cheng Peng, Pierre Millard, Anja Goldmann, Marli Tebaldi de Sordi, Kerstin Matussek, Annette Krökel, Cornelia Lauble, Denise Danz, Dr. Olivier Colombani, and Dr. Alexandre Terrenoire for a very nice working atmosphere. Special thanks

to Gabi Cantea, Evis Penott and Manuela Fink for their very nice companionship and co-operation.

Thanks to Gaby Oliver who has always being endowed with lot of patience in helping me out with lot of administration related things. Without her, it would have been nearly impossible for me to have understood all the german documents.

Last but not least, special thanks to my family members for their strong support, motivation and encouragement which has always being a driving force for working actively in abroad. Many thanks to John Bosco Stanislaus for his great efforts to stand by me for everything which relished my stay in Bayreuth and also for his great support and care whenever I worked in PC II.

Erklärung

Die vorliegende Arbeit wurde von mir selbstsändig verfasst und ich habe dabei keine anderen als die angegebenen Hilfsmittel und Quellen benutzt.

Ferner habe ich nicht versucht, anderweitig mit oder ohne Erfolg eine Dissertation einzureichen oder mich der Doktorprüfung zu unterziehen.

Bayreuth, den 29.11.2005

Sharmila Muthukrishnan